

クォークと原子核

クォークとレプトン 点状粒子

FERMIONS

matter constituents
spin = 1/2, 3/2, 5/2, ...

Leptons spin = 1/2		
Flavor	Mass GeV/c ²	Electric charge
ν_e electron neutrino	$<1 \times 10^{-8}$	0
e electron	0.000511	-1
ν_μ muon neutrino	<0.0002	0
μ muon	0.106	-1
ν_τ tau neutrino	<0.02	0
τ tau	1.7771	-1

Quarks spin = 1/2		
Flavor	Approx. Mass GeV/c ²	Electric charge
u up	0.003	2/3
d down	0.006	-1/3
c charm	1.3	2/3
s strange	0.1	-1/3
t top	175	2/3
b bottom	4.3	-1/3

物質を構成するのは、u, d, e, (ν_e)

低質量ハドロン

- バリオン

- ハイペロン (Λ , Σ , Ξ)

- ストレンジネス量子数を持つバリオン

S		Lifetims[s]	Main Decay channels	Mass [MeV/c ²]
0	P	Stable?		938.3
	n	887	$p e^- \bar{\nu}_e$ (100%)	939.6
-1	Λ	$2.63 \cdot 10^{-10}$	$\rho\pi$ (64%), $n\pi$ (36%)	1115.7
-1	Σ^\pm	$0.8 \cdot 10^{-10}$	$\rho\pi^0$ (52%), $n\pi^+$ (48%)	1189.4
	Σ^0	$7.4 \cdot 10^{-20}$	$\Lambda\gamma$ (~100%)	1192.6
	Σ^-	$1.48 \cdot 10^{-10}$	$n\pi^-$ (99.8%)	1197.4
-2	Ξ^0	$2.9 \cdot 10^{-10}$	$\Lambda\pi^0$ (~100%)	1315
	Ξ^-	$1.64 \cdot 10^{-10}$	$\Lambda\pi^-$ (~100%)	1321

- メソン (擬スカラ、ベクトル)

	Lifetims[s]	Main Decay channels	Mass [MeV/c ²]
π^\pm	$2.6 \cdot 10^{-8}$	$\mu^\pm \nu_\mu$ (~100%)	139.6
π^0	$8.4 \cdot 10^{-17}$	$e^\pm \nu_e$ (1.2×10^{-4})	135.0
K^\pm	$1.2 \cdot 10^{-8}$	$\mu^\pm \nu_\mu$ (64%)	493.6
	$8.9 \cdot 10^{-11}$	2π (~100%)	497.7
	$5.2 \cdot 10^{-8}$	3π (34%)	497.7
η η'	$5.5 \cdot 10^{-19}$	3π (56%), 2γ (39%)	547.4
	$3.3 \cdot 10^{-21}$	$\pi\pi\eta$ (65%), $\rho\gamma$ (30%)	957.8

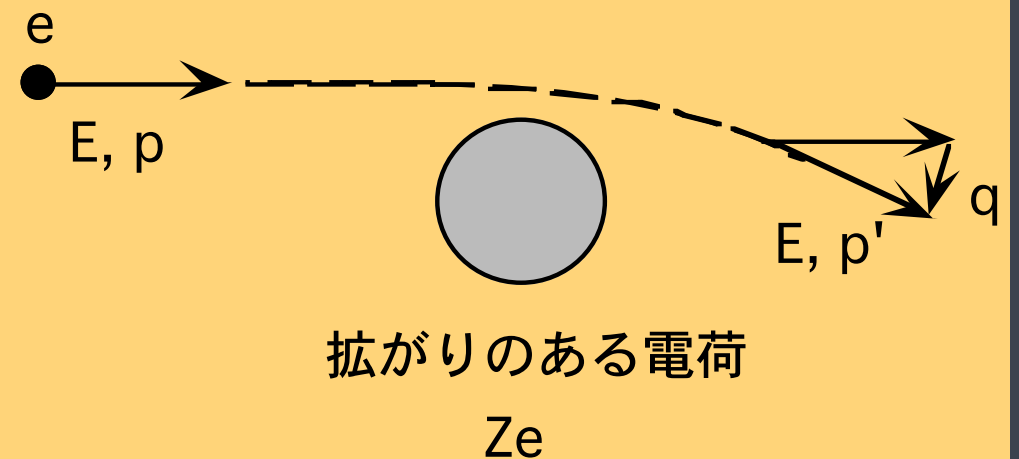
	Lifetims[s]	Main Decay channels	Mass [MeV/c ²]
ρ	$4.3 \cdot 10^{-24}$	2π (~100%)	769.9
K^\pm	$1.3 \cdot 10^{-24}$	$K\pi$ (~100%)	896.1(0) 891.6(-)
ω	$7.8 \cdot 10^{-23}$	3π (89%)	781.9
ϕ	$1.5 \cdot 10^{-22}$	$2K$ (84%), $\rho\pi$ (13%)	1014.9

電子散乱の実験



$$\frac{d\sigma}{d\Omega} = \frac{4(Ze^2)^2 E^2}{q^4} \left(1 - \frac{q^2}{4E^2}\right) = \left(\frac{d\sigma}{d\Omega}\right)_{\text{Mott}}$$

\uparrow Rutherford \uparrow Effect of electron helicity



$$\frac{d\sigma}{d\Omega} = \left(\frac{d\sigma}{d\Omega}\right)_{\text{Mott}} \times |F(q)|^2$$

$$F(q) = \int e^{iqr} \rho(r) dr$$

$\rho(r)$: 電荷分布

電子と陽子の散乱

$$\left(\frac{d\sigma}{d\Omega}\right)_{\text{exp}} = \left(\frac{d\sigma}{d\Omega}\right)_{\text{Mott}} \cdot |F(q^2)|^2$$

ローゼンブルースの公式

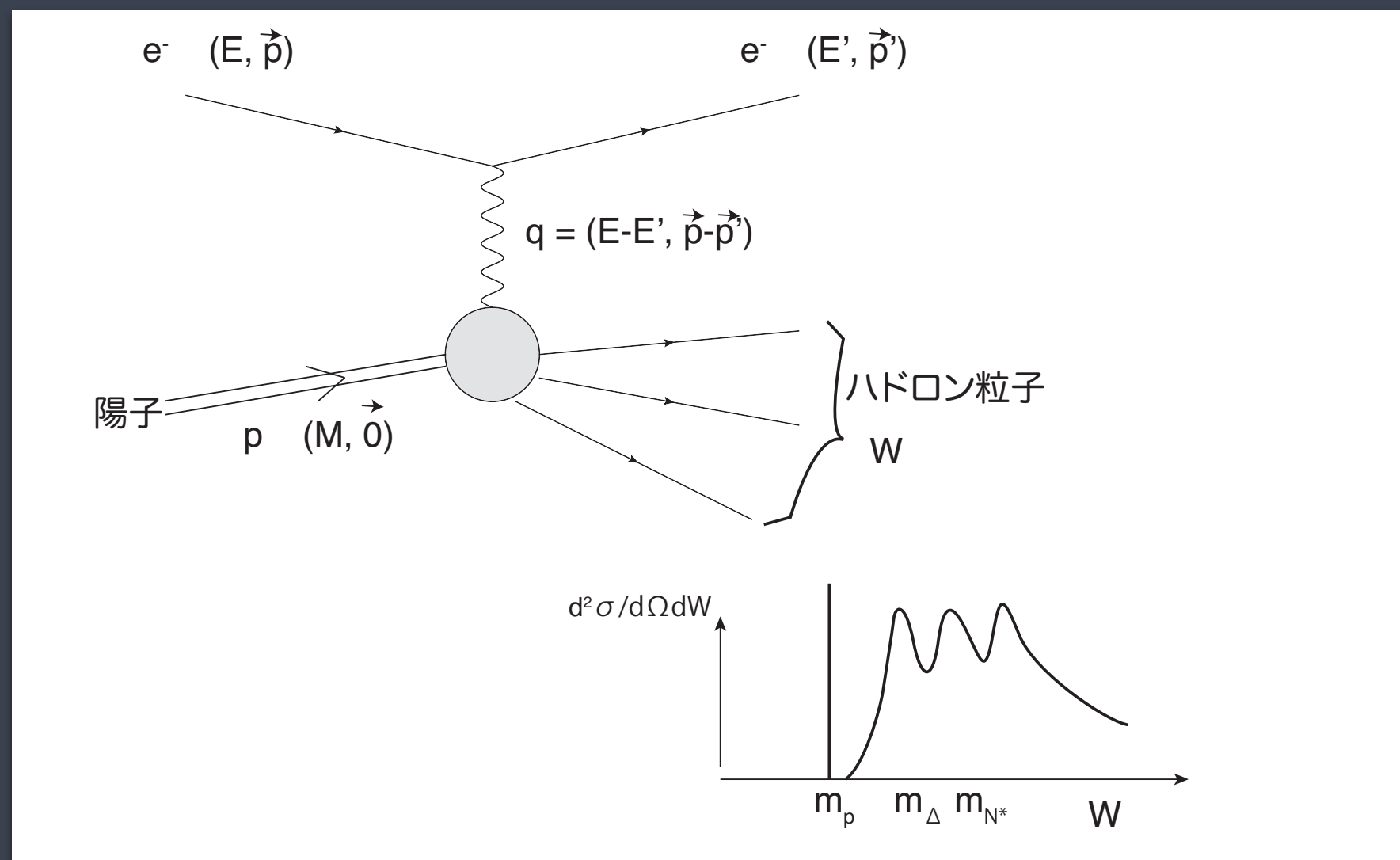
$$\left(\frac{d\sigma}{d\Omega}\right)_{\text{exp}} = \left(\frac{d\sigma}{d\Omega}\right)_{\text{Mott}} \cdot \left[\frac{G_E^2(q^2) + \tau G_M^2(q^2)}{1 + \tau} + 2\tau G_M^2(q^2) \tan^2 \frac{\theta}{2} \right], \tau = \frac{q^2}{4Mc^2}$$

$$G_E(q^2) = \frac{G_M(q^2)}{2.79} = \left(1 + \frac{q^2}{0.71(\text{GeV}/c)^2} \right)^{-2}$$

電気構造因子
磁気構造因子

陽子の平均 2 乗半径 = 0.81 fm

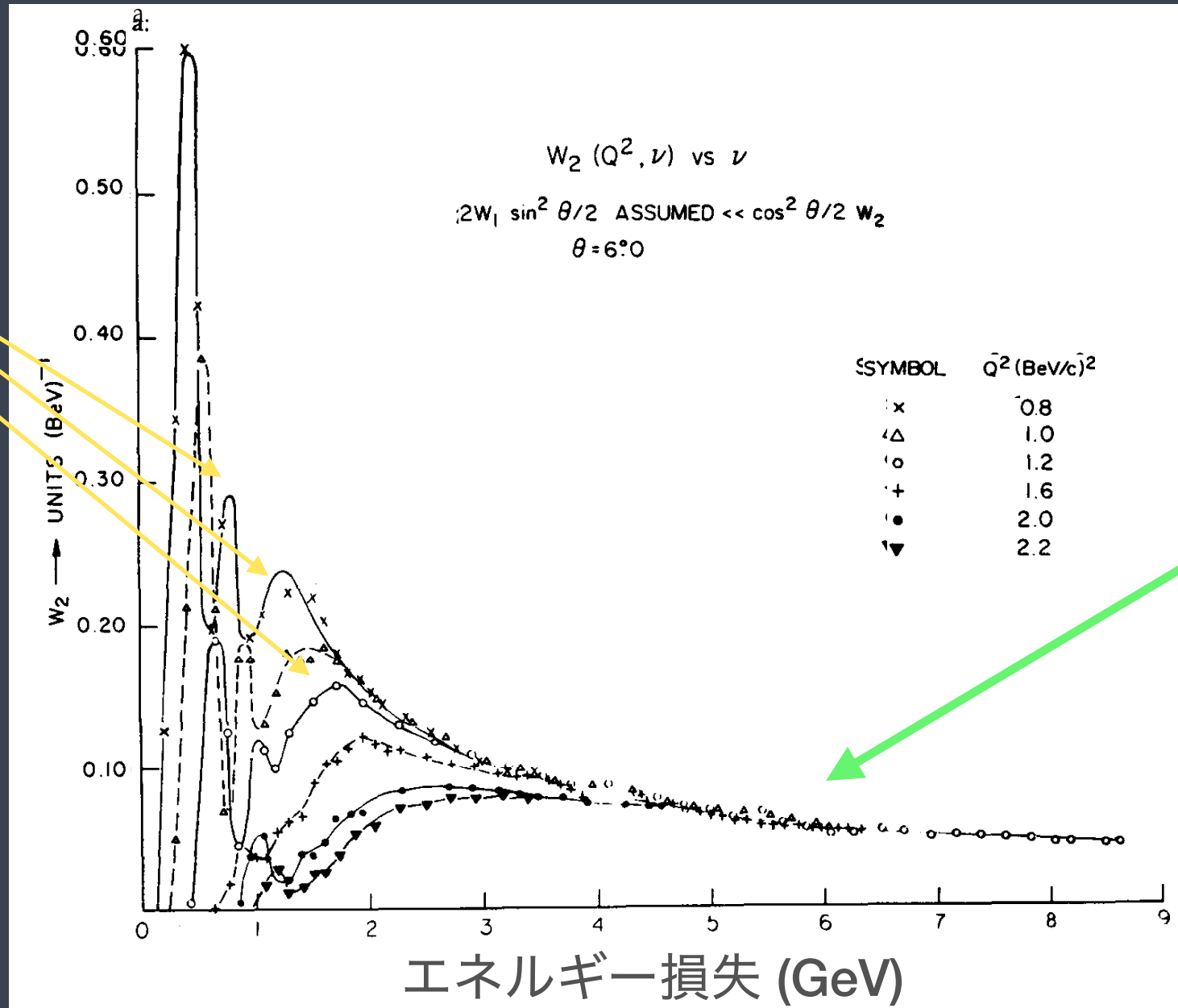
非弾性散乱の運動学



電子散乱のデータ: 高エネルギー

核子の
励起状態

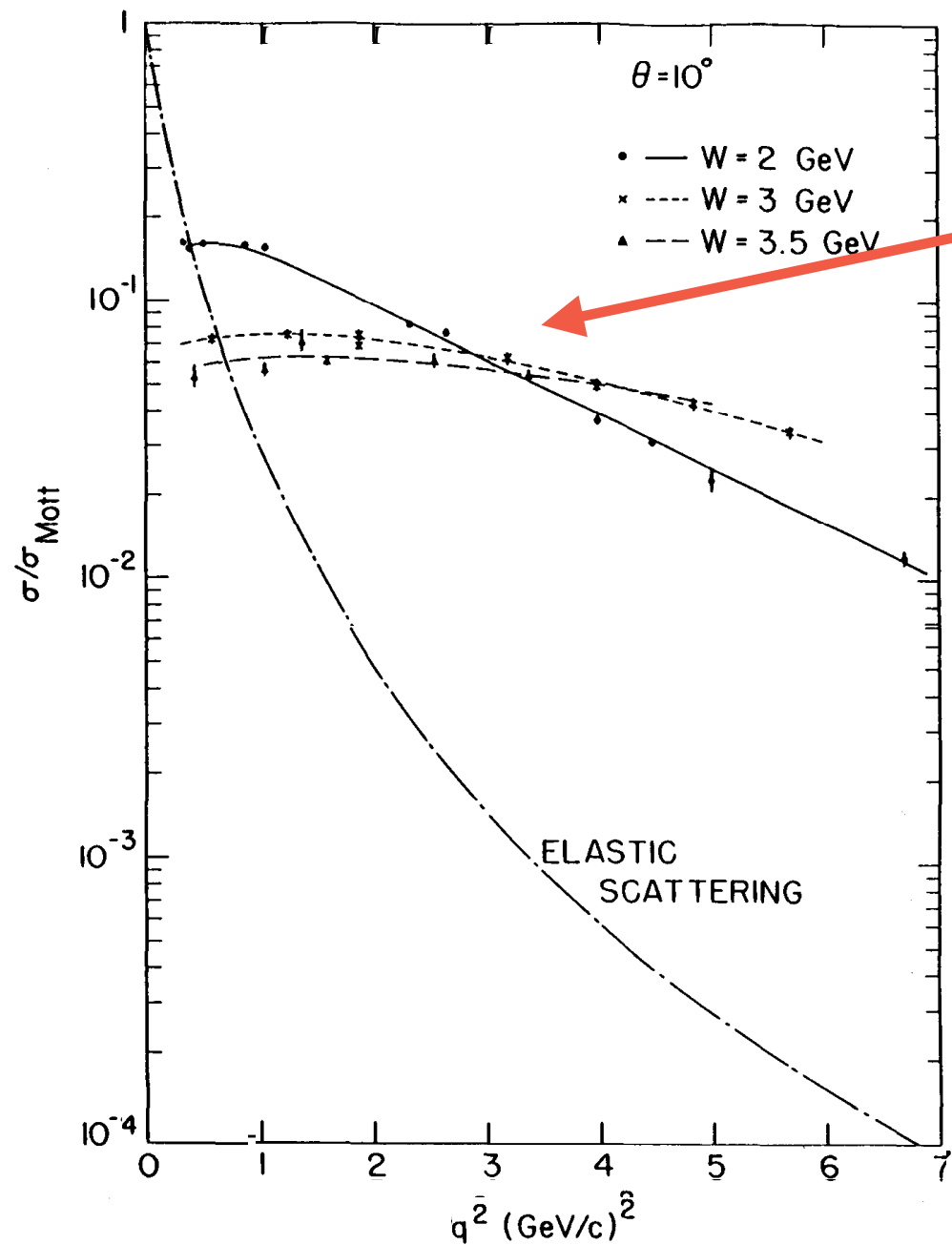
Δ, N^*



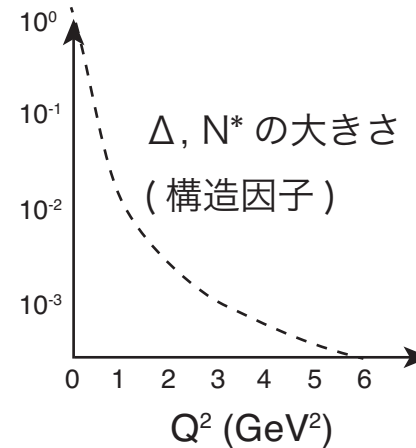
Deep
Inelastic
Sattering
(深部非弾性
散乱)

電子散乱のデータ (つづき)

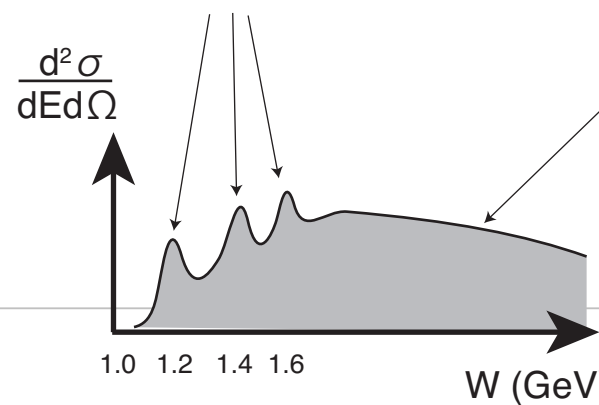
点電荷との散乱
(パートンの発見)



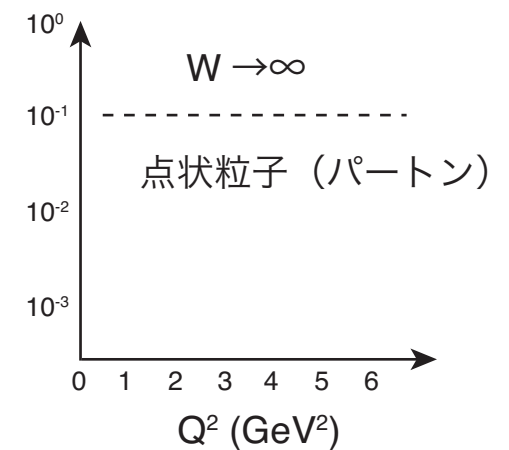
Mott 散乱との比



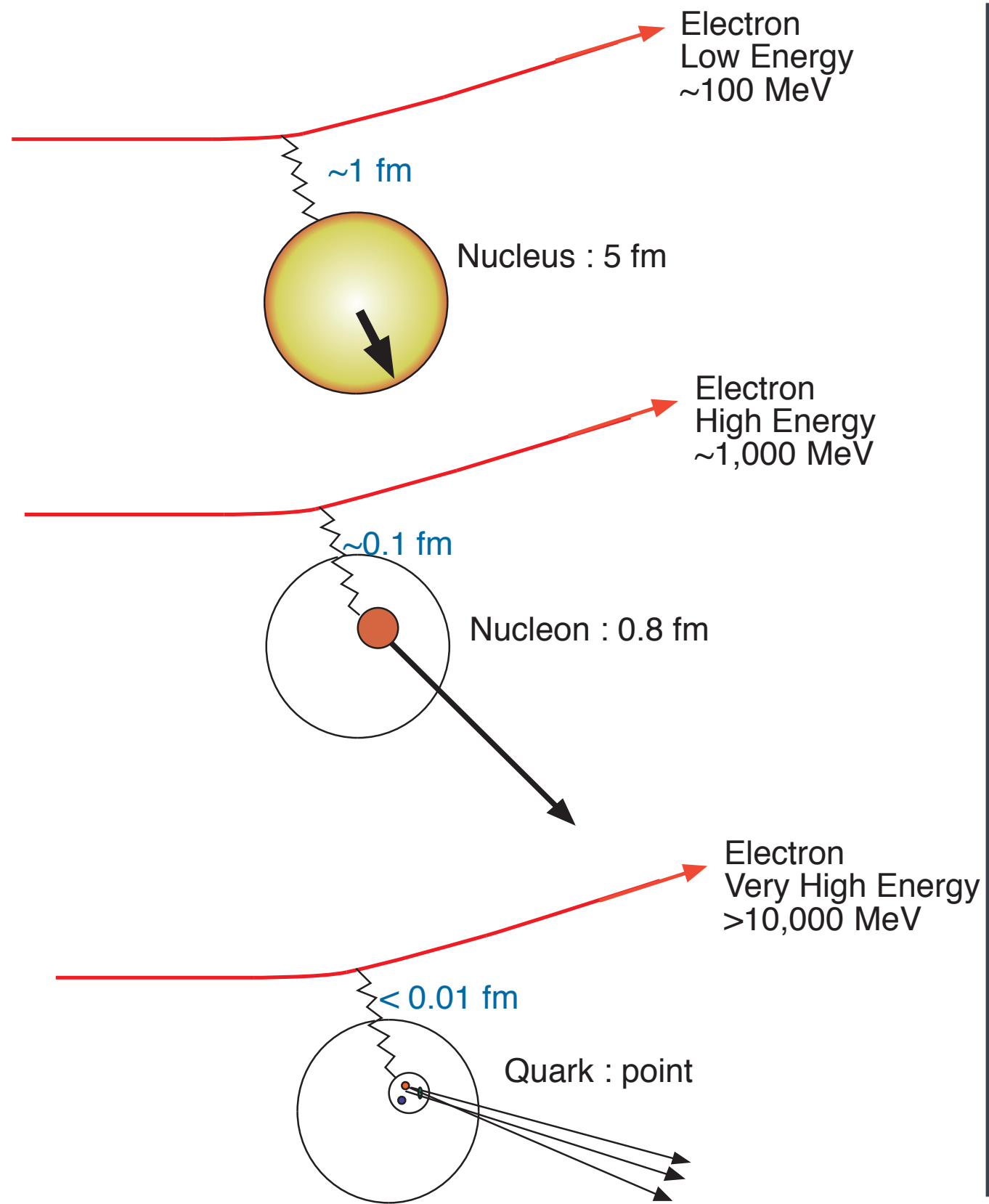
核子の励起状態 Δ , N^* の励起



Mott 散乱との比

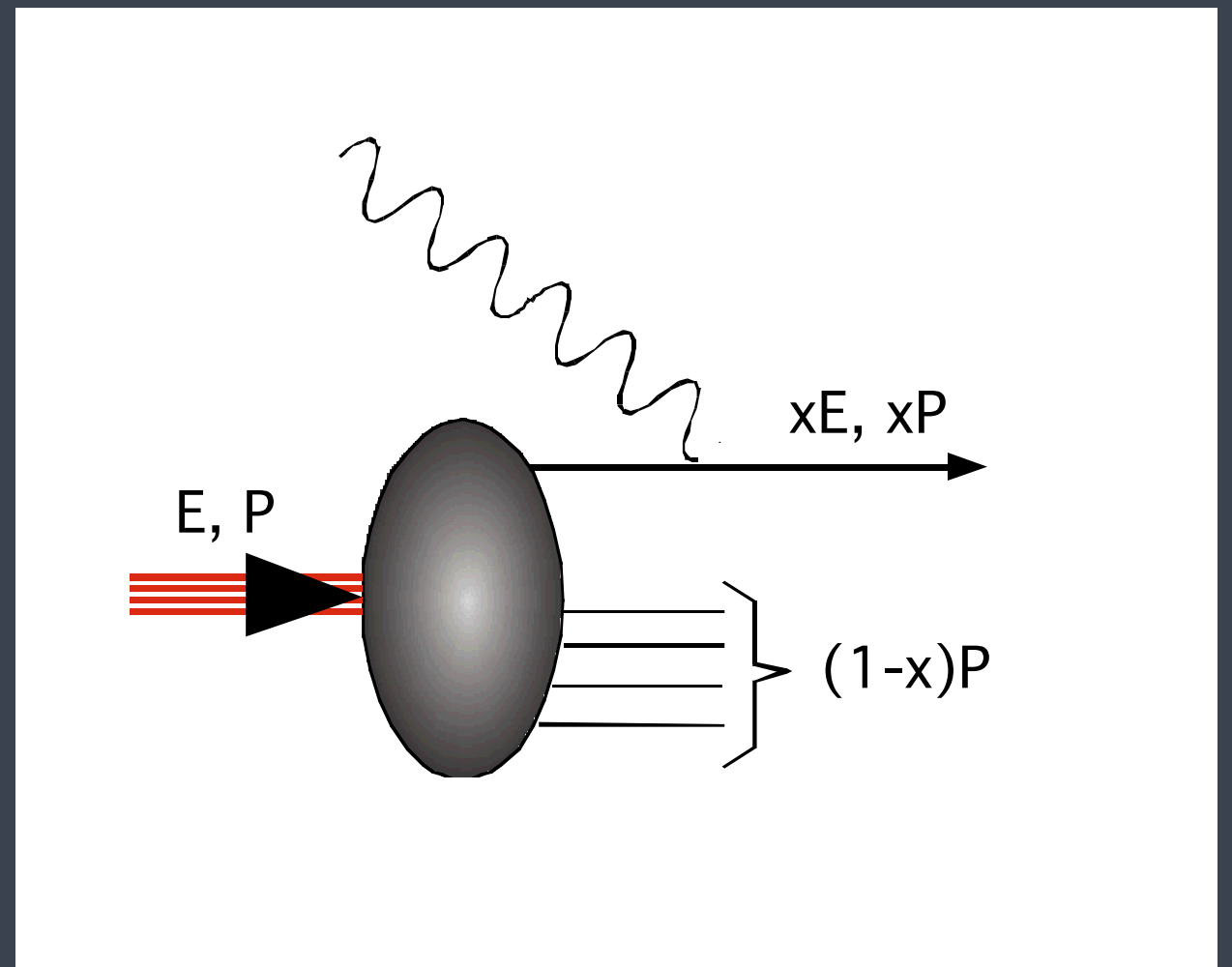


深部非弾性散乱



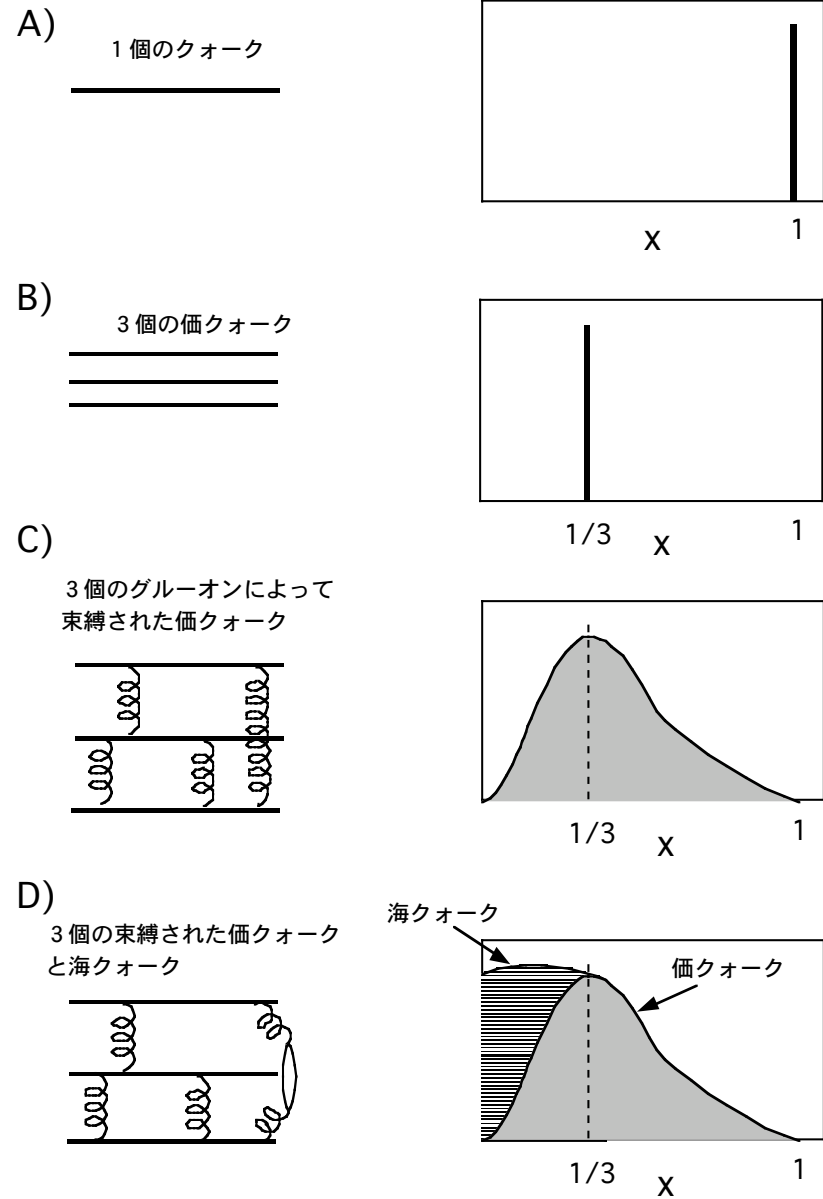
パートン模型

	陽子	パートン
エネルギー	E	xE
運動量	p_L	xp_L
	$p_T=0$	$p_T=0$
質量	M	xM

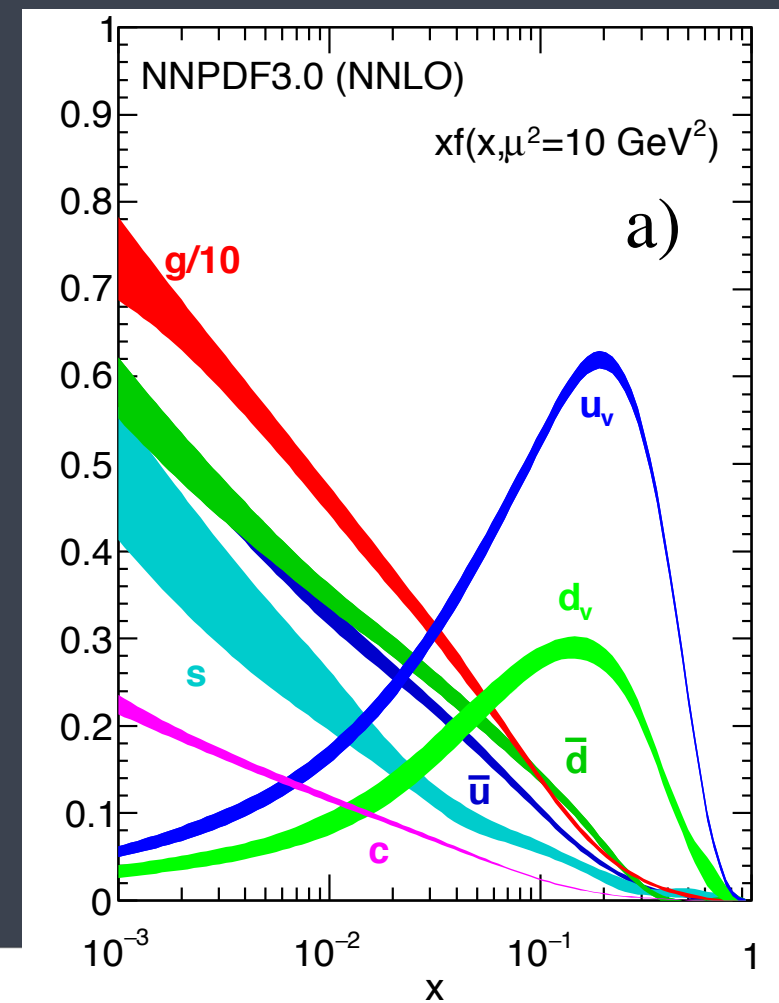


陽子の構造

パートンの運動量分布



全クォークが担う運動量～半分
 残りの半分はグルーオンが担う



パートンはクォーク？

- スピン1/2 : Callan-Gross関係式

$$2xF_1 = F_2$$

$$K_0 = F_2 / (xF_1) - 1$$

- 分数電荷: $-1/3e, +2/3e$

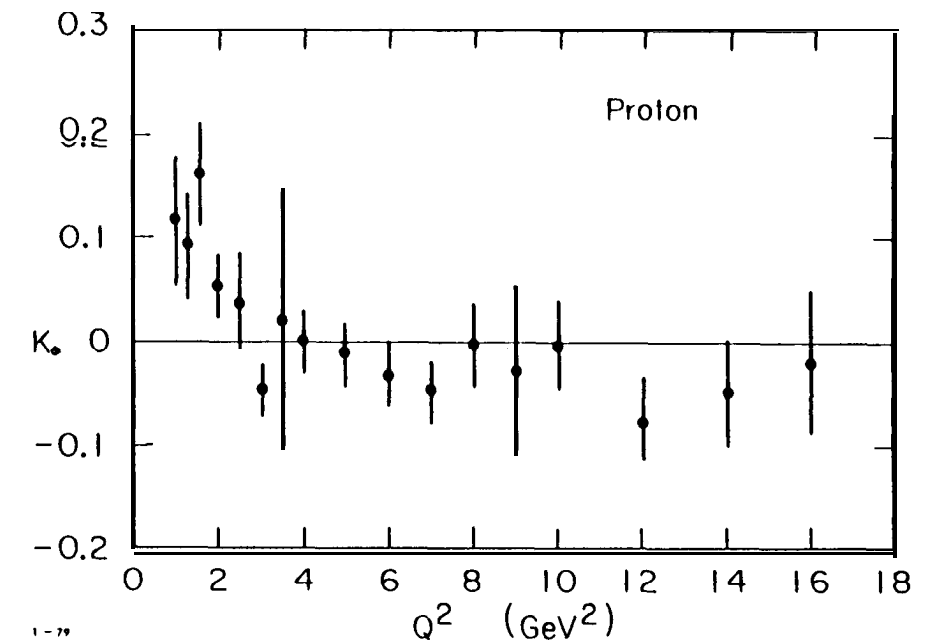


Fig. 18. The Callan-Gross relation: K_0 vs q^2 , where K_0 is defined in the text. These results established the spin of the partons as $1/2$.

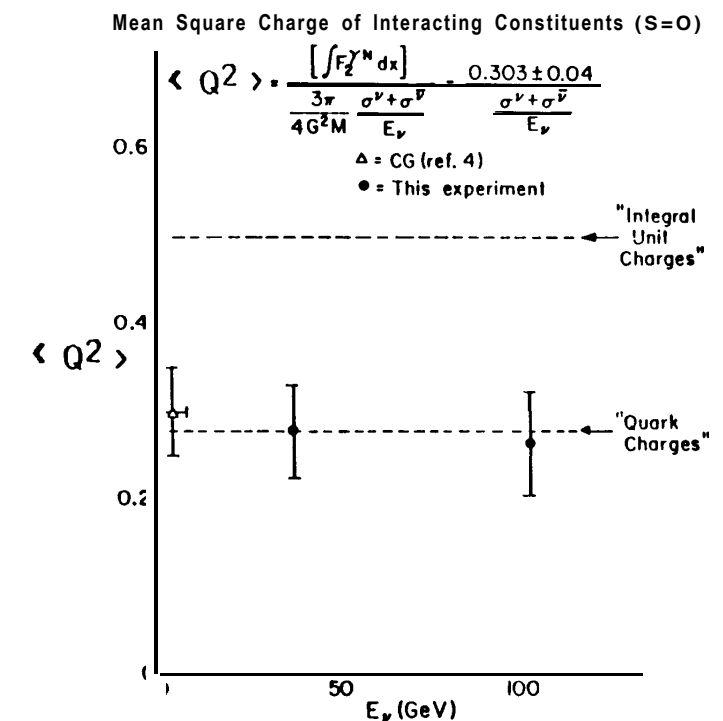
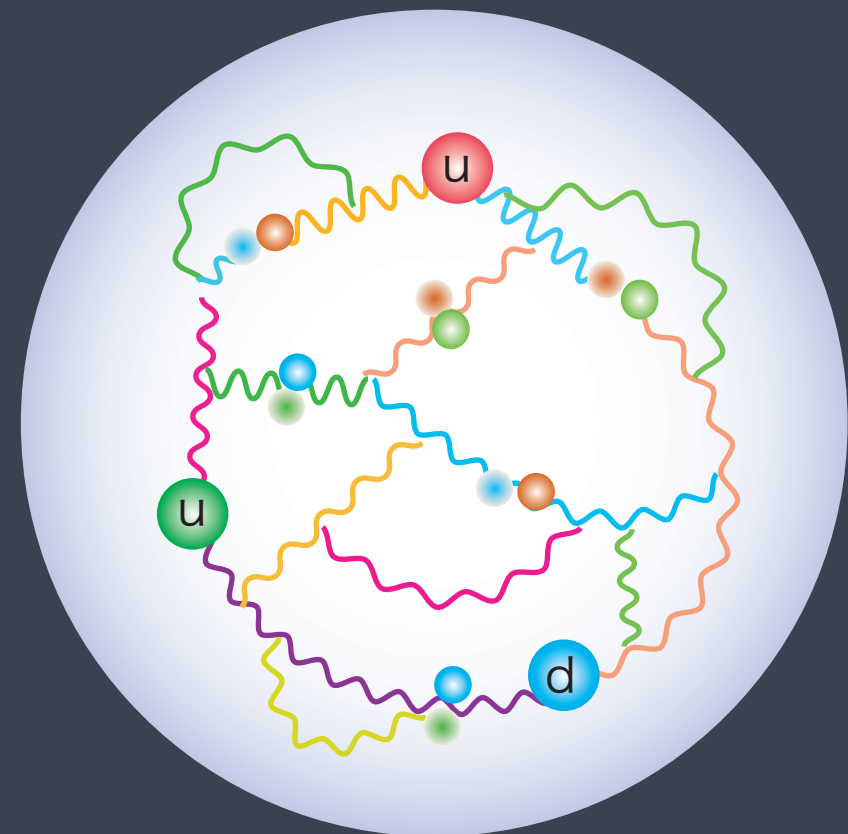


Fig. 11: Comparison of the ratio of integrated electron-nucleon and neutrino-nucleon structure functions to the value $5/18$ expected from quark charges. The open triangle data point is from Gargamelle and the filled-in circles are from the CIT-NAL Group. From Ref. [45]. The quantity $\langle Q^2 \rangle$ is the mean square charge of the quarks in a target consisting of an equal number of protons and neutrons.

陽子の内部構造

- ▶ 2個のuクォーク + 1個のdクォーク
 - ▶ グルーオン ~ 50%
 - ▶ 海クォーク ($q\bar{q}$)
- “色”がひしめき合う世界
- →外部は”白”



原子核のクォークによる記述は可能か？

- ▶ 原子核は、 Z 個の陽子と N 個の中性子から構成される($A=Z+N$)。

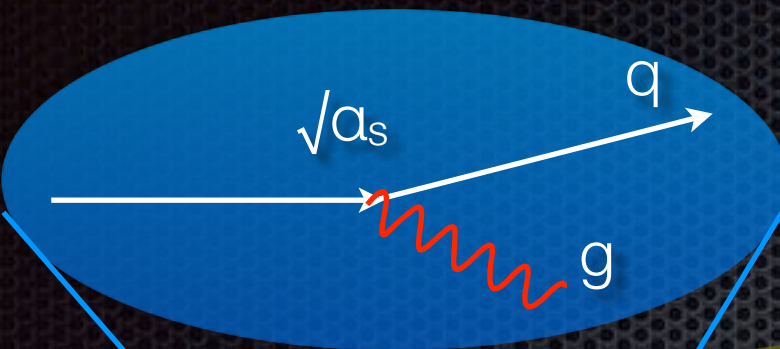


- ▶ 原子核は、 $3A$ 個のクォークから構成される。

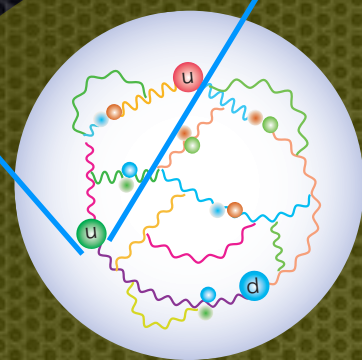
これまでのところ、そうでなければ説明できない現象は見つかっていない。

QCDの諸様相

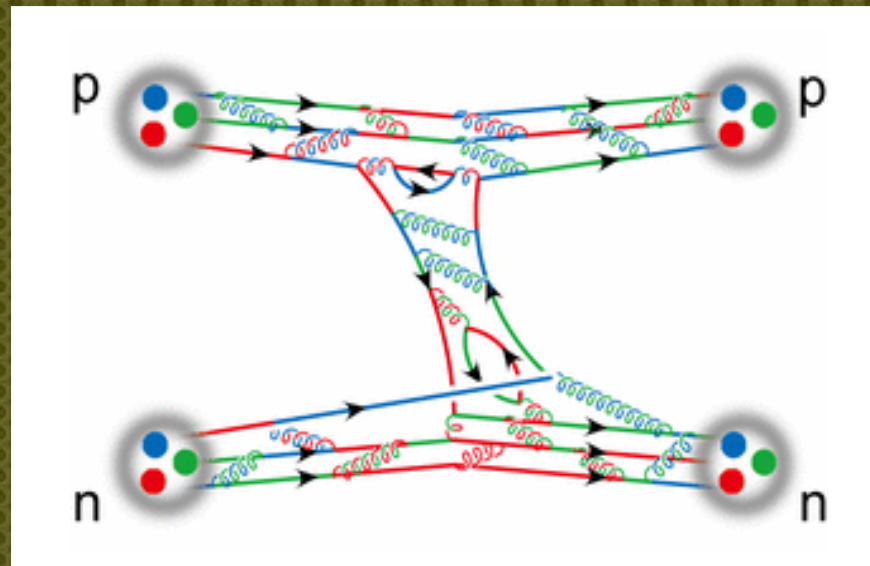
クォーク・グルーオンの力学
摂動論的QCD ← 漸近的自由性



クォーク多体系の世界
非摂動論的QCD



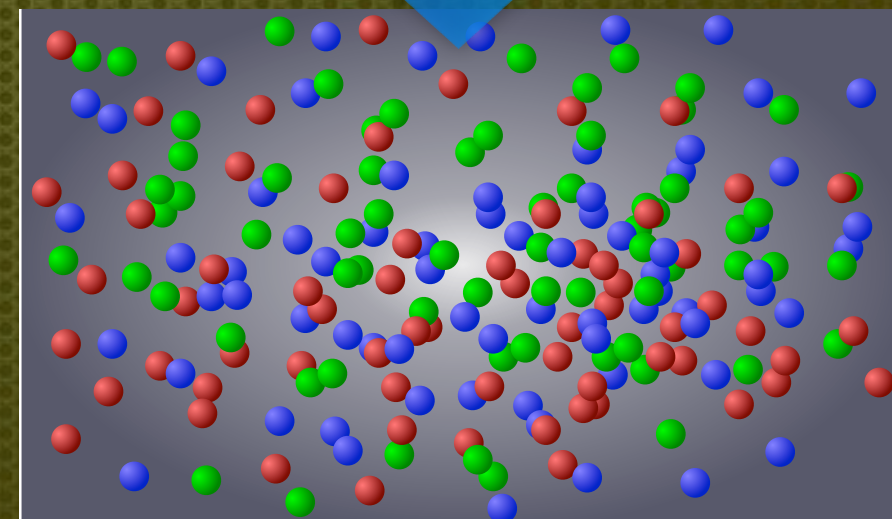
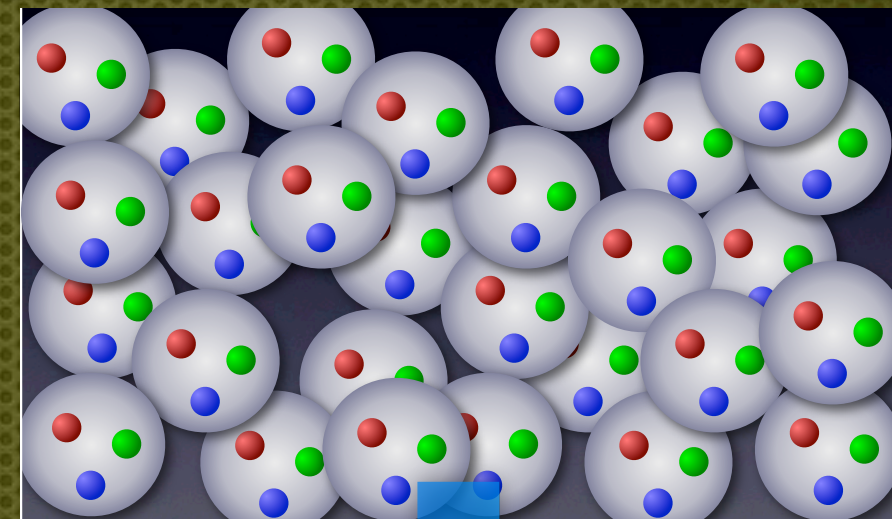
A=1
クォーク閉じ込め



A=2
バリオン間相互作用 (核力)

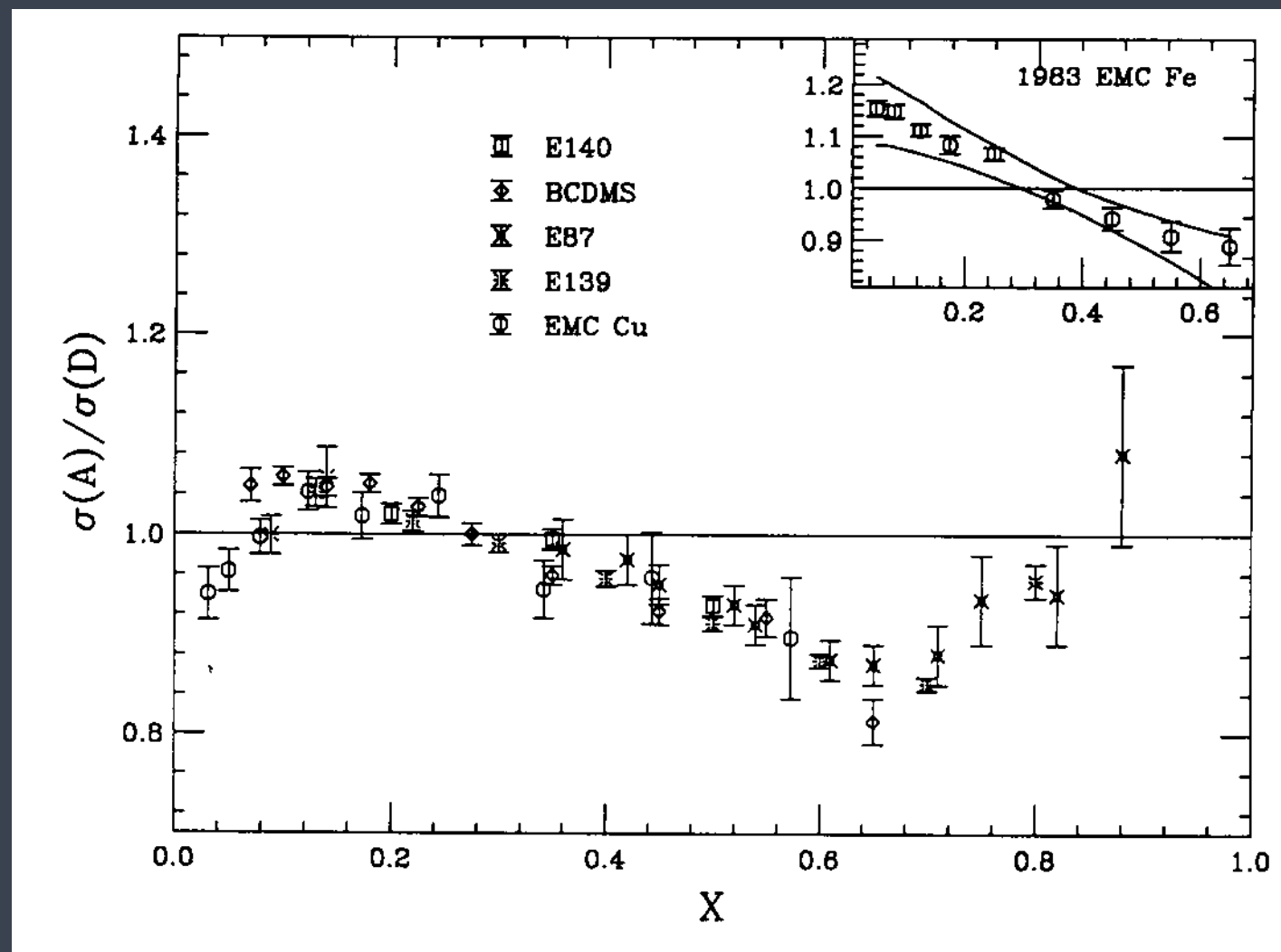
SU(3)_Fへの拡張

A=∞
高密度核物質：QCD相転移



マルチ・ストレンジネスの世界

EMC効果



原子核に束縛された陽子の
運動量分布は真空中と同じか？

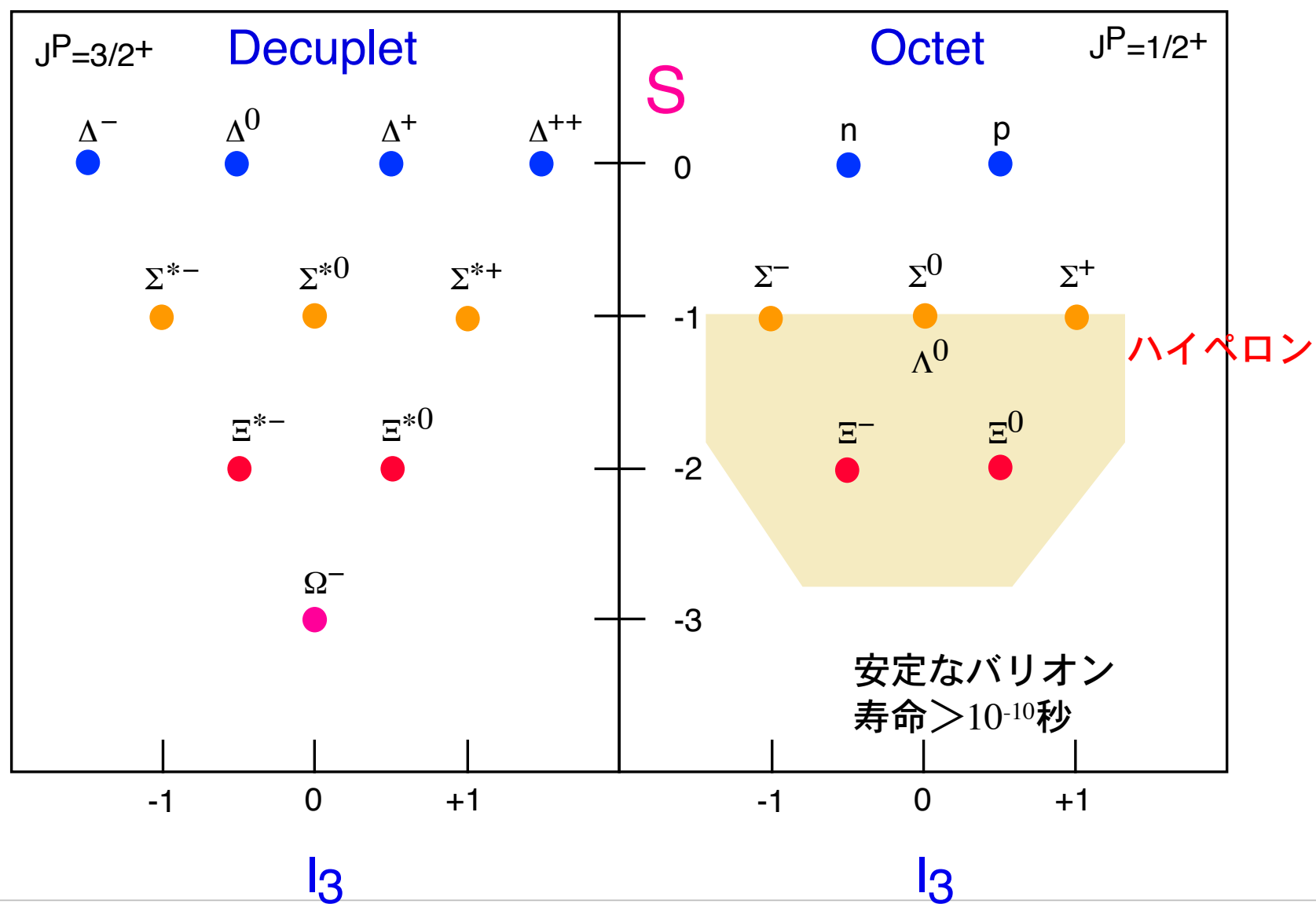
1994年

European Muon Collaboration

ハドロオンと原子核

バリオン族

バリオン多重項



$qqq: 3 \times 3 \times 3 = 10S + 8M + 8M + 1A$

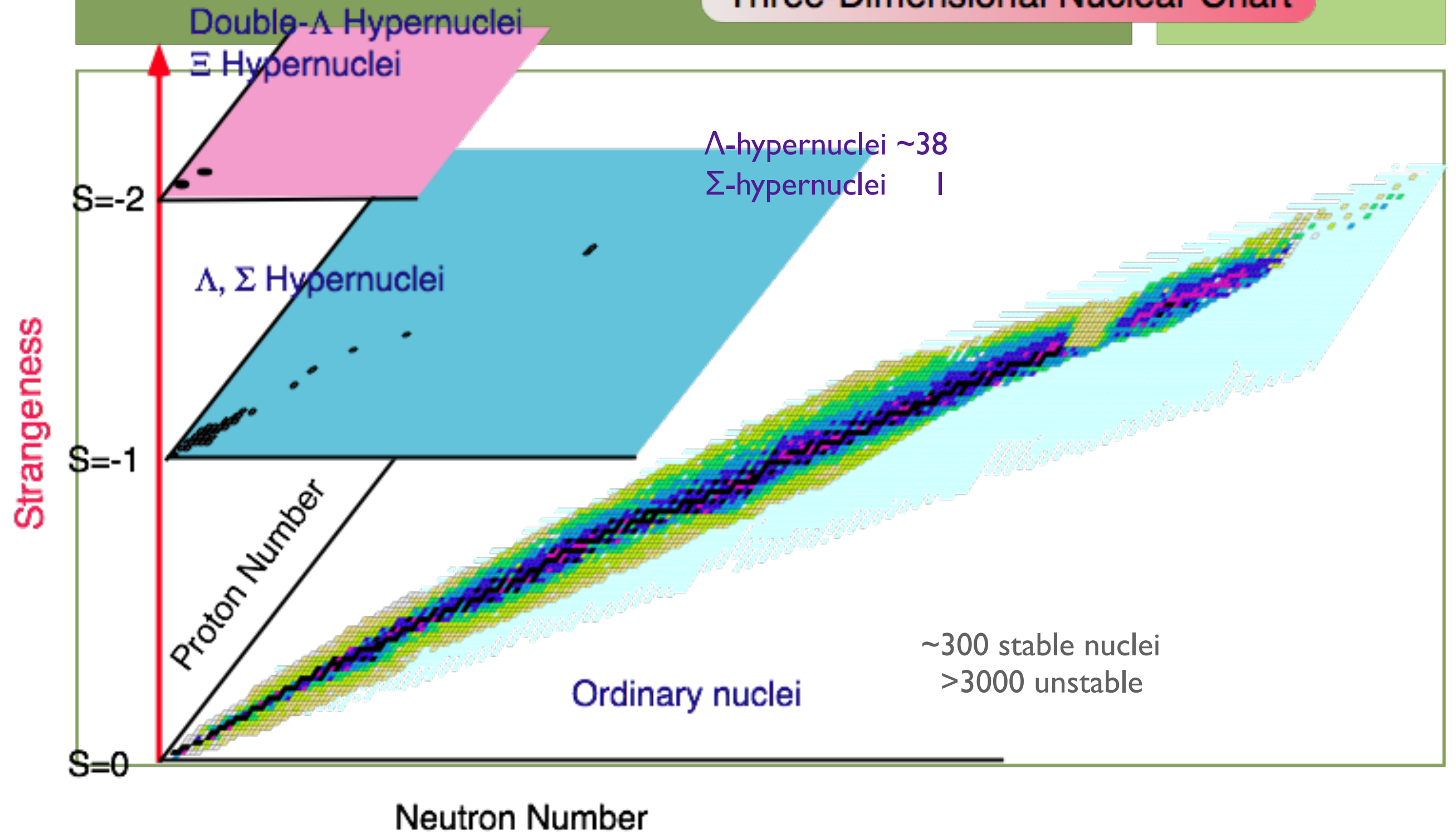
Hypernuclei

► A Nucleus with Hyperons

S		Lifetimes[s]	Main Decay channels	Mass [MeV/c ²]	Isospin
0	p: uud n: udd	Stable(?) 887	p e ⁻ ν _e (100%)	938.3 939.6	1/2
-1	Λ: uds	2.63×10 ⁻¹⁰	p π ⁻ (64%), n π ⁰ (36%)	1115.7	0
-1	Σ ⁺ : uus Σ ⁰ : uds Σ ⁻ : dds	0.8×10 ⁻¹⁰ 7.4×10 ⁻²⁰ 1.48×10 ⁻¹⁰	p π ⁰ (52%), n π ⁻ (48%) Λ γ (~100%) n π ⁻ (99.8%)	1189.4 1192.6 1197.4	1
-2	Ξ ⁰ : uss Ξ ⁻ : dss	2.9×10 ⁻¹⁰ 1.64×10 ⁻¹⁰	Λ π ⁰ (~100%) Λ π ⁻ (~100%)	1315 1321	1/2

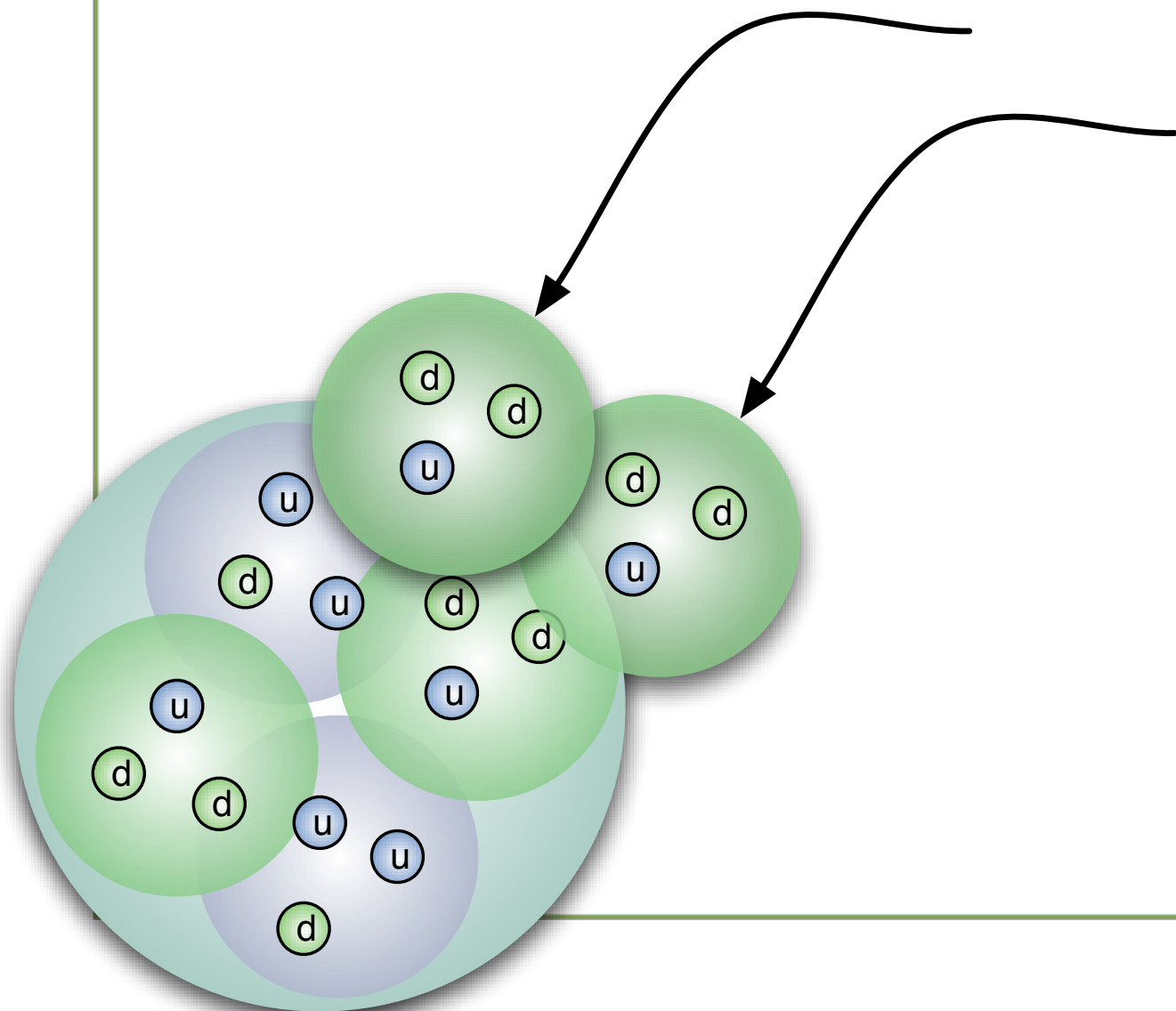
World of Strangeness Nuclear Physics

Three-Dimensional Nuclear Chart



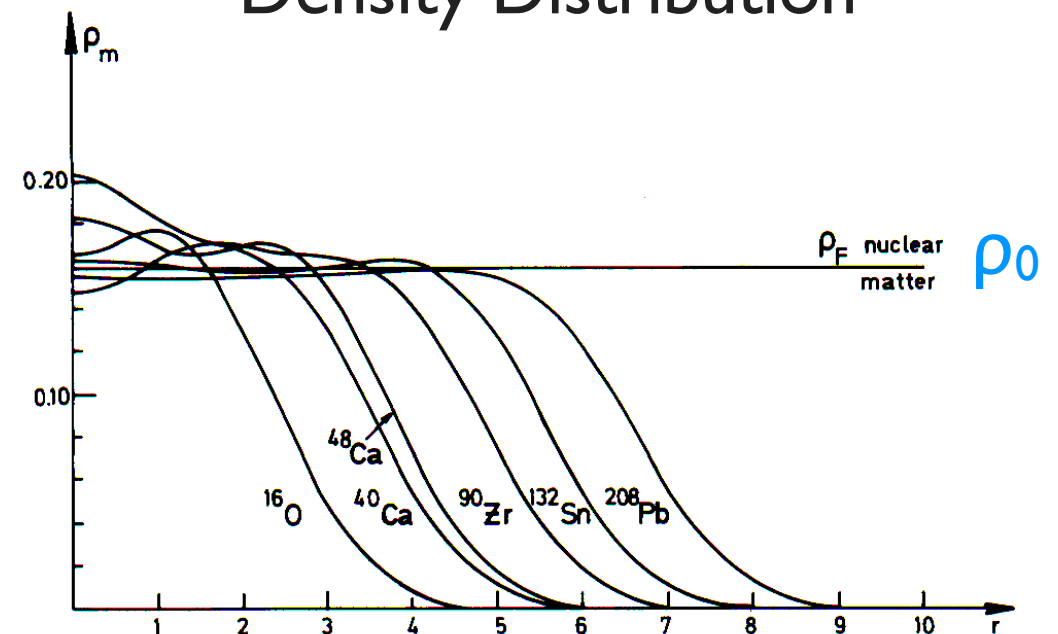
Normal Nuclei

- ▶ Many-Body systems composed of proton(uud)& neutron(udd)
 - ▶ Quark many-body systems with u & d quarks only
- Fermions



Saturation Density: $\rho_0 = 2.5 \times 10^{14} \text{ g/cm}^3$
 Binding Energy: 8 MeV/nucleon
 ← **Pauli Blocking, Repulsive core**

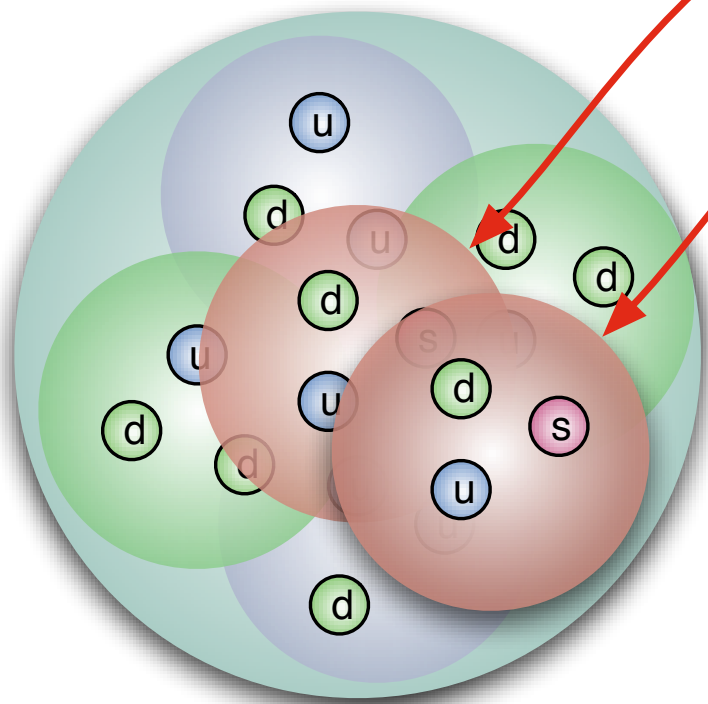
Density Distribution



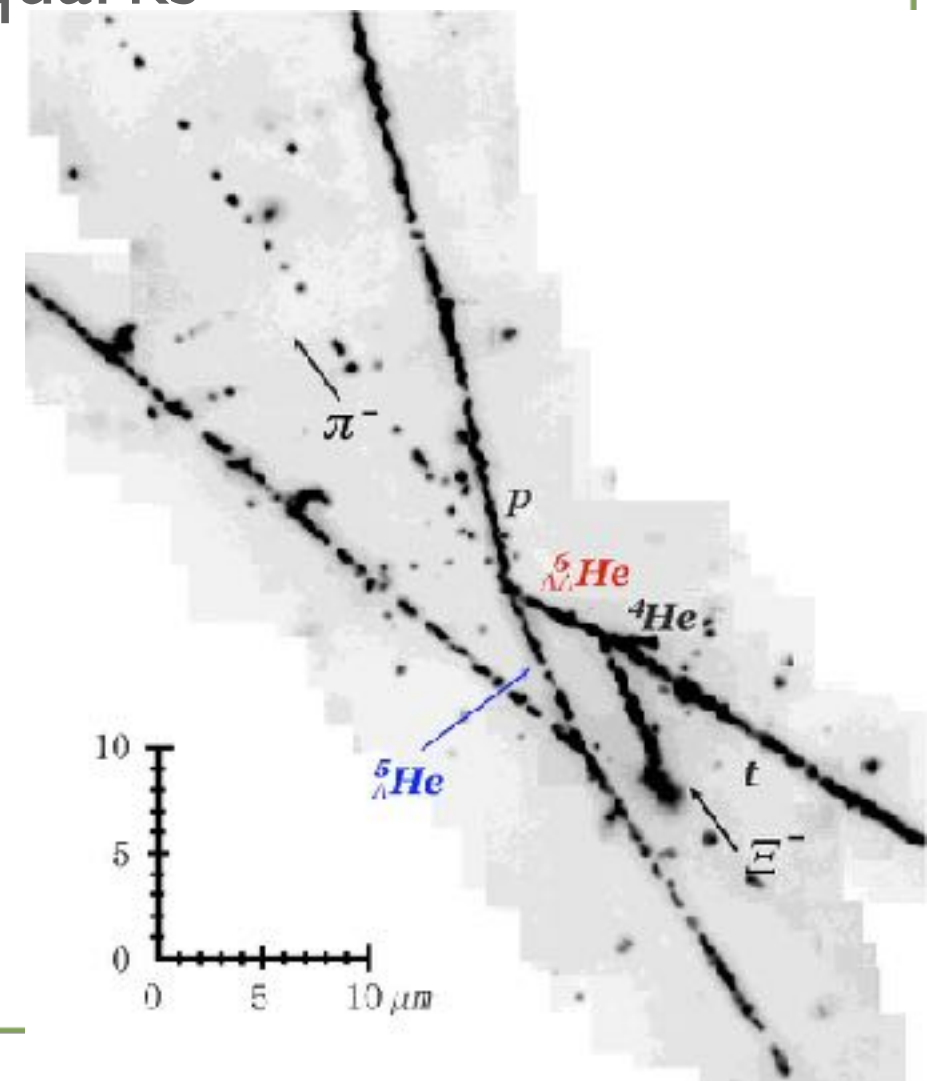
Hypernuclei

- ▶ Λ (uds)-Hypernuclei, Double- Λ Hypernuclei
- ▶ Quark many-body systems with u, d, & s quarks

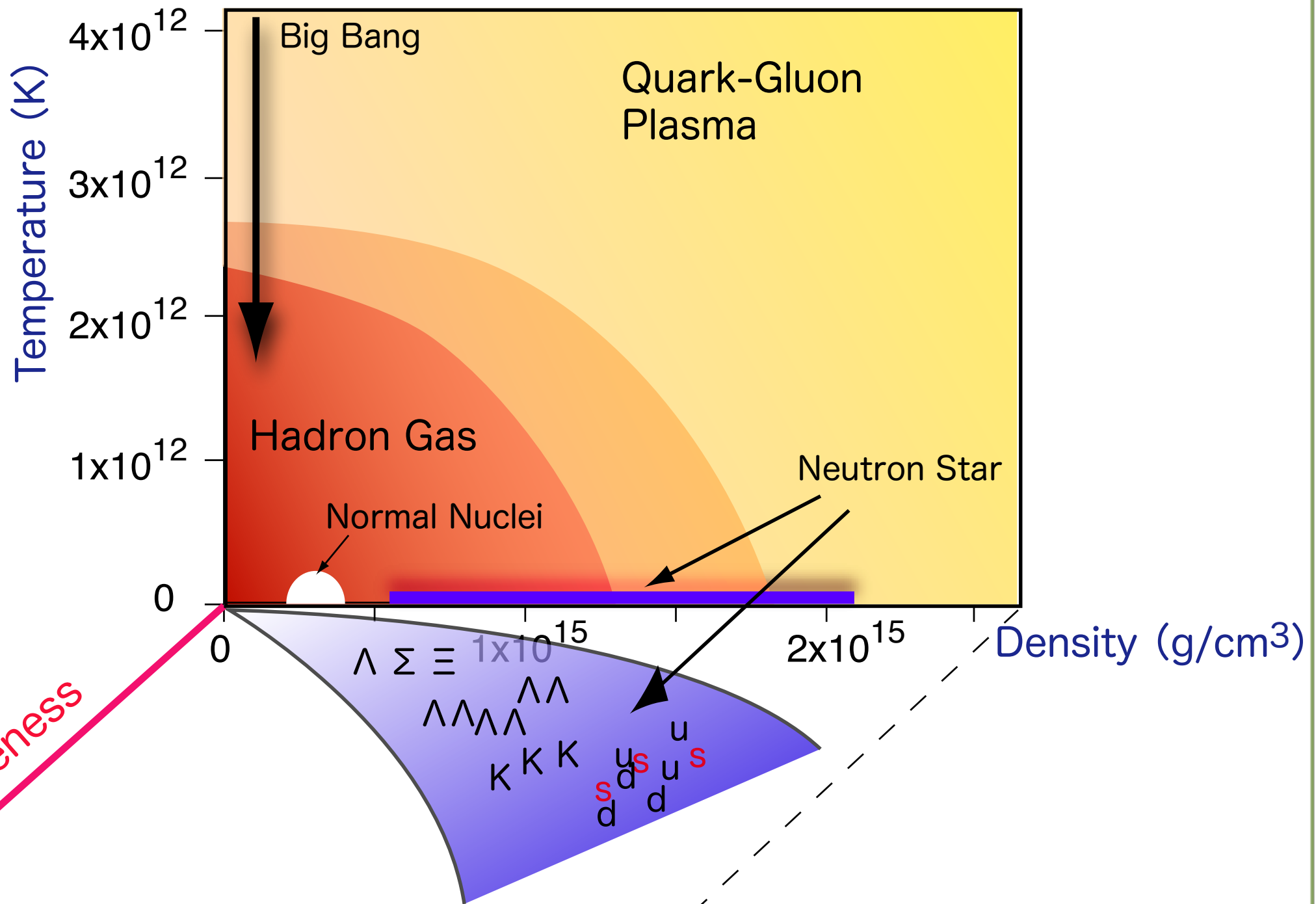
No Pauli Blocking
→ Higher Density



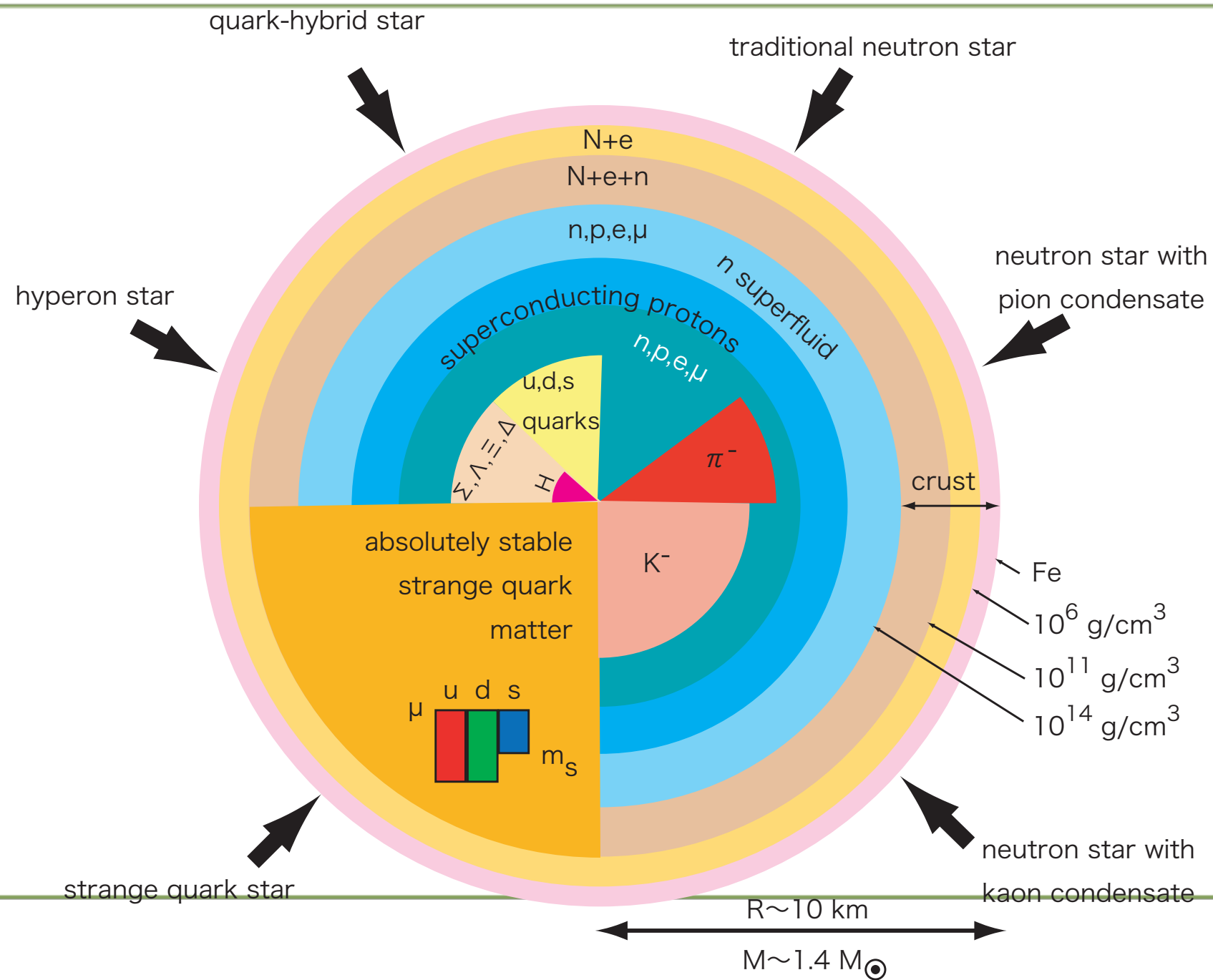
- ▶ Implant s quark(s) with u, d quarks



- ▶ Strangeness Degrees of Freedom
- ▶ Something beyond the “standard” Nuclear Physics



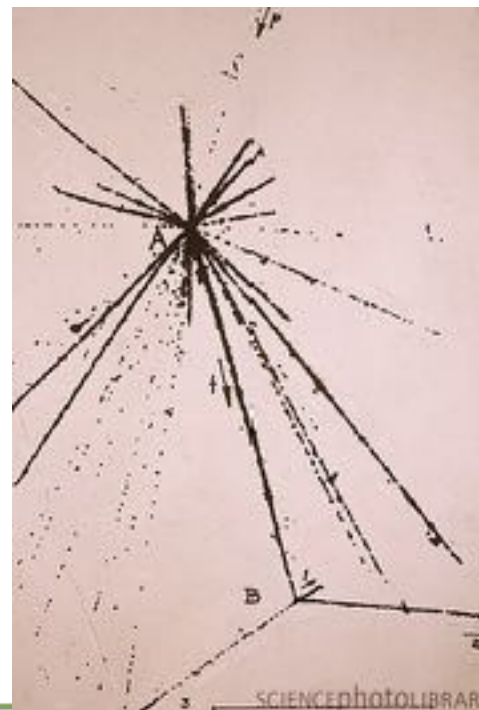
Neutron Star core ?



Brief history of Hypernuclear spectroscopy

- ▶ Discovery of Hyperfragments (1953) by M. Danysz and J. Pniewski
 - $\Lambda \sim p, n$
 - Discovery of V particles (1947) by G. Rochester and C. Butler

*ACTA PHYSICA POLONICA B 35 (2004)
901-927.*



Early days - 1950s~1960s

- ▶ Stopped K^- reactions in Nuclear emulsion and He bubble chamber
 - High efficiency for Hyperfragment formation
 - Identification of Light Hyperfragments
 - ${}^3_{\Lambda}H \sim {}^{15}_{\Lambda}N$
 - Binding energies of ground states
 - Spin assignments for several ground states

Stopped K^- on ${}^4\text{He}$

- ▶ Λ emission $\sim 70\%$
- ▶ Σ emission $\sim 30\%$
- ▶ Non-pionic $\sim 17\%$

TABLE III. Branching ratios for K^- absorption at rest.

Reaction	Events/(stopping K^-) (%)
$K^- \text{He}^4 \rightarrow \Sigma^+ \pi^- \text{H}^3$	9.3 ± 2.3
$\rightarrow \Sigma^+ \pi^- dn$	1.9 ± 0.7
$\rightarrow \Sigma^+ \pi^- pnn$	1.6 ± 0.6
$\rightarrow \Sigma^+ \pi^0 nnn$	3.2 ± 1.0
$\rightarrow \Sigma^+ nnn$	1.0 ± 0.4
Total $\Sigma^+ = (17.0 \pm 2.7)\%$	
$K^- \text{He}^4 \rightarrow \Sigma^- \pi^+ \text{H}^3$	4.2 ± 1.2
$\rightarrow \Sigma^- \pi^+ dn$	1.6 ± 0.6
$\rightarrow \Sigma^- \pi^+ pnn$	1.4 ± 0.5
$\rightarrow \Sigma^- \pi^0 \text{He}^3$	1.0 ± 0.5
$\rightarrow \Sigma^- \pi^0 pd$	1.0 ± 0.5
$\rightarrow \Sigma^- \pi^0 ppn$	1.0 ± 0.4
$\rightarrow \Sigma^- pd$	1.6 ± 0.6
$\rightarrow \Sigma^- ppn$	2.0 ± 0.7
Total $\Sigma^- = (13.8 \pm 1.8)\%$	
$K^- \text{He}^4 \rightarrow \pi^- \Lambda \text{He}^3$	11.2 ± 2.7
$\rightarrow \pi^- \Lambda pd$	10.9 ± 2.6
$\rightarrow \pi^- \Lambda ppn$	9.5 ± 2.4
$\rightarrow \pi^- \Sigma^0 \text{He}^3$	0.9 ± 0.6
$\rightarrow \pi^- \Sigma^0 (pd, ppn)$	0.3 ± 0.3
$\rightarrow \pi^0 \Lambda (\Sigma^0) (pnn)$	22.5 ± 4.2
$\rightarrow \Lambda (\Sigma^0) (pnn)$	11.7 ± 2.4
$\rightarrow \pi^+ \Lambda (\Sigma^0) nnn$	2.1 ± 0.7
Total $\Lambda (\Sigma^0) = (69.2 \pm 6.6)\%$	
Total $= \Lambda + \Sigma = (100_{-7}^{+0})\%$	

Hypernuclear Production by stopped K^-

- ▶ $\sim 10^{-3}$ per stopped K^- ; ... not so bad

TABLE IX. Calculated capture rates per stopped K^- (in units of 10^{-3}) for production of $1s_\Lambda$ states (1^- transition) and $1p_\Lambda$ states (0^+ and 2^+ transitions) and selected experimental rates.

Transition	Input	$^{12}_\Lambda\text{B}$ [3]	$^{12}_\Lambda\text{C}$ [2]	$^{16}_\Lambda\text{O}$ [2]
1^-	$[K_\chi]$	0.203	0.425	0.219
	$[K_{\text{DD}}]$	0.060	0.125	0.055
	Experimental rates	0.28 ± 0.08	0.98 ± 0.12	0.43 ± 0.06
0^+	$[K_\chi]$	0.096	0.216	0.134
	$[K_{\text{DD}}]$	0.011	0.021	0.020
2^+	$[K_\chi]$	0.547	1.052	0.872
	$[K_{\text{DD}}]$	0.192	0.410	0.330
$0^+ + 2^+$	$[K_\chi]$	0.643	1.268	1.006
	$[K_{\text{DD}}]$	0.203	0.431	0.350
	Experimental rates	0.35 ± 0.09	2.3 ± 0.3	1.68 ± 0.16

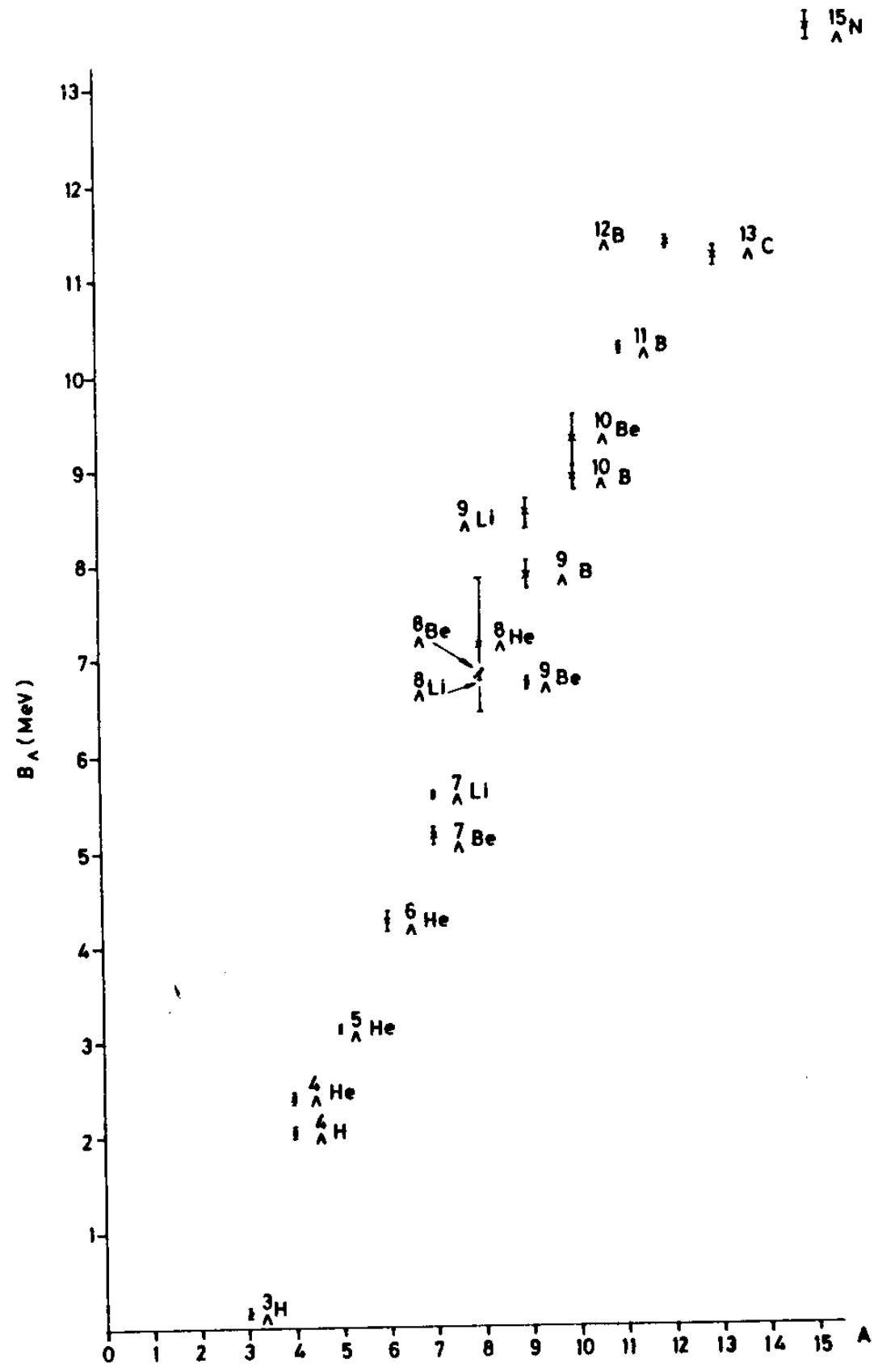
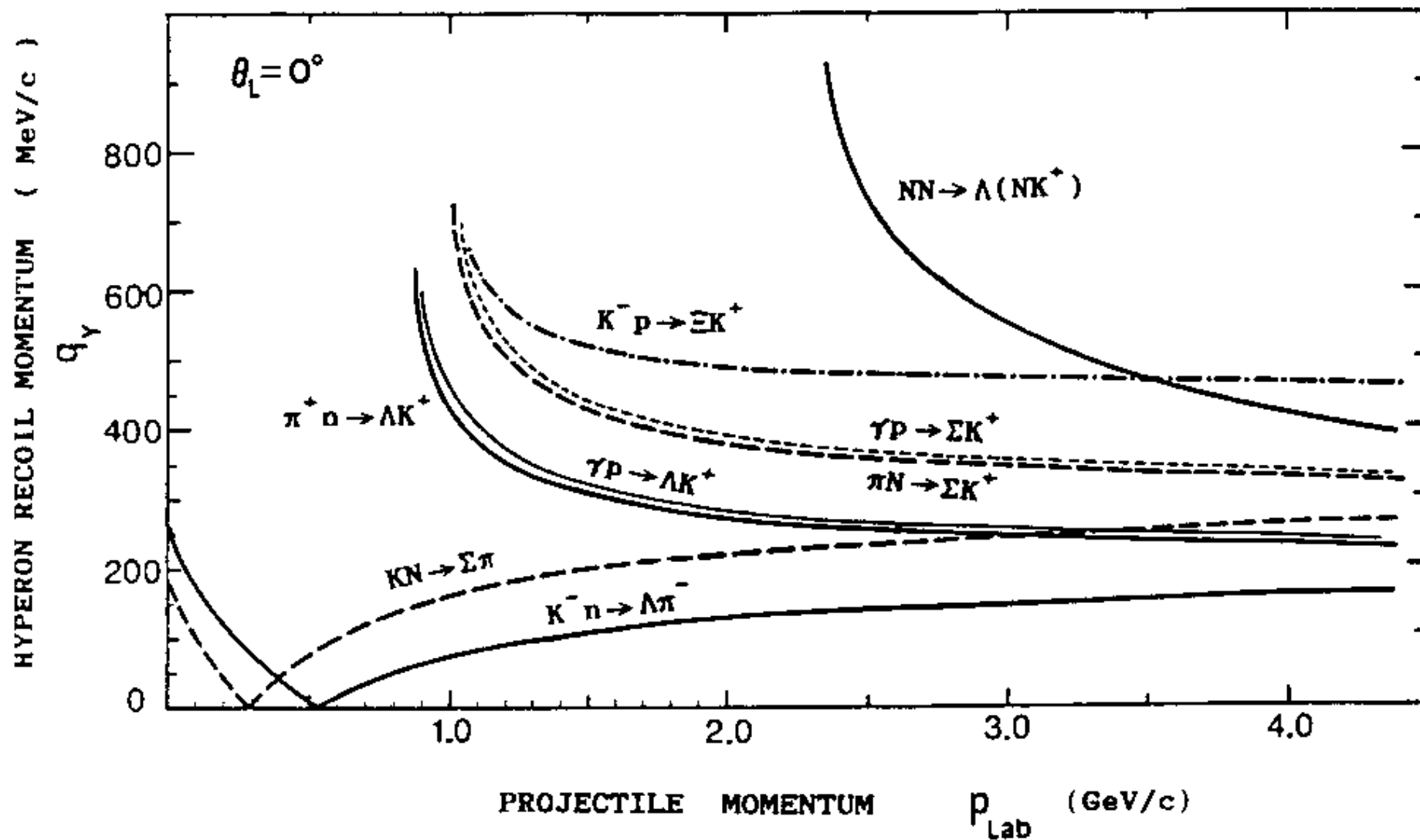


Fig. 10. Variation of the B_Λ values with the hypernuclear mass numbers.

In-flight (K^- , π^-) in 1970s

- ▶ Heidelberg-Saclay group
- ▶ “Magic momentum” - Recoilless condition
 - Population of Substitutional States: (p_n^{-1}, p_Λ)
 - Spectroscopic information on **Excited states**
 - Small Spin-Orbit splitting in Λ hypernuclei

Recoil Momentum of Hyperon



Data in the (K^-, π^-) reactions

► ${}^{16}_{\Lambda}\text{O}$

● $\delta_p = 0.8 \pm 0.7 \text{ MeV} \rightarrow V_{LS} = 4 \pm 2 \text{ MeV}$

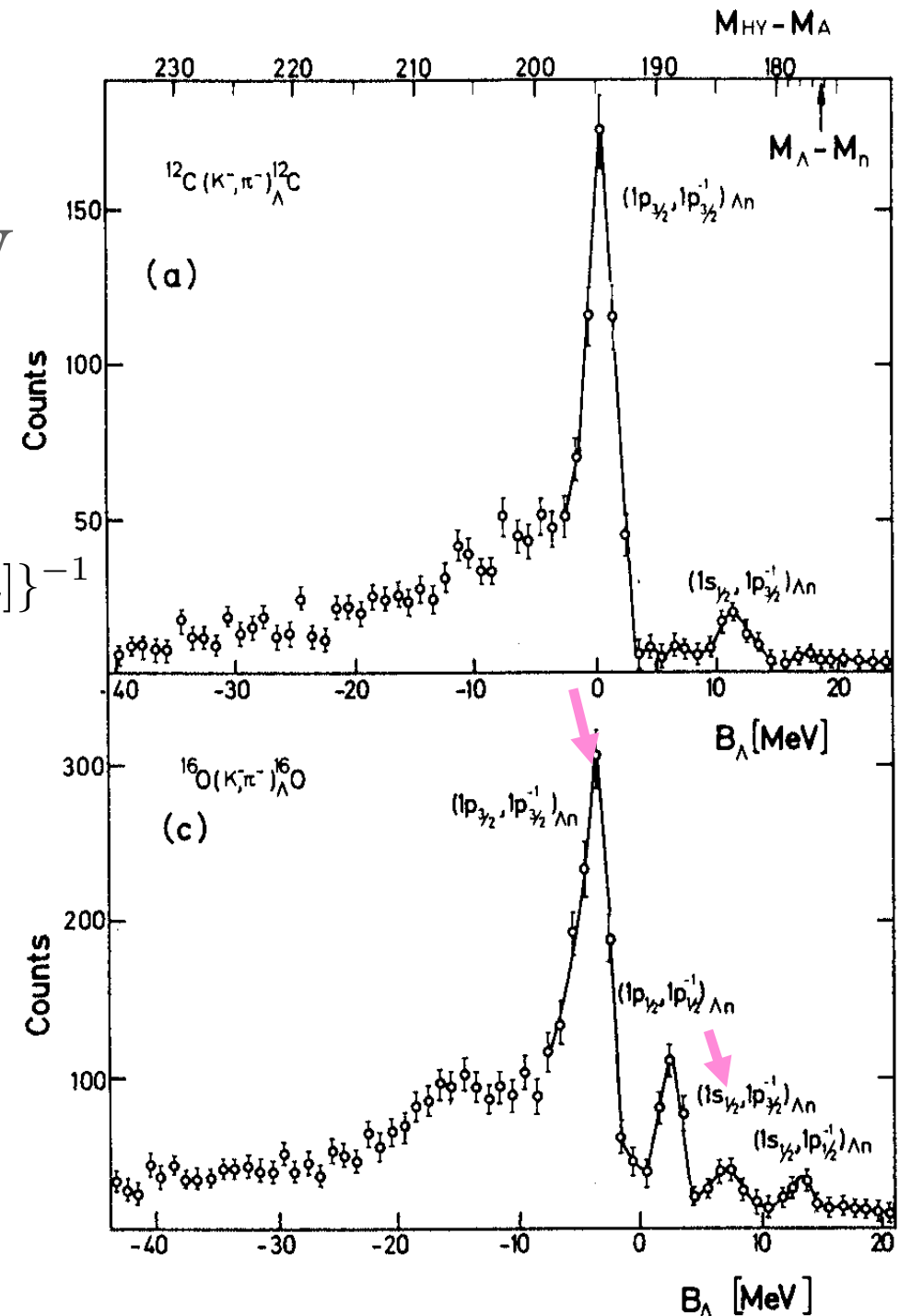
● $V_0 = 30 \text{ MeV}$

$$U_{\Lambda} = V_0^{\Lambda} f(r) + V_{LS}^{\Lambda} \left(\frac{\hbar}{m_{\pi} c} \right)^2 \frac{df(r)}{r dr} \vec{\ell} \cdot \vec{s}, \quad f(r) = \{1 + \exp[(r - R)/a]\}^{-1}$$



For ordinary nuclei:

$$V_0 \sim 50 \text{ MeV}, V_{LS} = 20 \text{ MeV}$$

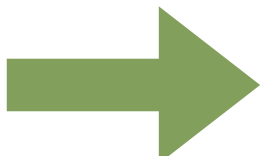


BNL-AGS & KEK-PS in 1980s ~

1990s

- ▶ Σ hypernuclei in (K^-, π^-)
 - narrow states \rightarrow not reconfirmed
 - one bound state ${}^4_{\Sigma}\text{He} \rightarrow$ confirmed
- ▶ Success of (π^+, K^+) Spectroscopy
- ▶ Success of Hypernuclear γ Spectroscopy
- ▶ H-particle search, Double- Λ hypernuclei

in the 21st century

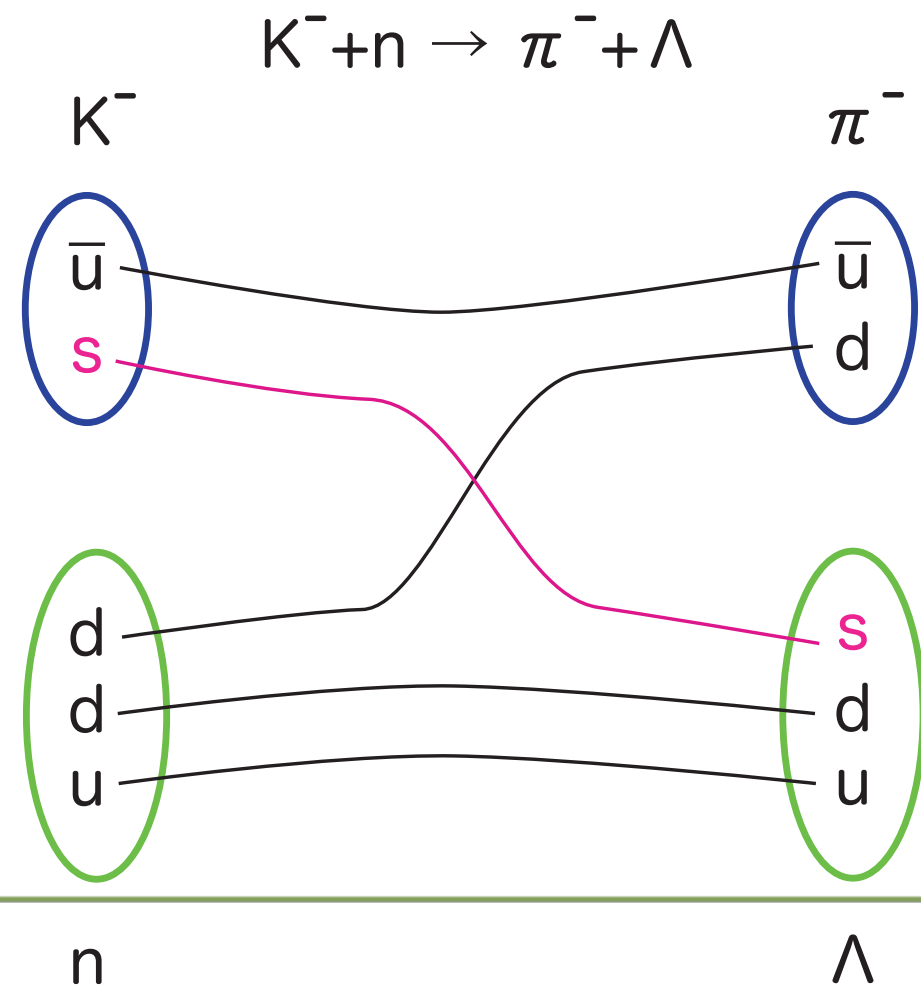
- ▶ $(e, e'K^+)$ at JLab
 - $\Delta E \sim 0.9 \text{ MeV}$  0.3 MeV
- ▶ $(K^-_{\text{stop}}, \pi^-)$ at DAFNE/FINUDA
 - $\Delta E \sim 0.7 \text{ MeV}$
- ▶ J-PARC, GSI, Mainz, ...

ハイパー核 の作り方

How to produce hypernuclei ?

► Strangeness exchange reactions: (K^- , π^-)

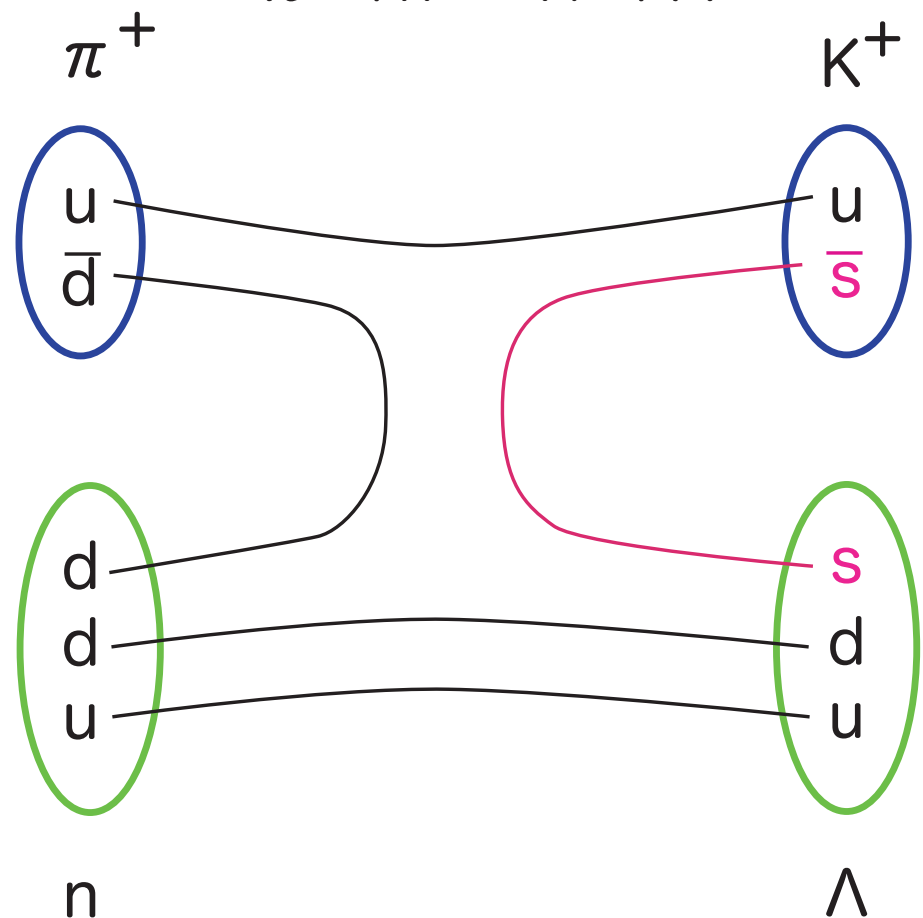
- Large cross section \sim mb/sr at 0 deg.
- K^- intensity limited



► Associated production: (π^+, K^+) , $(e, e'K^+)$

• Smaller cross sections: $\sim 10\mu\text{b}/\text{sr}$, $\sim 1\text{nb}/\text{sr}$

• High intensity beams: $> 10^6 \pi^+$, $> 10^{13} e^-$



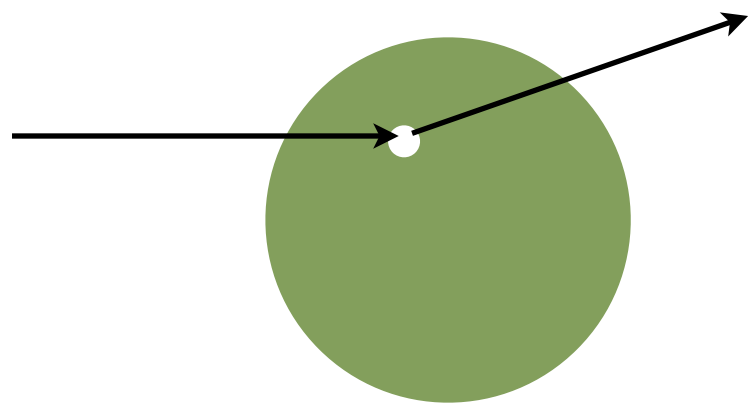
生成反応とその収量

	(K ⁻ ,π ⁻)	(π ⁺ ,K ⁺)	(e,e'K ⁺)
p _{BEAM} (GeV/c)	~0.7	1.05	1.8
dσ/dΩ(μb/sr)	1000	10	10 ⁻³
I _{BEAM} (s ⁻¹)	10 ⁺⁵	10 ⁺⁶	>10 ⁺¹³
ΔΩ (msr)	20	100	20
n _x (g/cm ²)	3	3	0.1
ΔE (MeV)	3	2	0.2
Relative Yield	2	1	>3

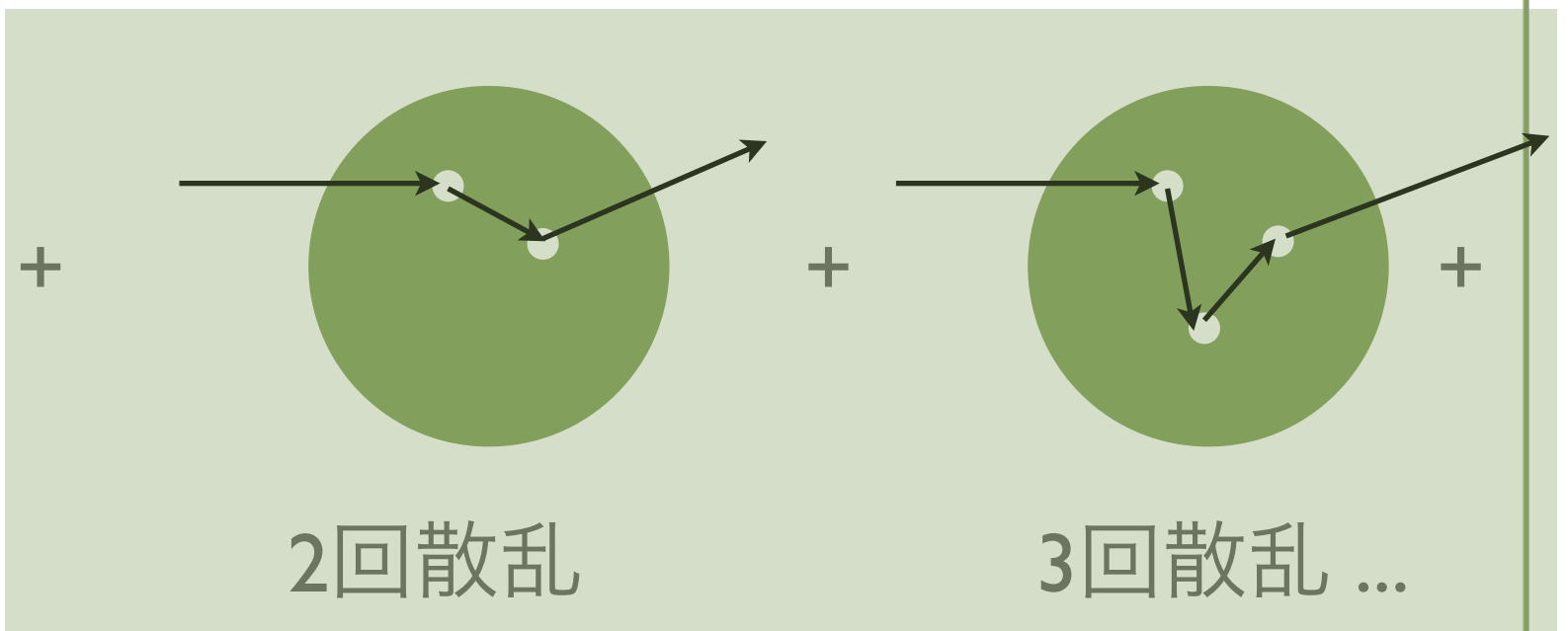
反応機構

- ▶ DWIA (Distorted Wave Impulse Approximation)

- ▶ Impulse Approx. : $p_{\text{inc}} \rightarrow \text{high}$, $\lambda = h/p \rightarrow \text{small} \ll 1 \text{ fm}$



1回散乱



2回散乱

3回散乱 ...

- ▶ 核内での遷移振幅 ~ 自由散乱の遷移振幅

▶ 1 + “2” → 3 + “4”

$$\left(\frac{d^2 \sigma_{fi}}{d\Omega_3 dE_3} \right)_{lab} = \frac{p_3 E_3}{(2\pi)^2 v_1} |T_{fi}|^2 \delta(\omega - E_1 + E_3)$$

$$T_{fi} = \langle \chi_3^{(-)} | \langle f | \sum_j t_j | i \rangle | \chi_1^{(+)} \rangle$$

▶ t_j : 素過程反應

▶ $\chi_3^{(-)}$, $\chi_1^{(+)}$: 平面波(PWIA)、 or 歪曲波(DWIA)

Distorted Wave

- ▶ Eikonal Approximation: $E \gg U, \rho R \gg 1$

$$\chi^{(+)}(b, z) = e^{ipz} \phi(b, z)$$

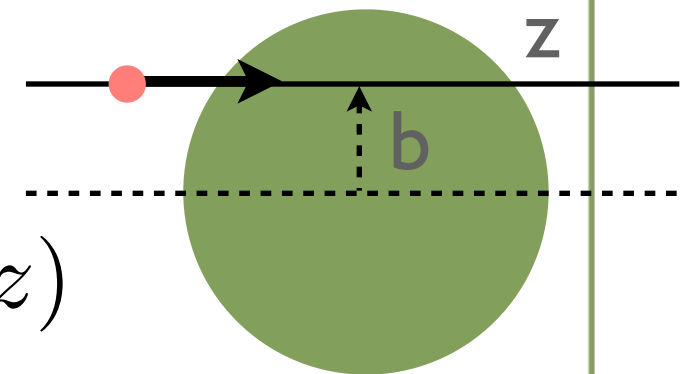
$$[-\nabla^2 + \mu^2 - \omega^2] \chi^{(+)}(b, z) = -2\omega U \chi^{(+)}(b, z)$$

$$\phi = \exp\left\{-i v^{-1} \int_{-\infty}^z U(b, z') dz'\right\}$$

$$2\omega U(b, z) = p\sigma^{tot} \rho(b, z)$$

$$\chi_3^{(-)*}(\mathbf{r}) \chi_1^{(+)}(\mathbf{r}) = \exp\left\{i\mathbf{q} \cdot \mathbf{r} - \frac{1}{2} \sigma_{eff} \int_{-\infty}^{\infty} \rho(b, z') dz'\right\}$$

Mean free path = $1/\rho\sigma = 1/(4 \text{ fm}^2)(0.15 \text{ fm}^{-3}) = 1.6 \text{ fm}$, $\sigma = 40 \text{ mb}$



→核表面での反応が支配的

Effective nucleon number

- ▶ 素過程($1+2 \rightarrow 3+4$)での微分断面積を使う

$$\left(\frac{d^2 \sigma_{fi}}{d\Omega_3 dE_3} \right)_{lab} = \beta \left(\frac{d\sigma}{d\Omega_3} \right)_{lab} N_{eff}(\theta_{lab}; i \rightarrow f) \delta(\omega + E_3 - E_1)$$

$$\beta = \left(1 + \frac{E_3^{(0)} p_3^{(0)} - p_1 \cos \theta_{lab}}{E_4^{(0)} p_3^{(0)}} \right) \frac{p_3 E_3}{p_3^{(0)} E_3^{(0)}}$$

2体系((0))から多体系への運動学因子

Spectroscopic Information

- ▶ Mass → Binding Energy
 - ▶ Missing Mass measurement in in-flight reactions
 - ▶ Weak decays of Hyperfragments
- ▶ Spin Assignment
 - ▶ Weak Decay
 - ▶ Gamma Decay

$^{208}\text{Pb}(e,e'p)$

- ▶ $zA_N(e,e'p) z-1A'_N$: nucleon hole state
- ▶ Deep Hole States \rightarrow Large Spreading Width $>$ a few MeV

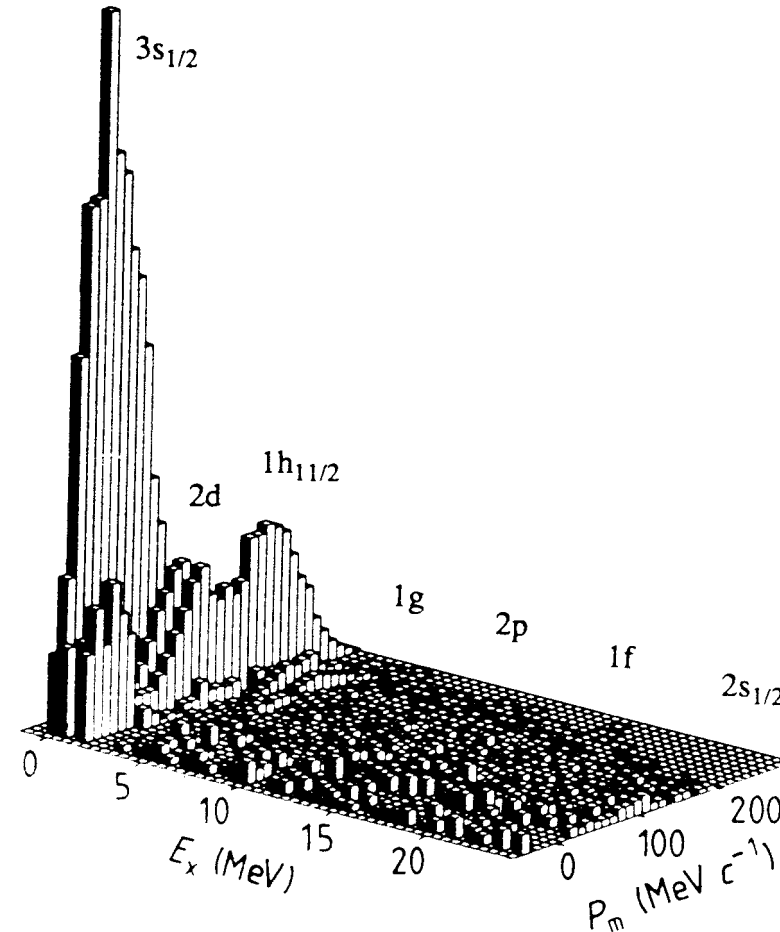
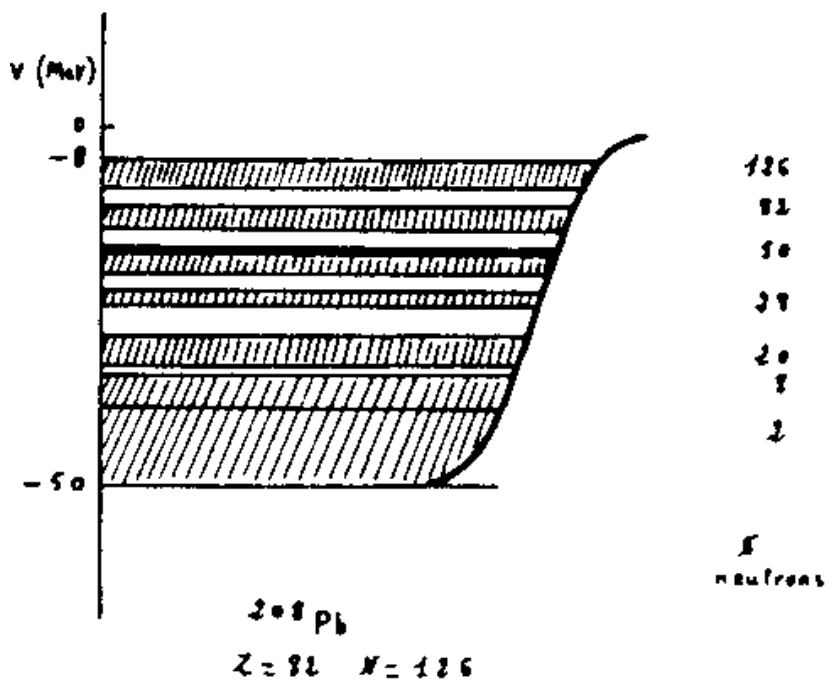


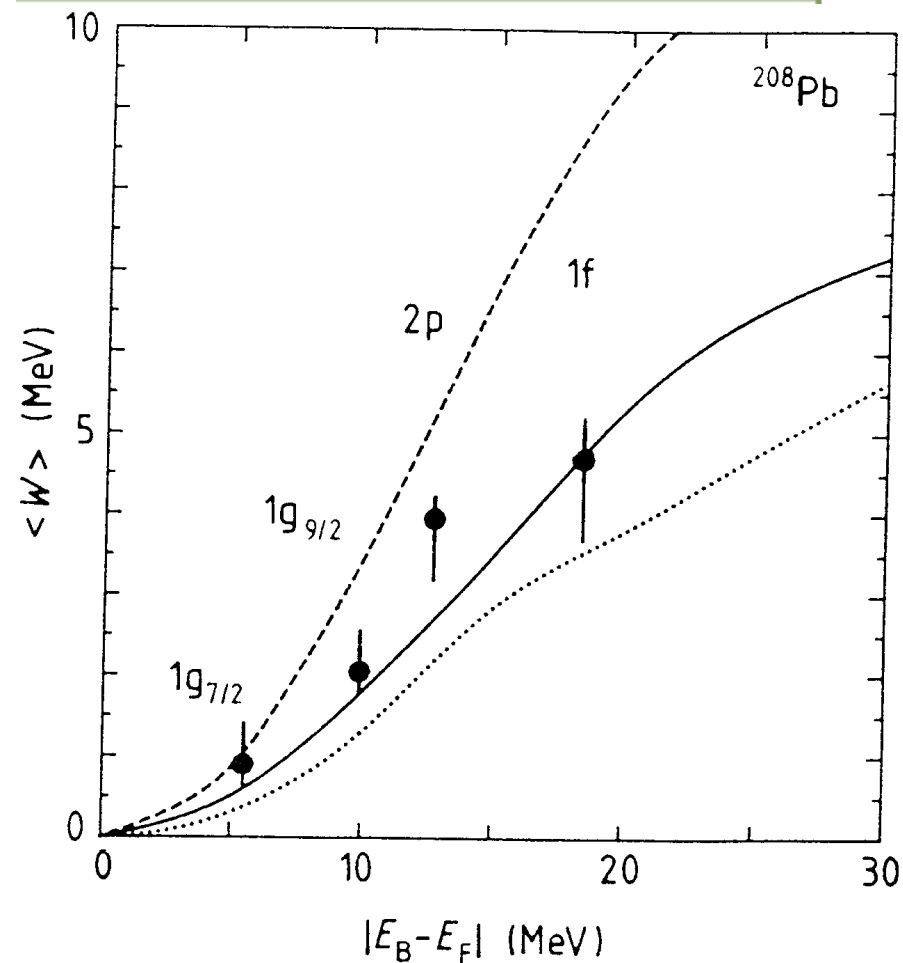
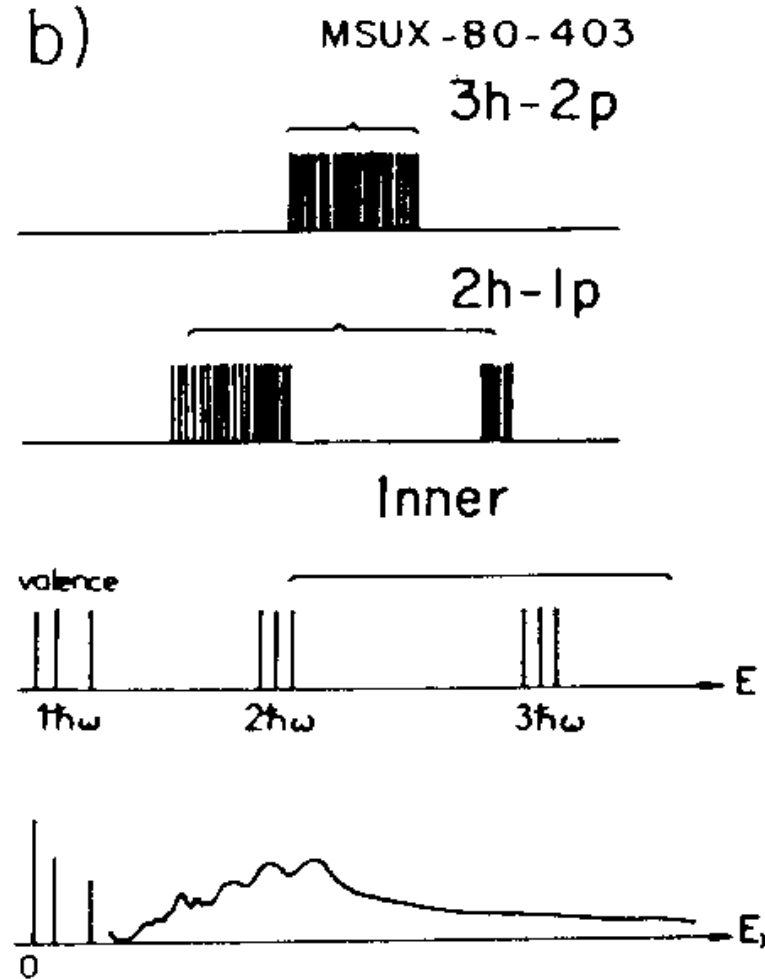
Figure 32. Experi
 $^{208}\text{Pb}(e,e'p)^{207}\text{Tl}$.



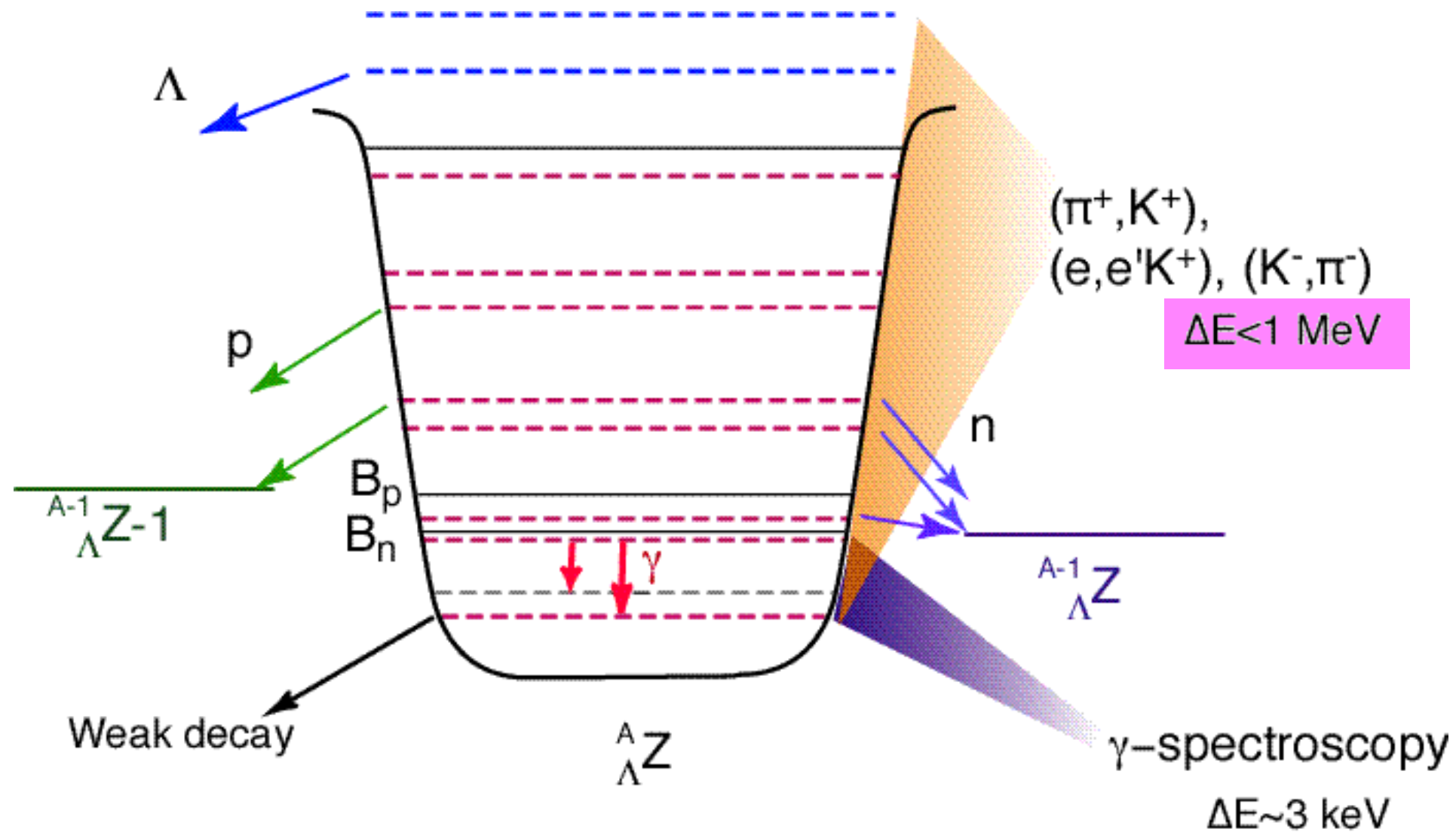
a)



b)



Excited levels of Λ -hypernuclei



Monochromatic Peak

► Mesonic decay of Hyperfragments

► ${}^4_{\Lambda}\text{H}$

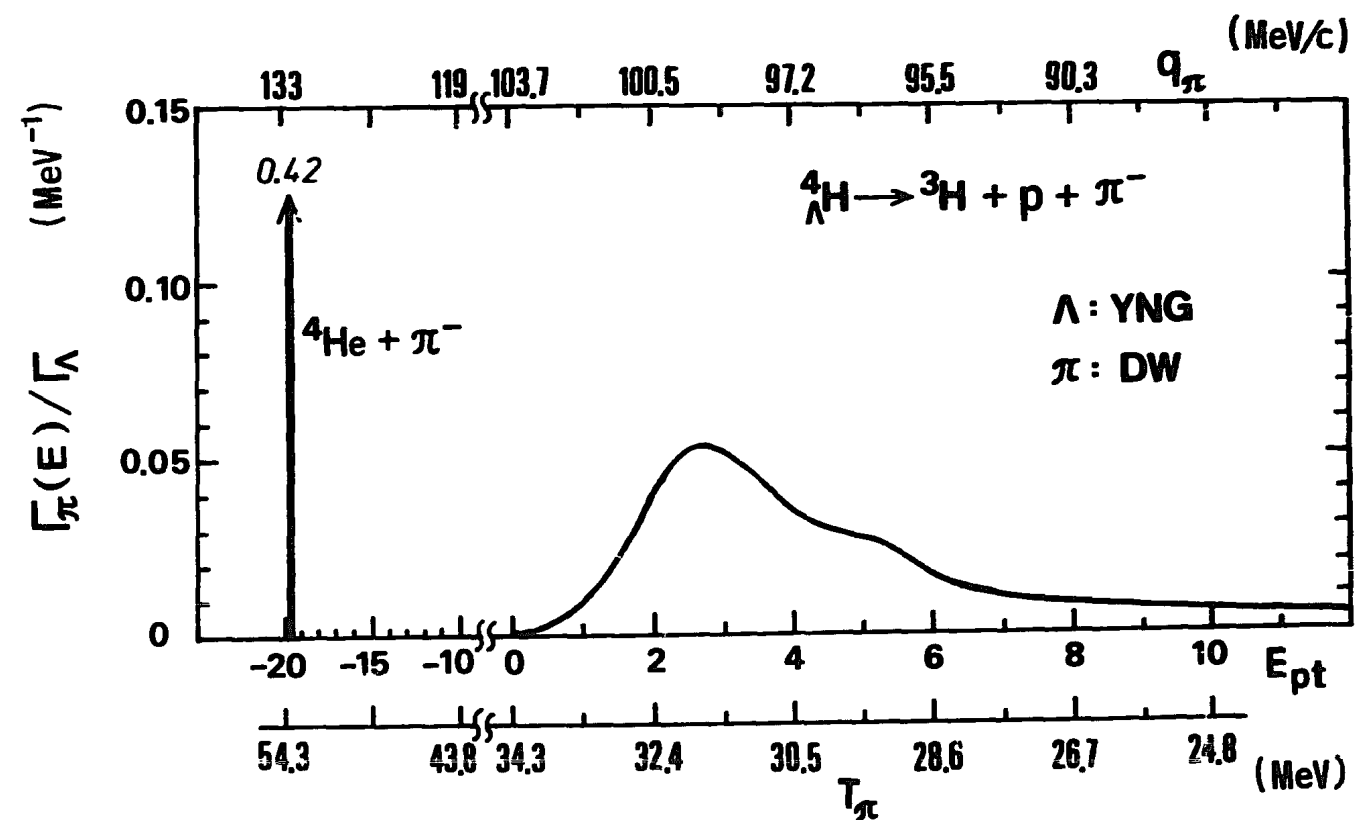


Fig. 9. The theoretical π^{-} decay spectrum $\Gamma_{\pi^{-}}({}^4_{\Lambda}\text{H})/\Gamma_{\Lambda}$ as a function of the proton- ${}^3\text{H}$ relative energy E_{pt} .

Quasi-monochromatic

- ${}^5_{\Lambda}\text{He} \rightarrow \pi^- + p + {}^4\text{He}$; $p_{\pi} = 99.9 \text{ MeV}/c$, $\Delta p \sim 1.4 \text{ MeV}/c$

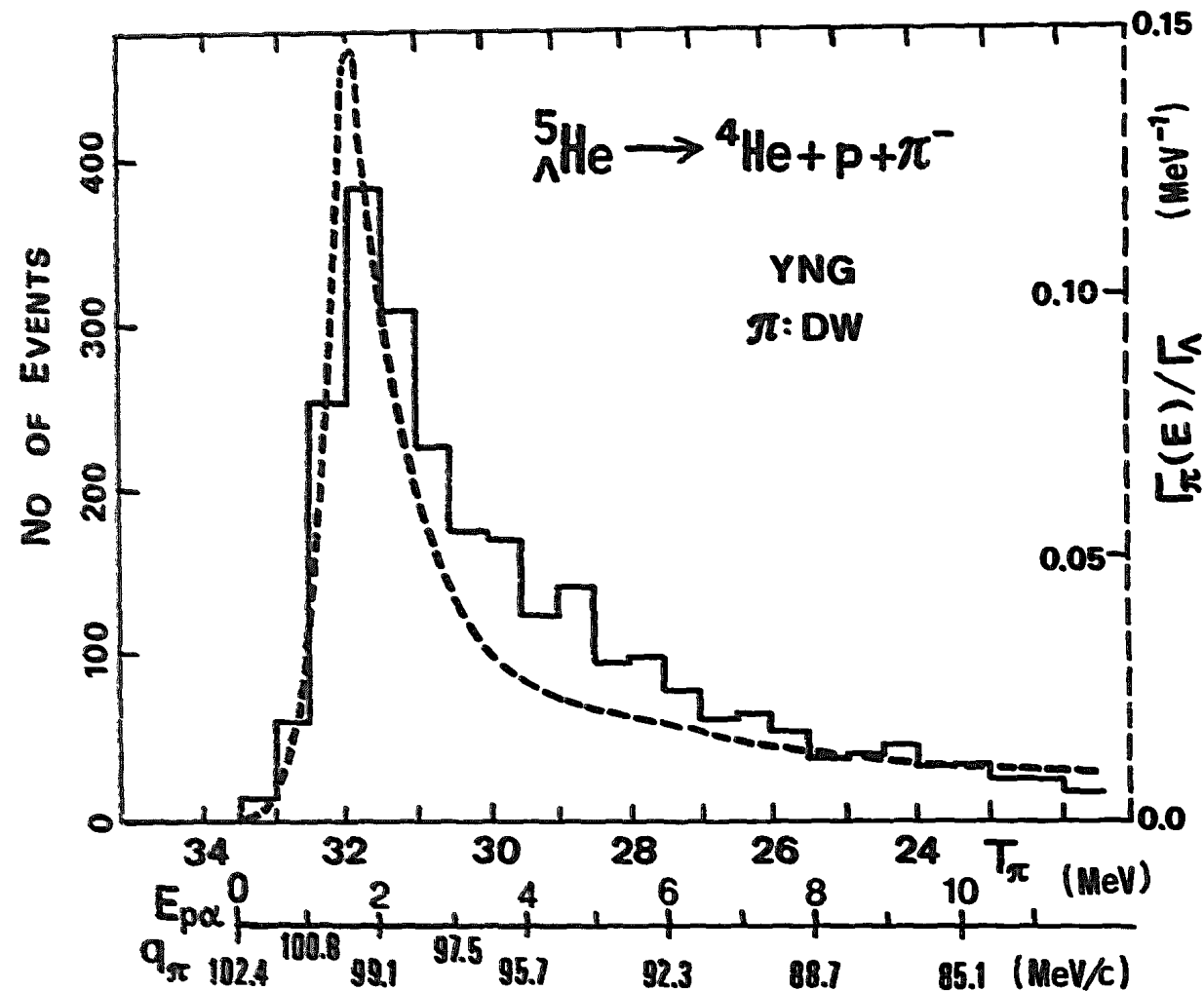


Fig. 4. The theoretical π^- decay spectrum $\Gamma_{\pi^-}({}^5_{\Lambda}\text{He})/\Gamma_1$ with YNG drawn as a function of the $p\alpha$ relative energy $E_{p\alpha}$ is compared with the observed π^- decay spectrum taken in the emulsion experiment^{18,33}). The calculated π^- decay rate is compared with the experimental values^{12,20}) in table 1 and fig. 5.

Mesonic Decay Rate

- $\Gamma_{\pi}/\Gamma_{\Lambda} \sim 0.4 - 0.6$ for light fragments

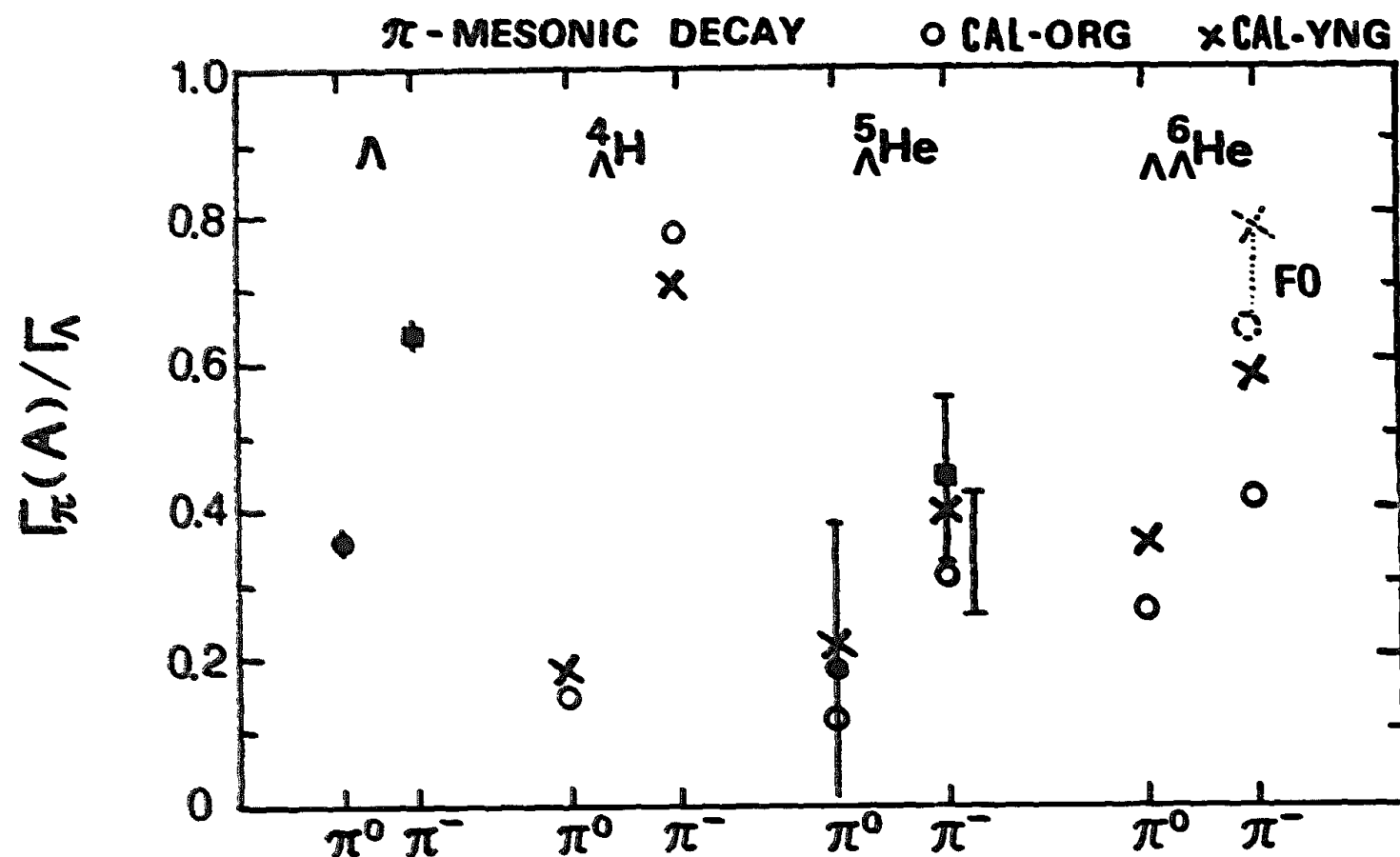
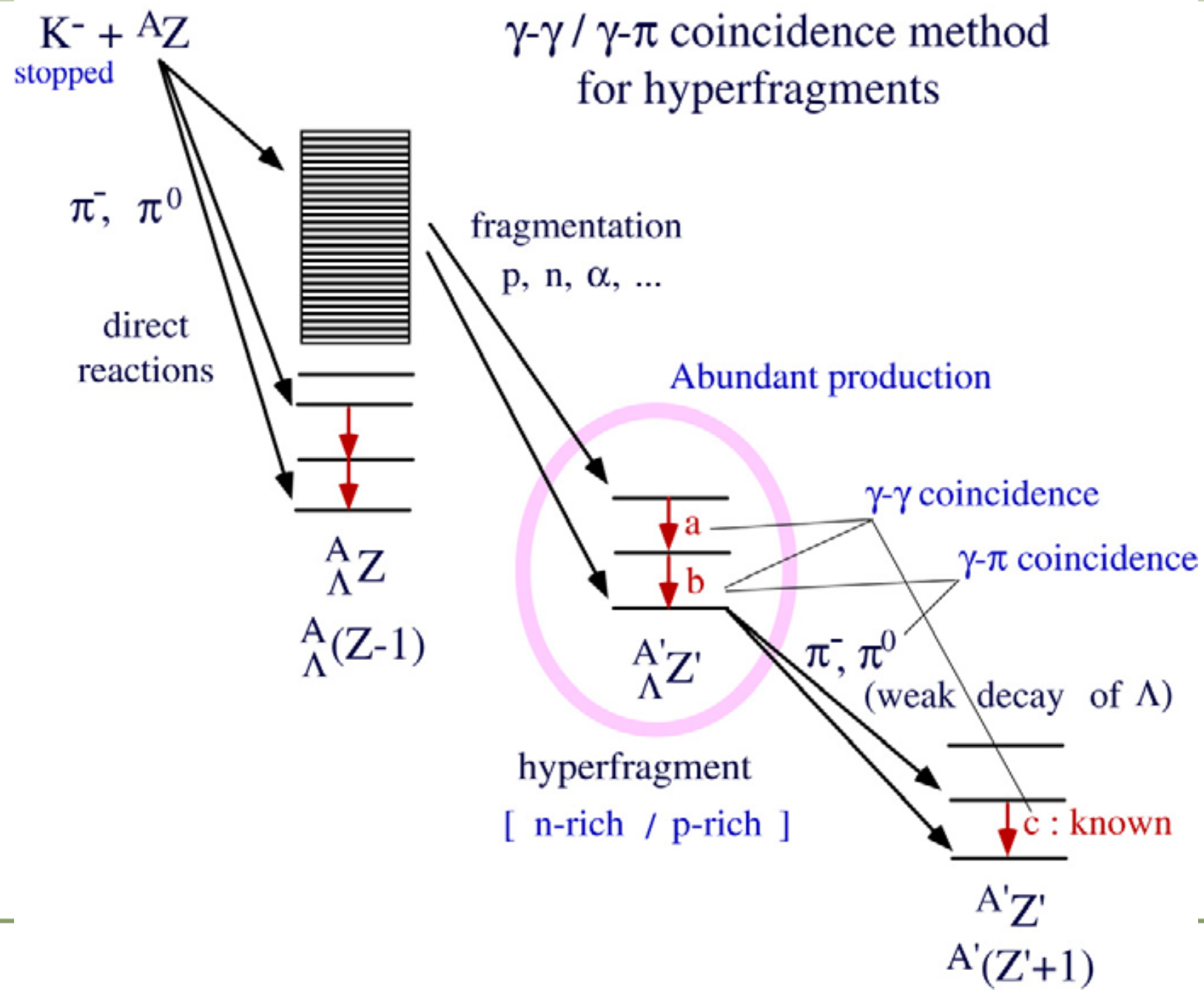
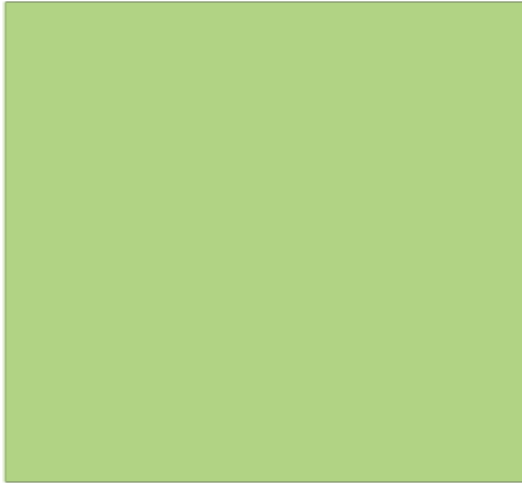


Fig. 5. Summary of the theoretical π -decay rates in units of Γ_{Λ} . The open circle and the cross correspond to ORG and YNG, respectively. The π^- decay rates of ${}^6_{\Lambda\Lambda}\text{He}$ in the case of the F0 .1.1 interaction are also shown. The experimental values for ${}^5_{\Lambda}\text{He}$ are taken from refs. ^{12,20}).

γ -ray spectroscopy





- ▶ Charged-particle Spectroscopy

- ▶ magnetic spectrometer: $\Delta p/p > 10^{-4}$

- ▶ $\Delta E = 0.3 \sim 2 \text{ MeV}$

- ▶ Absolute Energy Level

- ▶ selectivity for produced states

- ▶ Gamma-ray Spectroscopy: Low detection efficiency

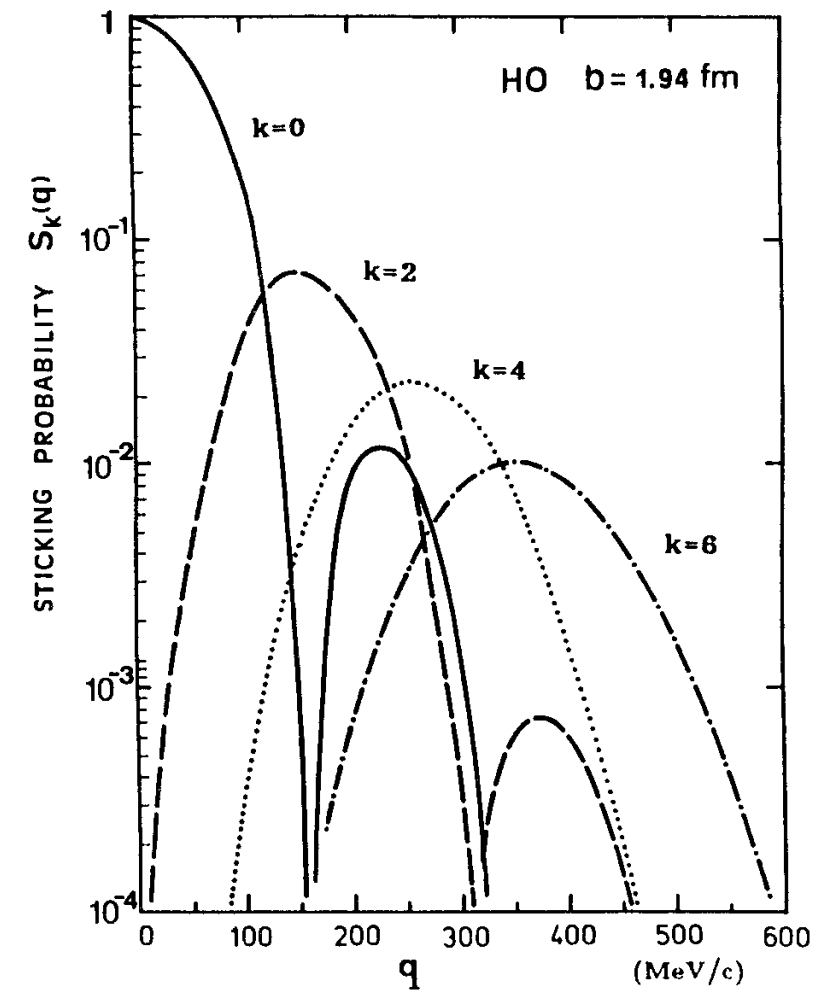
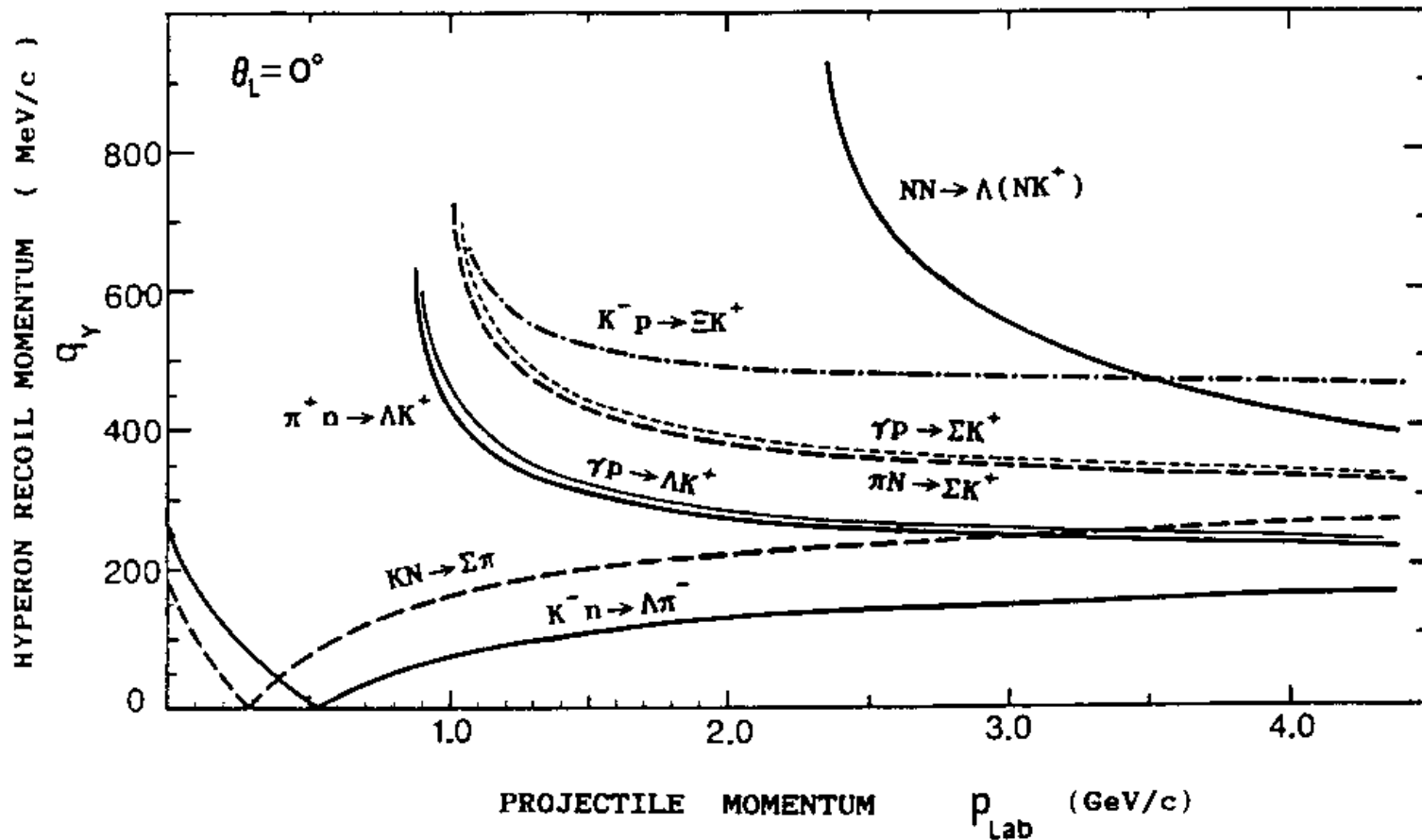
- ▶ NaI($\sim 100 \text{ keV}$), Ge($2\text{-}3 \text{ keV}$): **Excellent Resolution**

- ▶ Energy level separation

- ▶ Low-lying states below particle-emission threshold

Sticking probabilities

$$S_k(q; n_N l_N, n_Y l_Y) = \left| \langle \phi_{n_Y l_Y}^{HO}(r) | j_k(qr) | \phi_{n_N l_N}^{HO}(r) \rangle \right|^2$$



► (K⁻, π⁻): $q < 100$ MeV/c $\rightarrow \Delta \ell = 0$ dominant

Angular Distributions

- ▶ $\Delta l = 0$
 - ▶ $s_N \rightarrow s_\Lambda$
 - ▶ $p^{1/2}_N \rightarrow p^{1/2}_\Lambda$
- ▶ $\Delta l = 1$
 - ▶ $p^{3/2}_N \rightarrow s^{1/2}_\Lambda$
- ▶ $\Delta l = 2$
 - ▶ $p^{1/2}_N \rightarrow p^{3/2}_\Lambda$

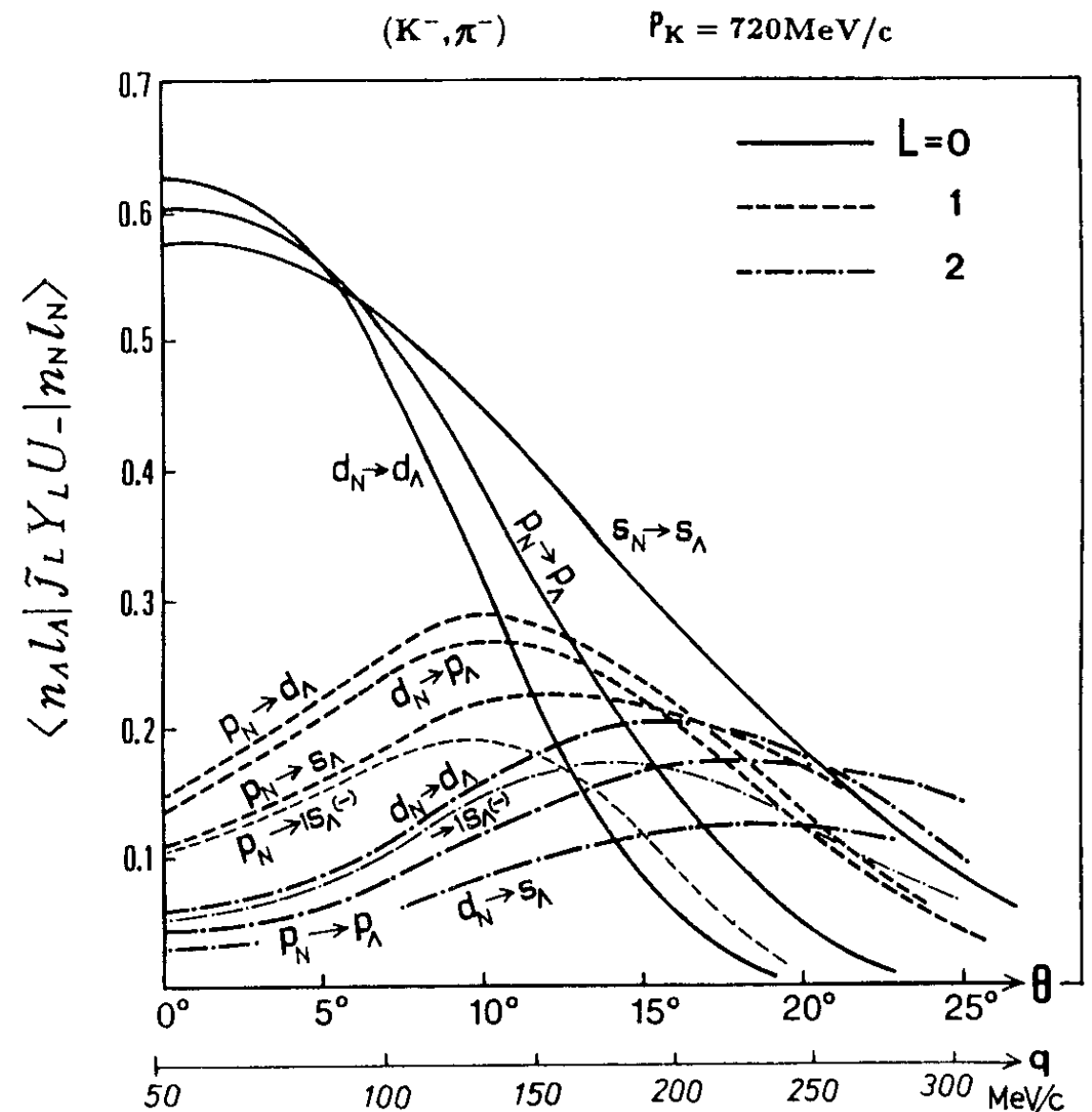
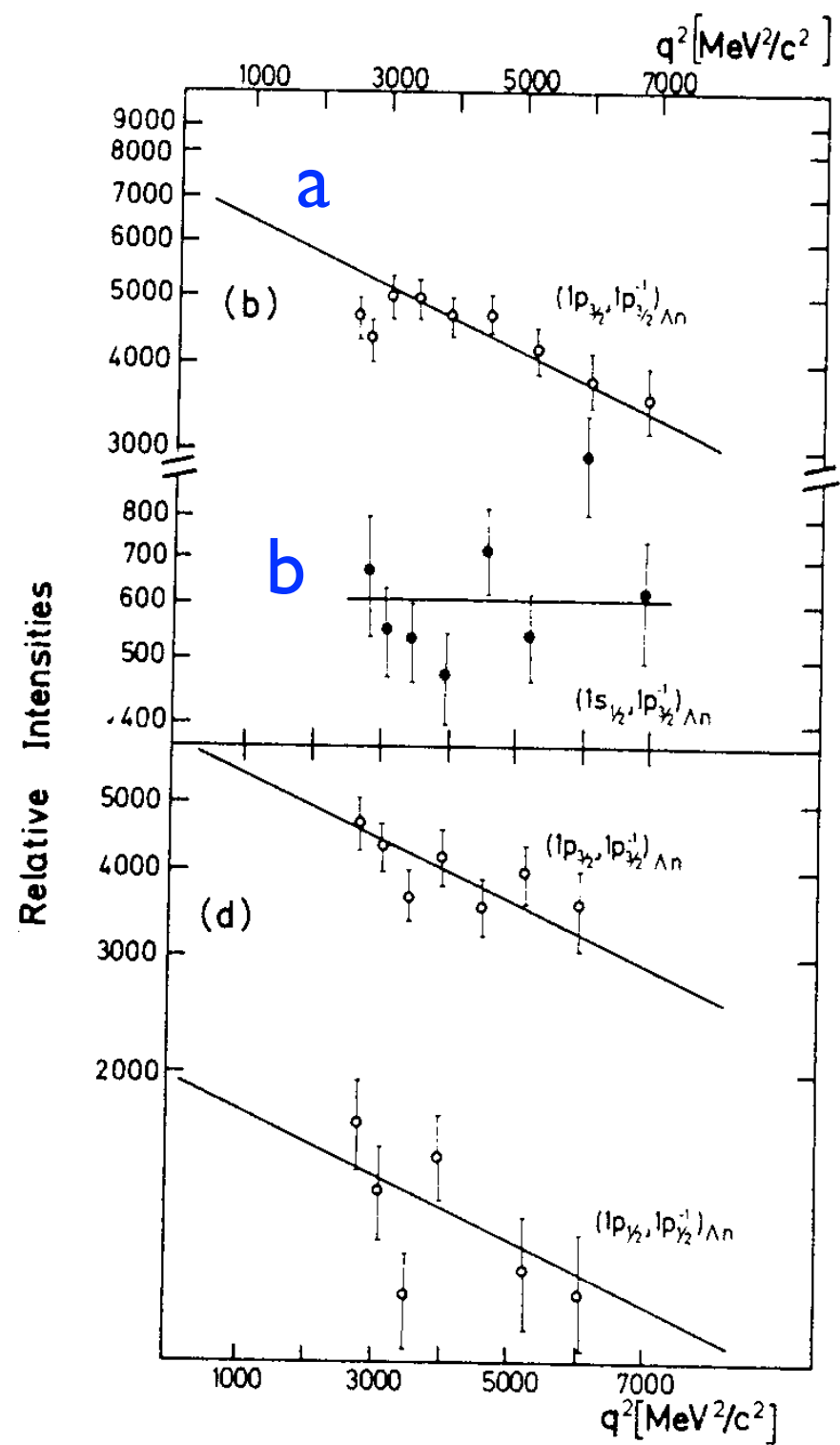
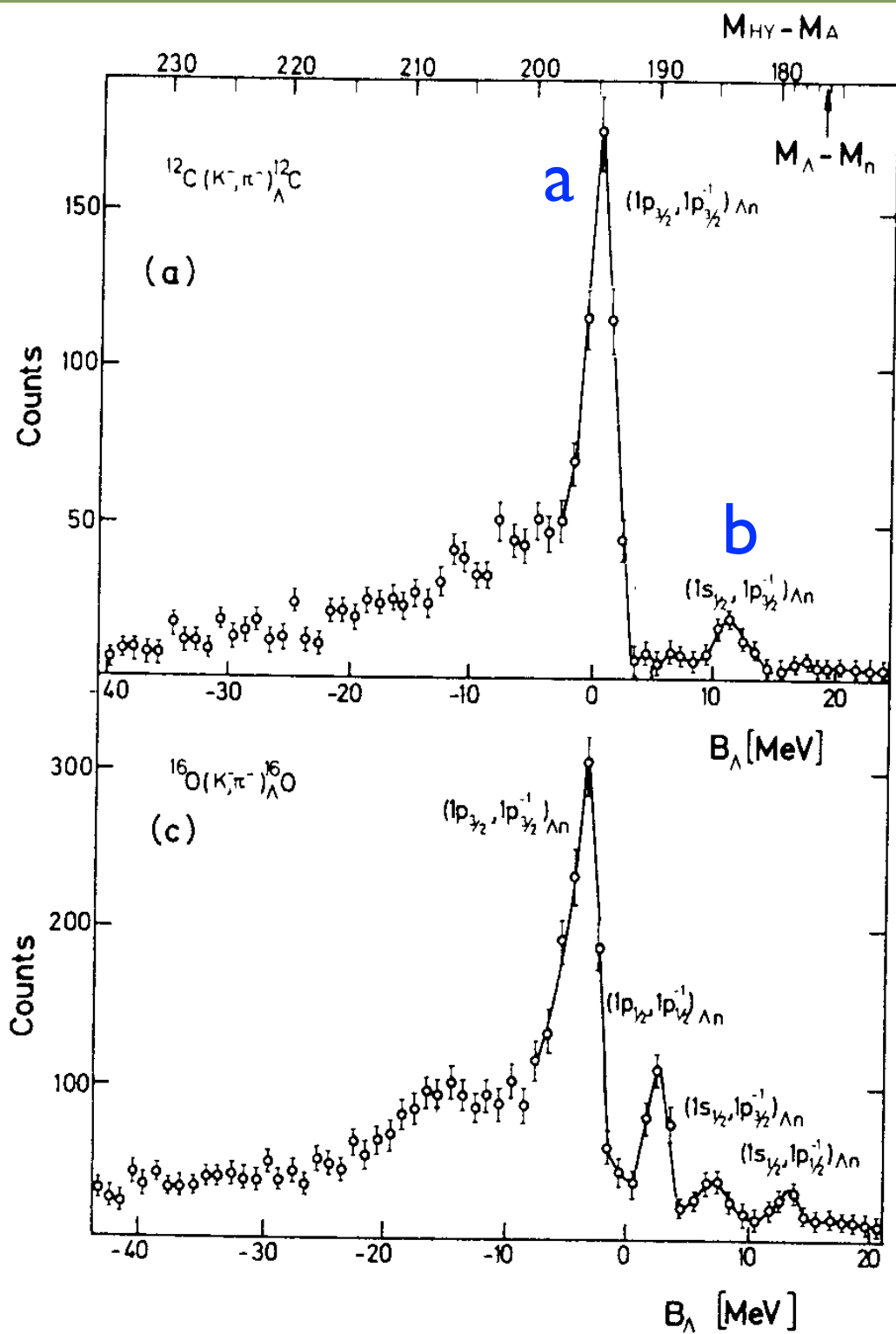


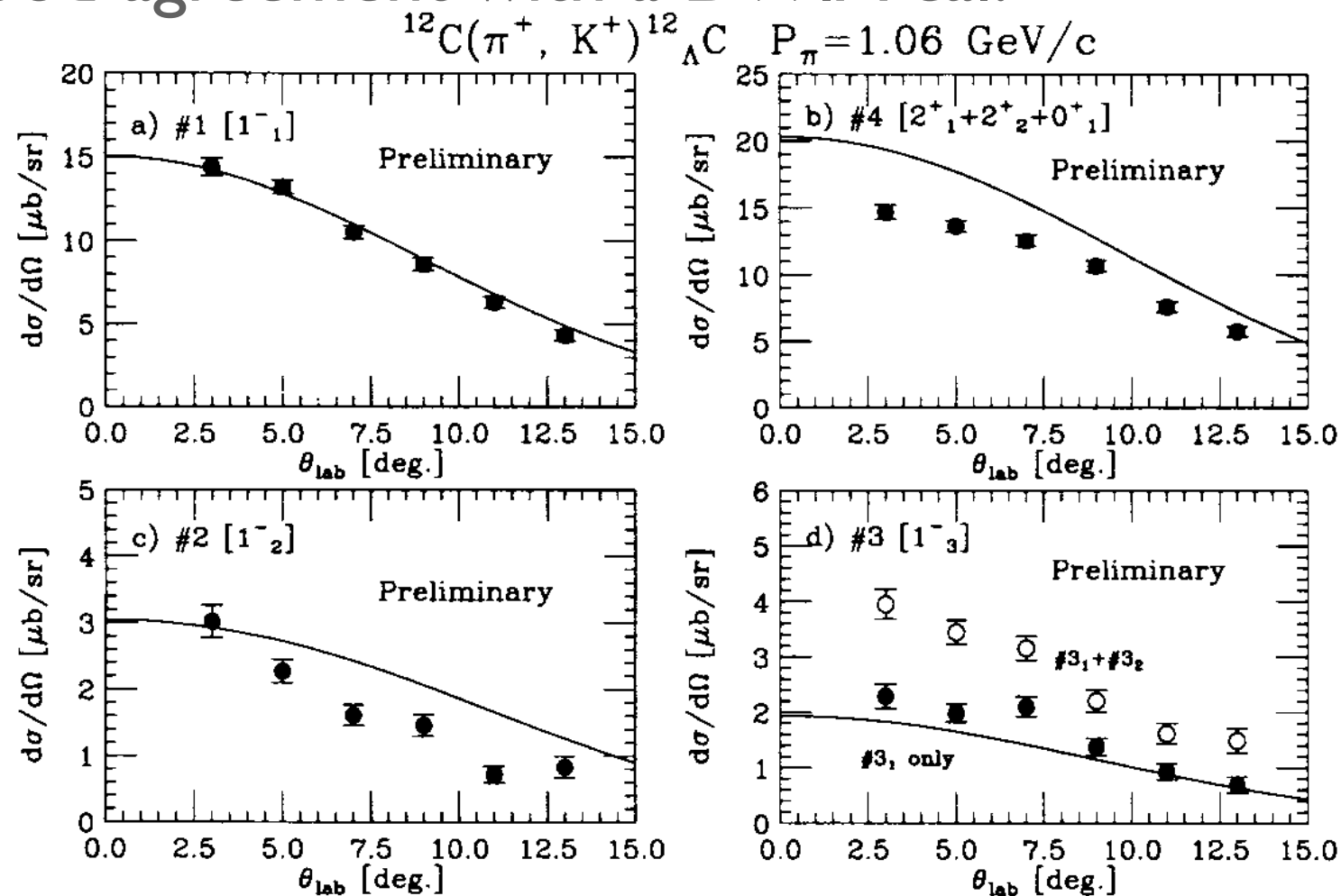
Fig. 4.1. θ -dependence of the single-particle transition matrix element $\langle n_\Lambda l_\Lambda | \tilde{J}_L Y_L U_- | n_N l_N \rangle$ calculated for the (K^-, π^-) reaction at $p_K = 720 \text{ MeV}/c$.²⁵⁵

(K^-, π^-) on ^{12}C & ^{16}O



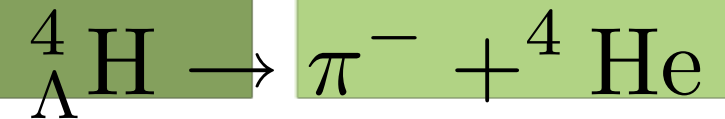
Angular distribution in (π^+, K^+)

- Small change of q
- $^{12}\Lambda C$: good agreement with a DWIA cal.



T. Takahashi et al., Nucl. Phys. A670 (2000) 265c.
 Cal. by K. Itonaga et al., Phys. Rev. C49 (1994) 1045.

Spin of ${}^4_{\Lambda}\text{H}$ (I)



- ▶ ${}^4_{\Lambda}\text{H} = {}^3\text{H}(1/2) + \Lambda(1/2)$
- ▶ Initial State: $J=0$ or 1
- ▶ Final State: $\pi(0^{-}), {}^4\text{He}(0^{+})$
 - ▶ s-wave ($J=0$) or p-wave ($J=1$)
 - ▶ isotropic or $\cos^2\Theta$

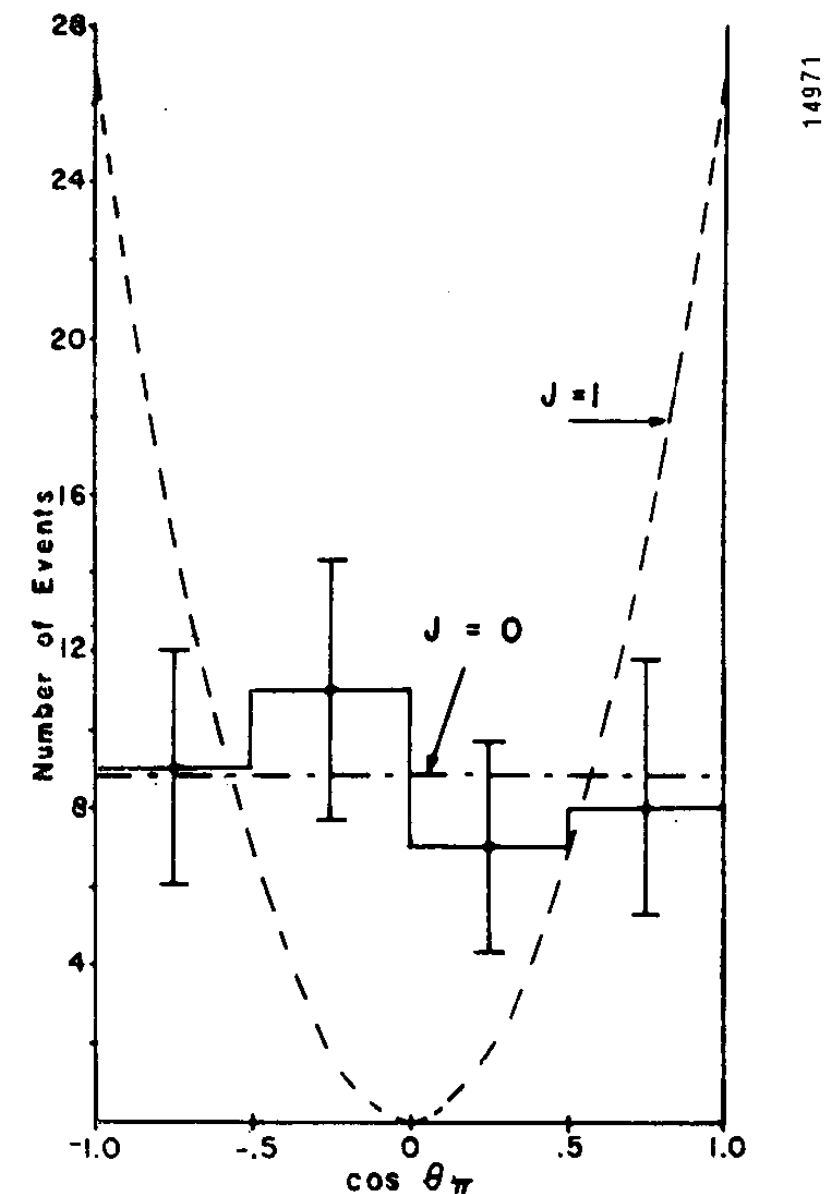


Fig. 1 The angular distribution of the π^{-} from the decay ${}^4_{\Lambda}\text{H} \rightarrow \pi^{-} + {}^4\text{He}$, for hyperfragments produced in the capture reaction $\text{K}^{-} + {}^4\text{He} \rightarrow {}^4_{\Lambda}\text{H} + \pi^0$.

Spin of ${}^4_{\Lambda}\text{H}$ (2)

► $R_4 = ({}^4_{\Lambda}\text{H} \rightarrow \pi^- + {}^4\text{He}) / (\text{all } \pi^- \text{ decays of } {}^4_{\Lambda}\text{H})$

► v.s. $p^2/(s^2+p^2)$

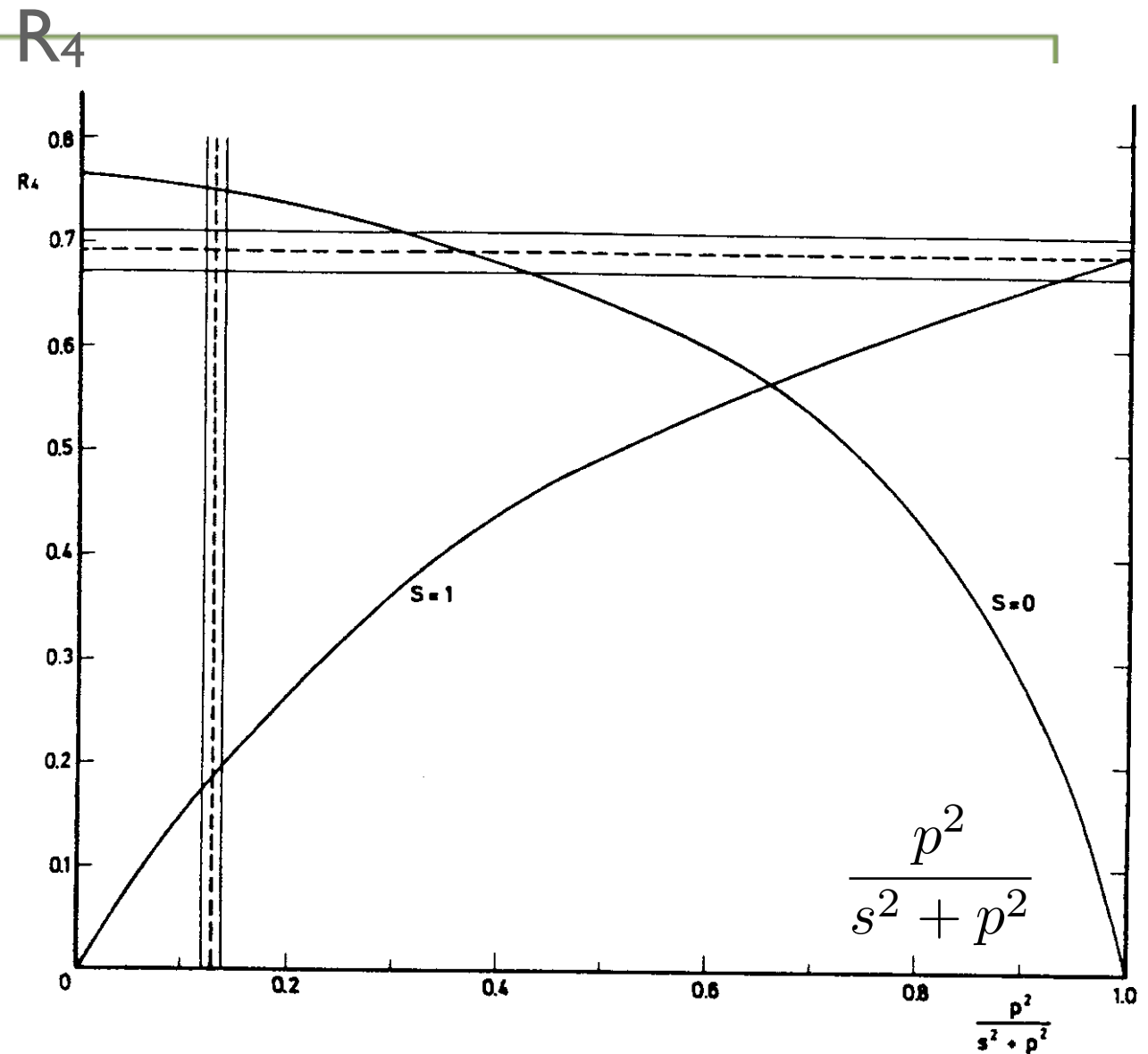
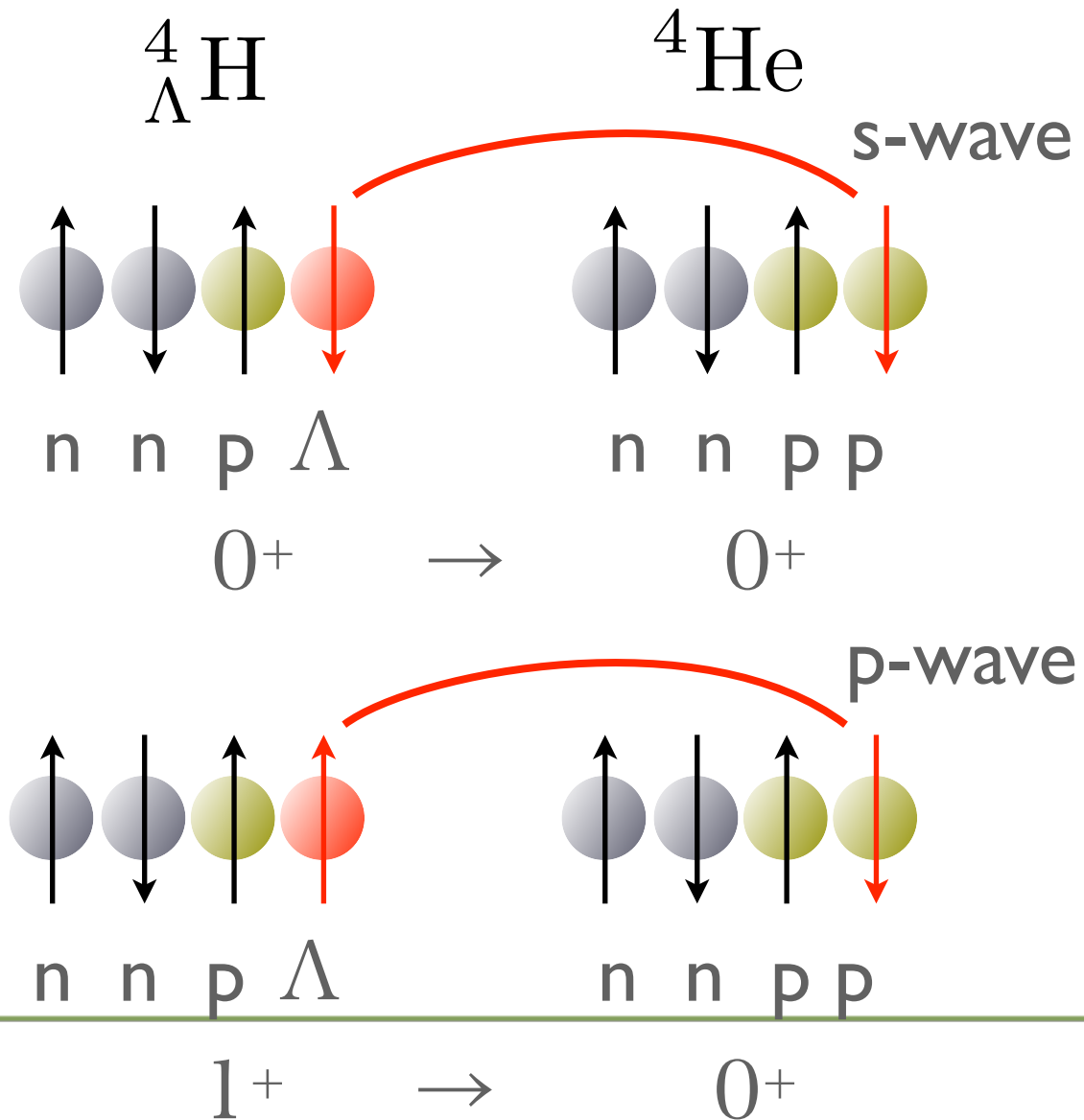


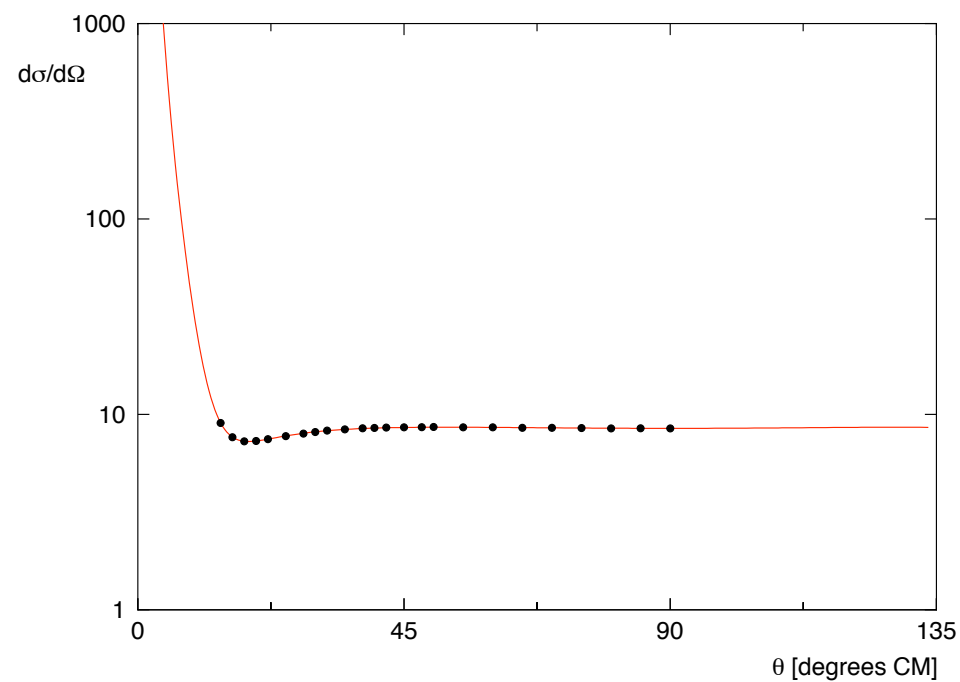
Fig. 3. The ratio $R_4 = ({}^4_{\Lambda}\text{H} \rightarrow \pi^- + {}^4\text{He}) / (\text{all } \pi^- \text{ mesonic decays of } {}^4_{\Lambda}\text{H})$ as a function of $p^2/(p^2+s^2)$. The curves illustrate the results of the calculations made by Dalitz and Liu [4] for $J({}^4_{\Lambda}\text{H}) = 0$ and 1.

Motivations of Hypernuclear Spectroscopy

- ▶ Extract YN and YY interactions
 - difficulties in YN and YY scattering measurements
- ▶ Hyperon as an impurity
 - structure change, new symmetry, etc.
- ▶ Hyperon in nuclei
 - effective mass, magnetic moment, etc.

Realistic Nuclear Force

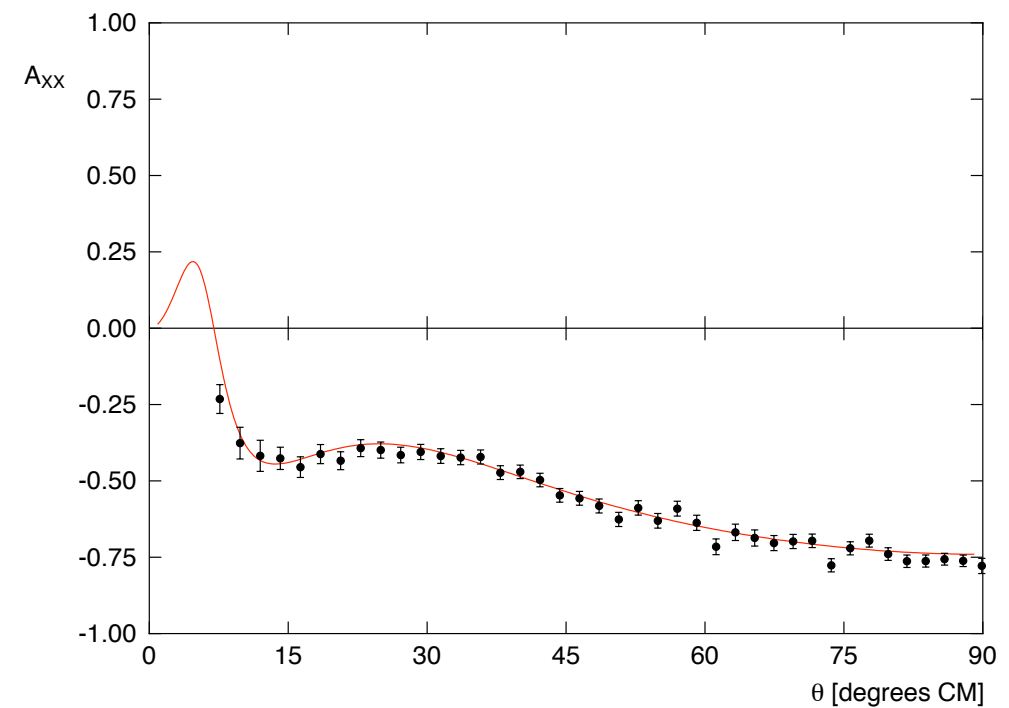
- ▶ Based on a lot of pp & pn scattering data:
 - ▶ ~5900 $d\sigma/d\Omega$, >2000 Pol., + 1700 data



pp observable $d\sigma/d\Omega$ at $T_{lab} = 50.06$ MeV

— PWA93

• Berdoz et al., SIN(1986)



pp observable A_{xx} at $T_{lab} = 350.0$ MeV

— PWA93

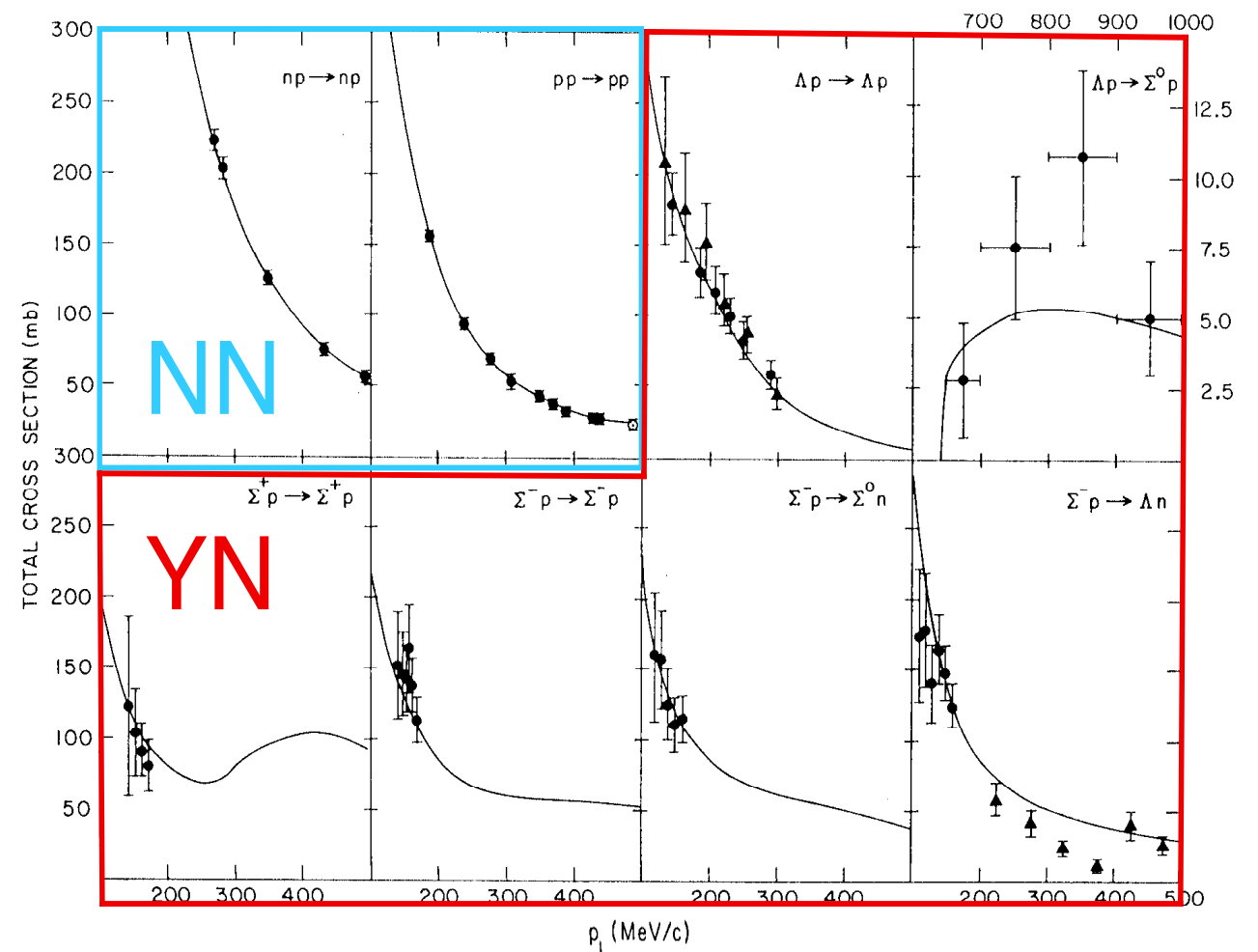
• von Przewoski et al., IUCF(1998)

Hyperon-Nucleon Scattering

$\Sigma^\pm p, \Lambda p$: only 38 data points

- $\Xi^- p$ elastic scattering and $\Xi^- p \rightarrow \Lambda \Lambda$ reaction
- Asymmetry in Λp and $\Sigma^+ p$ elastic scattering

$\Lambda^+ p, \Sigma^+ p, \Sigma^- p$ and $\Xi^- p$ scattering

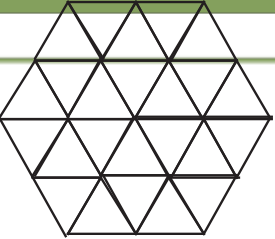


from Dover & Feshbach Ann.Phys.198(90)321

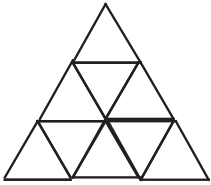
Need high quality data with high statistics

Baryon-Baryon Interaction

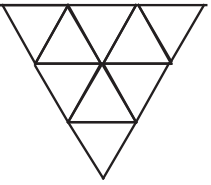
Baryon-Baryon Systems in SU(3)

27_s 

- S=0 NN(T=1)
- S=-1 ΣN(T=3/2)ΣN-ΛN(T=1/2)
- S=-2 ΣΣ(T=2)ΞN-ΣΛ-ΣΣ(T=1)ΞN-ΣΣ-ΛΛ(T=0)
- S=-3 ΞΣ(T=3/2)ΞΣ-ΞΛ(T=1/2)
- S=-4 ΞΞ(T=1)

10_a 

- S=0 NN(T=0)
- S=-1 ΣN-ΛN(T=1/2)
- S=-2 ΞN-ΣΛ(T=1)
- S=-3 ΞΣ(T=3/2)

10_a 

- S=-1 ΣN(T=3/2)
- S=-2 ΞN-ΣΛ-ΣΣ(T=1)
- S=-3 ΞΣ-ΞΛ(T=1/2)
- S=-4 ΞΞ(T=0)

8_s 

- S=-1 ΣN-ΛN(T=1/2)
- S=-2 ΞN-ΣΛ(T=1)ΞN-ΣΣ-ΛΛ(T=0)
- S=-3 ΞΣ-ΞΛ(T=1/2)

8_a 

- S=-1 ΣN-ΛN(T=1/2)
- S=-2 ΞN-ΣΛ-ΣΣ(T=1)ΞN(T=0)
- S=-3 ΞΣ-ΞΛ(T=1/2)

1_s • S=-2 ΞN-ΣΣ-ΛΛ(T=0)

► Understanding of the flavor SU(3) baryon-baryon interaction

• Y-N, Y-Y < N-N ?

Repulsive or Attractive ?

• Repulsive cores in Y-N/Y-Y ?
What's the origin ?

• Spin-dependent forces in Y-N/Y-Y.

• Dibaryons

H Dibaryon ?

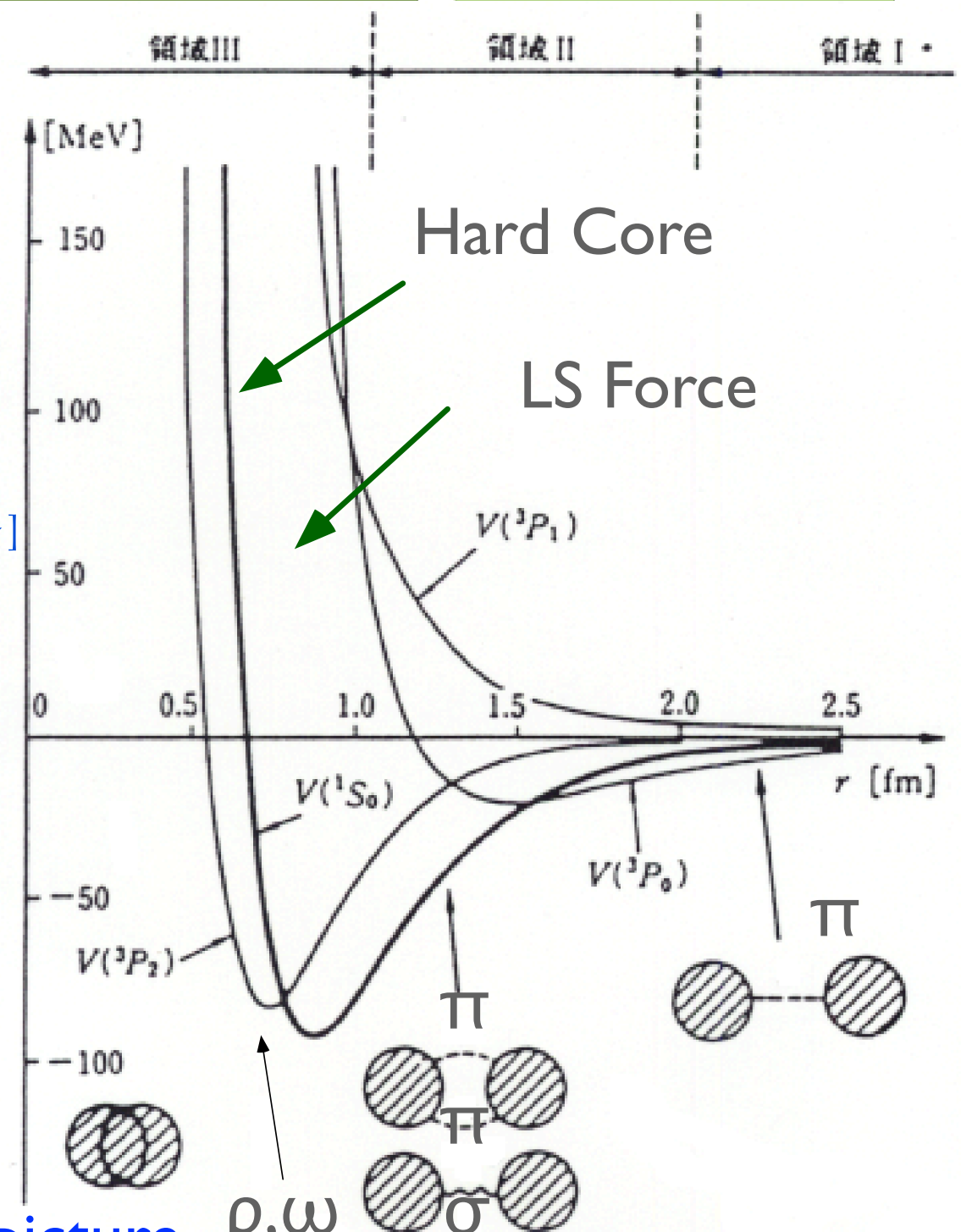
Do we understand the Nuclear Force ?

Short-range forces (=repulsive core, LS force) determine the “basic properties of nucleus” (=saturation, magic number).

from textbook by Tamagaki

Quark Cluster Model

- NN repulsive core → color magnetic int.
 Δ -N mass difference
 ↓
 H dibaryon ($SU_f(3) \times SU_f(3)$ singlet) $[u \uparrow u \downarrow d \uparrow d \downarrow s \uparrow s \downarrow]$
 = Attractive core in $\Lambda \Lambda - \Xi N$ channel
- ΣN ($I=3/2, S=1$) strongly repulsive core
 ← quark Pauli blocking
- LS force → quark gluon exchange
 → Λ : very small
 Σ : as large as N



quark-gluon picture

meson exchange picture

Theory Interest in Flavor Nuclear Physics

- Recent Model building:

1. Nijmegen models: OBE and ESC Soft-core (SC)

[Rijken, Phys.Rev. C73, 044007 \(2006\)](#)

[Rijken & Yamamoto, Phys.Rev. C73, 044008 \(2006\)](#)

[Rijken & Yamamoto, arXiv:nucl-th/060874 \(2006\)](#)

2. Chiral-Unitary Approach model

[Sasaki, Oset, and Vacas, Phys.Rev. C74, 064002 \(2006\)](#)

3. Jülich Meson-exchange models

[Haidenbauer, Meissner, Phys.Rev. C72, 044005 \(2005\)](#)

4. Jülich Effective Field Theory models

[Polinder, Haidenbauer, Meissner, Nucl.Phys. A 779, 244 \(2006\)](#)

5. Quark-Cluster-models: QGE + RGM

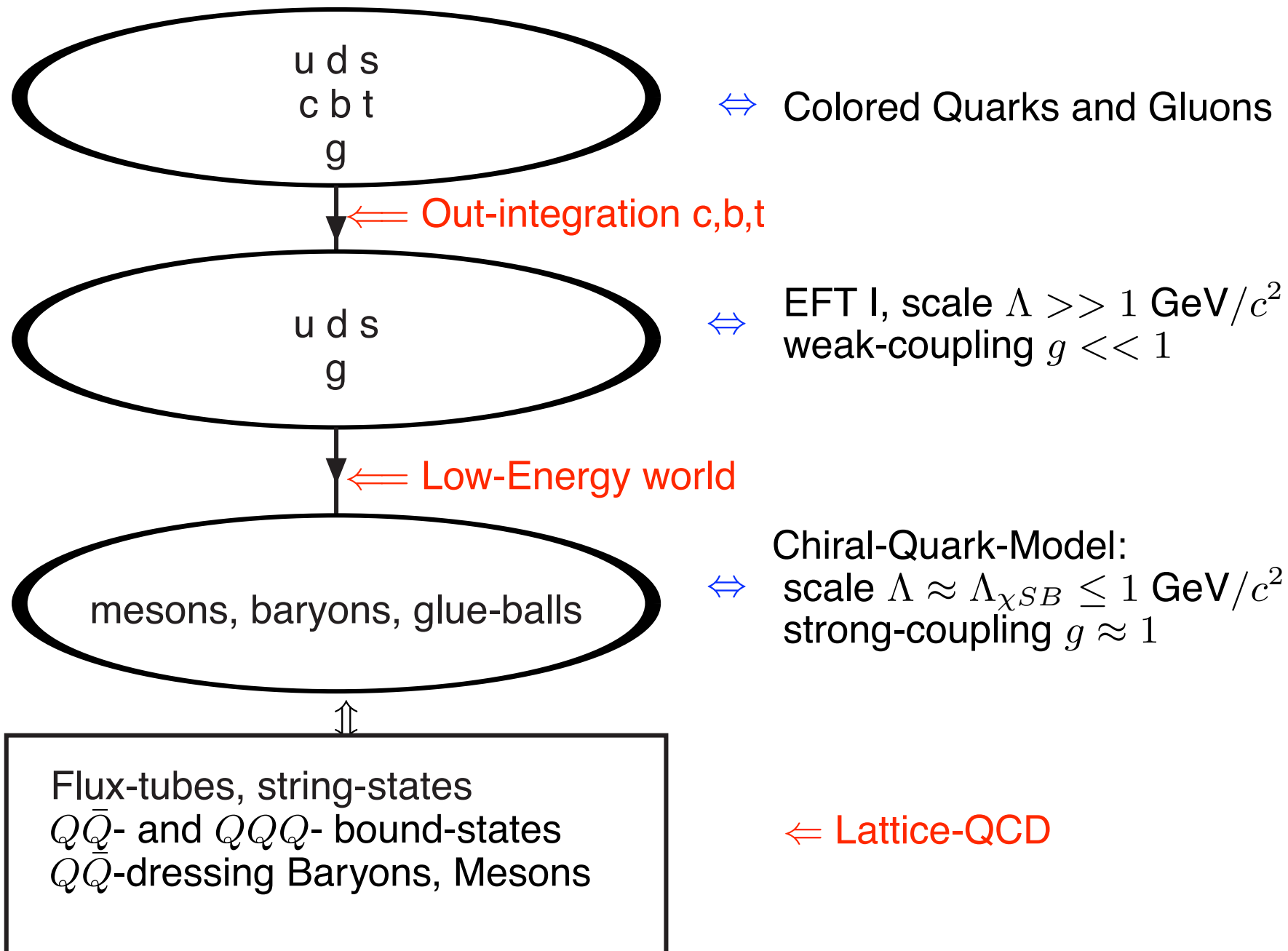
[Fujiwara et al, Progress in Part. & Nucl.Phys. 58, 439 \(2007\)](#)

[Valcarce et al, Rep.Progr.Phys. 68, 965 \(2005\)](#)

Th.A. Rijken

QCd-world I

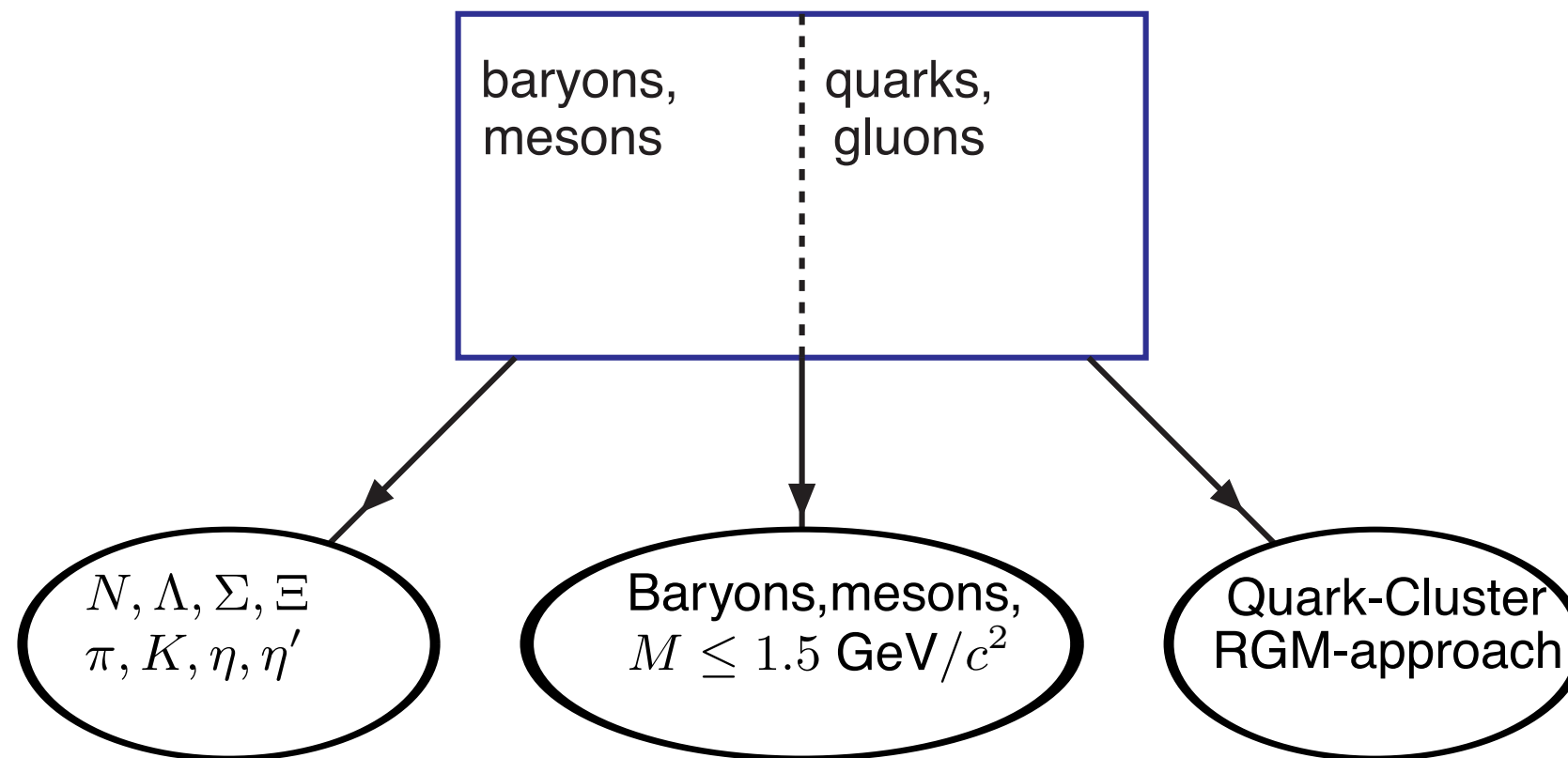
QCD-world I: mesons and baryons



Th.A. Rijken

QCD-world II

QCD-world II: Baryon/Meson-baryon Interactions



Goldstone-boson exch.
+ contact-terms
Chiral Pert. Models:
Van Kolck, Epelbaum,
Bonn-Jülich, Barcelona, etc.

Meson-exchange models
Nijmegen NSC97, ESC04,
Ehime, Jülich, etc.

Quark-Gluon-
+ OBE-exchange
Tokyo, Kyoto-Niagatta,
Tübingen, Salamanca,
Nanjing, etc.

Th.A. Rijken

Quark Pauli principle

► $(0s)^6$ is not allowed for $[51]$

$$[222]_c \times [51]_{sf} \times [6]_o \neq [1^6]$$

► n: $-|ddu\rangle\{2|++-\rangle-|+-+\rangle-|-++\rangle\}/3\sqrt{2}$

► Σ^- : $|dds\rangle\{2|++-\rangle-|+-+\rangle-|-++\rangle\}/3\sqrt{2}$

$SU(6)_{fs}$ -contents of the various potentials
on the isospin, spin basis.

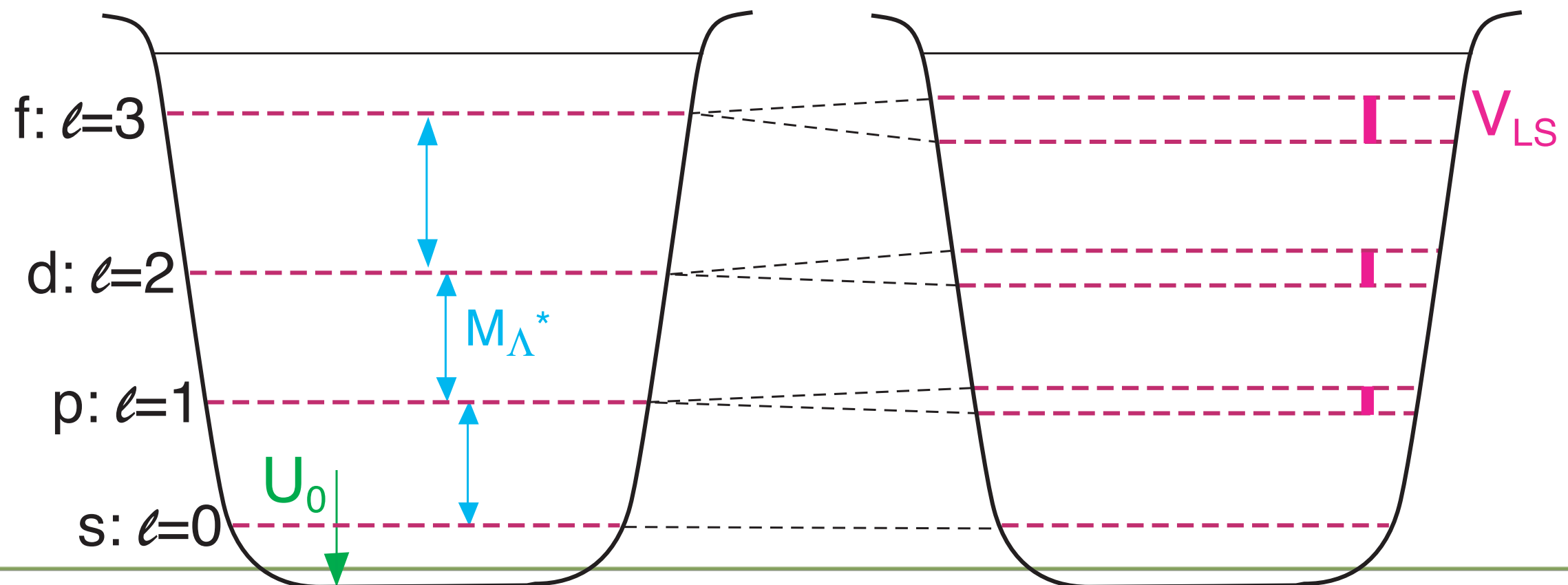
	(S, I)	$V = aV_{[51]} + bV_{[33]}$
$NN \rightarrow NN$	$(0, 1)$	$V_{NN}(I = 1) = \frac{4}{9}V_{[51]} + \frac{5}{9}V_{[33]}$
$NN \rightarrow NN$	$(1, 0)$	$V_{NN} = \frac{4}{9}V_{[51]} + \frac{5}{9}V_{[33]}$
$\Lambda N \rightarrow \Lambda N$	$(0, 1/2)$	$V_{\Lambda\Lambda} = \frac{1}{2}V_{[51]} + \frac{1}{2}V_{[33]}$
$\Lambda N \rightarrow \Lambda N$	$(1, 1/2)$	$V_{\Lambda\Lambda} = \frac{1}{2}V_{[51]} + \frac{1}{2}V_{[33]}$
$\Sigma N \rightarrow \Sigma N$	$(0, 1/2)$	$V_{\Sigma\Sigma} = \frac{17}{18}V_{[51]} + \frac{1}{18}V_{[33]}$
$\Sigma N \rightarrow \Sigma N$	$(1, 1/2)$	$V_{\Sigma\Sigma} = \frac{1}{2}V_{[51]} + \frac{1}{2}V_{[33]}$
$\Sigma N \rightarrow \Sigma N$	$(0, 3/2)$	$V_{\Sigma\Sigma} = \frac{4}{9}V_{[51]} + \frac{5}{9}V_{[33]}$
$\Sigma N \rightarrow \Sigma N$	$(1, 3/2)$	$V_{\Sigma\Sigma} = \frac{8}{9}V_{[51]} + \frac{1}{9}V_{[33]}$

Hypernuclear structure and ΛN interaction

$$V_{\Lambda N} = U_0 + V_S \sigma_N \cdot \sigma_\Lambda + V_{\Lambda} \ell_{N\Lambda} \cdot \sigma_\Lambda + V_N \ell_{N\Lambda} \cdot \sigma_N + V_{TS} S_{I2}$$

(a) Central Attraction Only

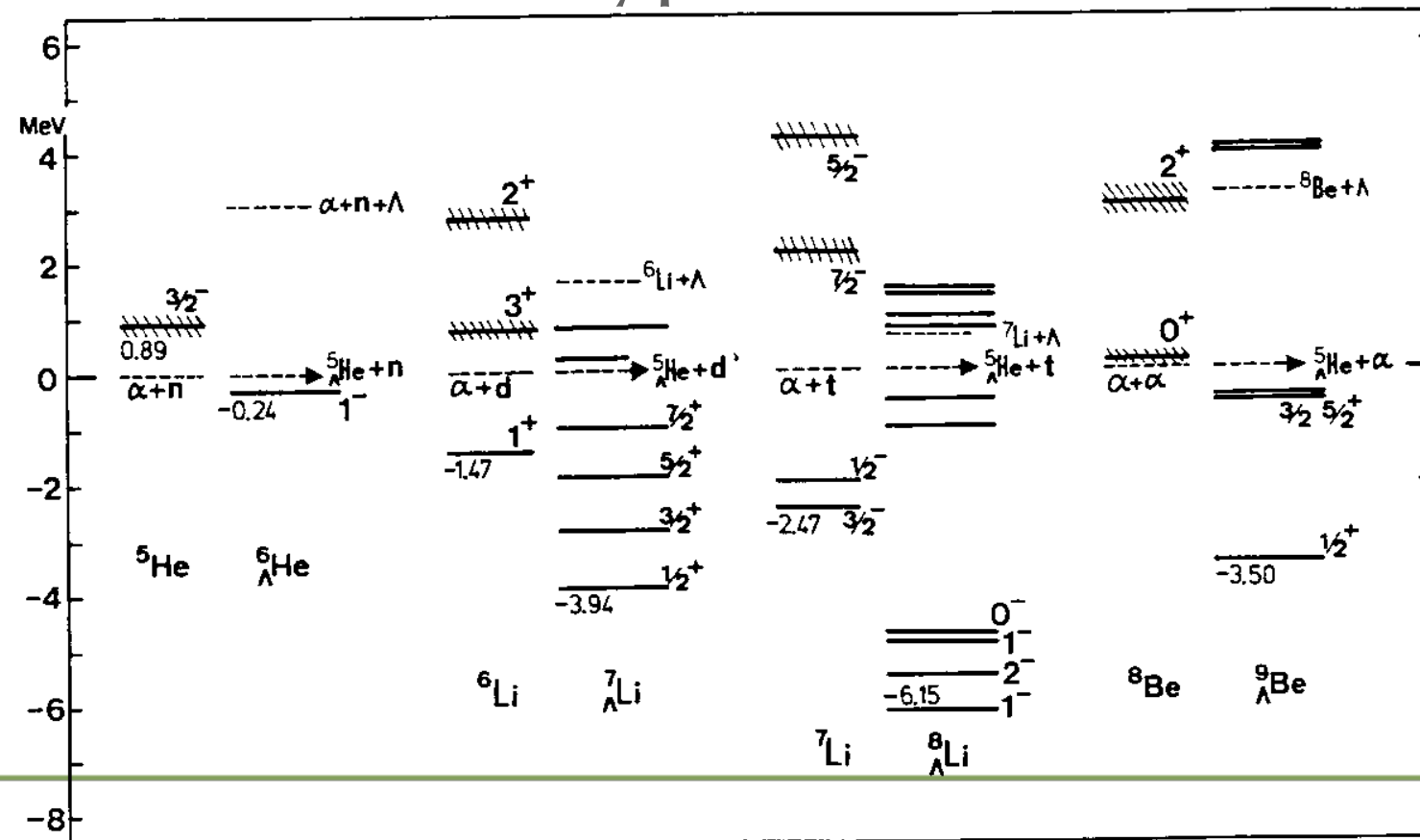
(b) Central + Spin-Orbit Force



Impurity Effect - I

▶ Glue-like role

- Energetical stabilization
- Resonant states in neutron-rich nuclei
→ Bound states in Λ -hypernuclei

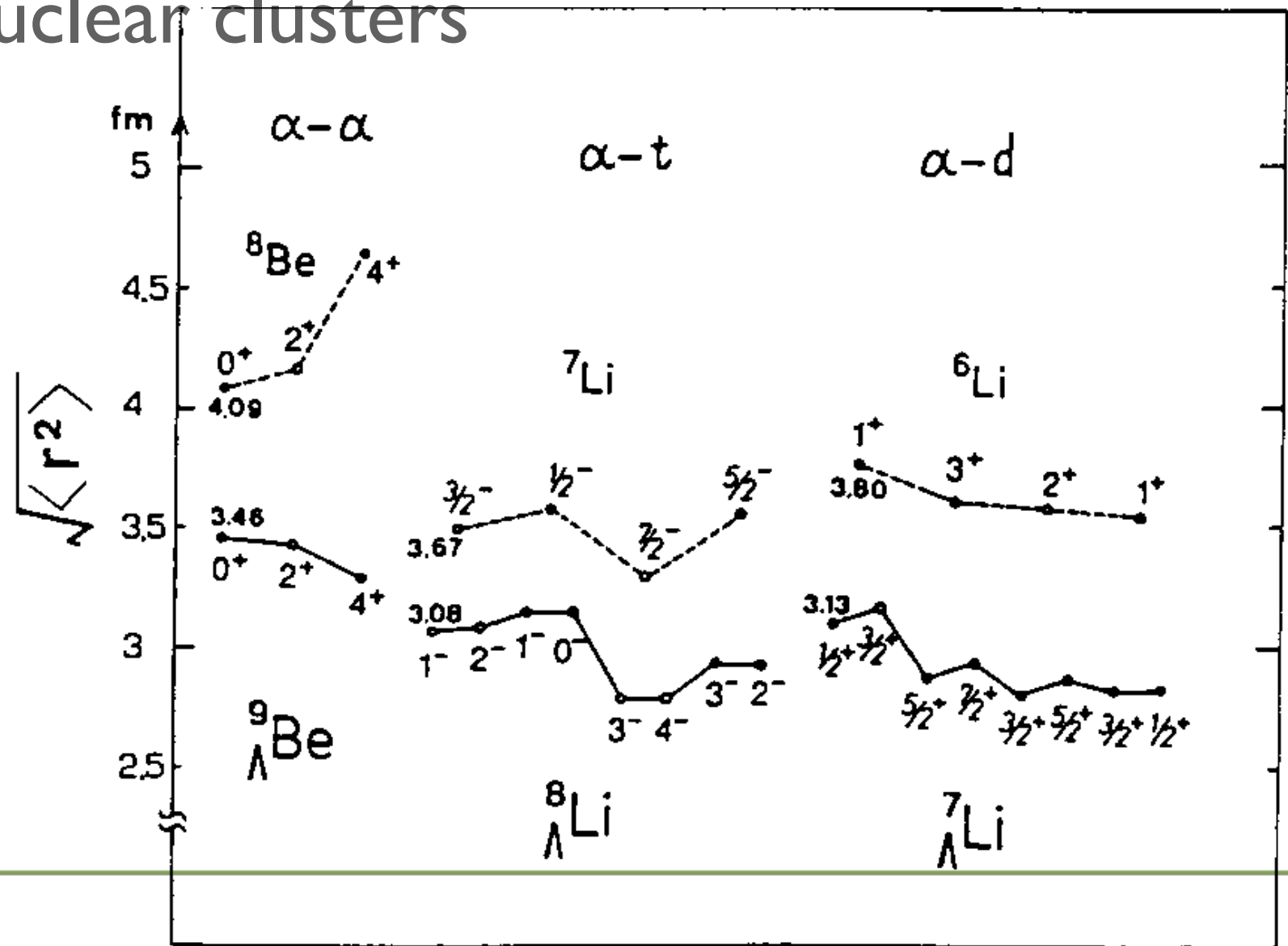


Impurity Effect -2

- ▶ Structure Change
- ▶ Shrinkage of nuclear clusters

$$B(E2) \propto |\langle f | e r^2 Y_2 | i \rangle|^2$$

$$\propto R^4 \text{ or } (\beta \langle r^2 \rangle)^2$$

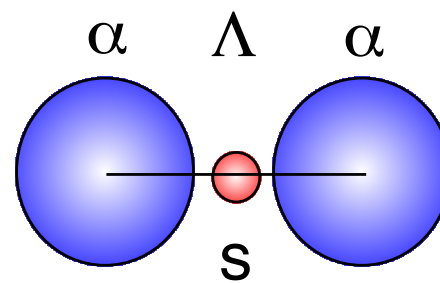
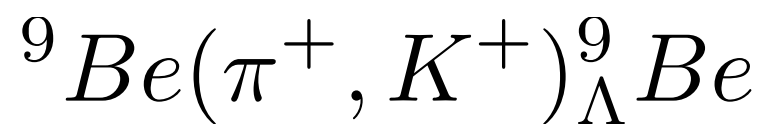


Impurity Effect -3

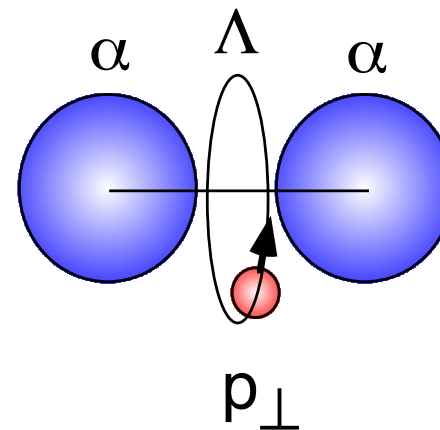


► New symmetry:

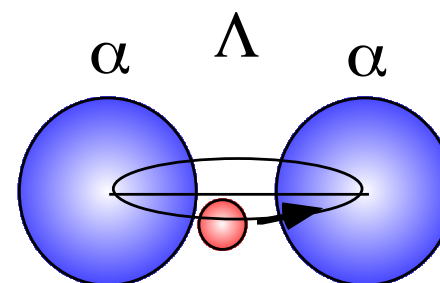
- Supersymmetric state or
Genuine hypernuclear state


 $[(\alpha\alpha)\otimes s\Lambda]$

8Be-analog


 $[(\alpha\alpha)\otimes p_{\perp}\Lambda]$

9Be-analog


 $[(\alpha\alpha)\otimes p_{\parallel}\Lambda]$

Genuine hypernuclear

p_{\parallel}

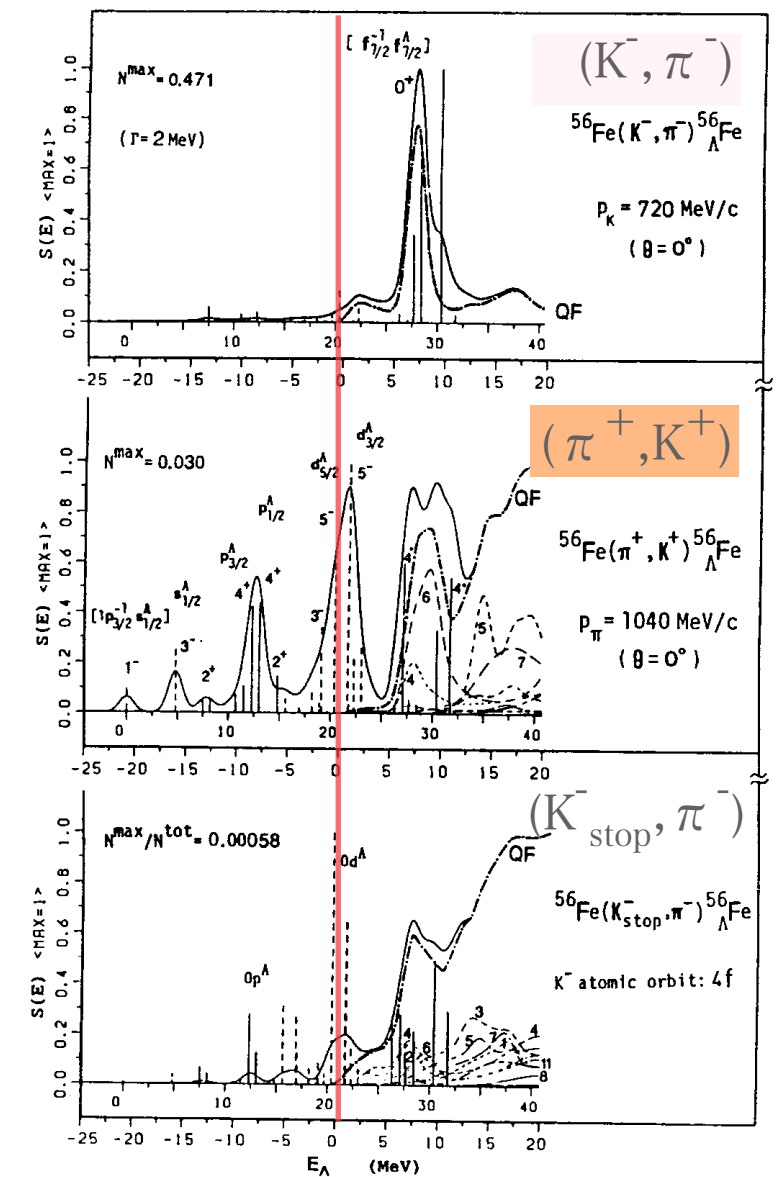
(π^+, K^+) Spectroscopy

► Merits

- ✱ Large momentum transfer $q \sim 350$ MeV/c
- ✱ Efficiently produces deeply-bound states
- ✱ Low backgrounds: γ , n

► Demerits

- ✱ No difference in angular distributions



(π^+, K^+) Spectroscopy

■ Reaction mechanism:

■ Dover, Ludeking, Walker, Phys. Rev. C22(1980) 2073.

■ Success at BNL(1985, 1988)

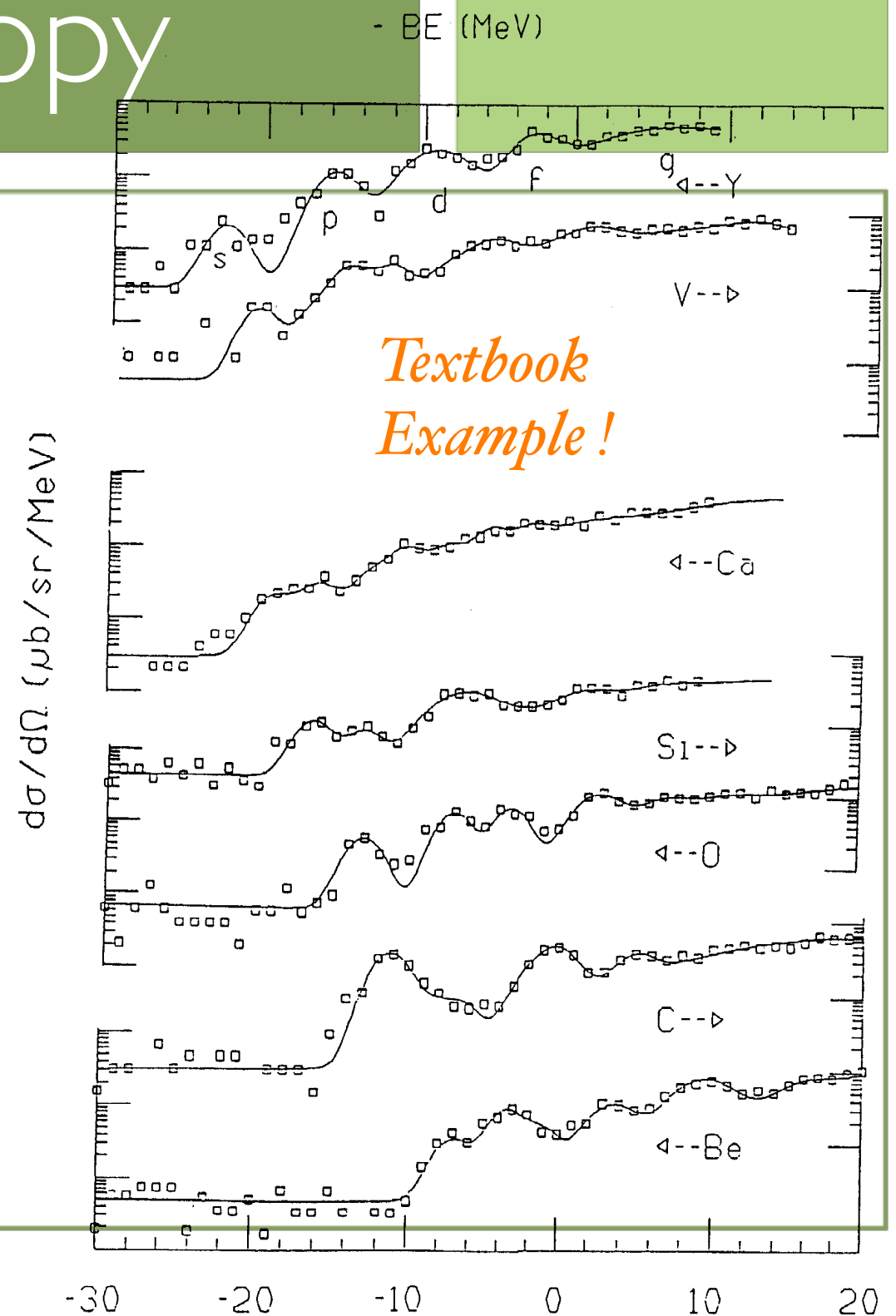
■ $\Delta E \sim 3$ MeV

■ Up to $^{89}_{\Lambda}Y$

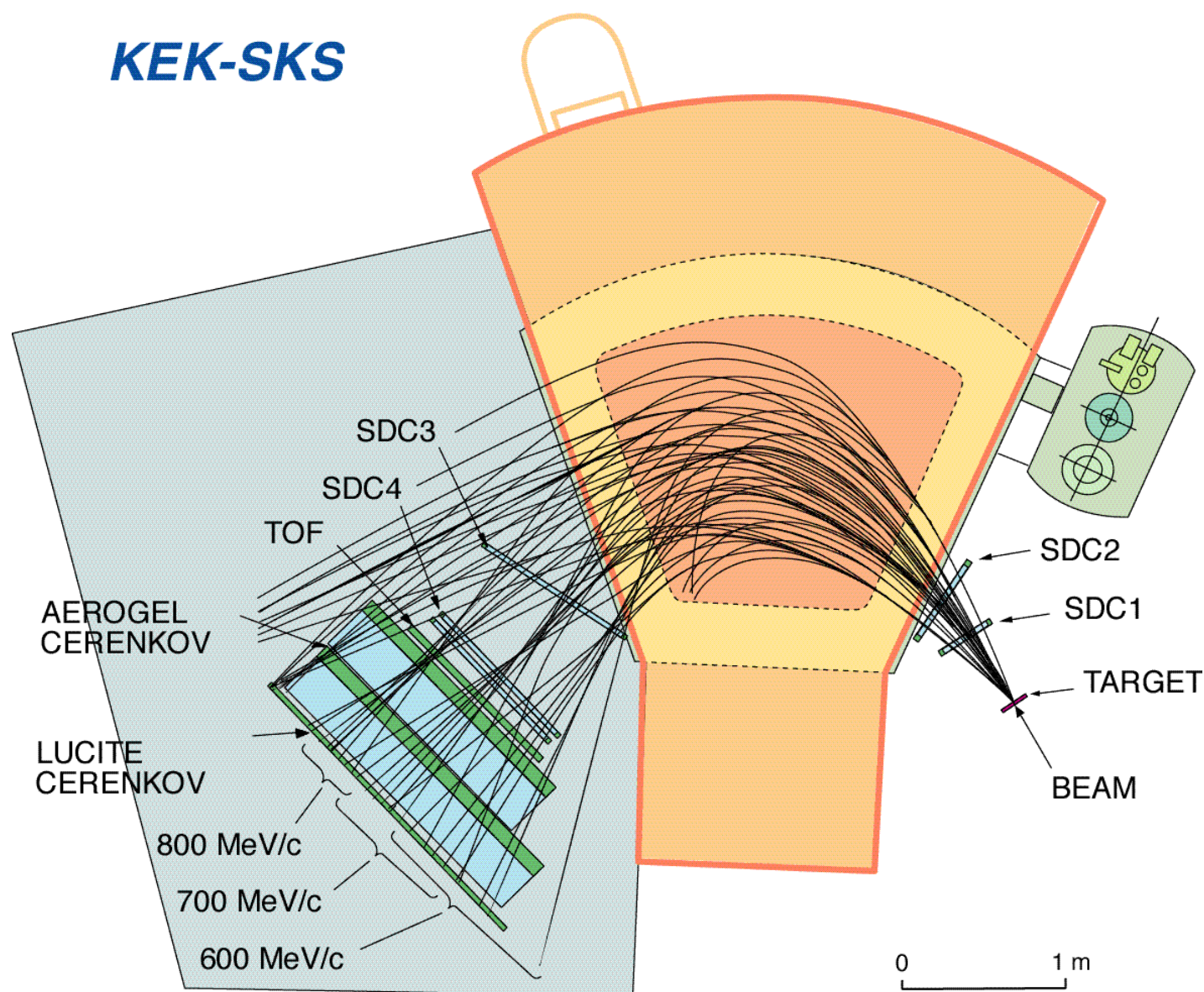
► $q \sim 350$ MeV/c

✓ natural-parity stretched states

✓ $[(\ell_N j_N)^{-1} (\ell_{\Lambda} j_{\Lambda})]$ with $J = \ell_N + \ell_{\Lambda}$



SKS spectrometer at KEK-PS



- Superconducting Kaon Spectrometer for the (π^+ , K^+) reactions
- Constructed by INS, Univ. of Tokyo, from 1987 to 1990
- In operation since 1992
- $B_{\max} = 3T$ (500A)
- Pole Gap = 50 cm
- 10.6 MJ stored
- Cold Mass ~ 4.5 t
- ~ 280 tons

Design Specifications of the SKS

- Momentum resolution:
0.1%(FWHM) at 720 MeV/c
- Solid angle: **100 msr**
 - To get enough yields
- Short Flight Path: ~5 m
 - To reduce K^+ decays
- Initial Goal of Energy Resolution:
2 MeV(FWHM)

Challenges in the SKS

- Good Energy Resolution: <2 MeV(FWHM)
- Magnetic Field Mapping: $\Delta B/B < 10^{-3}$
 - Fully automated 3D positioning system
 - (120,000points x 7excitations) in 1.5 months
 - Very careful calibrations
- 3 T magnet with very low heat leak
- He transfer line with rotation capability

Momentum resolution

► K6 Beamline

- Matrix representations for magnets

$$\vec{x}'_{out} = QQDQQ\vec{x}_{in}$$

$$\vec{x} = (x, y, \theta \equiv dx/dz, \varphi \equiv dy/dz, \delta \equiv (p - p_0)/p_0)$$

- $\langle x' | \theta \rangle \sim 0$

- Resolution in 1st order

$$\frac{\langle x' | x \rangle \sigma_x}{\langle x' | \delta \rangle}$$

$$QQDQQ = \begin{pmatrix} \langle x' | x \rangle & \langle x' | y \rangle & \langle x' | \vartheta \rangle & \langle x' | \varphi \rangle & \langle x' | \delta \rangle \\ \langle y' | x \rangle & \langle y' | y \rangle & \langle y' | \vartheta \rangle & \langle y' | \varphi \rangle & \langle y' | \delta \rangle \\ \langle \vartheta' | x \rangle & \langle \vartheta' | y \rangle & \langle \vartheta' | \vartheta \rangle & \langle \vartheta' | \varphi \rangle & \langle \vartheta' | \delta \rangle \\ \langle \varphi' | x \rangle & \langle \varphi' | y \rangle & \langle \varphi' | \vartheta \rangle & \langle \varphi' | \varphi \rangle & \langle \varphi' | \delta \rangle \\ 0 & 0 & 0 & 0 & 1 \end{pmatrix}$$

(π, K^+) experiments with SKS

- ▶ E140a: ^{10}B , ^{12}C , ^{28}Si , ^{89}Y , ^{139}La , ^{208}Pb

■ Phys. Rev. C 53 (1996) 1210.

- ▶ E336: ^7Li , ^9Be , ^{13}C , ^{16}O

■ Nucl. Phys. A 639 (1998) 93c, Nucl. Phys. A 691 (2001) 123c.

- ▶ E369: ^{89}Y , ^{51}V , ^{12}C in high-resolution

■ Phys. Rev. C 64 (2001) 044302.

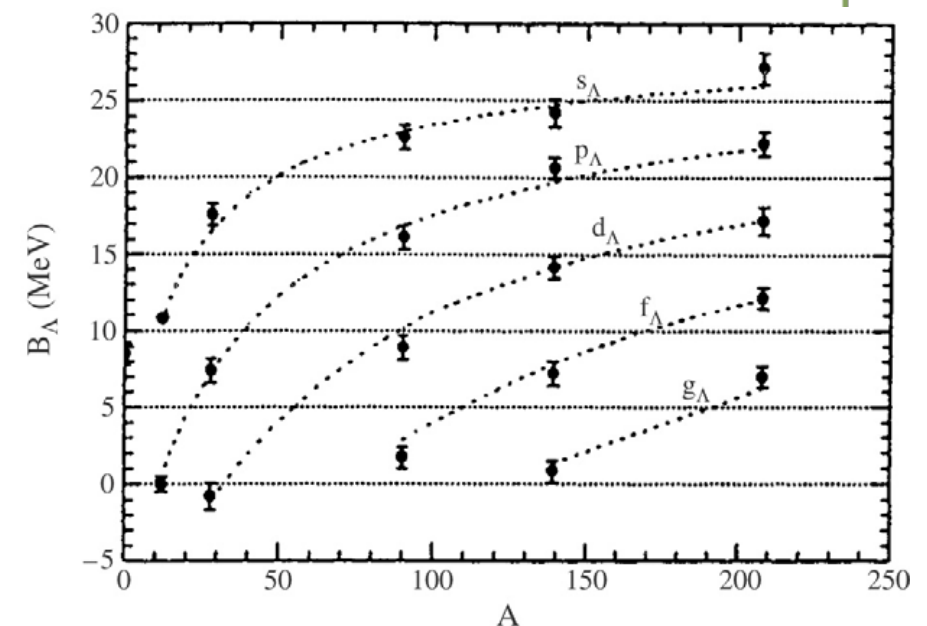
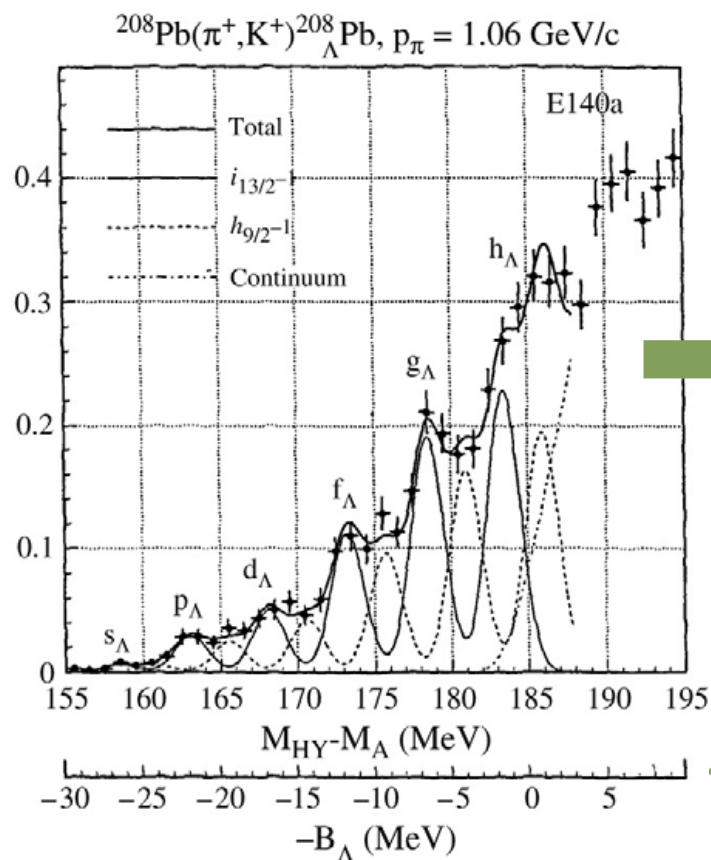
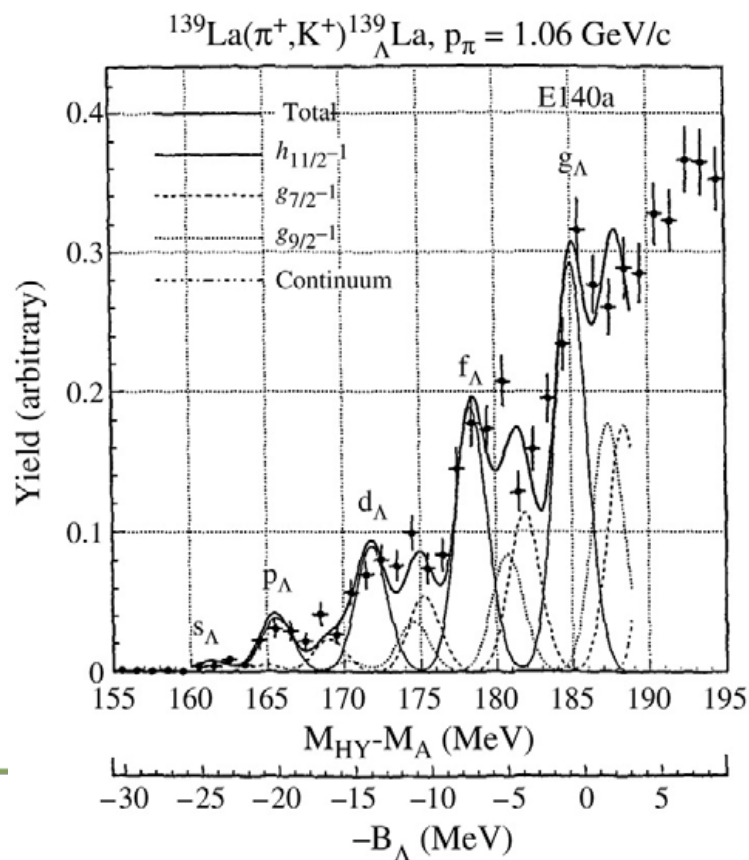
- ▶ E521: $^{10}\text{B}(\pi^-, K^+)$

■ Phys. Rev. Lett. 94 (2005) 052502.

E140a:

First (π^+, K^+) exp. with the SKS

- Targets: ^{10}B , ^{12}C , ^{28}Si , ^{89}Y , ^{139}La , ^{208}Pb
 - $^{12}\Lambda\text{C}$: First observation of core-excited states
 - Confirmed Λ Shell Structures up to $^{208}\Lambda\text{Pb}$

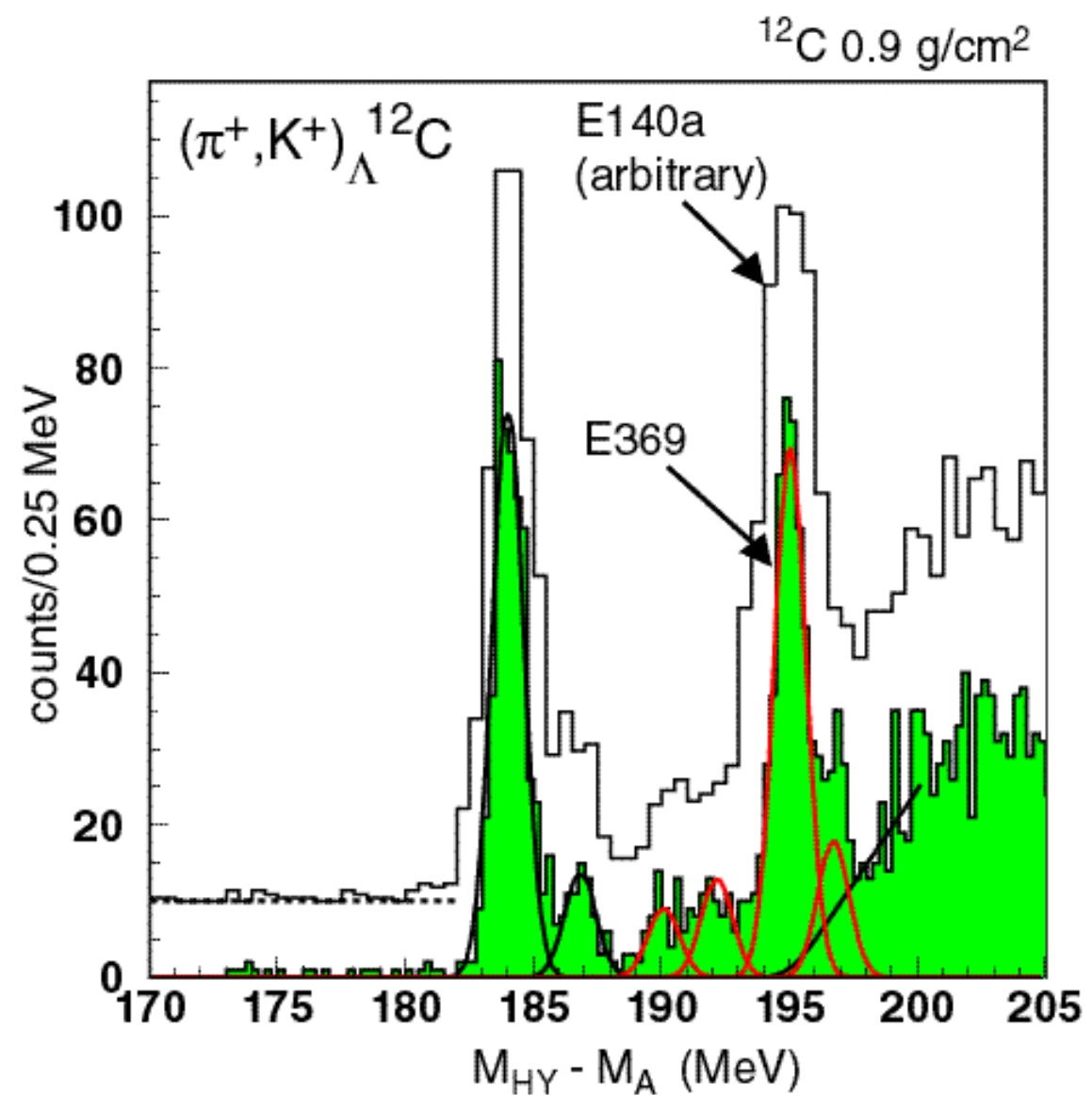


E369: Λ ^{12}C

- Best energy resolution
- $\Delta E(\text{FWHM})$
= 1.45 MeV

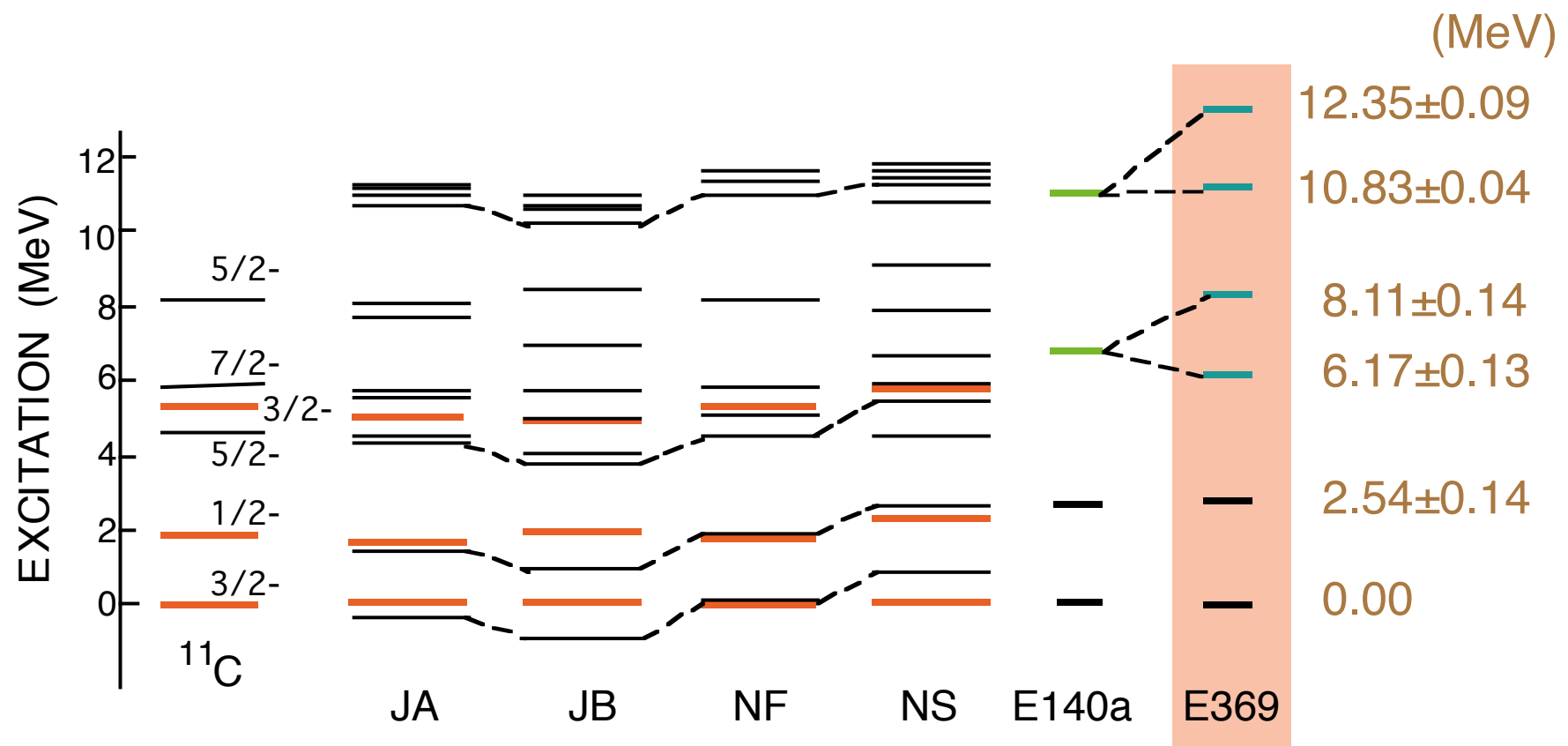


- 2.0 MeV



Core-excited states of $\Lambda^{12}\text{C}$

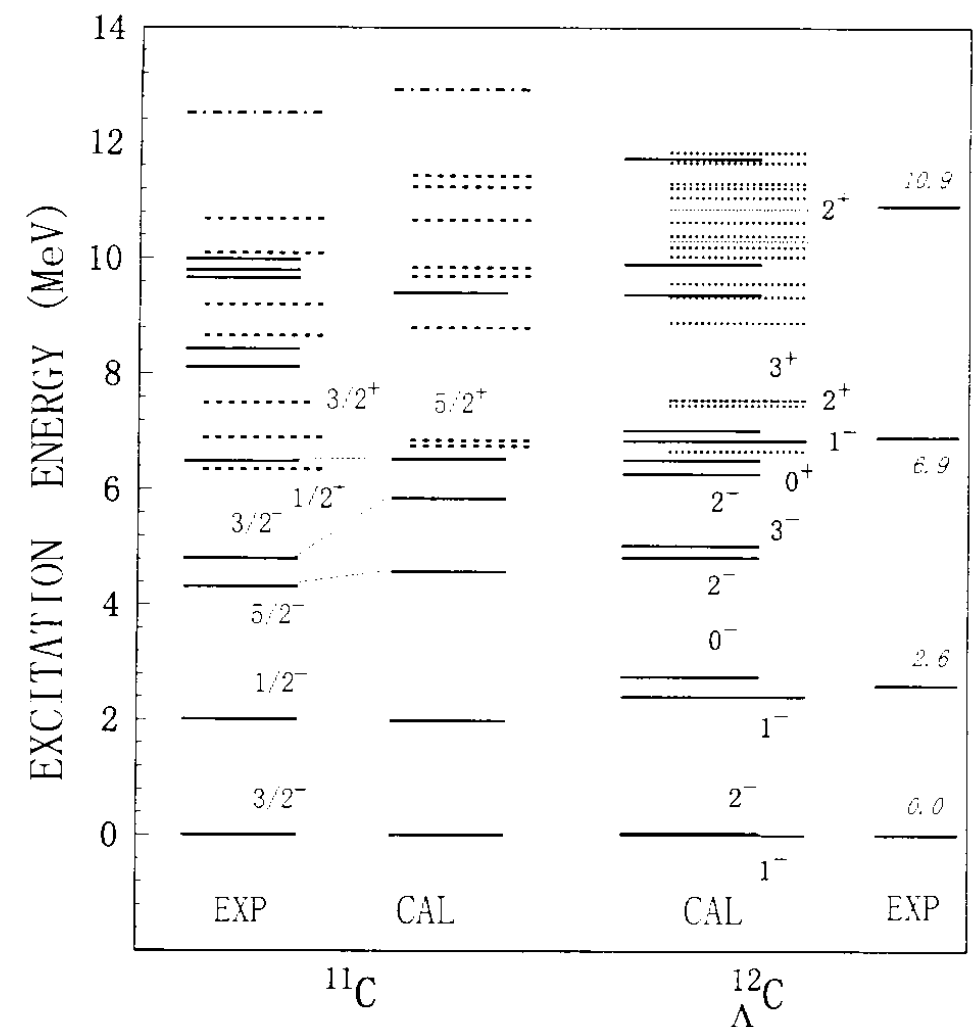
- New states are resolved.
Effects of ΛN spin-dependent forces



Parity-mixing intershell coupling

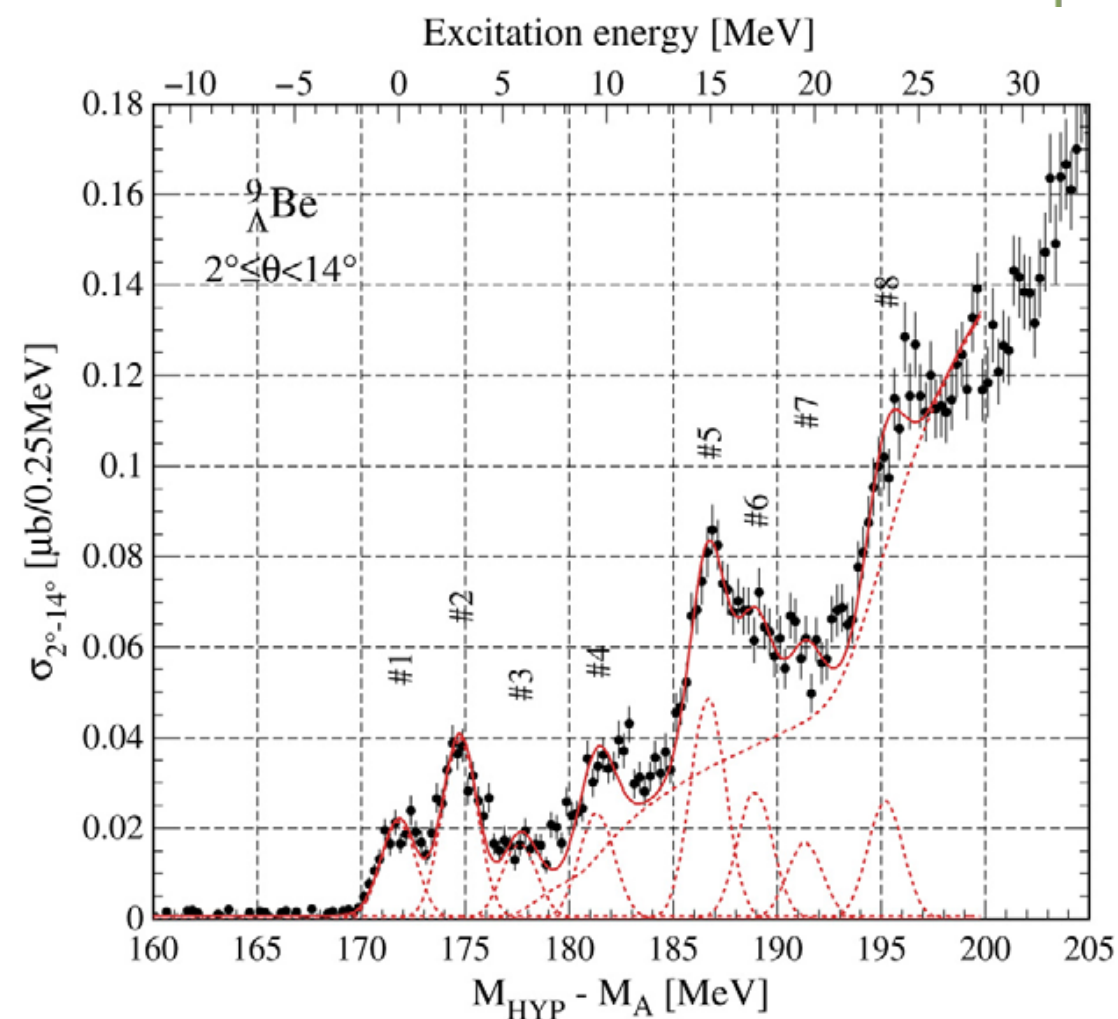
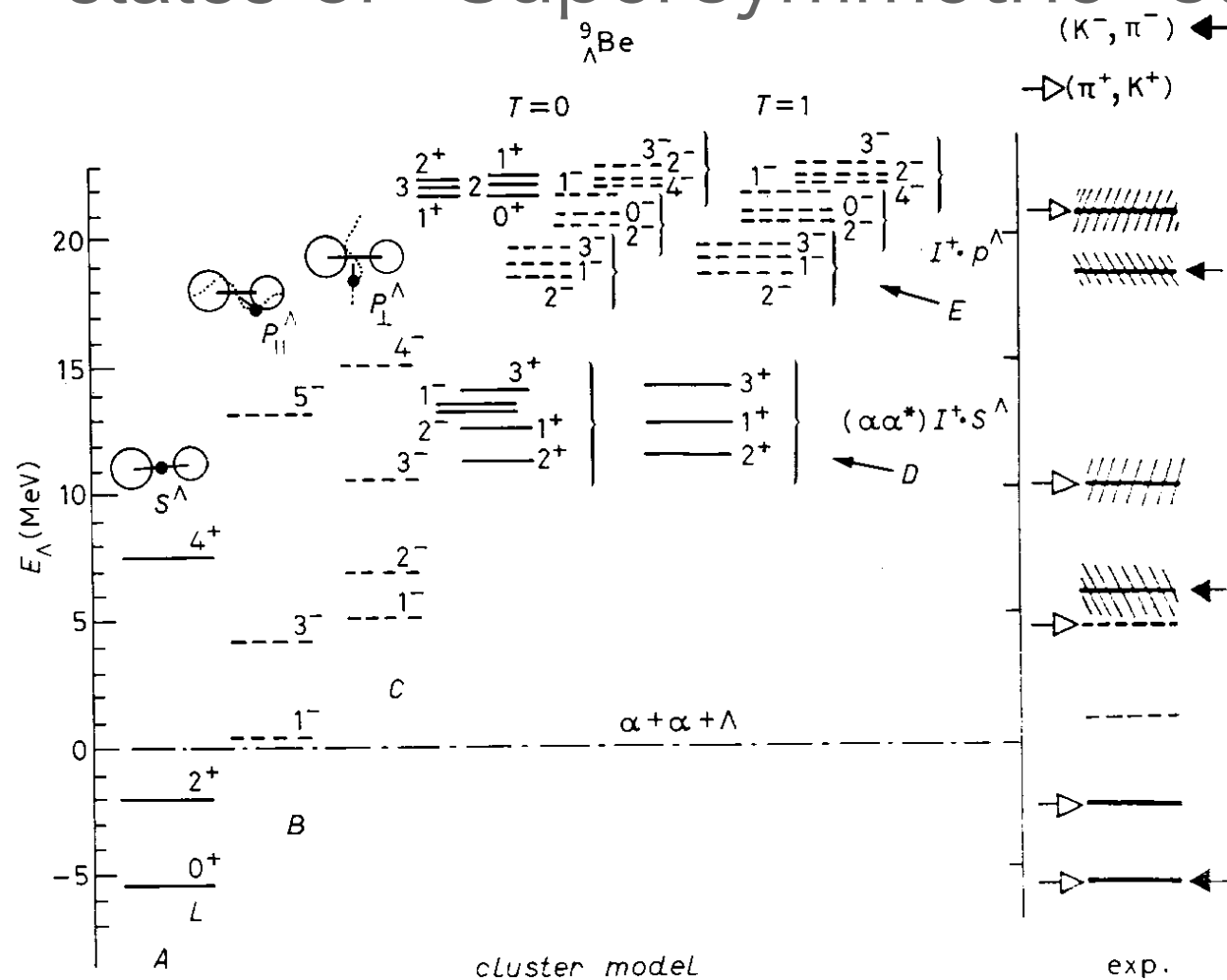
- T. Motoba, in HYP97 (Nucl. Phys. A 639 (1998) 135c.)

$$|{}_{\Lambda}^{12}\text{C}; J^+\rangle = [s^4 p^7]_- \otimes 1p^{\Lambda} + \left\{ [s^4 p^6 (sd)^1]_+ + [s^3 p^8]_+ \right\} \otimes 1s^{\Lambda}$$

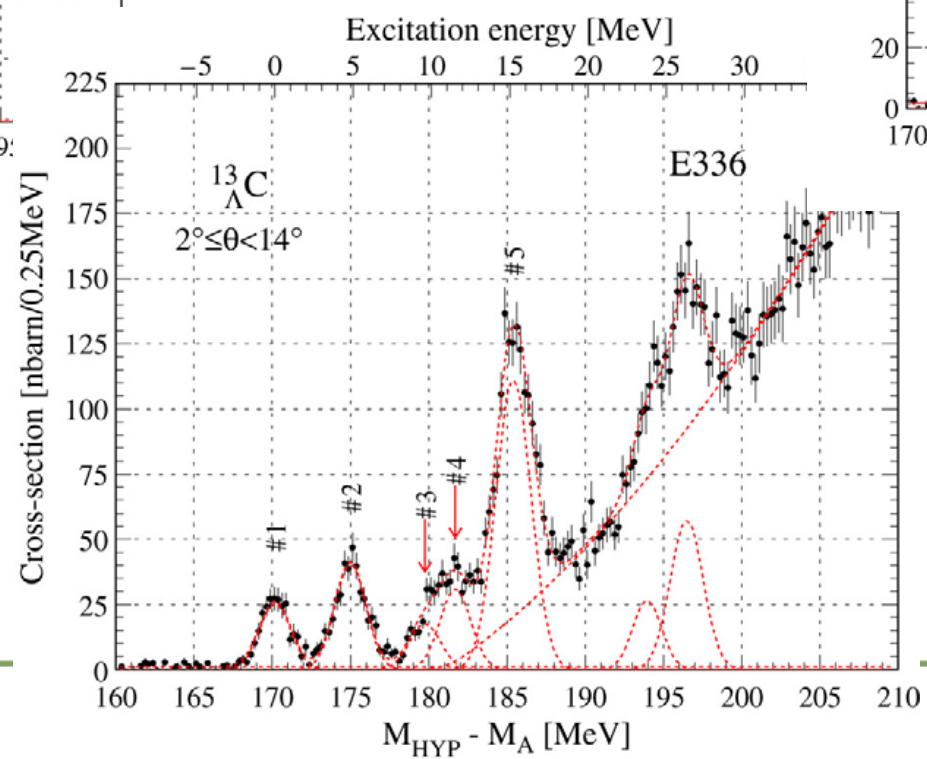
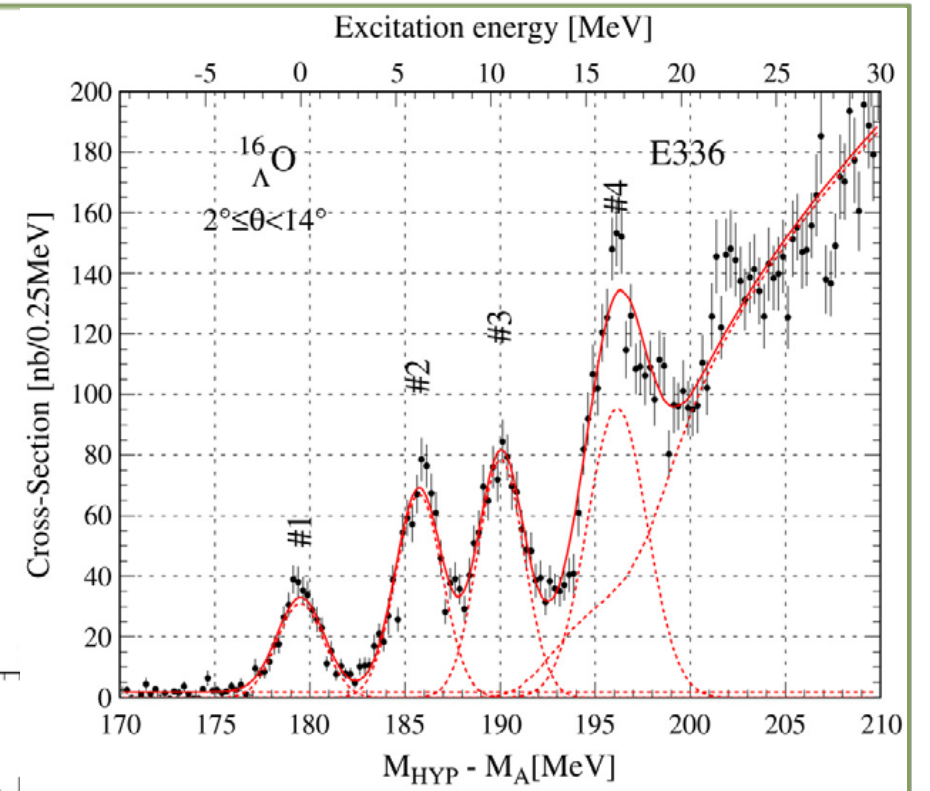
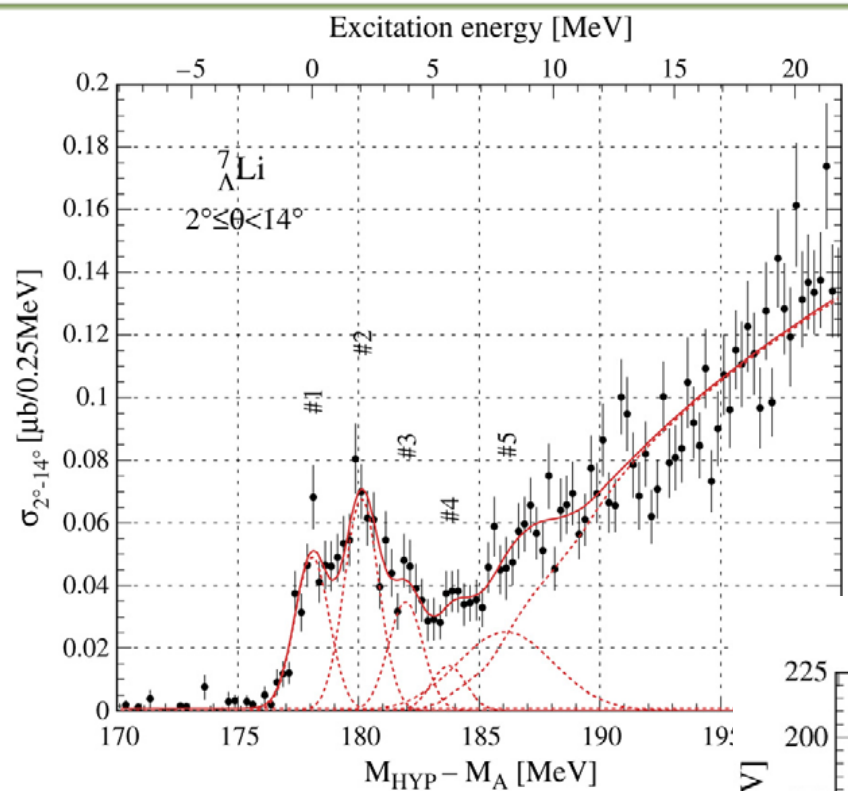


E336: ${}^9_{\Lambda}\text{Be}$

- Observation of “genuine” hypernuclear states or “Supersymmetric” states

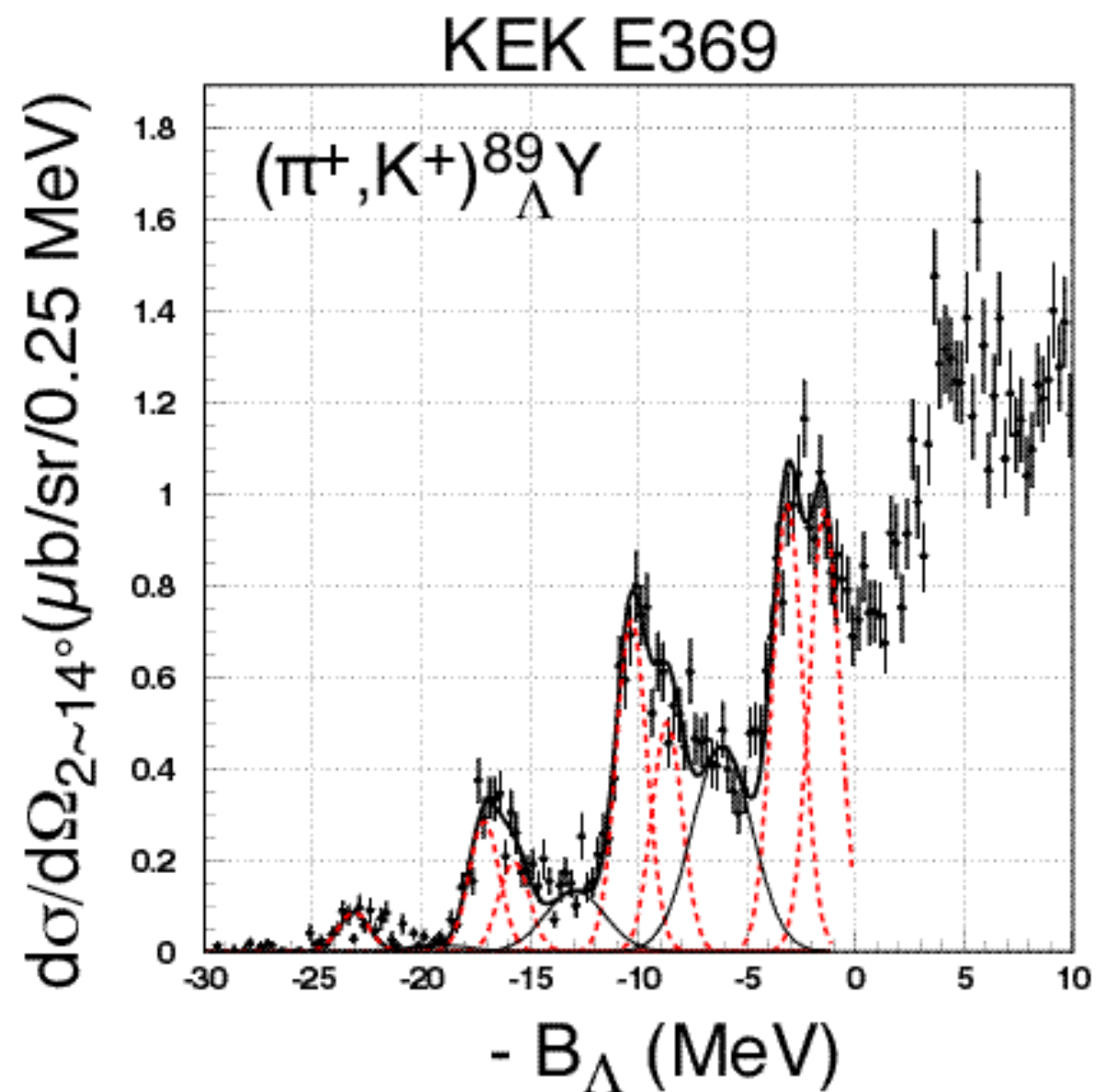


E336: $\Lambda^7\text{Li}$, $\Lambda^{13}\text{C}$, $\Lambda^{16}\text{O}$



E369: $\Lambda^{89}\text{Y}$

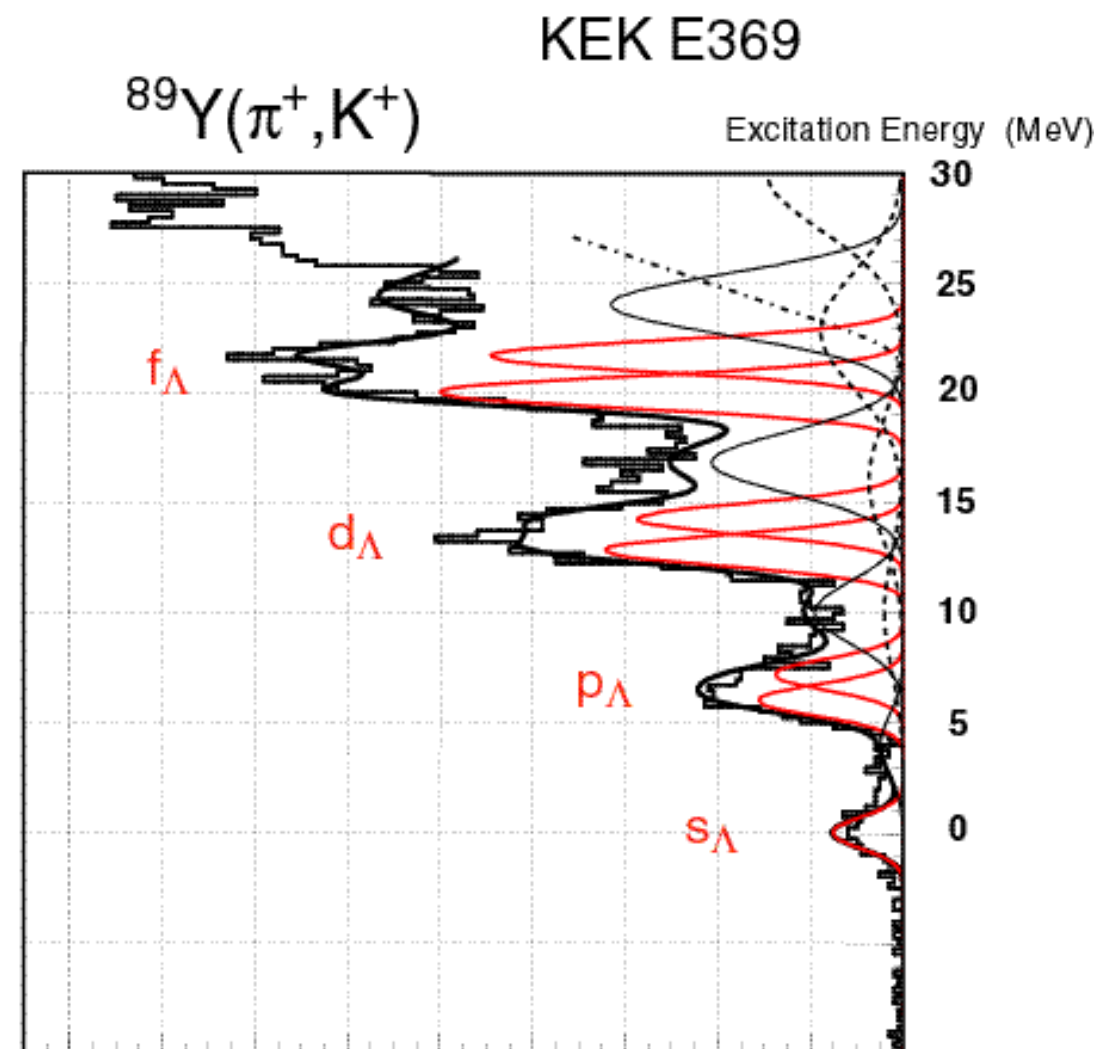
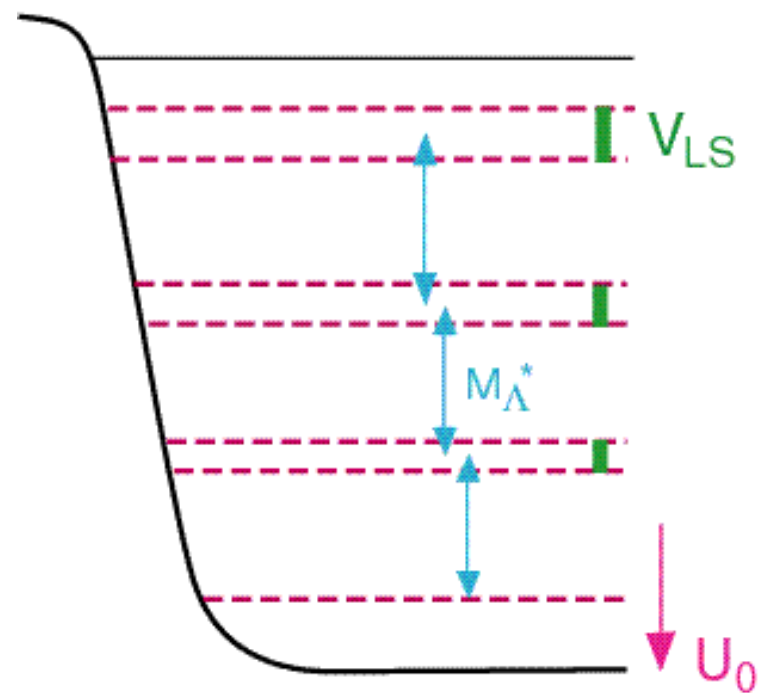
- $B_{\Lambda S} = 23.1 \pm 0.1$ MeV
- Energy Splitting
 - $\Delta E_f = 1.70 \pm 0.10$ MeV
 - $\Delta E_d = 1.63 \pm 0.14$ MeV
 - $\Delta E_p = 1.37 \pm 0.20$ MeV
- Peak Ratio
 - $R/L_f = 0.99 \pm 0.07$
 - $R/L_d = 0.69 \pm 0.06$
- Extra n-hole at $+4.1 \pm 0.1$ MeV, width = 3.2 ± 0.2 MeV



Single-particle motion of Λ in heavy hypernuclei

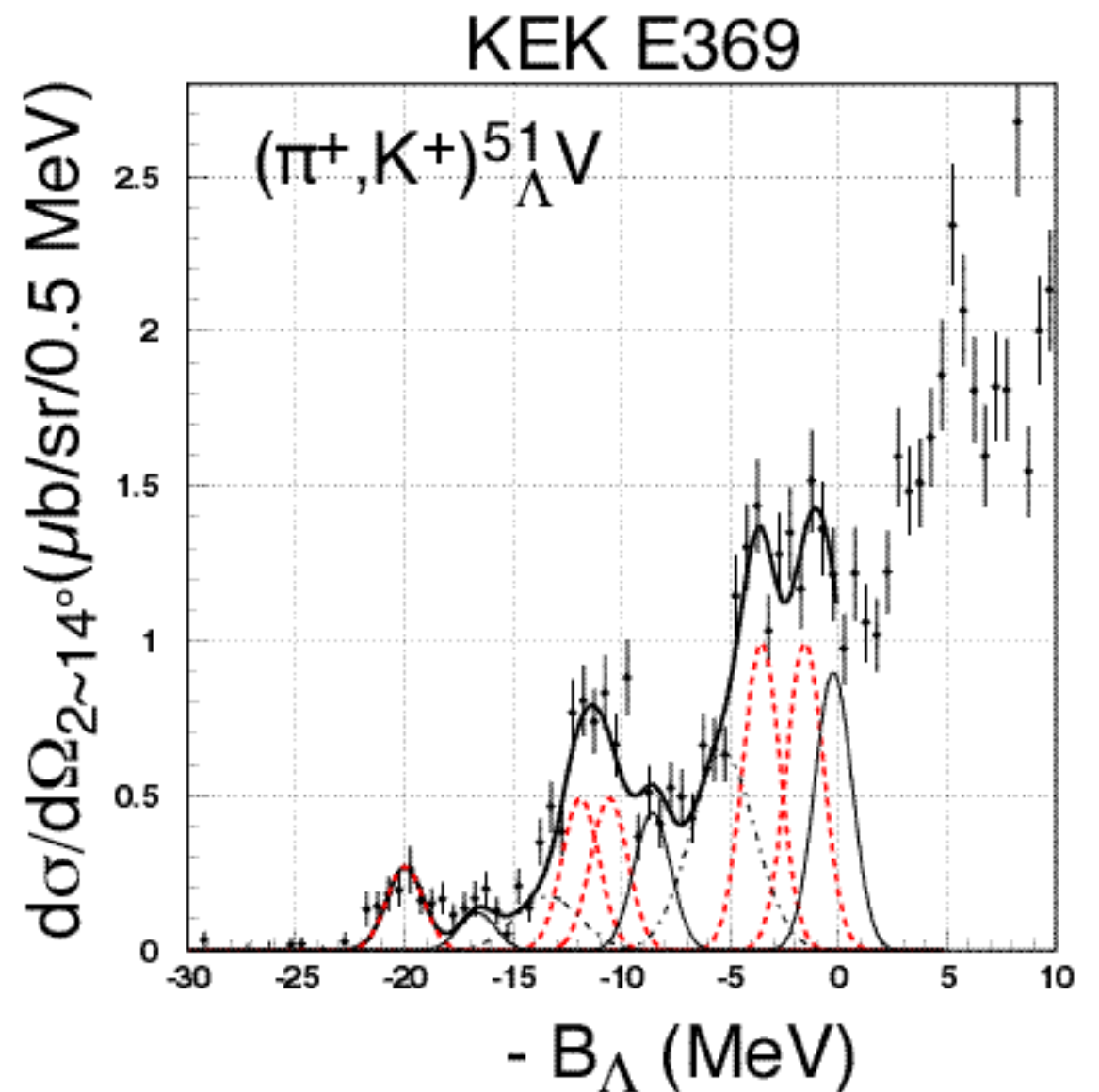
- $U_0 = -30.5$ MeV
- $M_{\Lambda}^* = 0.7 \sim 0.8 \times M_{\Lambda}$

by Y. Yamamoto



E369: $\Lambda^5 1V$

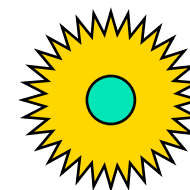
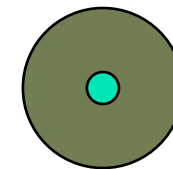
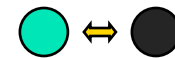
- Splitting in d-(and p-) orbit(s)
- $B_{\Lambda S} = (20 \pm 0.13) + 0.56$ MeV
- Width = 1.95 MeV
- Peak Ratio = 1 (fixed)
 - Extra n-holes
 - At $+3.3 \pm 0.2$ MeV, width = 1.95 MeV
 - At $+6.6 \pm 0.2$ MeV, width = 3.46 MeV



Heavy Λ -Hypernuclei

■ *A bridge to strange matter*

- 2-body Y-N interaction
 - Baryon-baryon interactions in $SU(3)_f$
 - Short range part: meson picture or quark picture ?
- Light hypernuclei ($A < \sim 20$)
 - Fine structure \longleftrightarrow Spin-dependent interactions
 - Cluster structure
- Heavy hypernuclei ($A > \sim 80$)
 - Single-particle potential: $U_0(r), m_{\Lambda}^*(r), V_{\Lambda NN}, \dots$
- Neutron star ($A \sim 10^{57}$): $\rho > 5 \rho_0$
 - Hyperonization \longrightarrow Softening of E.O.S.
 - Superfluidity



E52 I: Production of neutron-rich Λ hypernuclei by the (π^-, K^+) double-charge-exchange reaction

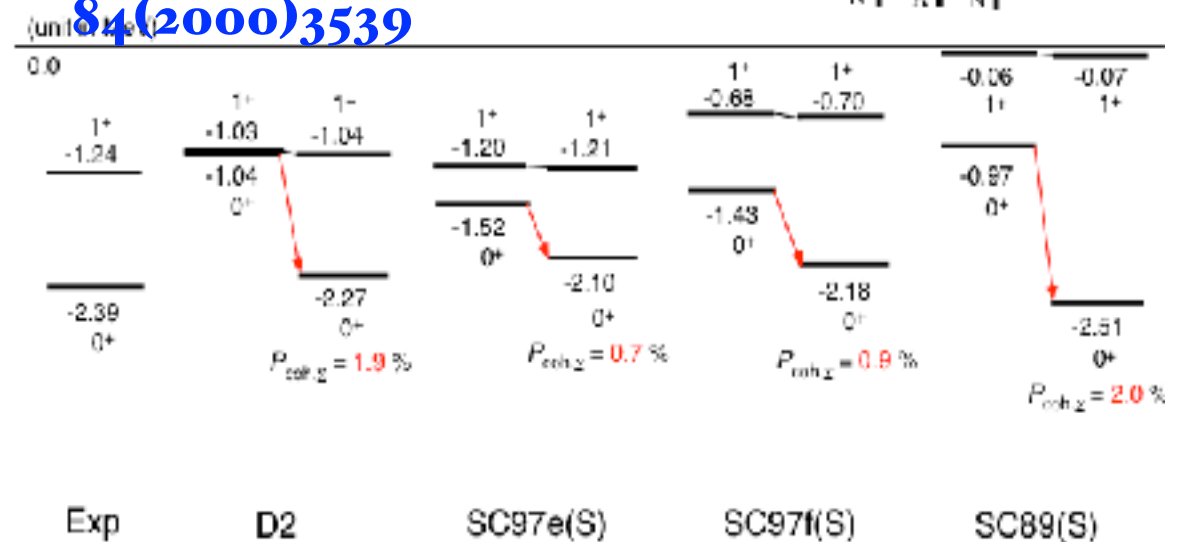
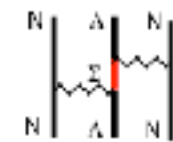
A pilot experiment for spectroscopic studies of
the neutron-rich Λ hypernuclei via the (π^-, K^+) reaction

Production cross section/ Background (sensitivity)
⇒ Understanding of the Reaction Mechanism

Akaishi et al.
PRL

84(2000)3539

^4He



Λ - Σ coherent coupling in $A=4$ hypernuclei



...solved an underbinding problem,
known as an overbinding problem in

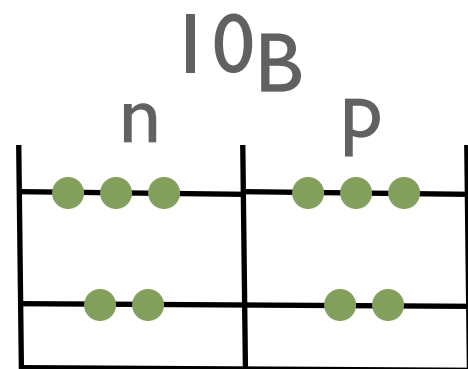


Y.Akaishi *et al.*, PRL84(2000)3539

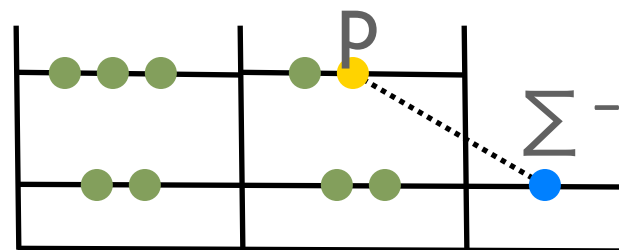
To be confirmed/examined in other examples

In the (π, K^+) reaction...

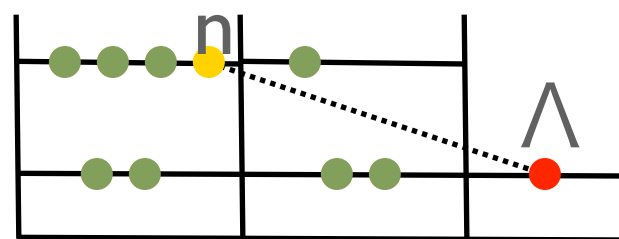
(KEK-E521, Fukuda *et al.*)



Two-step

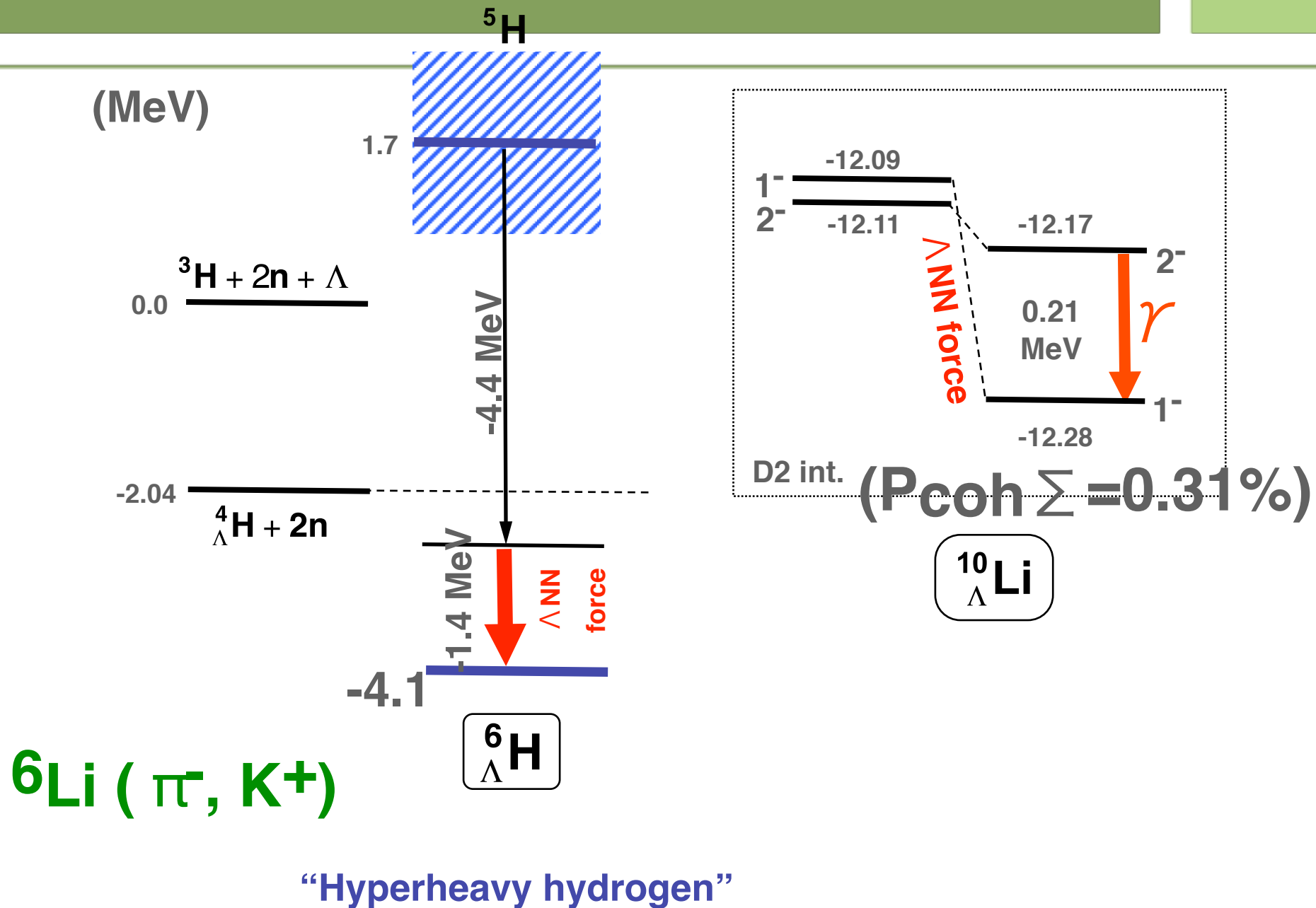


Coherent coupling



Effect of Coherent Σ mixing in n-rich hypernuclei

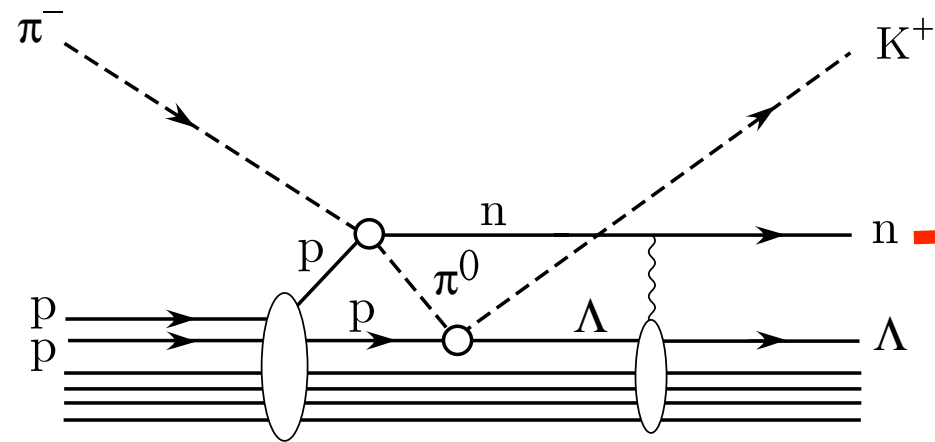
Superheavy hydrogen



Reaction mechanism

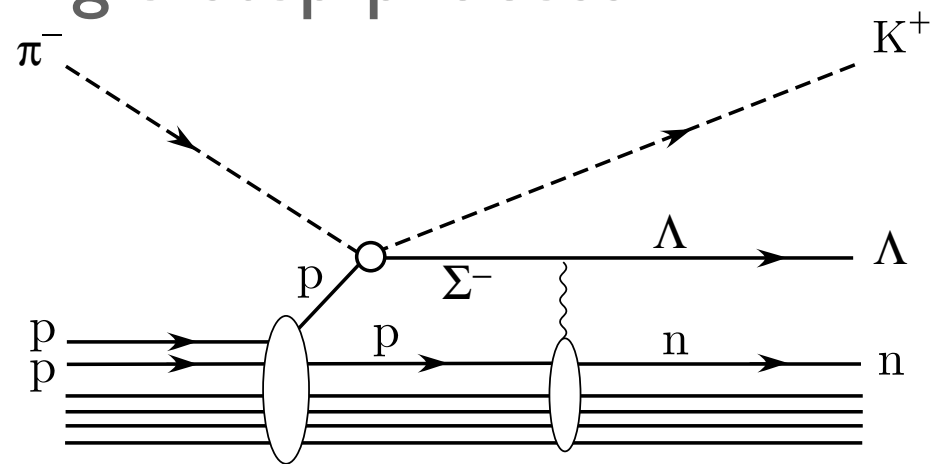
Tretyakova, Akaishi et al.

► Two-step process:



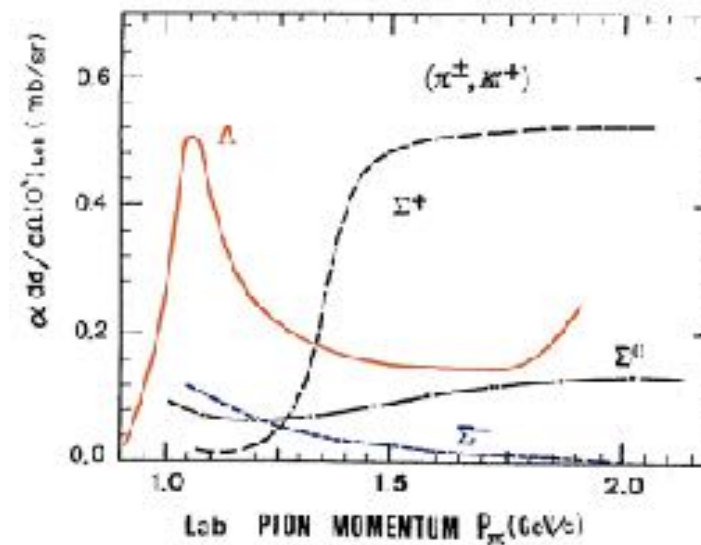
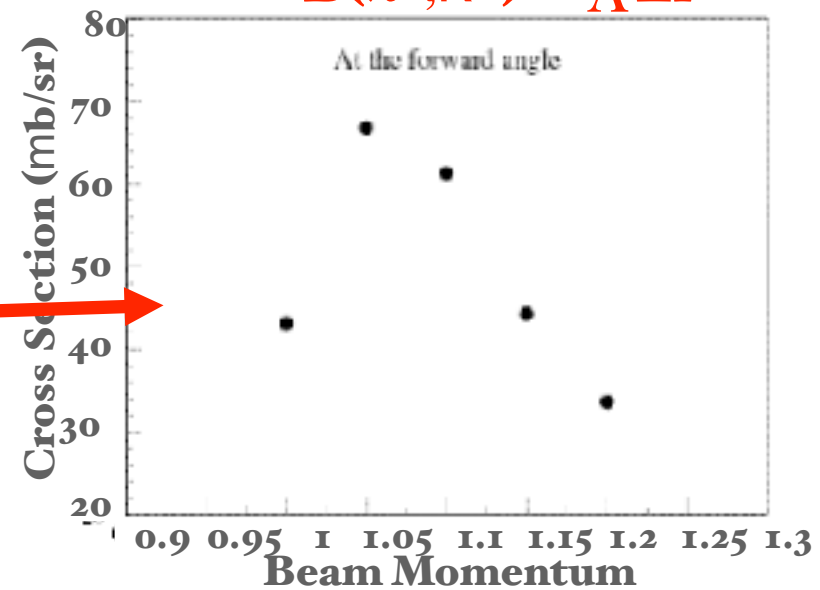
(a)

► Single-step process



(b)

$^{10}\text{B}(\pi^-, \text{K}^+)^{10}\text{B} \Lambda \text{Li}$



Experimental Results

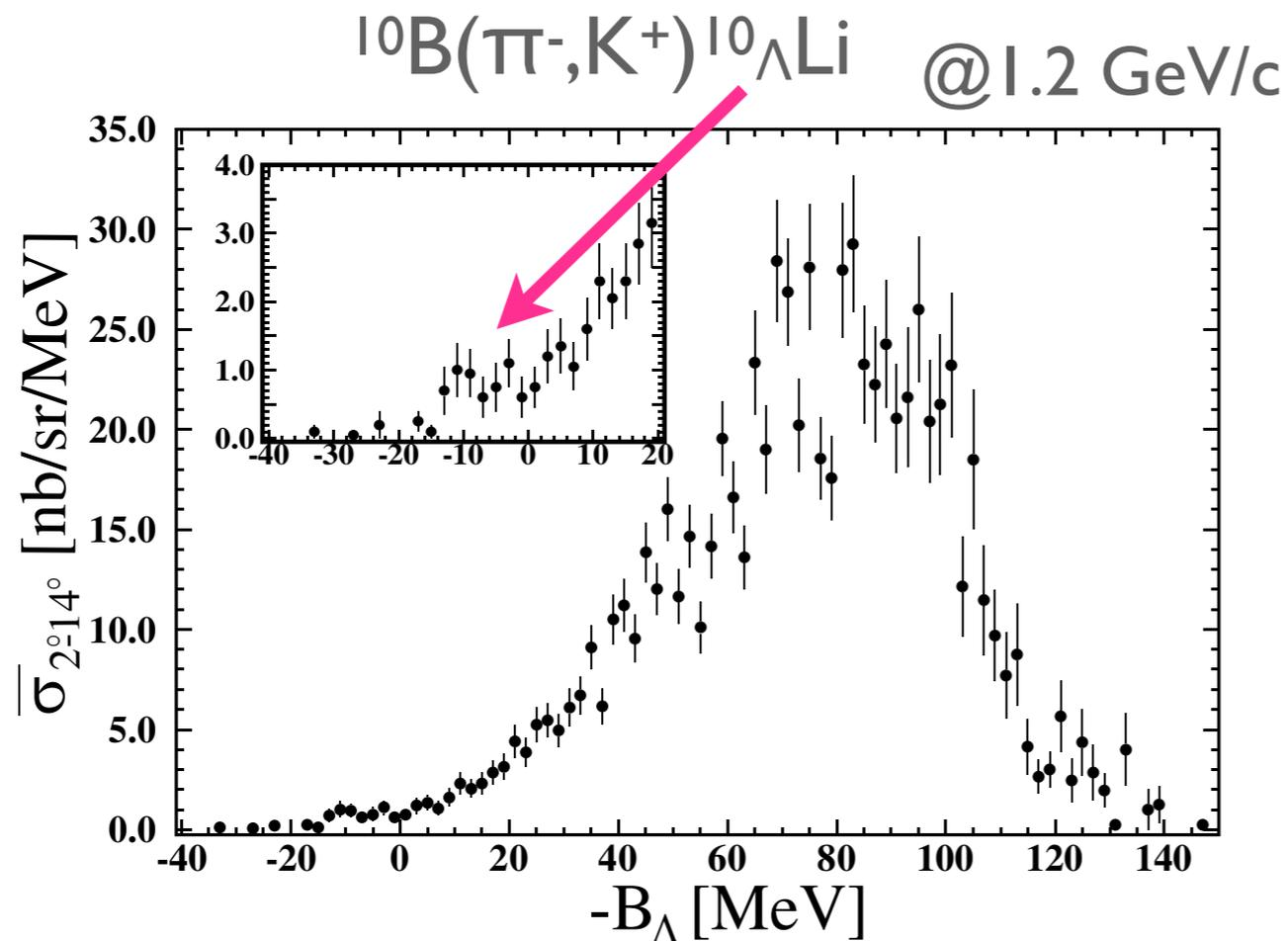


FIG. 3. Missing-mass spectrum of the (π^-, K^+) reaction on a ^{10}B target at 1.2 GeV/c. The horizontal and vertical axes are the same as Fig. 2. An expanded view near the Λ bound region is shown in the inset.

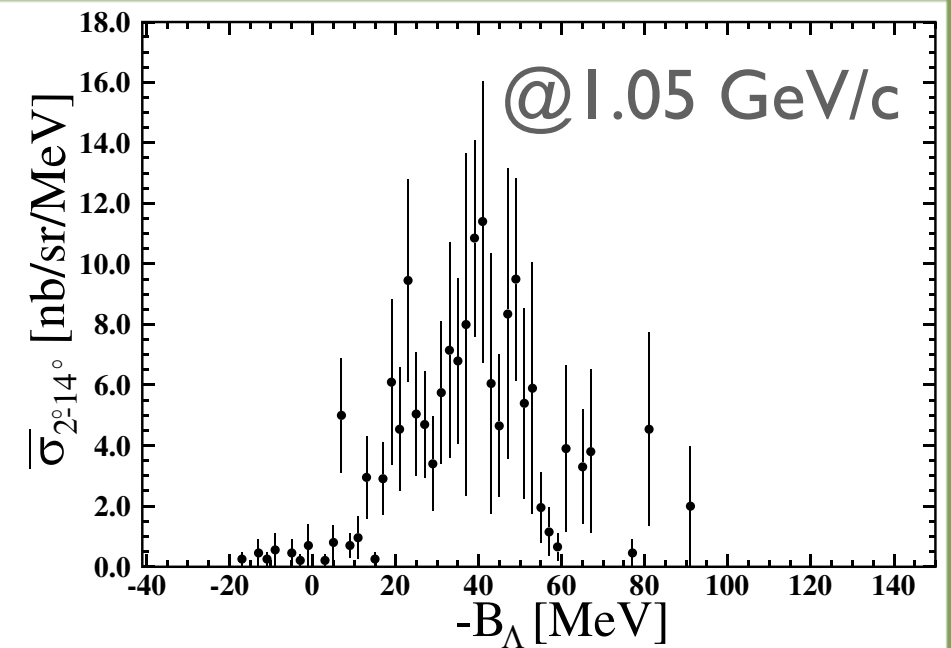


FIG. 2. Missing-mass spectrum of the (π^-, K^+) reaction on a ^{10}B target at 1.05 GeV/c. The horizontal axis shows the binding energy of a Λ , whereas the vertical axis shows the cross section in terms of nb/sr/MeV.

Ratio of the Λ production cross section (π^-, K^+) to (π^+, K^+)

TABLE I. Hypernuclear production cross sections for the bound region averaged over the scattering angle from 2° to 14° . The cross section with an asterisk shows a lower limit by extrapolating the quasifree components linearly. The quoted errors are statistical.

Reaction	Cross Section	
	1.05 GeV/c	1.2 GeV/c
$^{12}\text{C}(\pi^+, K^+)_{\Lambda}^{12}\text{C}$	$18.0 \pm 0.7 \mu\text{b/sr}$	$17.5 \pm 0.6 \mu\text{b/sr}$
$^{10}\text{B}(\pi^+, K^+)_{\Lambda}^{10}\text{B}$	$7.8 \pm 0.3 \mu\text{b/sr}$	
$^{10}\text{B}(\pi^-, K^+)_{\Lambda}^{10}\text{Li}$	$5.8 \pm 2.2 \text{ nb/sr}$	$11.3 \pm 1.9 \text{ nb/sr}$ $9.6 \pm 2.0^* \text{ nb/sr}$

Σ mixing ?

- ▶ T. Harada et al., PRC 79 (2009) 014603.

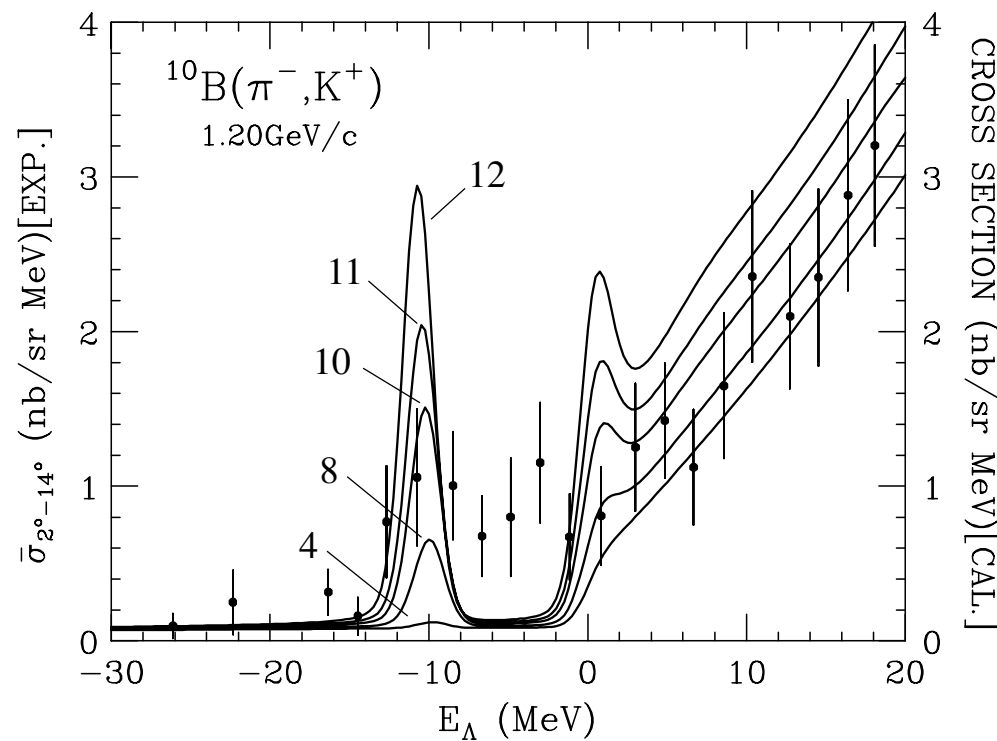


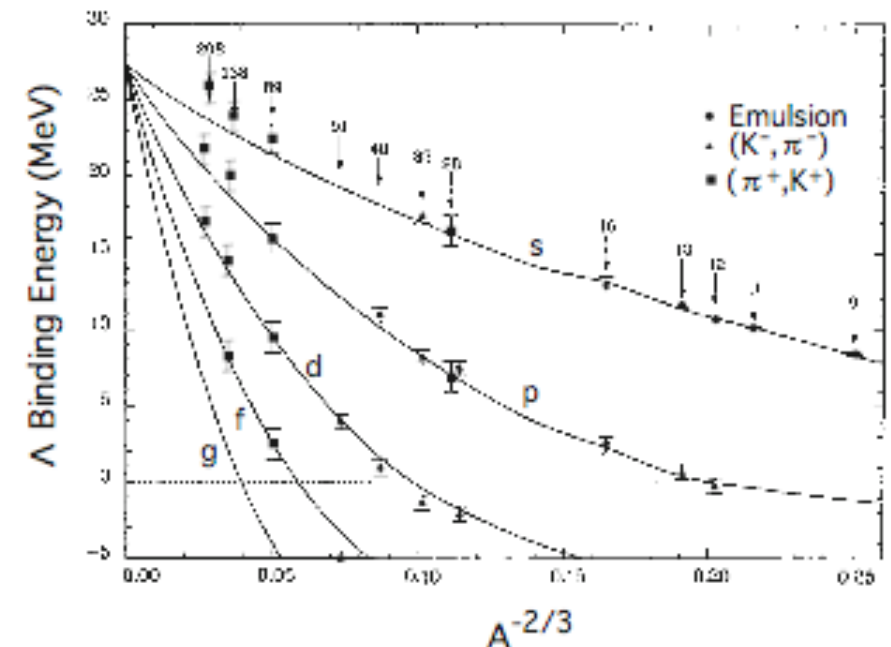
FIG. 3. Calculated inclusive Λ spectra obtained by the one-step mechanism near the Λ threshold in the $^{10}\text{B}(\pi^-, K^+)$ reaction at 1.20 GeV/c (6°), by changing $V_{\Sigma\Lambda}$ for the Λ - Σ coupling potential. The experimental data are taken from Ref. [12]. The solid curves denote $V_{\Sigma\Lambda} = 4, 8, 10, 11,$ and 12 MeV when $-W_\Sigma = 20$ MeV, with a detector resolution of 2.5 MeV FWHM.

$$P_\Sigma \sim 0.47 - 0.68\%$$

Summary

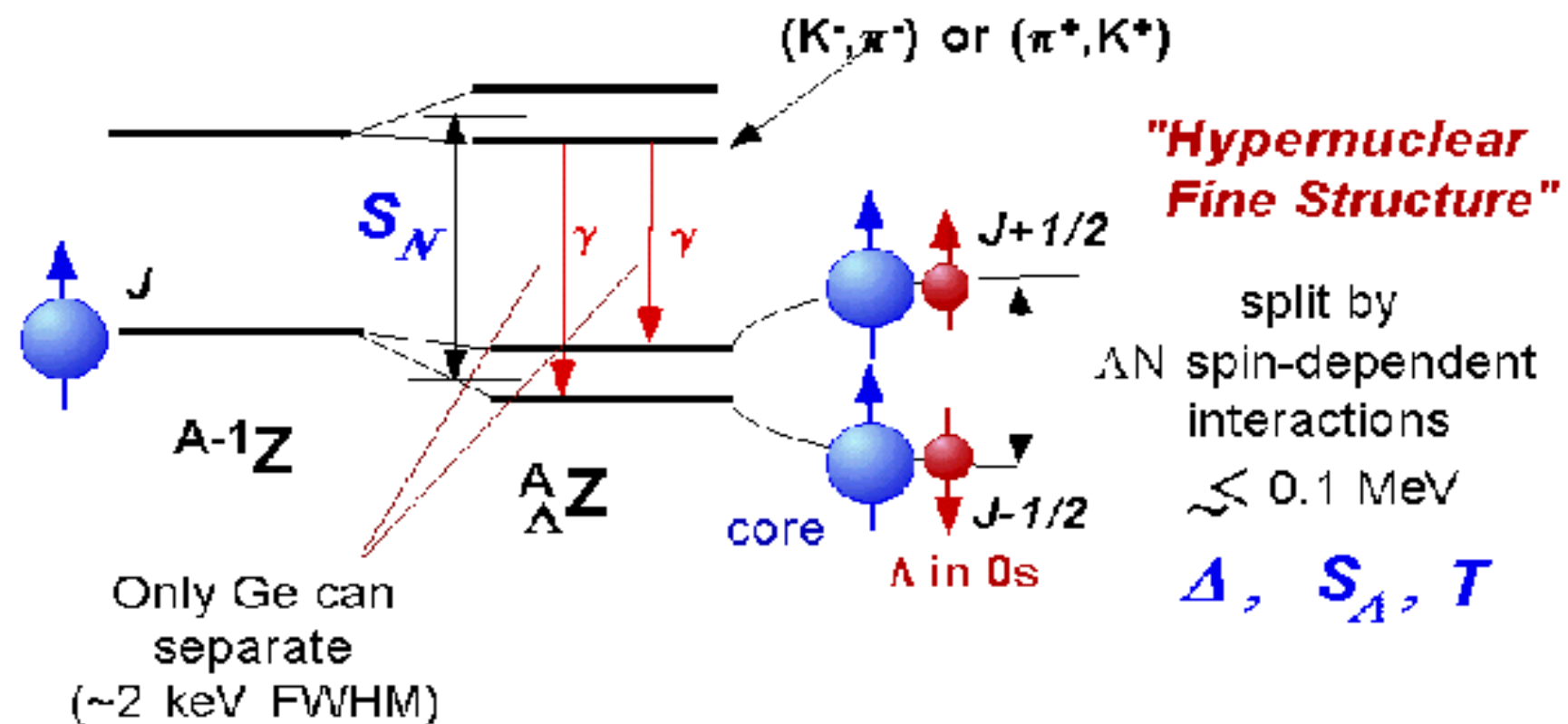
on (π, K) spectroscopy

- ▶ The (π, K) Spectroscopy has been successful.
 - ▶ Gross feature of Single-particle levels of Λ
 - ▶ Effective for Heavy Λ hypernuclei
 - ▶ *High-resolution spectroscopy ($\Delta E \sim 0.2$ MeV) will be interesting*
 - ▶ Possibility to study neutron-rich hypernuclei with (π^-, K^+)



γ spectroscopy

- Low-lying levels of Λ hypernucleus



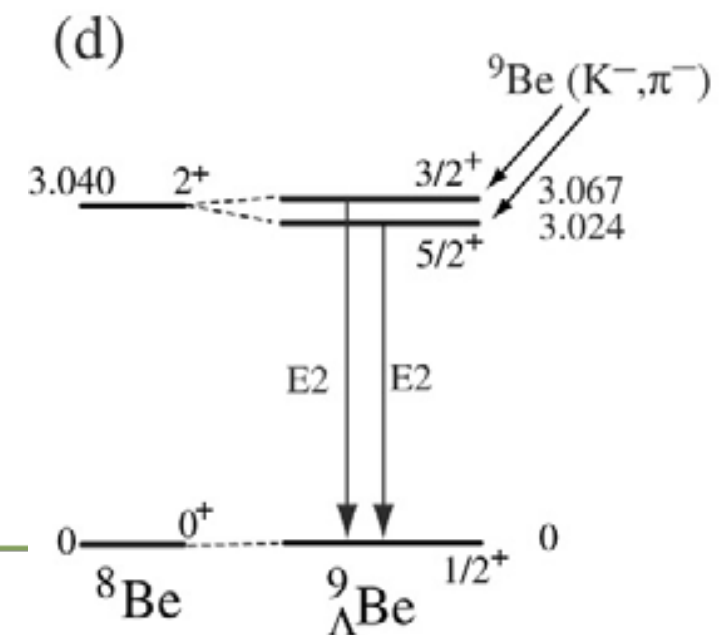
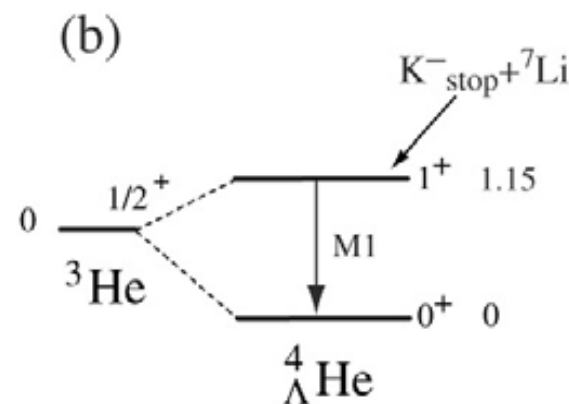
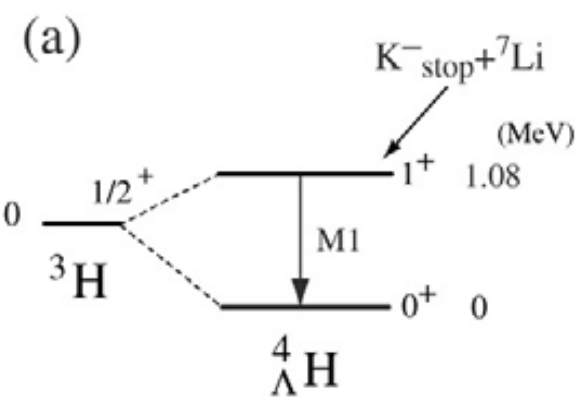
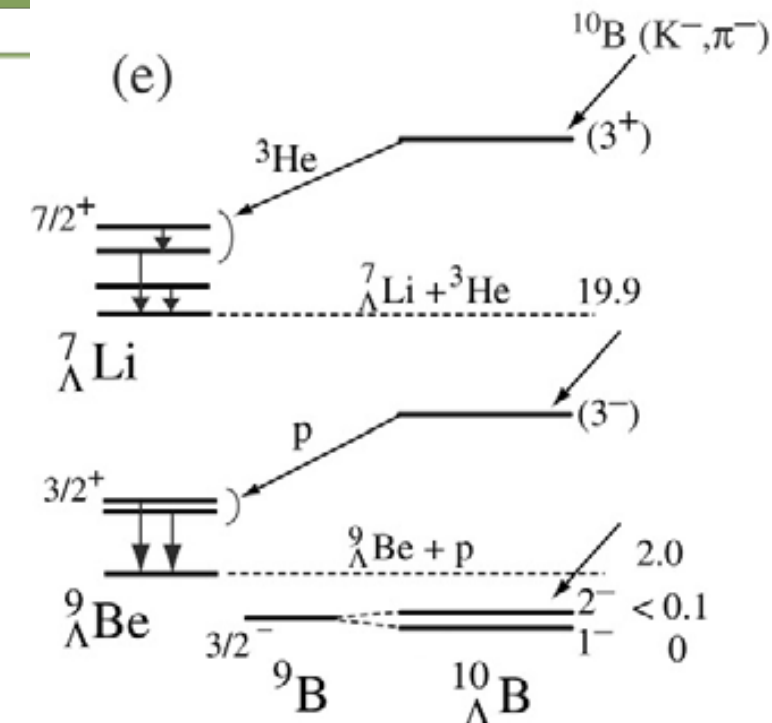
- 2-body ΛN effective interaction

$$V_{\Lambda N}^{\text{eff}} = V_0(r) + \underbrace{V_\sigma(r)}_{\Delta} \vec{s}_A \vec{s}_N + \underbrace{V_\Lambda(r)}_{S_A} \vec{l}_{\Lambda N} \vec{s}_A + \underbrace{V_N(r)}_{S_N} \vec{l}_{\Lambda N} \vec{s}_N + \underbrace{V_T(r)}_T S_{12}$$

p-shell : 4 radial integrals for $p_N s_A$ w.f.

Hypernuclear γ -rays before Hyperball

${}^4_{\Lambda}\text{H}, {}^4_{\Lambda}\text{He}$	$1.10 \pm 0.04 \text{ MeV}$	Nal
${}^7_{\Lambda}\text{Li}$	$2.034 \pm 0.023 \text{ MeV}$	Nal
${}^9_{\Lambda}\text{Be}$	$3.079 \pm 0.04 \text{ MeV}$	Nal
${}^{10}_{\Lambda}\text{B}$	not observed	Ge



Hyperball

(Tohoku/ Kyoto/ KEK, 1998)

- Large acceptance for small hypernuclear γ yields

Ge (r.e. 60%) x 14

$\Delta\Omega \sim 15\%$

$\eta_{\text{peak}} \sim 3\%$ at 1 MeV

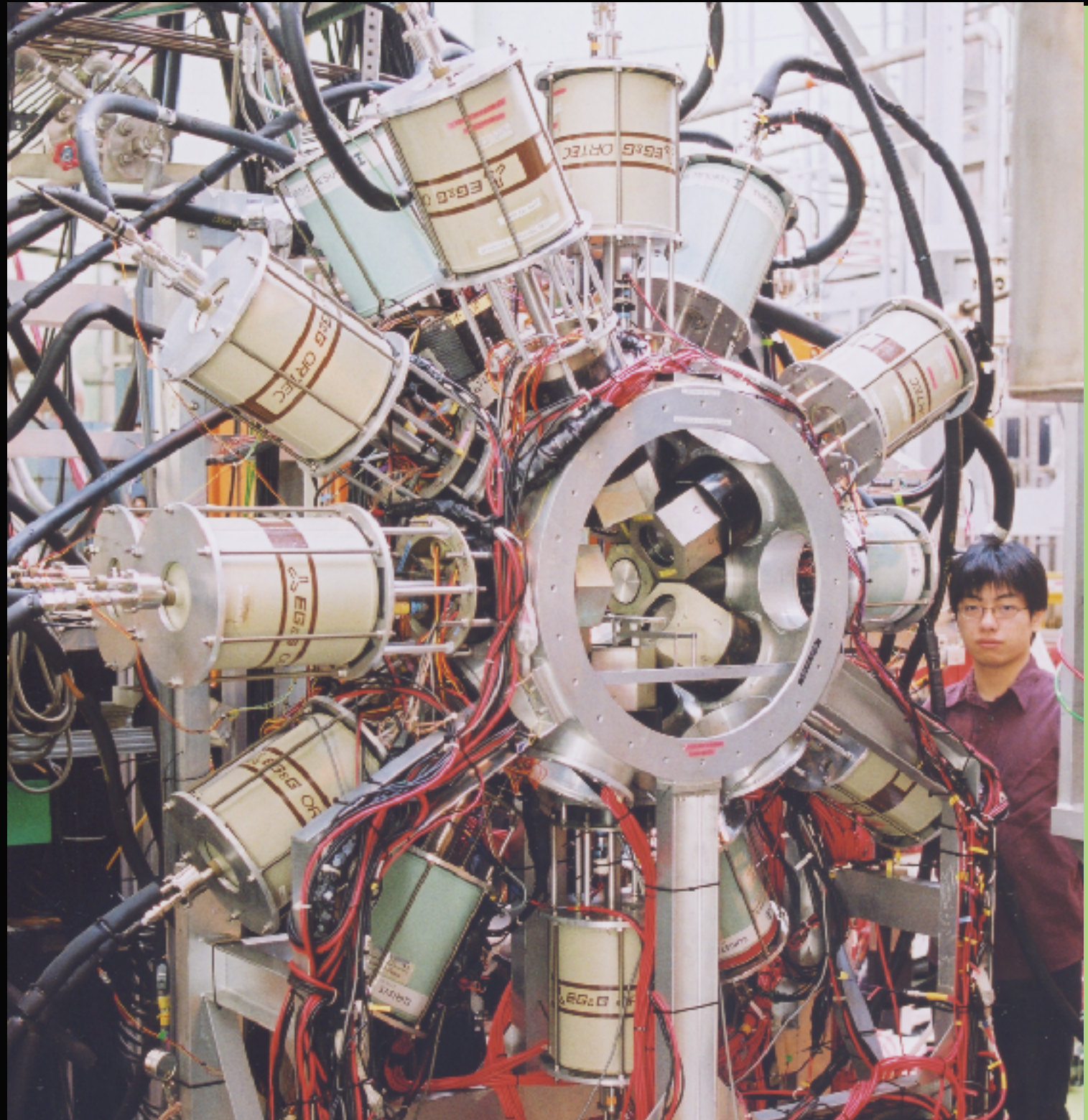
- High-rate electronics for huge background

1 TeV/sec, 100 kHz

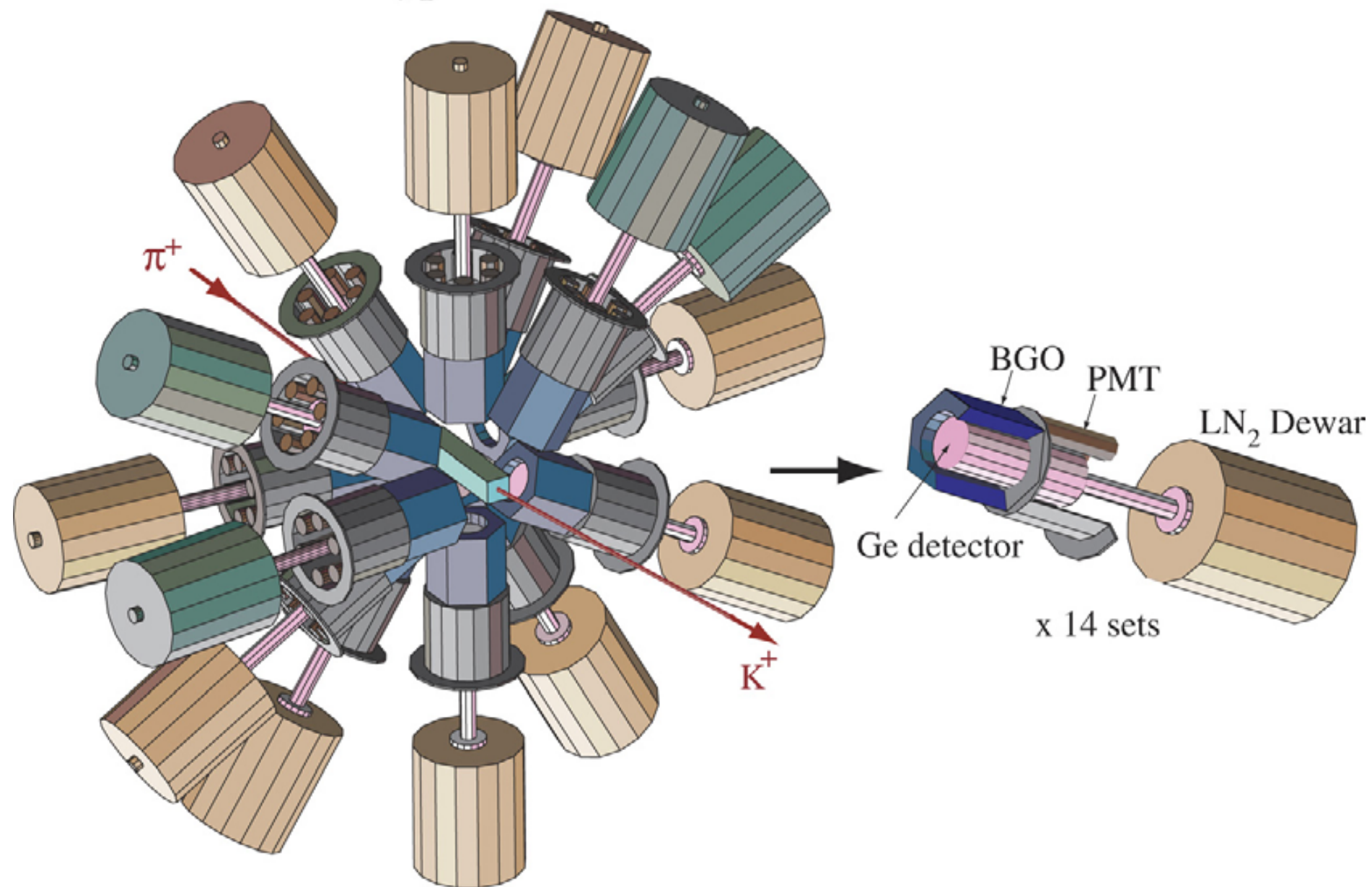
- BGO counters for π^0 and Compton suppression

Resolution of hypernuclear spectroscopy

1 MeV \rightarrow 2 keV FWHM



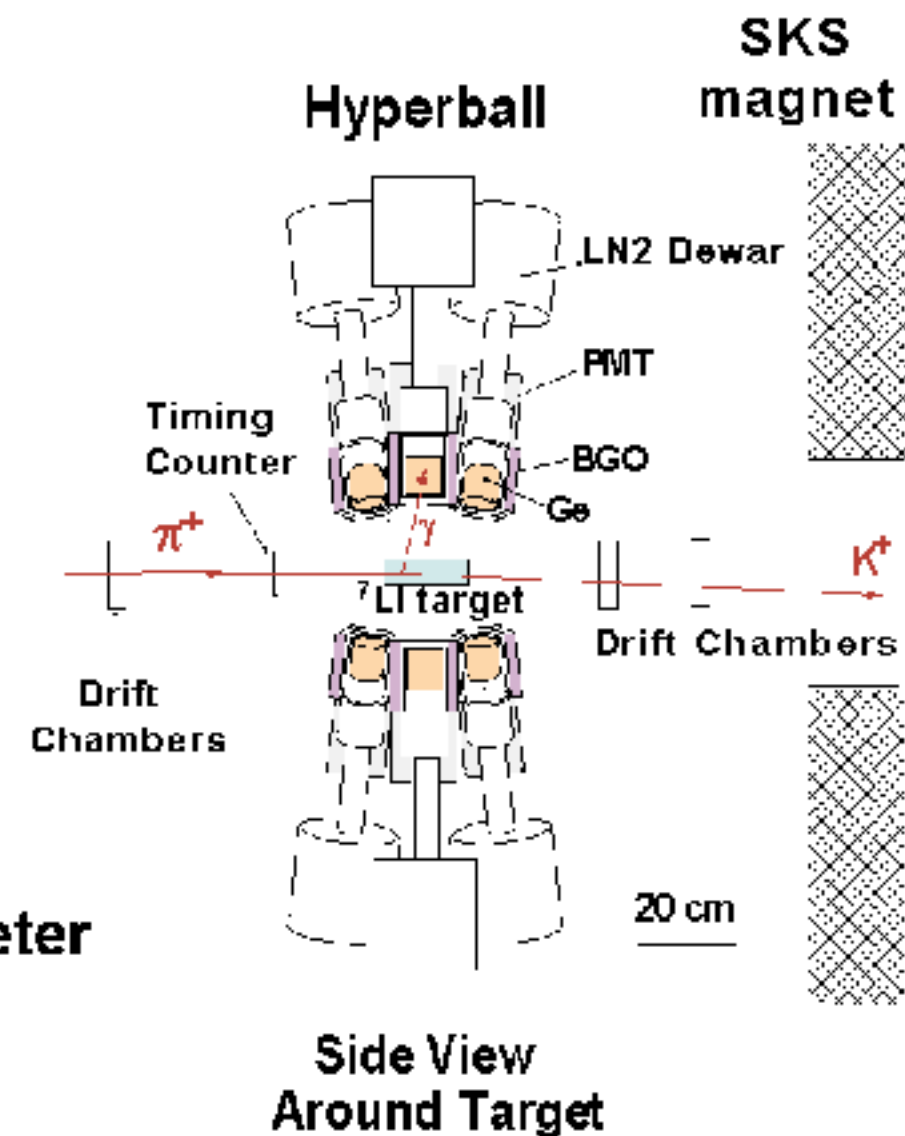
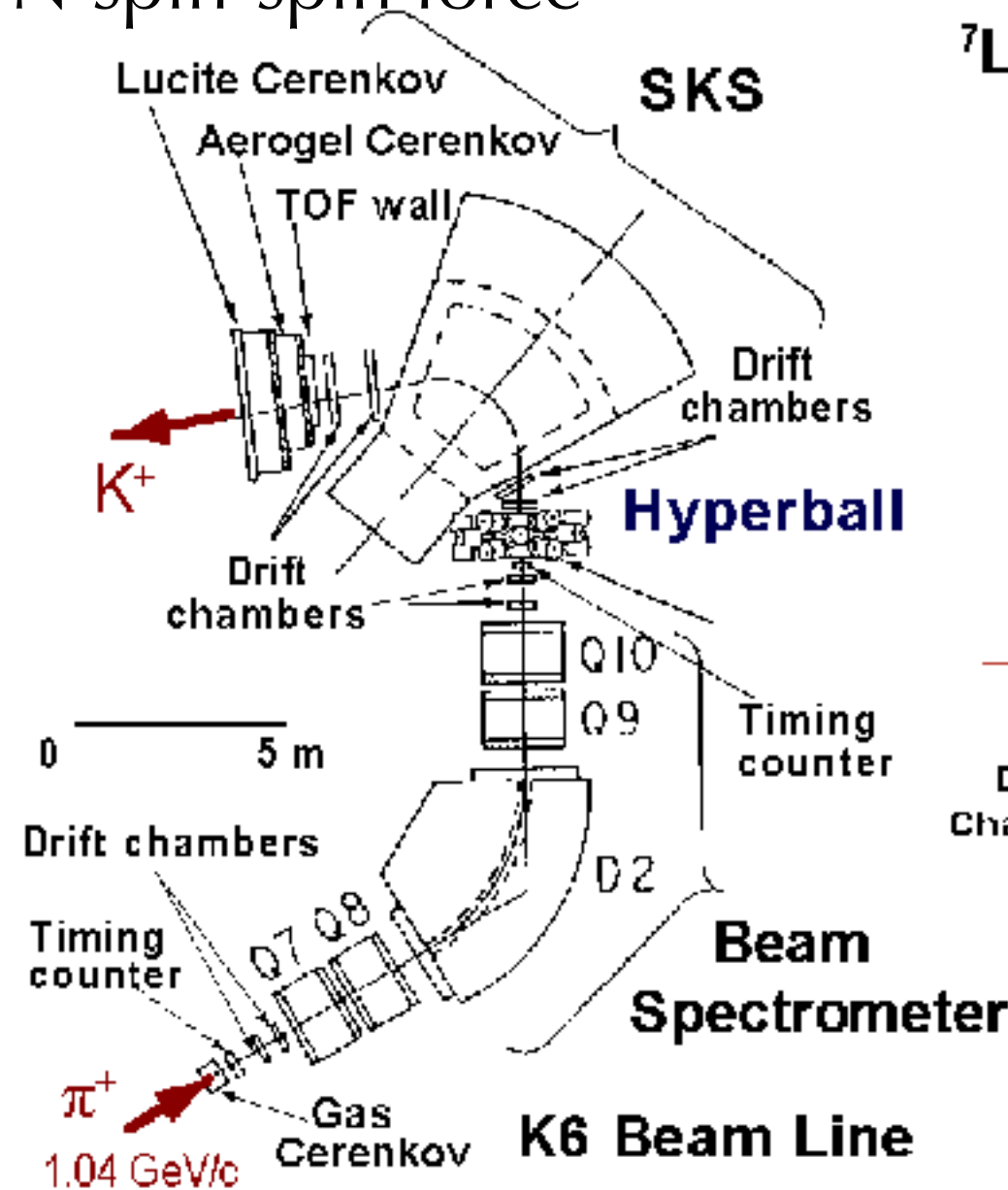
Hyperball



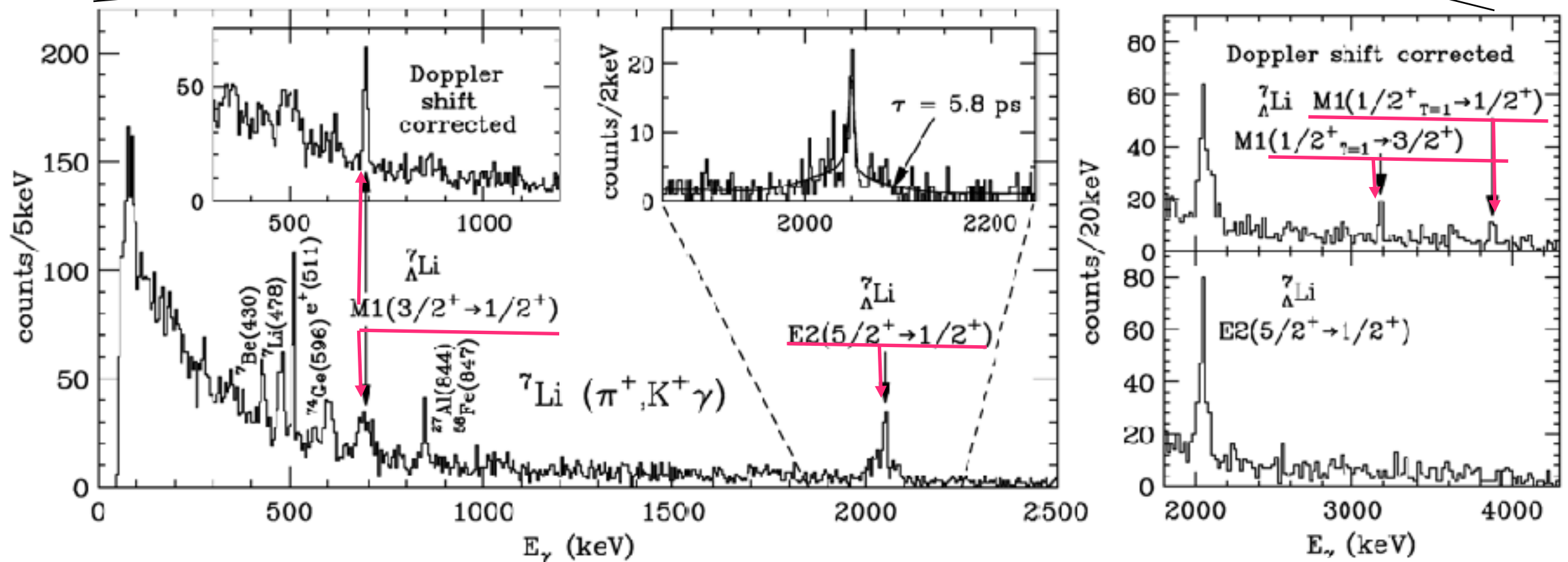
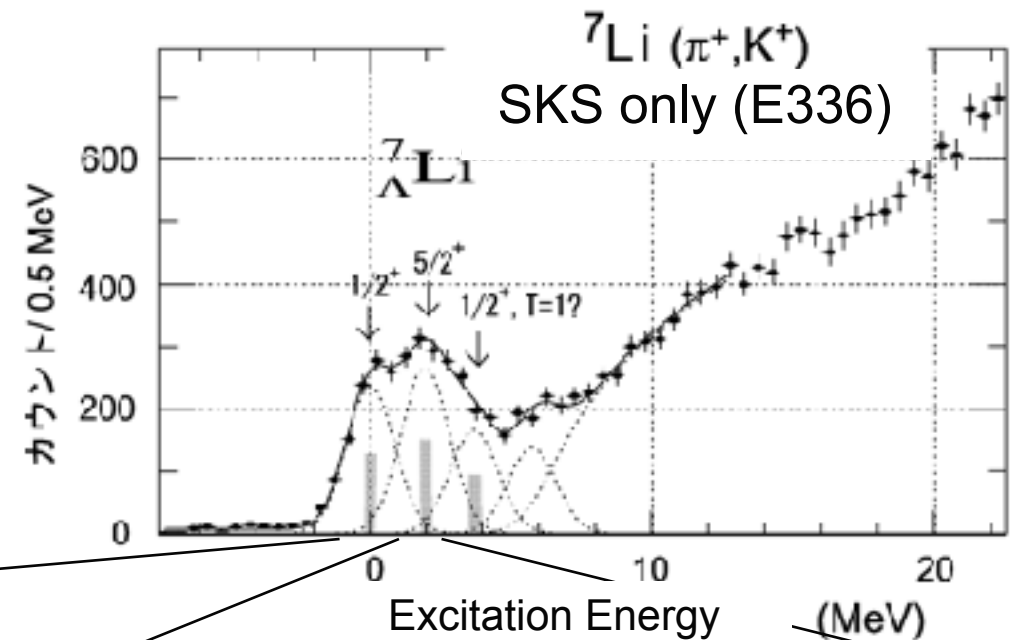
E419: γ spectroscopy of ${}^7_{\Lambda}\text{Li}$

- ▶ First exp. with Hyperball
- ▶ B(E2) \rightarrow shrinking effect
- ▶ Spin-flip M1 \rightarrow Λ N spin-spin force

Setup for KEK-E419

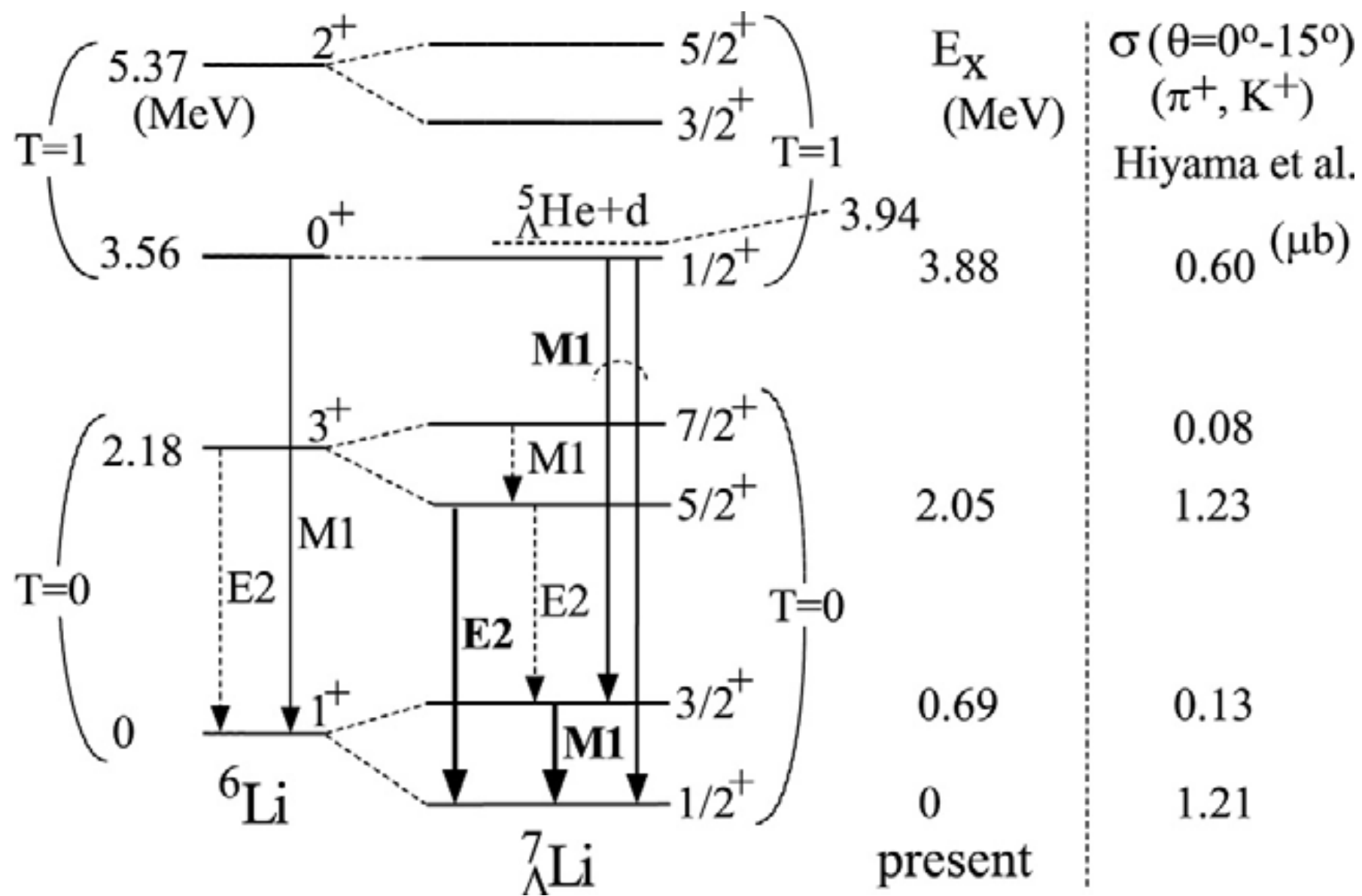


E419: SKS+Hyperball



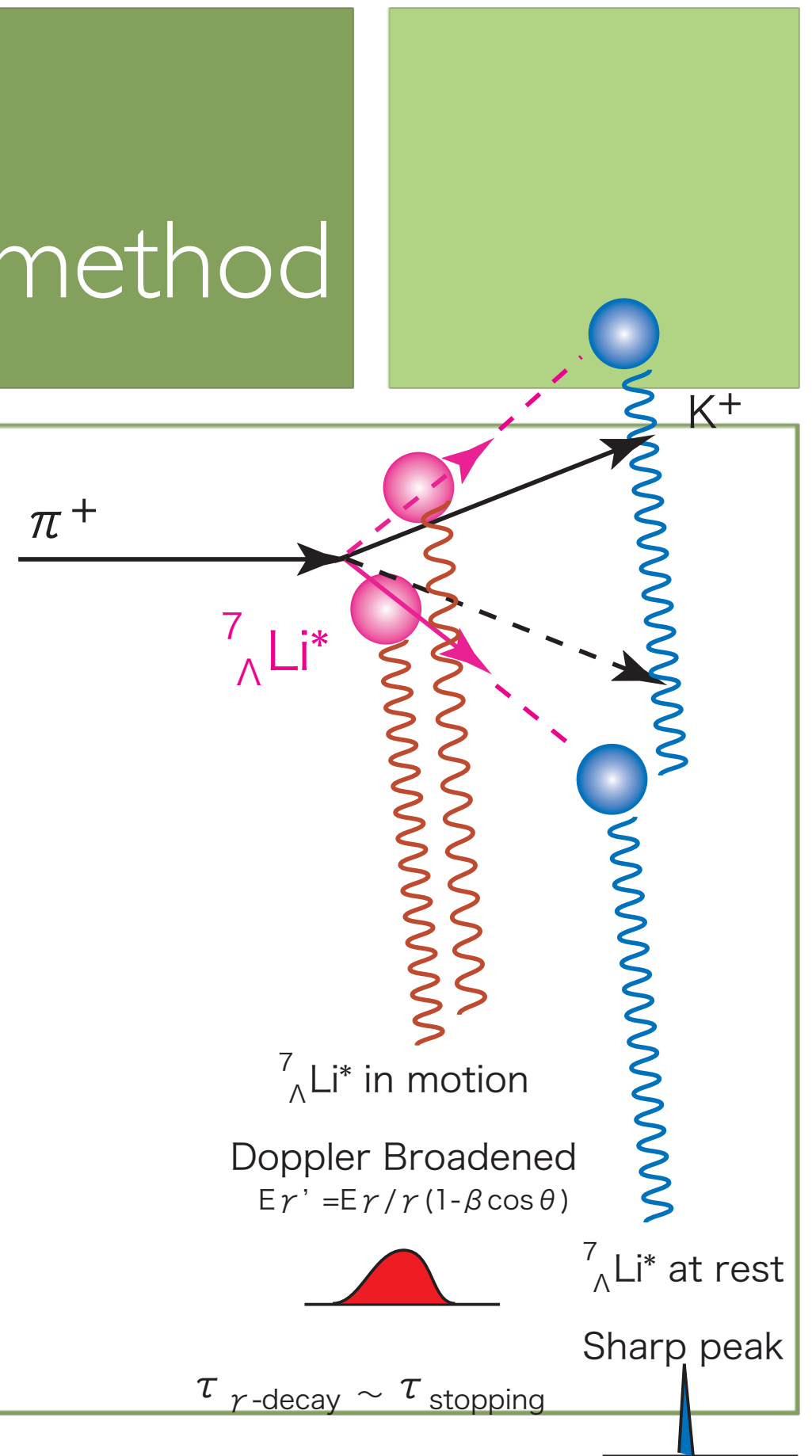
Tamura et al., PRL 94(2000) 5963

First observation of well-identified hypernuclear γ rays with Ge.



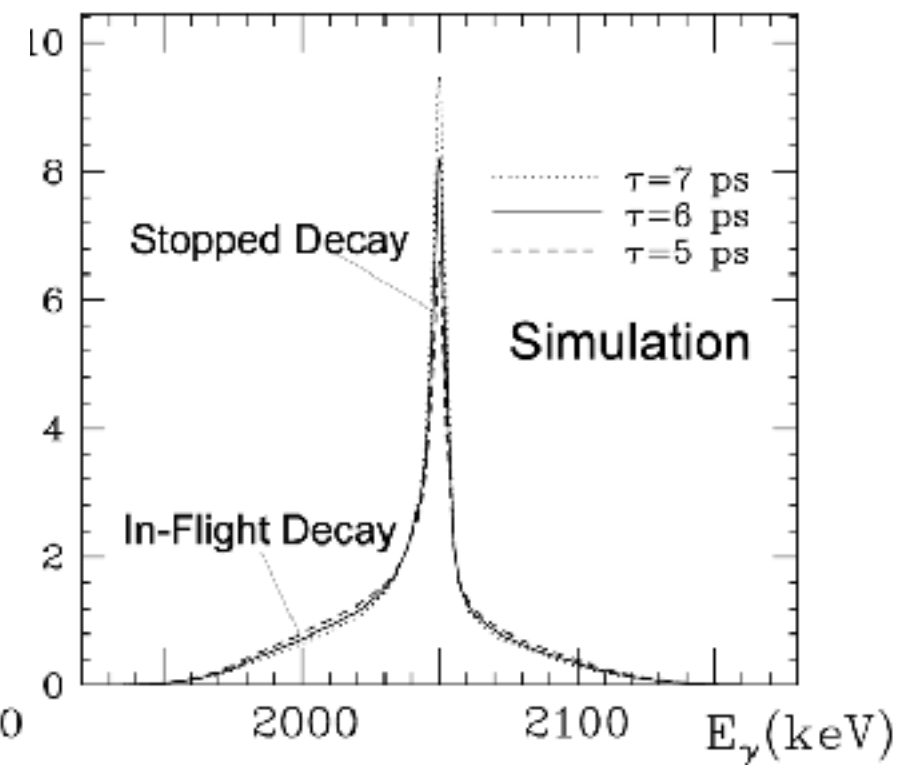
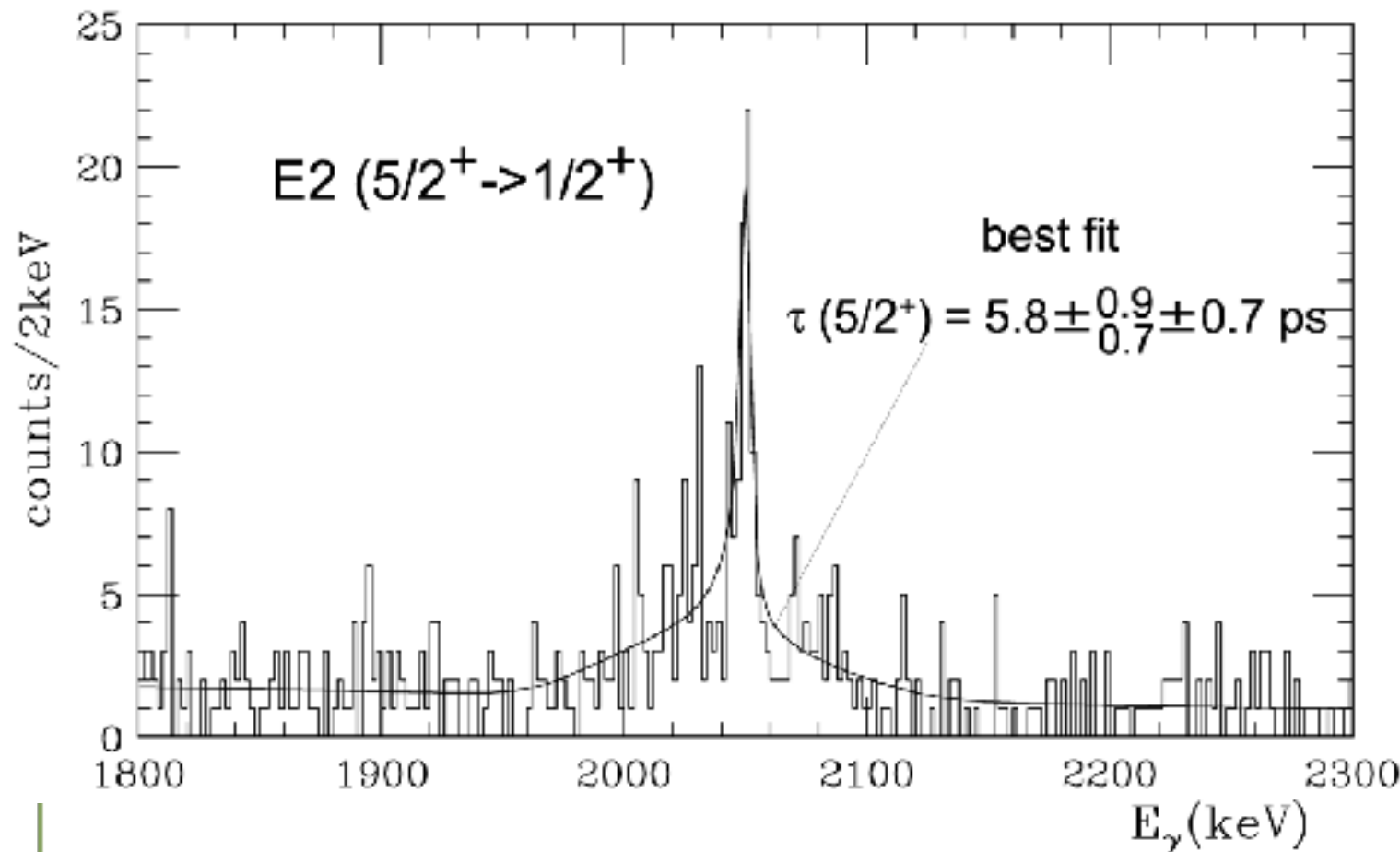
Doppler shift attenuation method

- ▶ $\tau_{\gamma\text{-decay}} \sim \tau_{\text{stopping}}$
- ▶ 5.8 ps 13 ps
- ▶ mixture of a sharp peak and a broad peak



Lifetime and B(E2)

Lifetime Measurement
using Doppler Shift Attenuation Method



$$\Gamma(E2; 5/2^+ \rightarrow 1/2^+) = BR / \tau (5/2^+) = 1.22 \times 10^9 E^5 B(E2)$$

$$BR = 93.6 \pm 3.8 \%$$

$$[\text{weak decay } (230 \pm 40 \text{ ps})^{-1}, BR(5/2^+ \rightarrow 3/2^+) = 3.8 \pm 0.5 \%$$

$$\Rightarrow B(E2) = 3.6 \pm 0.5 \pm 0.5_{0.4} e^2 \text{fm}^4$$

B(E2)

$$\Gamma(E(M)\lambda : I_i \rightarrow I_f) = \frac{8\pi(\lambda + 1)}{\lambda[(2\lambda + 1)!!]^2} \frac{1}{\hbar} \left(\frac{\omega}{c}\right)^{2\lambda+1} B(E(M)\lambda; I_i \rightarrow I_f)$$

$$\begin{aligned} B(E(M)\lambda; I_i \rightarrow I_f) &= \sum_{\mu M_f} |\langle I_f M_f | \mathcal{M}(E(M)\lambda, \mu) | I_i M_i \rangle|^2 \\ &= \frac{1}{2I_i + 1} |\langle I_f || \mathcal{M}(E(M)\lambda) || I_i \rangle|^2 \end{aligned}$$

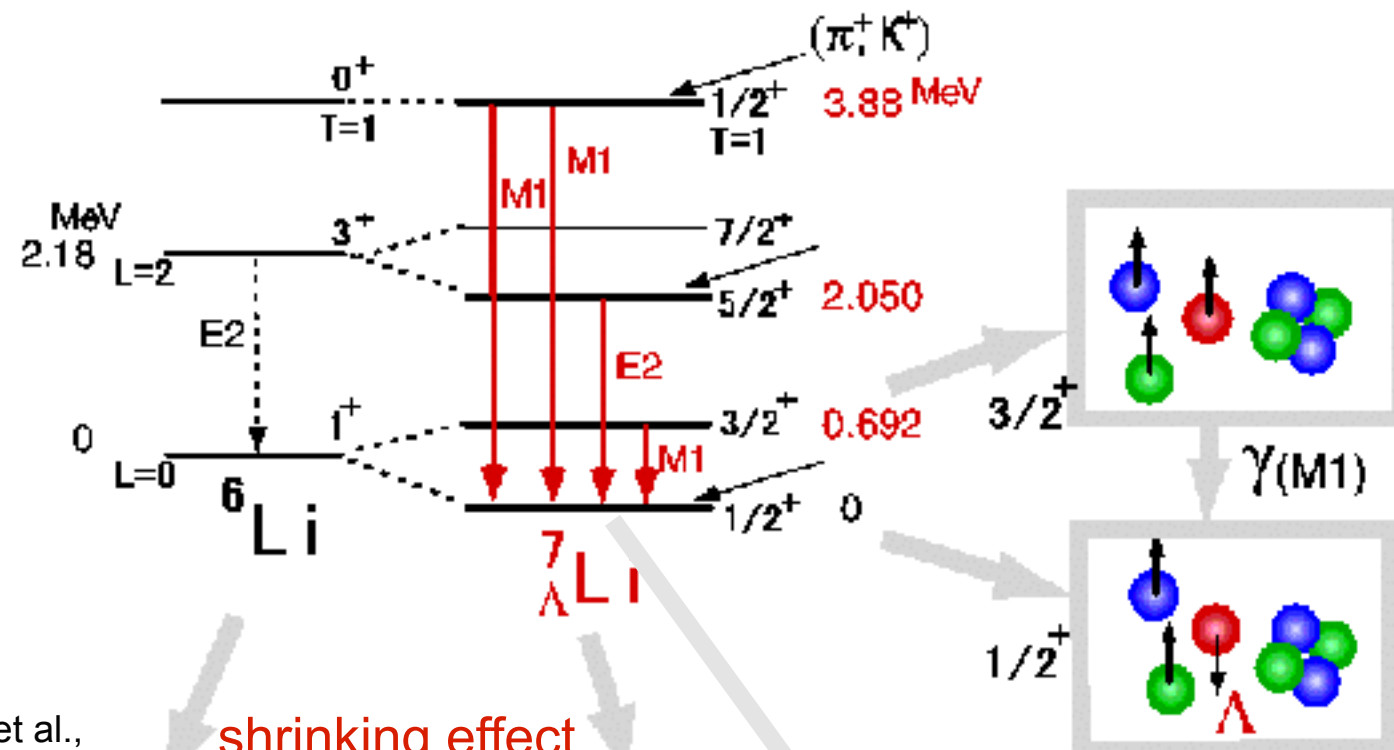
$$\mathcal{M}(E\lambda, \mu) = \int \rho(\vec{r}) r^\lambda Y_{\lambda\mu}(\hat{r}) d\tau$$

$$\mathcal{M}(M\lambda, \mu) = \frac{-1}{c(\lambda + 1)} \int \vec{j}(\vec{r}) \cdot (\vec{r} \times \nabla) r^\lambda Y_{\lambda\mu}(\hat{r}) d\tau$$

$$\Gamma(E1) = 1.59 \times 10^{15} (E)^3 B(E1)$$

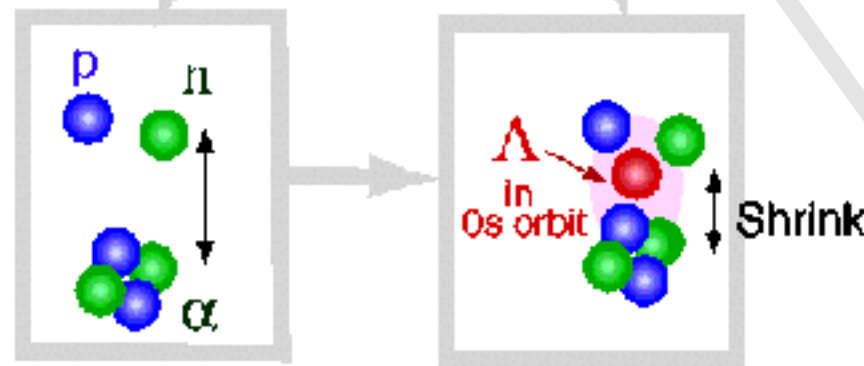
$$\Gamma(E2) = 1.22 \times 10^9 (E)^5 B(E2) \quad \text{in } e^2(\text{fm})^{2\lambda}$$

Summary on ${}^7_{\Lambda}\text{Li}$



Predicted by Motoba et al.,
Prog.Theor.Phys.
70 (1983) 189.

shrinking effect



spin-spin interaction

$$\Delta = 0.50 \text{ MeV}$$

N-LS interaction

$$S_N \sim -0.4 \text{ MeV}$$

PRL 84 (2000) 5983

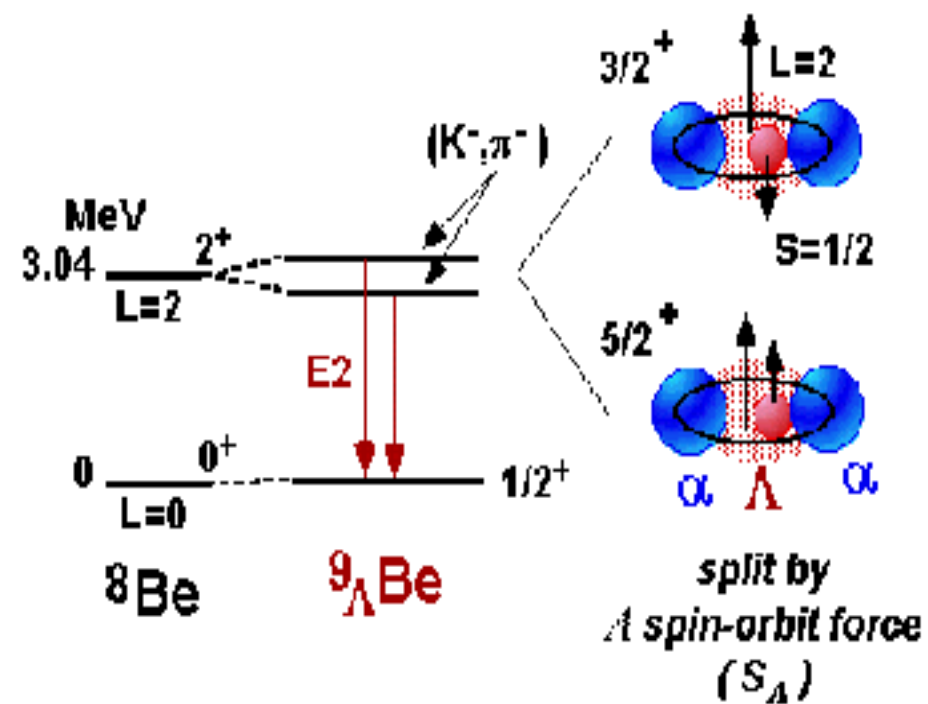
$$B(E2) \propto |\langle f | e r^2 Y_2 | i \rangle|^2$$

$$\propto R^4 \text{ or } (\beta \langle r^2 \rangle)^2$$

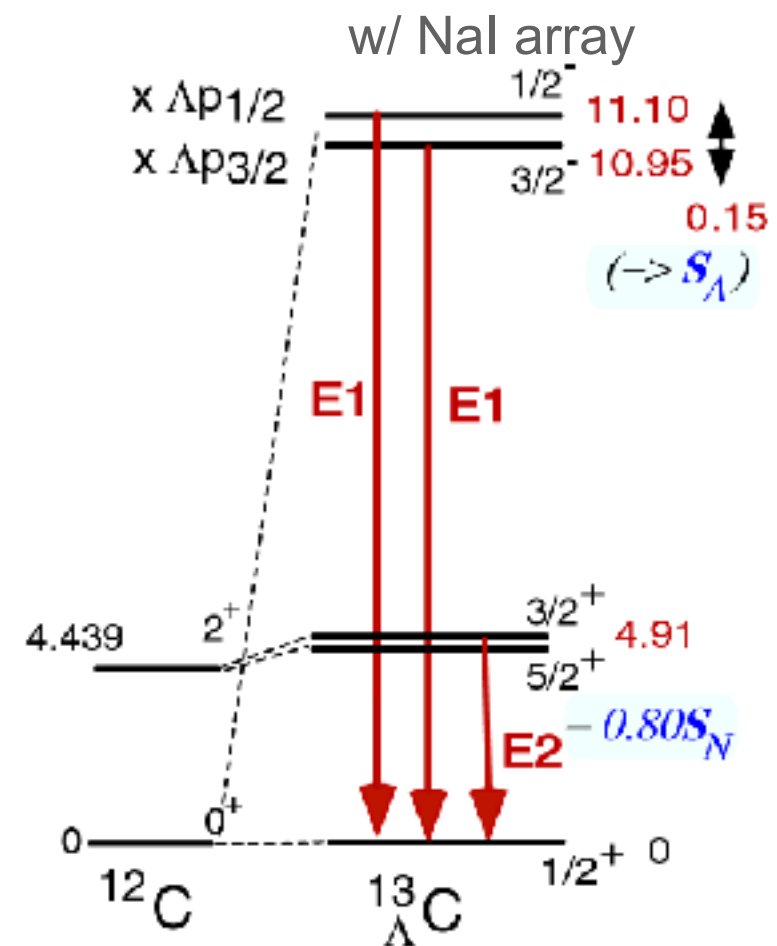
$B(E2) \text{ [e}^2 \text{fm}^4\text{]}$
 $10.9 \pm 0.9 \longrightarrow 3.6 \pm 0.5 \pm 0.5$
 $\Rightarrow 19 \pm 4\% \text{ shrinkage by } \Lambda$
 Tanida et al., PRL 86(2001) 1982

ΛN spin-orbit force

${}^9\text{Be} (K^-, \pi^- \gamma) {}^9\Lambda\text{Be}$
BNL E930-1



${}^{13}\text{C} (K^-, \pi^- \gamma) \text{BNL E929}$



Ajimura et al., PRL 86 (2001) 4255

$^{13}_{\Lambda}C$

$p_{1/2}$, $p_{3/2}$ single-particle level splitting

$$E(1/2^-) - E(3/2^-) = 152 \pm 54 \pm 36 \text{ keV}$$

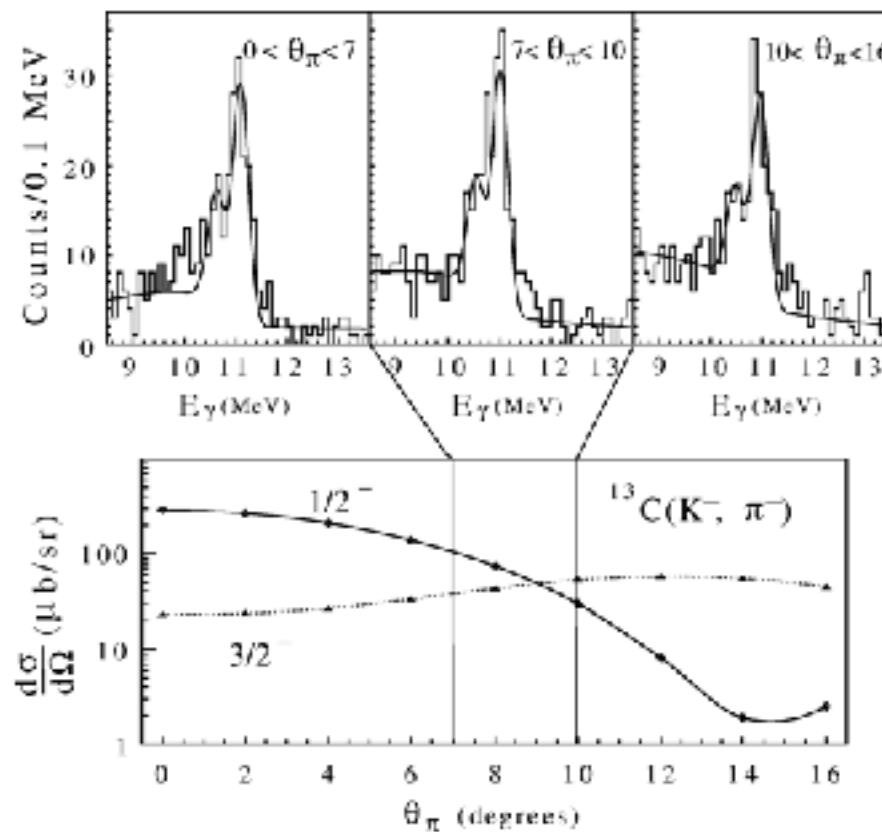


FIG. 2. γ ray spectra taken in coincidence with scattered π^- 's (upper panel) and differential cross section of $1/2^-$ and $3/2^-$ states calculated by Motoba [18] (lower panel) are shown.

-forward

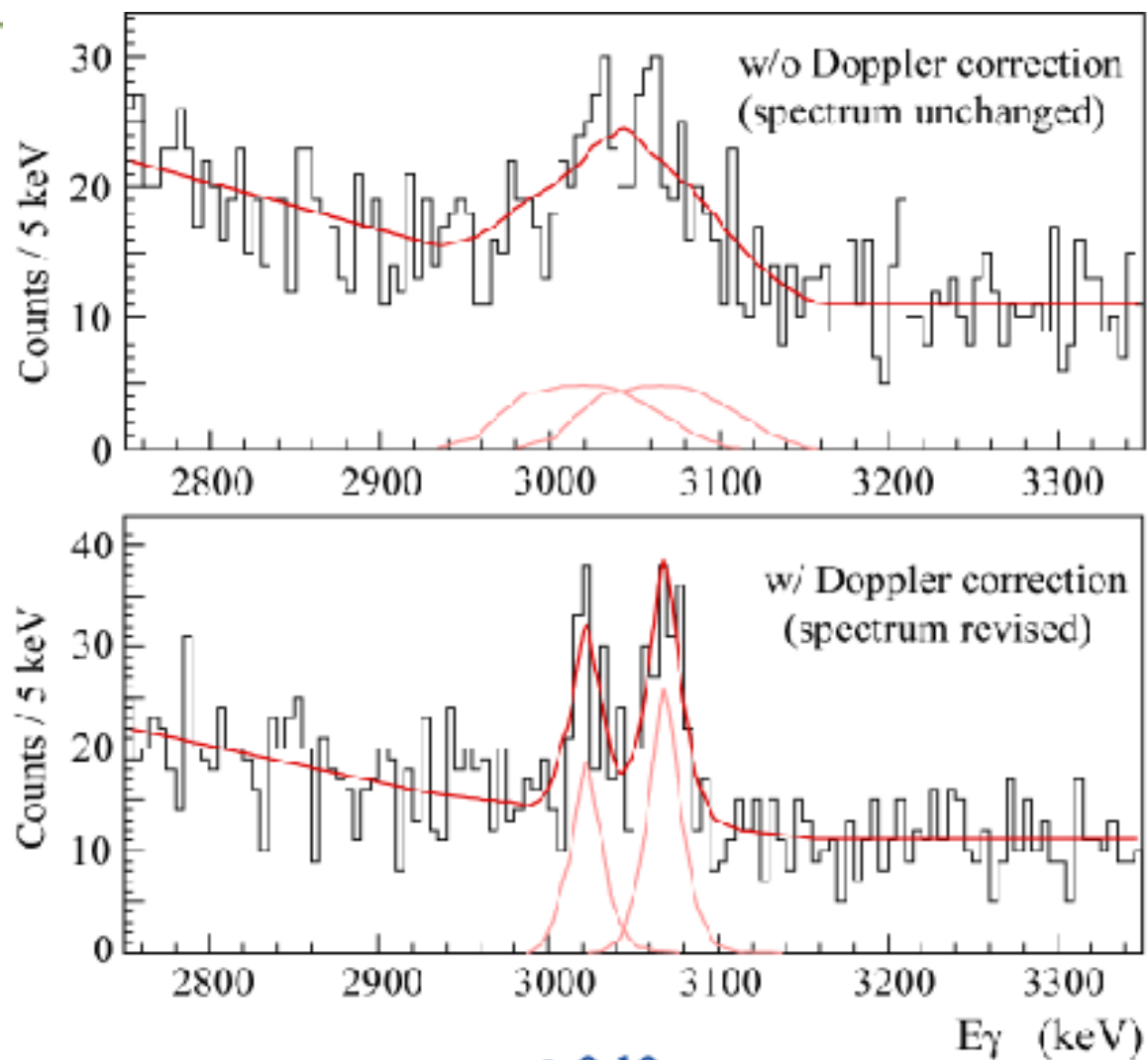
$$(p_{1/2,n}^{-1}, p_{1/2,\Lambda}) \quad \Delta L=0$$

-backward

$$(p_{1/2,n}^{-1}, p_{3/2,\Lambda}) \quad \Delta L=2$$

${}^9_{\Lambda}\text{Be}$

Revised



Revised
Results

$\tau < 0.10$ ps
 $\Delta E = 43 \pm 5$ keV
 $E = 3024 \pm 3 \pm 1, 3067 \pm 3 \pm 1$ keV
 $\chi^2 / \text{dof} = 1.22$

Hiyama et al: PRL 85 (2000) 270

$E(3/2^+) - E(5/2^+)$
 Meson exch. 0.08 - 0.20 MeV
 quark 0.035 - 0.040 MeV

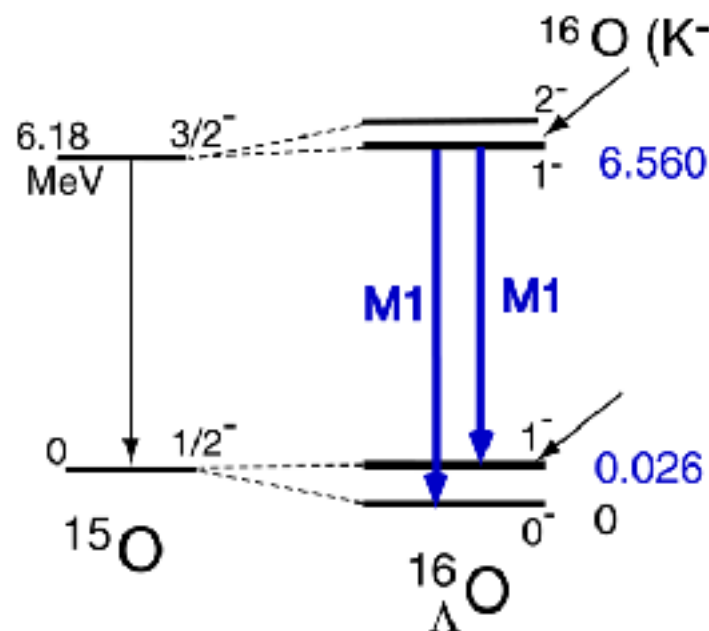
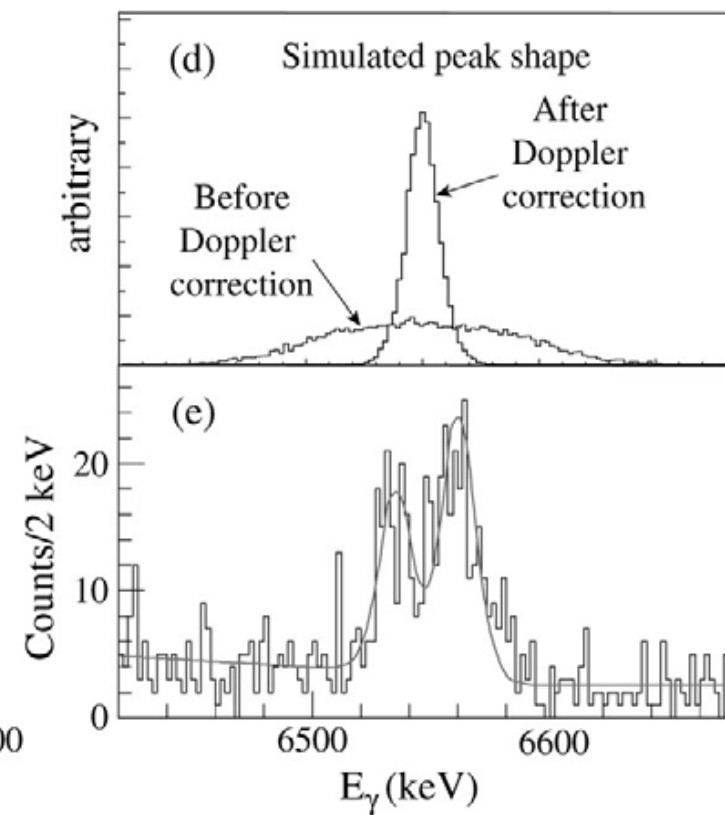
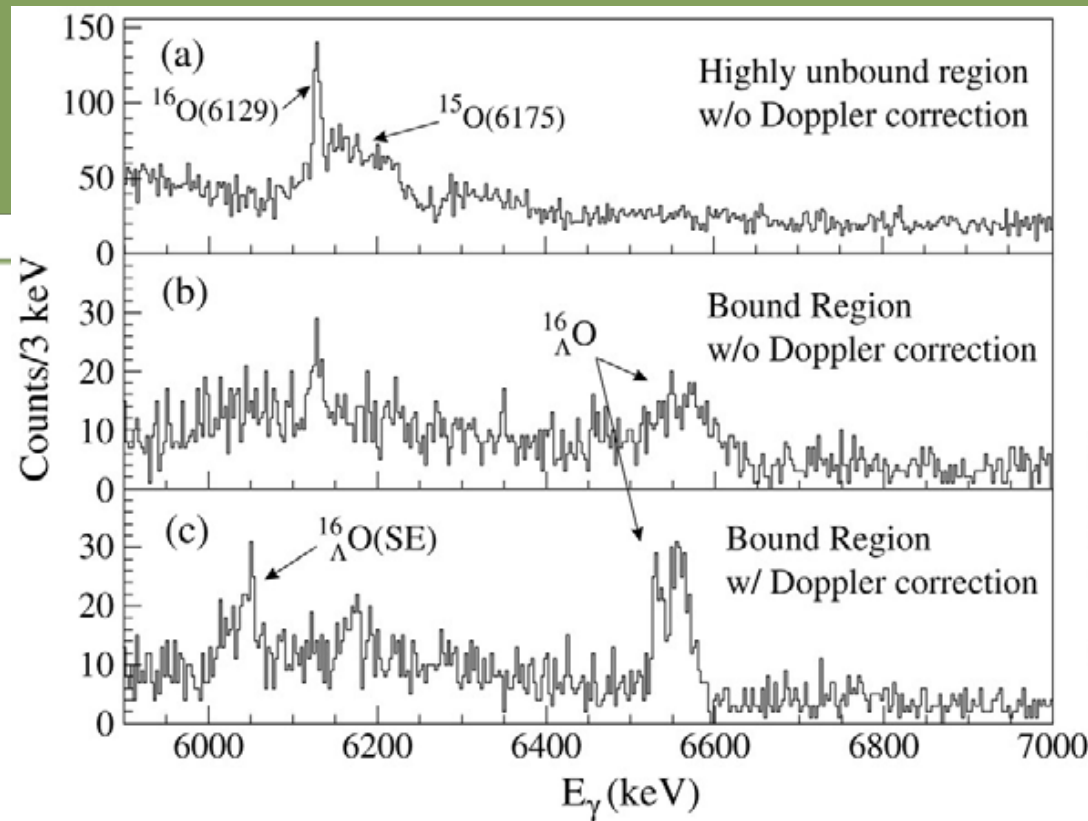
• Millener:

$E(3/2^+) - E(5/2^+)$
 $= -0.035 \Delta - 2.465 S_{\Lambda} + 0.936 T$

$S_{\Lambda} = -0.02$ MeV

Consistent with
 very small LS splitting in ${}^{13}_{\Lambda}\text{C}$

$^{16}_{\Lambda}\text{O}$



$$\Delta E = 26.1 \pm 1.4 \pm 0.6 \text{ keV}$$

$$E(1^-) - E(0^-) = -0.39 \Delta + 1.4 S_{\Lambda} - 0.005 S_N + 7.8 T + LS$$

(Millener, 2001)

$$\leftarrow \Delta = 0.46 \text{ MeV}, S_{\Lambda} = -0.01 \text{ MeV}$$

$$\rightarrow T = 26 - 32 \text{ keV}$$

First info. on T

	ND	NF	NSC89	NSC97f
T	18	33	36	54 (keV)

Some of Meson Exchange model predictions agree

Summary of p-shell levels

► $\Delta=0.48$ MeV, $S_\Lambda=-0.01$ MeV, $S_N=-0.43$ MeV, $T=0.03$ MeV

Table 18

Energies of the four hypernuclear level spacings that are described in terms of the spin-dependent ΛN interaction parameters obtained by Millener's shell model calculations [101]

Hypernuclear levels	Shell model calculation by Millener	$\Lambda\Sigma$ (MeV)	Exp. (MeV)
${}^7_\Lambda\text{Li}$ $E(3/2^+) - E(1/2^+)$	$1.444\Delta + 0.054S_\Lambda + 0.016S_N - 0.271T$	+0.071	0.692
${}^7_\Lambda\text{Li}$ $\overline{E(7/2^+, 5/2^+)}$ $- \overline{E(3/2^+, 1/2^+)}^a$	$-0.05\Delta + 0.07S_\Lambda + 0.70S_N - 0.08T$ $+ \Delta E_{\text{core}}^b$		1.858
${}^9_\Lambda\text{Be}$ $E(3/2^+) - E(5/2^+)$	$-0.037\Delta - 2.464S_\Lambda + 0.003S_N + 0.994T$	-0.008	0.043
${}^{16}_\Lambda\text{O}$ $E(1^-) - E(0^-)$	$-0.382\Delta + 1.378S_\Lambda - 0.004S_N + 7.850T$	-0.014 ^c	0.026

Experimental energies obtained by the Hyperball experiments are also shown. The effect of the Λ - Σ coupling estimated by Millener is listed as $\Lambda\Sigma$.

^a $\overline{E(J_1, J_2)} = [(2J_1 + 1)E(J_1) + (2J_2 + 1)E(J_2)] / (2J_1 + 2J_2 + 2)$ denotes the center of gravity energy for the doublet (J_1, J_2) .

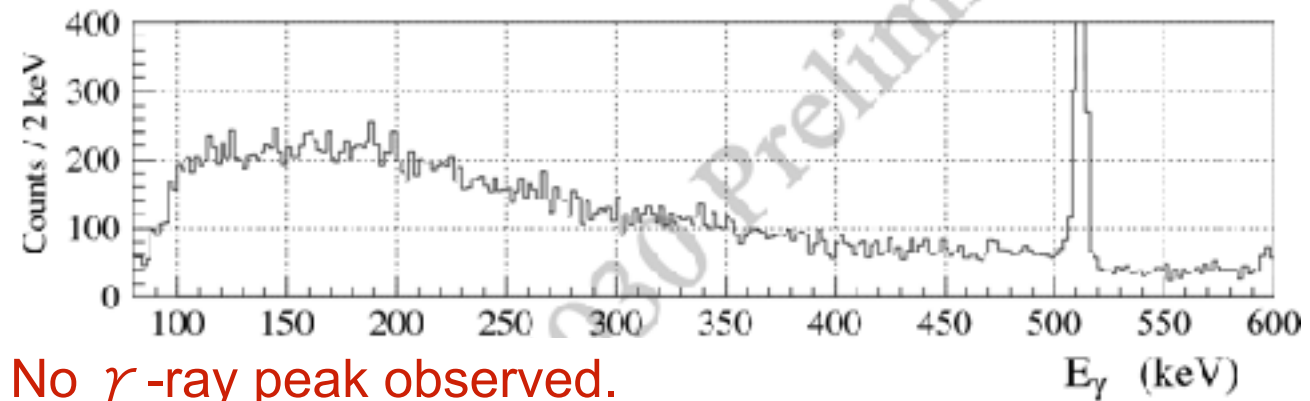
^b $\Delta E_{\text{core}} = E({}^6\text{Li}; 3^+) - E({}^6\text{Li}; 1^+) = 2.186$ MeV.

^c A small 1^- mixing effect of 0.016 MeV is added to a Λ - Σ coupling effect of -0.030 MeV.

γ spectrum of $^{10}_{\Lambda}\text{B}$ (E930-2)

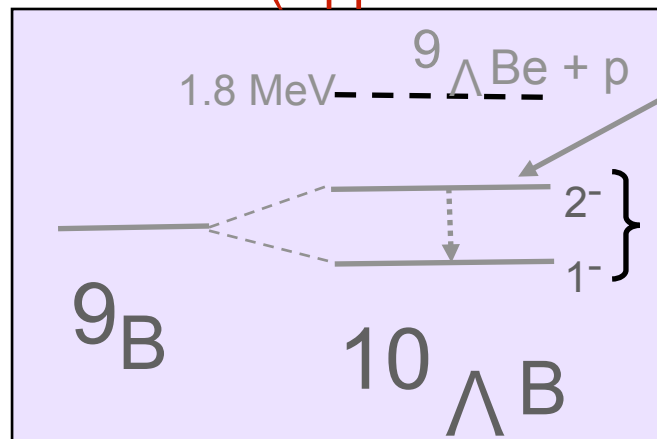
$^{10}\text{B} (\text{K}^-, \pi^-) ^{10}_{\Lambda}\text{B}$

$-40 < -B_{\Lambda}^* < -10 \text{ MeV}$ *uncalibrated
(5 MeV lower than the $^9_{\Lambda}\text{Be}$ gate)



No γ -ray peak observed.

(Upper limit to be determined.)



(K^-, π^-)

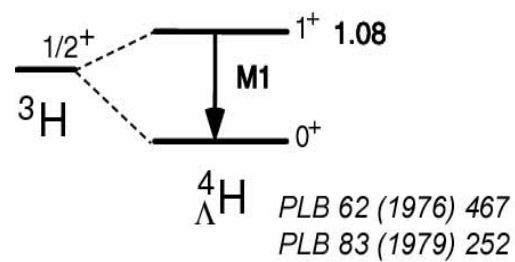
$< 100 \text{ keV}$ $\delta \sim 200 \text{ keV}$ from $\Delta = 0.5 \text{ MeV}$

Confirmed

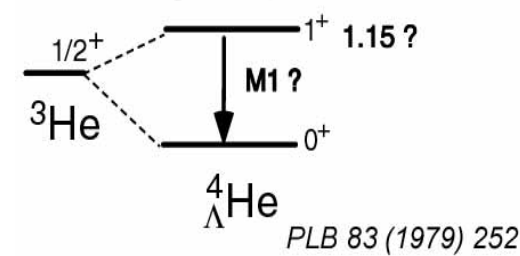
Chrien et al., Phys. Rev. C 41 (1990) 1062.

Summary of Hypernuclear γ rays

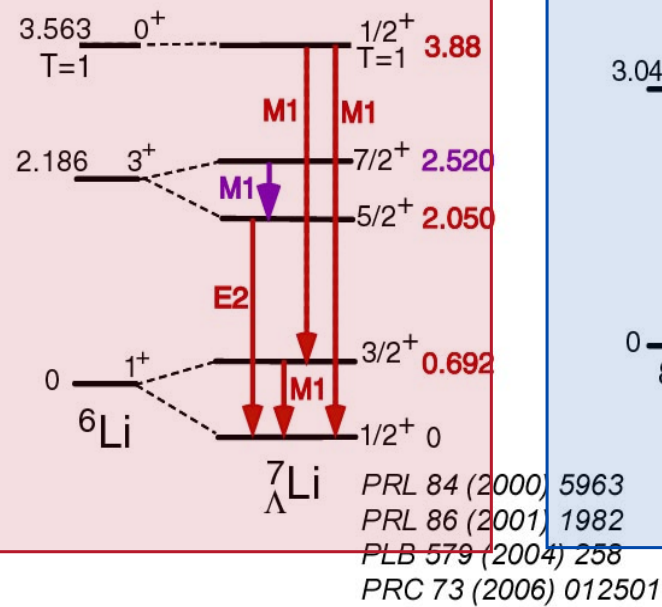
${}^7\text{Li}$ etc. ($K^-_{\text{stop}}, \gamma \pi^-$)



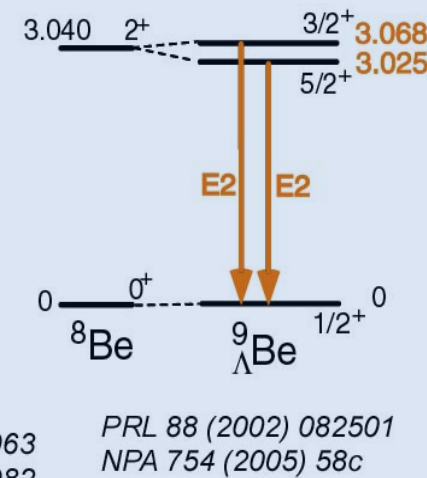
${}^7\text{Li}$ ($K^-_{\text{stop}}, \gamma \pi^0$)



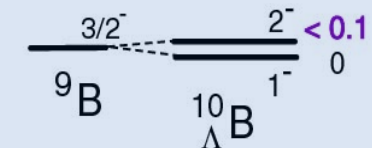
${}^7\text{Li}$ ($\pi^+, K^+\gamma$) KEK E419



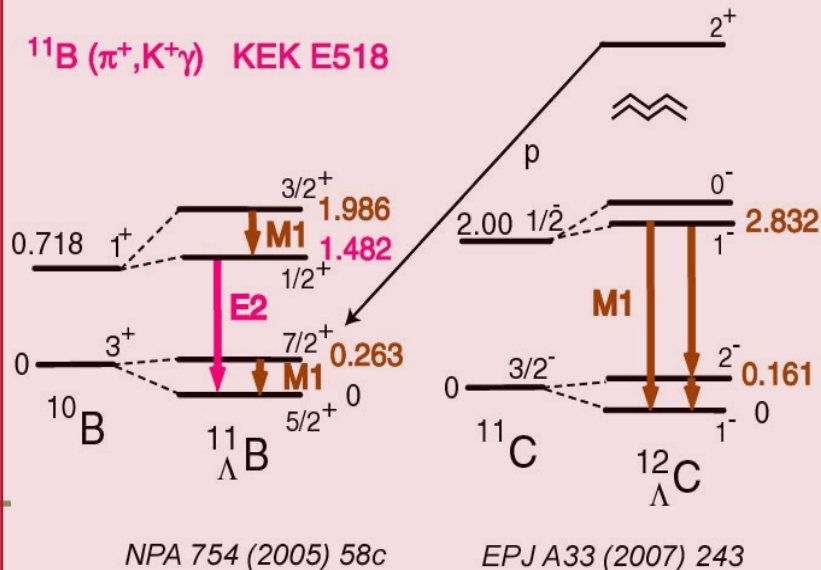
${}^9\text{Be}$ ($K^-, \pi^-\gamma$) BNL E930('98)



${}^{10}\text{B}$ ($K^-, \pi^-\gamma$) BNL E930('01)

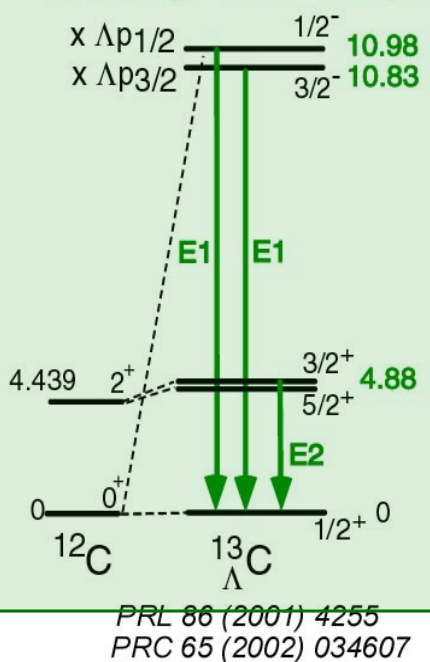


${}^{12}\text{C}$ ($\pi^+, K^+\gamma$) KEK E566

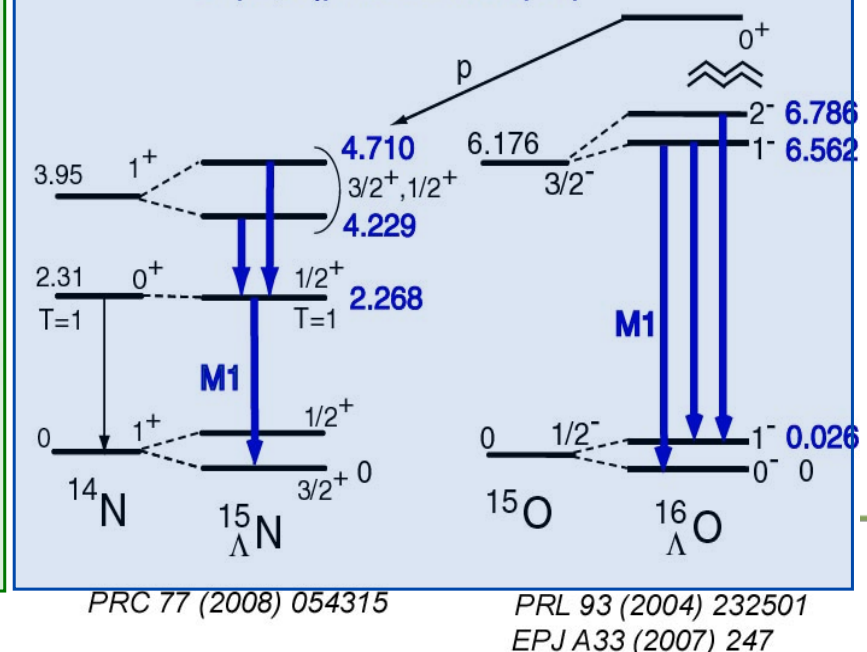


${}^{11}\text{B}$ ($\pi^+, K^+\gamma$) KEK E518

${}^{13}\text{C}$ ($K^-, \pi^-\gamma$) BNL E929 (NaI)

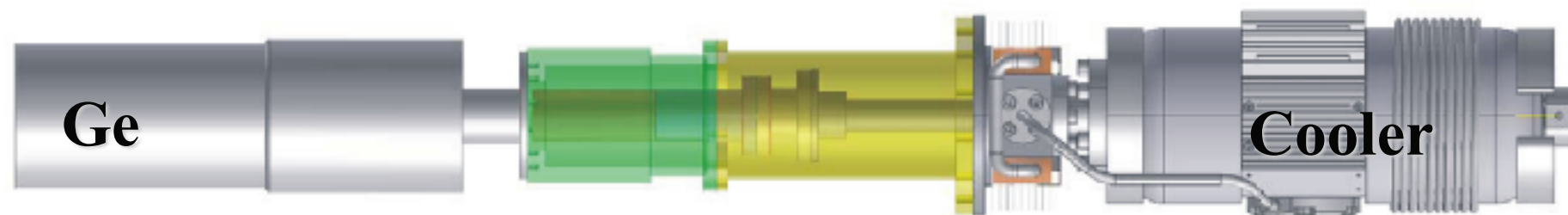
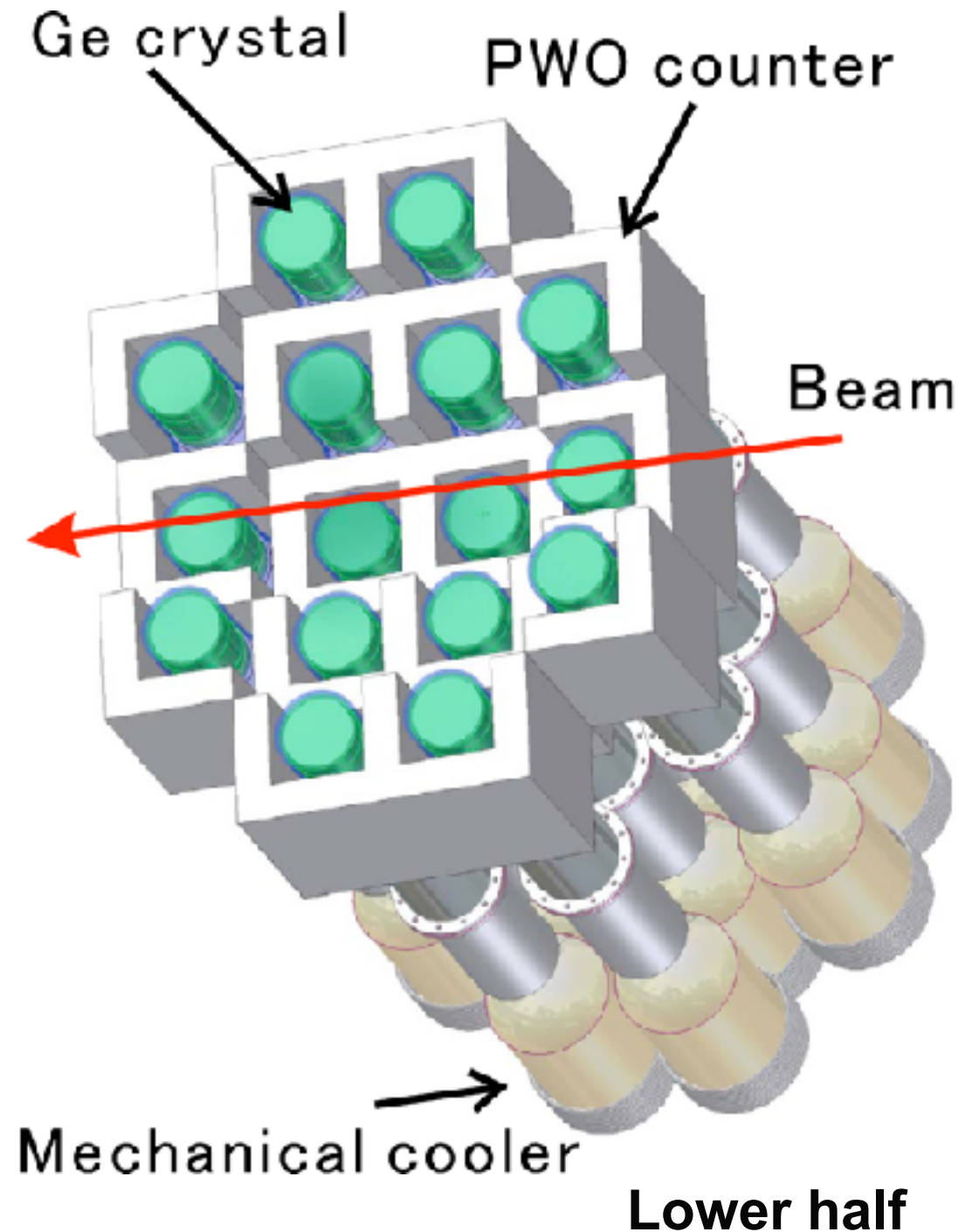


${}^{16}\text{O}$ ($K^-, \pi^-\gamma$) BNL E930('01)

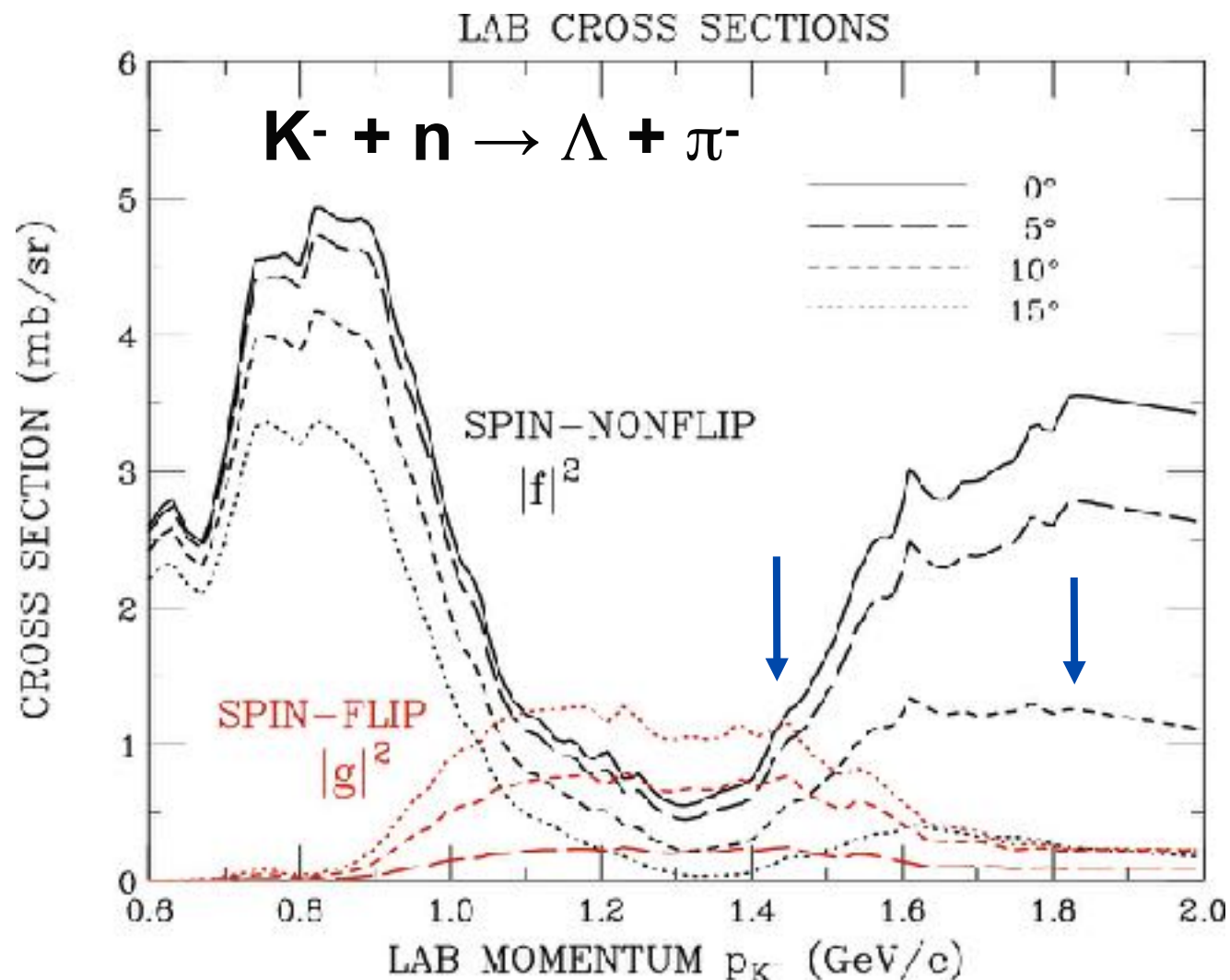


Hyperball-J

- Ge (single, r.e.~60%) x ~32
→ peak efficiency ~6% at 1 MeV
(x ~3 of Hyperball)
- Mechanical cooling
 - Lower temp. for less radiation damage
 - Save space for flexible arrangement
- PWO background suppression counters replaced from BGO for higher rate
- Waveform readout (under development)
=> Rate limit $\sim 2 \times 10^7$ particles /s
(x5 of Hyperball)



Best K- beam momentum



Both spin-flip and nonflip states should be produced.

→ $p_K = 1.1$ or 1.5 GeV/c

$p_K = 1.1$ GeV/c : K1.1 + “SKS” (ideal)
 $p_K = 1.5$ GeV/c : K1.8 + SKS (realistic)

High K/π ratio to minimize radiation damage to Ge detectors

→ Double-stage separation. K1.8BR is not good.

Beam and Setup

$(K^-, \pi^- \gamma)$ at $p_K = 1.5 \text{ GeV}/c$

Both spin-flip and nonflip states produced
Spin assignment from angular distribution

■ Spectrometer: SksMinus

$\Delta p \sim 4 \text{ MeV}$ (FWHM)

$\Omega \sim 110 \text{ msr}$

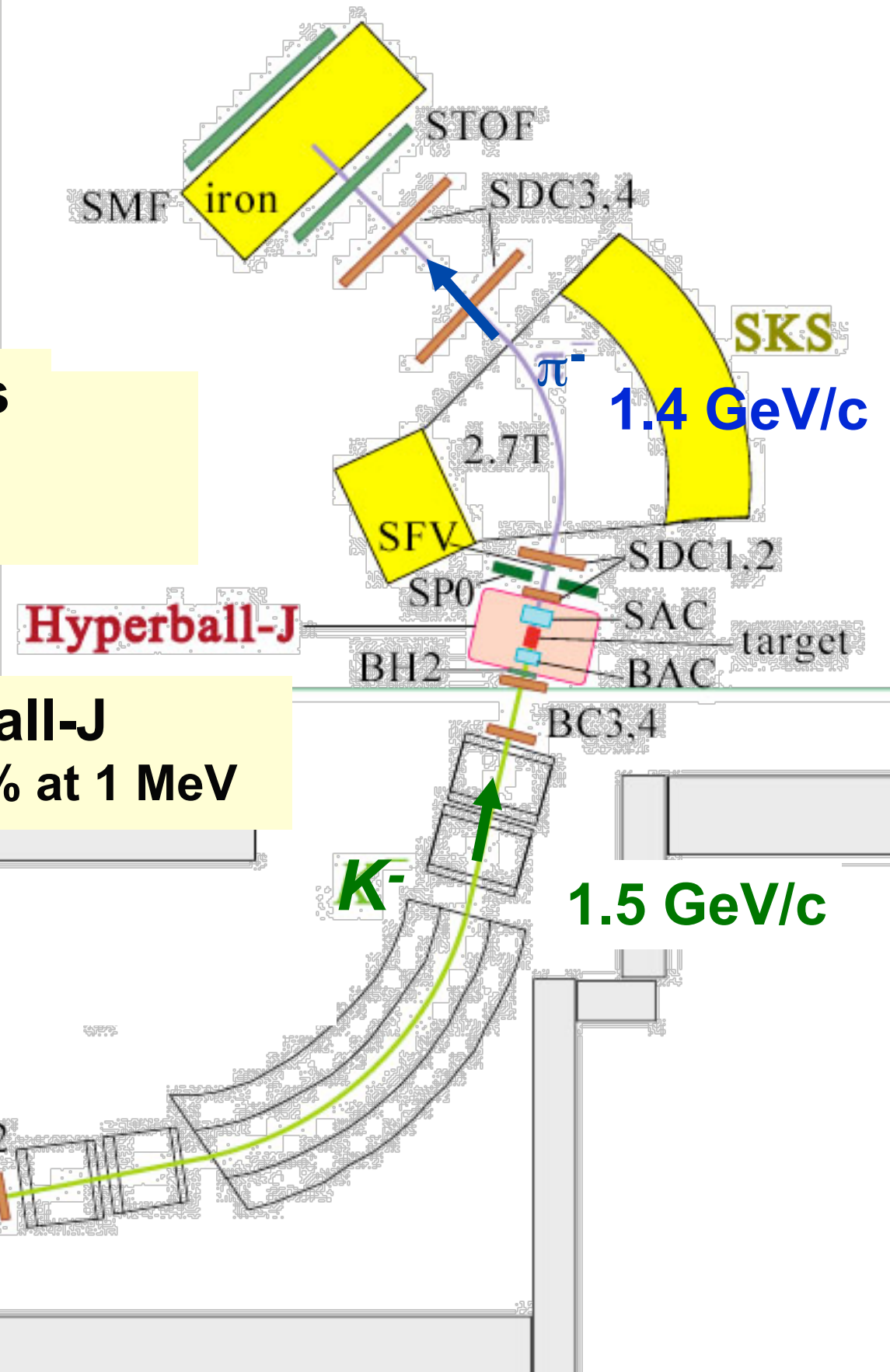
■ Hyperball-J

$\varepsilon \sim 6\%$ at 1 MeV

■ Beamline: K1.8

$0.5 \times 10^6 \text{ K/spill}$ at $1.5 \text{ GeV}/c$ ($9 \mu\text{A}$)

$K/\pi \gg 1$

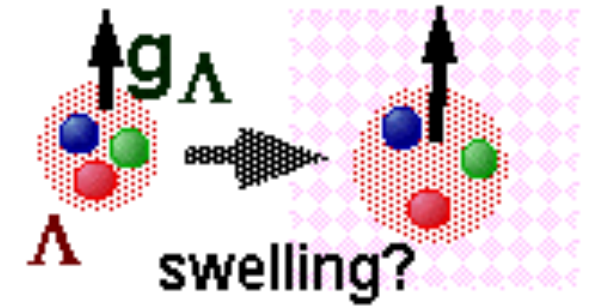


g factor of Λ in nucleus

■ Motivation

μ_Λ in nucleus \rightarrow medium effect of baryons

Can be investigated using a Λ in 0s orbit

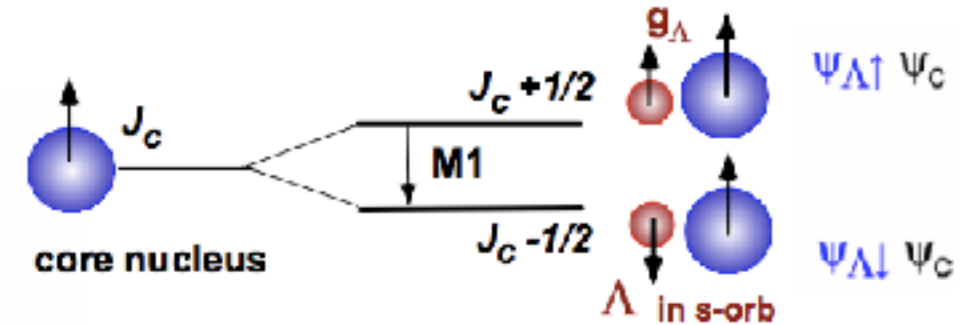


■ B(M1) of Λ -spin-flip M1 transition $\rightarrow g_\Lambda$

$$\begin{aligned}
 B(M1) &= (2J_{up} + 1)^{-1} |\langle \Psi_{low} \| \mu \| \Psi_{up} \rangle|^2 \\
 &= (2J_{up} + 1)^{-1} |\langle \psi_{\Lambda\downarrow} \psi_c \| \mu \| \psi_{\Lambda\uparrow} \psi_c \rangle|^2 \\
 \mu &= g_c J_c + g_\Lambda J_\Lambda = g_c J + (g_\Lambda - g_c) J_\Lambda
 \end{aligned}$$

$$= \frac{3}{8\pi} \frac{2J_{low} + 1}{2J_c + 1} (g_\Lambda - g_c)^2 \quad [\mu_N^2]$$

Reduction of constituent q mass?
Swelling?



■ How to measure

Doppler-shift attenuation method :

applied to “hypernuclear shrinkage”
in ${}^7_\Lambda\text{Li}$ ($5/2^+ \rightarrow 1/2^+$) from B(E2)

$$\Gamma = BR / \tau = \frac{16\pi}{9} E_\gamma^3 B(M1)$$

PRL 86 ('01)1982

■ Preliminary data (statistical error only) from ${}^7_\Lambda\text{Li}$ ($3/2^+ \rightarrow 1/2^+$) (BNL E930)

$$g_\Lambda = -1.1^{+0.6}_{-0.4} \mu_N \longleftrightarrow g_\Lambda(\text{free}) = -1.226 \mu_N \quad \rightarrow < 5\% \text{ accuracy at J-APRC}$$

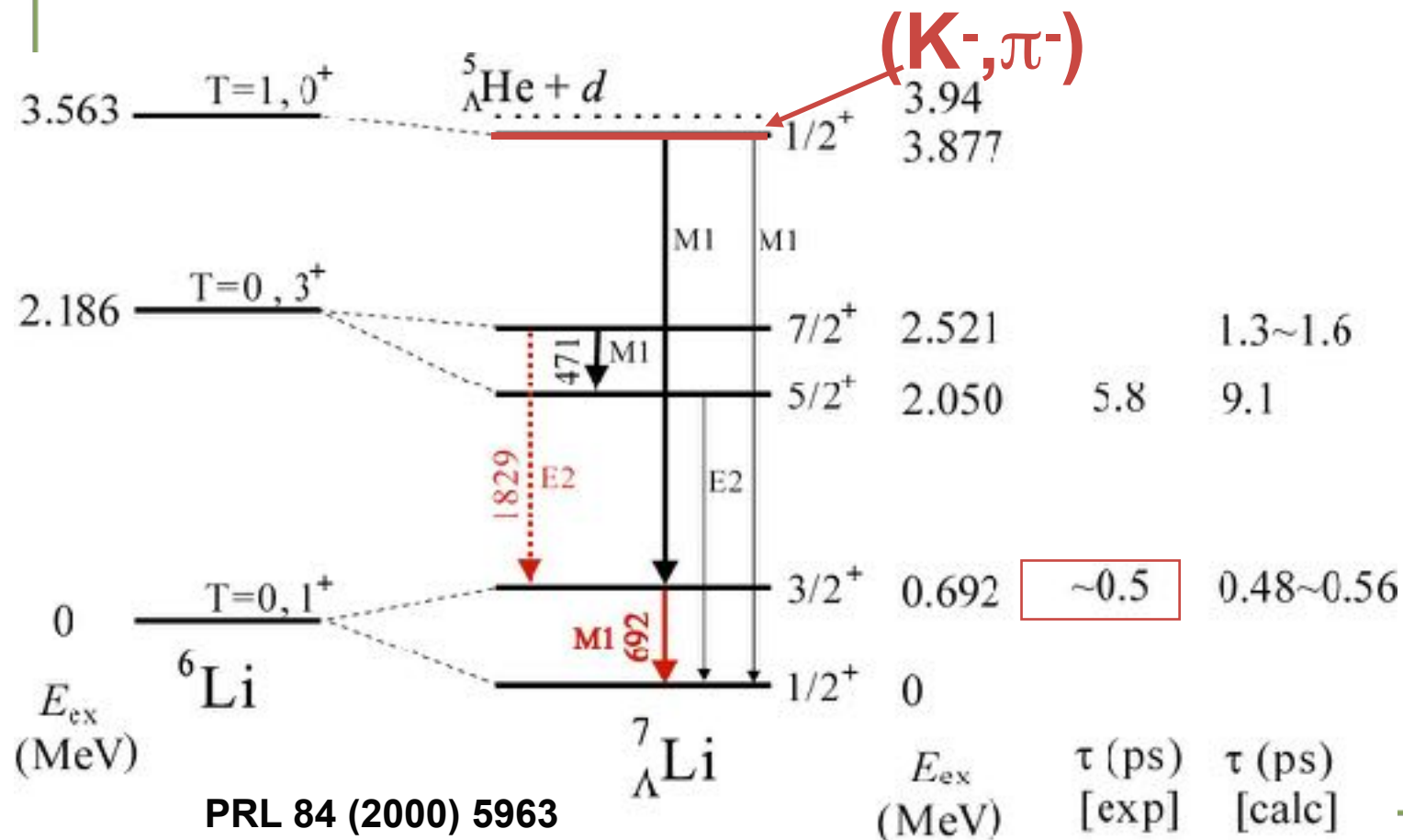
Proposed B(M1) measurement

Difficulties in B(M1) measurement

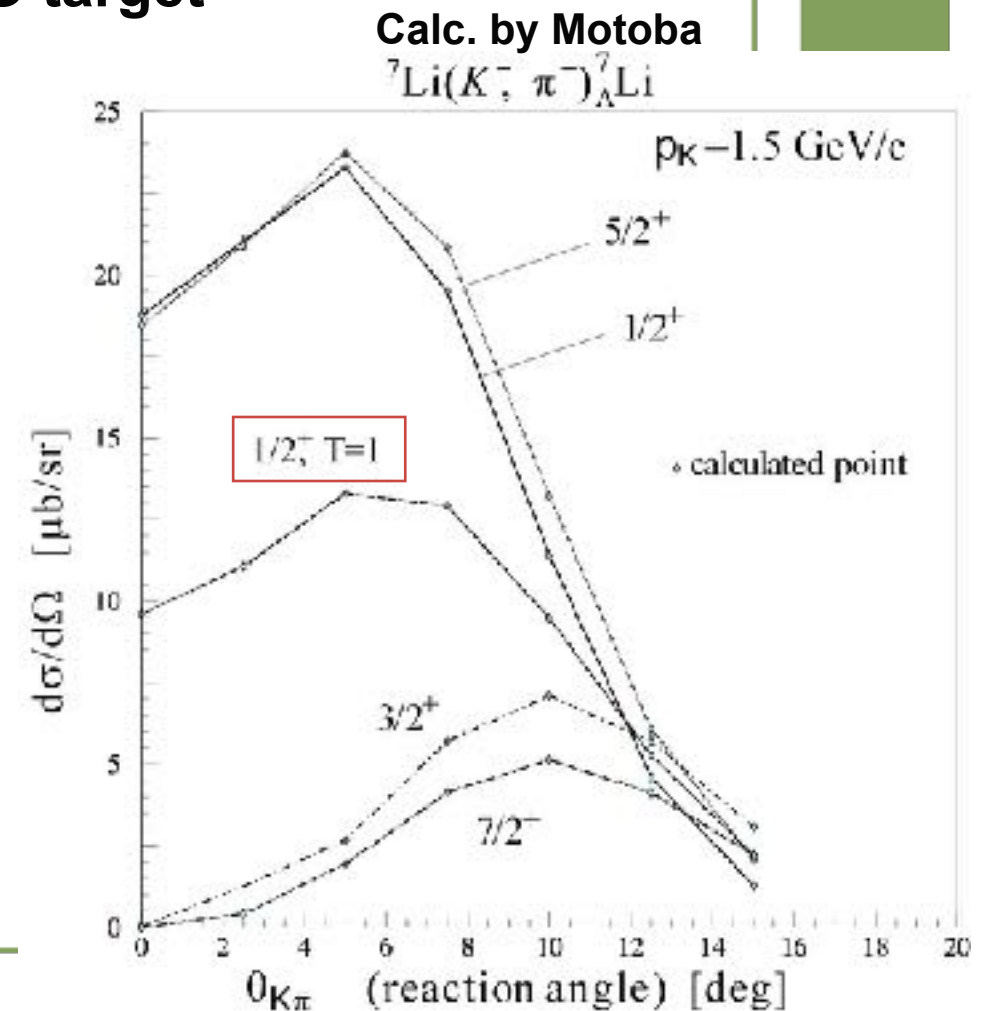
- Doppler Shift Attenuation Method works only when $\tau < t_{\text{stop}}$
 - τ is very sensitive to E_γ because $B(M1) \propto 1/\tau \propto E_\gamma^3$. But E_γ is unknown.
 - Cross sections and background cannot be accurately estimated.
- Previous attempts: $^{10}_\Lambda\text{B}$, $^{11}_\Lambda\text{B}$ (E_γ too small $\rightarrow \tau \gg t_{\text{stop}}$), $^7_\Lambda\text{Li}$ (by product: indirect population)

To avoid ambiguities, we use the best-known hypernucleus, $^7_\Lambda\text{Li}$.

- Energies of all the bound states and B(E2) were measured,
- γ -ray background level was measured,
- cross sections are reliably calculated.
- $\tau = 0.5\text{ps}$, $t_{\text{stop}} = 2\text{-}3\text{ ps}$ for 1.5 GeV/c (K^- , π^-) and Li_2O target



PRL 84 (2000) 5963
PRC 73 (2006) 012501



Expected yield and sensitivity

Yield estimate

$$N_K = 0.5 \times 10^6 / \text{spill}$$

$$\text{Target } (^7\text{Li in Li}_2\text{O}) = 20\text{cm} \times 2.0\text{g/cm}^3 \times 14/30 \times 0.934 / 7 \times 6.02 \times 10^{23}$$

$$\int d\sigma/d\Omega(1/2;1) \Delta\Omega \times \text{BR}(1/2^+;1 \rightarrow 3/2^+) = 0.84 \mu\text{b} \times 0.5$$

$$\varepsilon(\text{Ge}) \times \varepsilon(\text{tracking}) = 0.7 \times 0.6$$

→

$$\text{Yield } (3/2^+ \rightarrow 1/2^+) = 7.3 / \text{hr} (1000 \text{ spill})$$

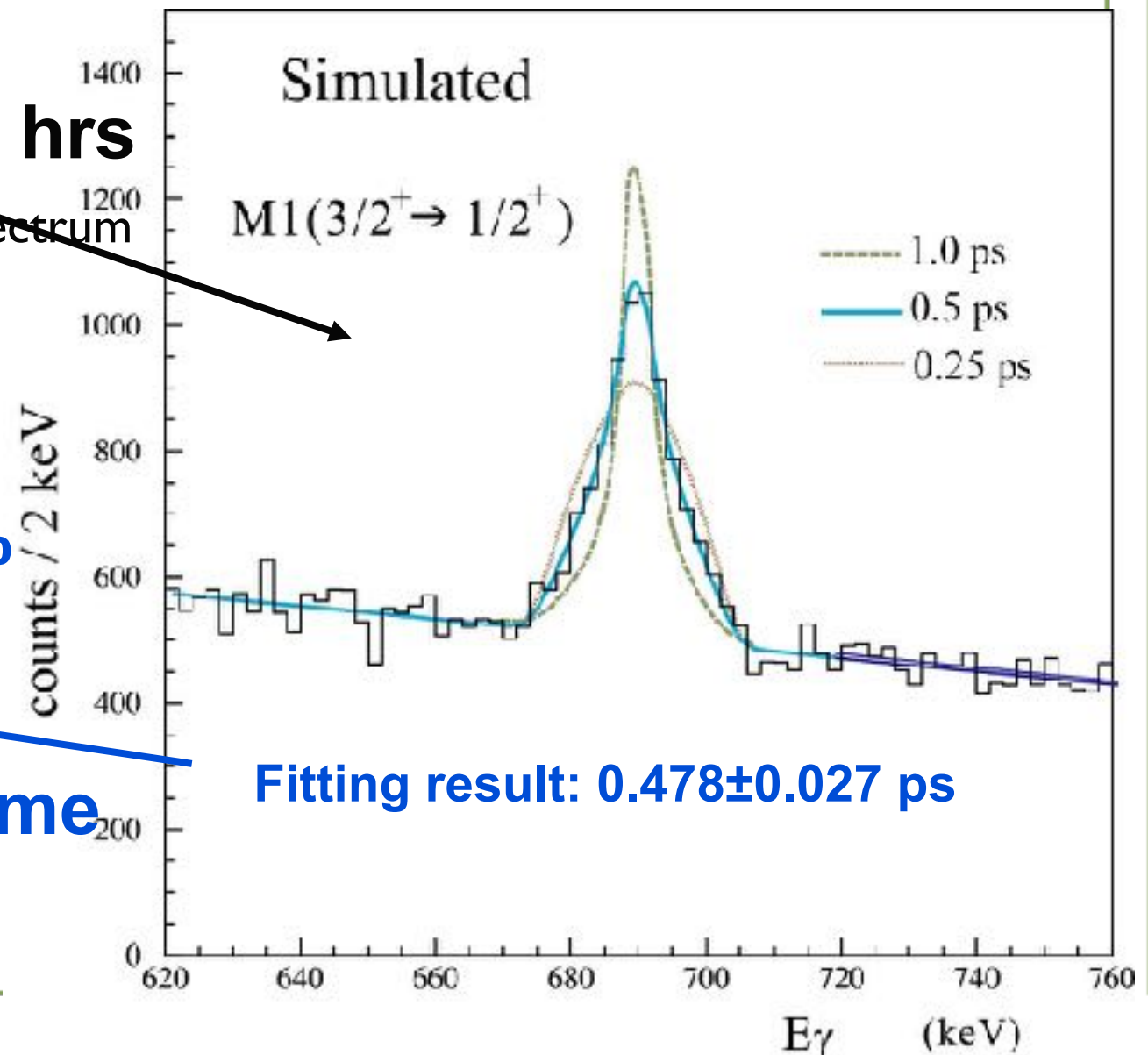
$$= \mathbf{3600 / 500 \text{ hrs}}$$

Background estimated from E419 $^7_\Lambda\text{Li}$ spectrum

■ **Stat. error** $\Delta\tau/\tau = 5.4\%$

$$\rightarrow \frac{\Delta|g_\Lambda - g_c|}{|g_\Lambda - g_c|} \sim 3\%$$

■ **Syst. error < 5%**
mainly from stopping time



Σ

Hypernuclei

History of Σ Hypernuclei

- Σ^- atom X-ray : Level shifts, widths
 - CERN('75), RAL('78), BNL('93)
 - $^{12}\text{C} \sim ^{208}\text{Pb}$, 23 data points
 - $V_{\text{opt}}(r) = t_{\text{eff}} \cdot Q(r)$ (C.J.Batty, Nucl. Phys. A372 (81) 433)
 - $-\text{Re } V_{\text{opt}}(0) \sim 25\text{-}30 \text{ MeV}$, **Attractive**
 - $-\text{Im } V_{\text{opt}}(0) \sim 10\text{-}15 \text{ MeV}$, **Absorptive**
 - $\Sigma\text{N} \rightarrow \Lambda\text{N}$ conversion (strong interaction)
 - Σ hypernuclei may exist, but the widths are broad
 - **No Spectroscopy $\Gamma \sim 2\text{Im}V$**

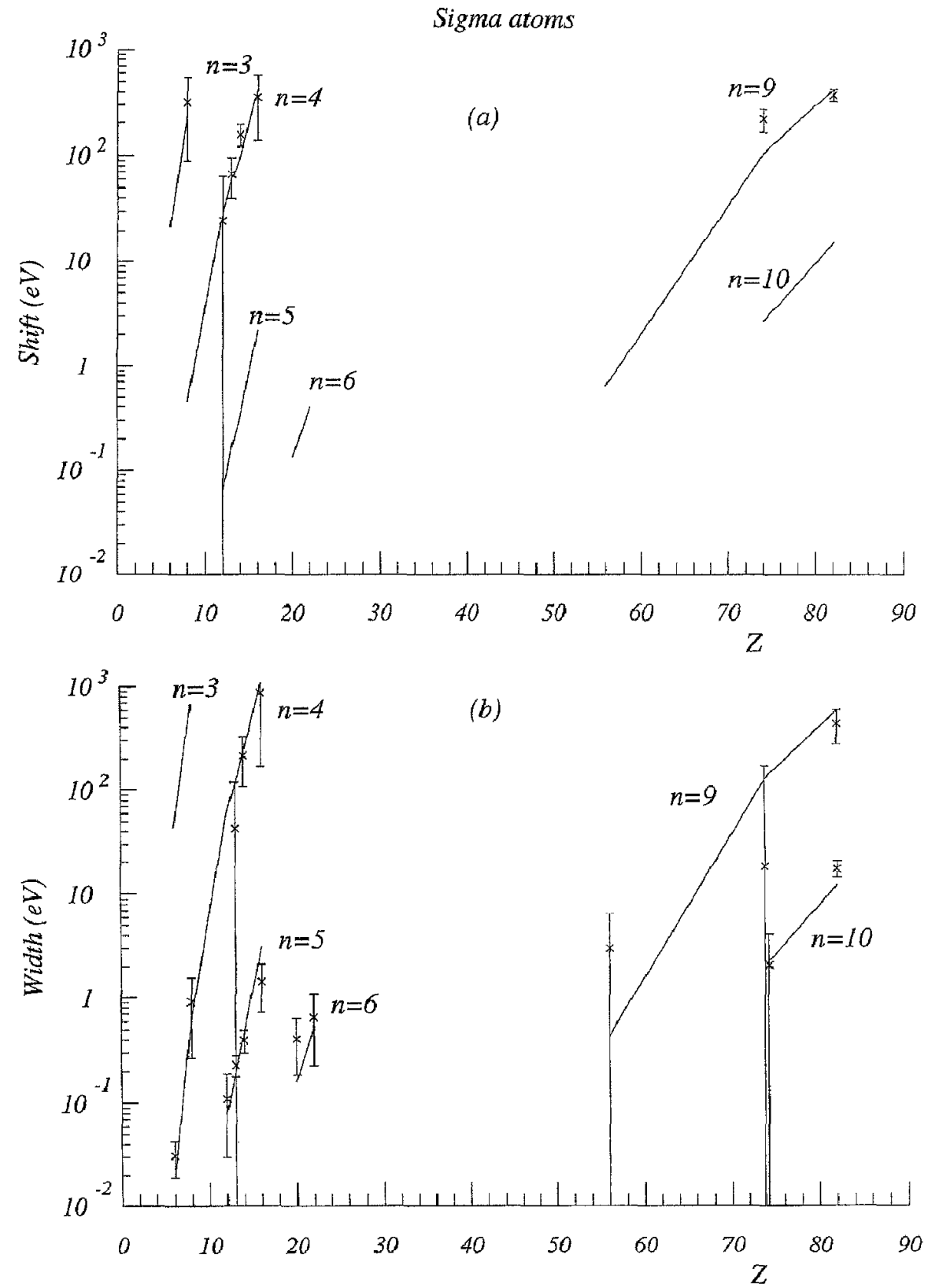


Fig. 9. Shift and width values for sigma atoms. The continuous lines join points calculated with the best-fit optical potential discussed in Section 6.2.

Σ -Nucleus potential

- Σ -atom X-ray

C.J.Batty et al., NP A372(81)433.

$$V(r) + iW(r) = -\left(\frac{4\pi\hbar^2}{2\mu}\right)\left(1 + \frac{\mu}{M_N}\right)\bar{a}\rho(r) \quad \bar{a} = 0.35 + i0.19 : \text{scattering - length,}$$
$$= -(28 + i15)\text{MeV}\rho(r)/\rho_0 \quad \mu : \text{reduced - mass}$$

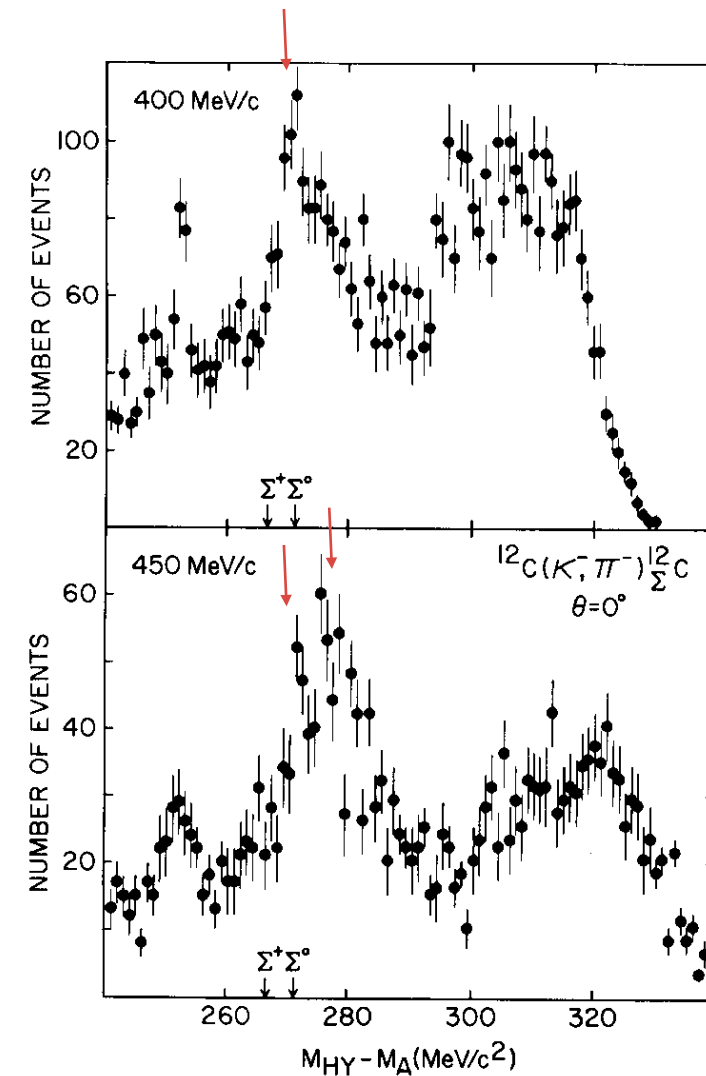
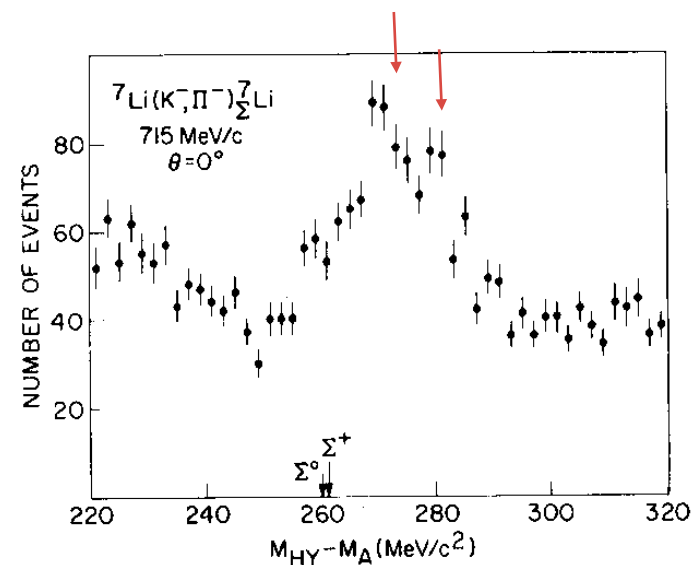
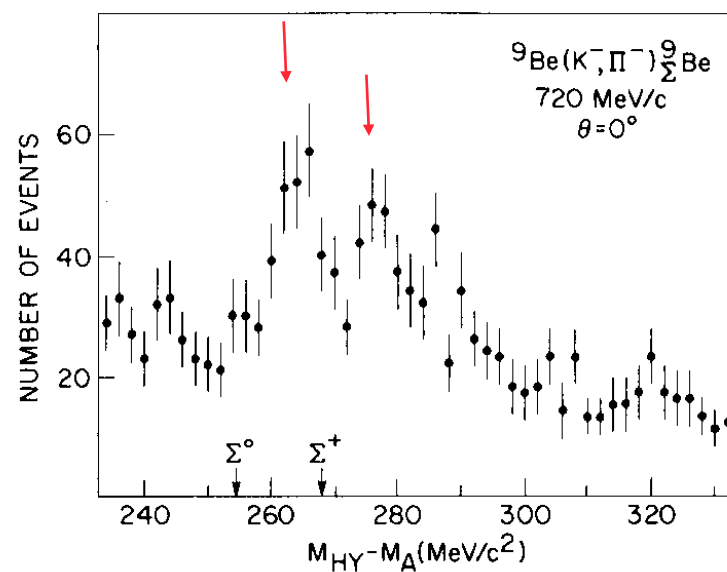
- DWIA analysis: Green Function method

Morimatsu and Yazaki, NP A483(88)493,

R.S.Hayano, NP A478(88)113c.

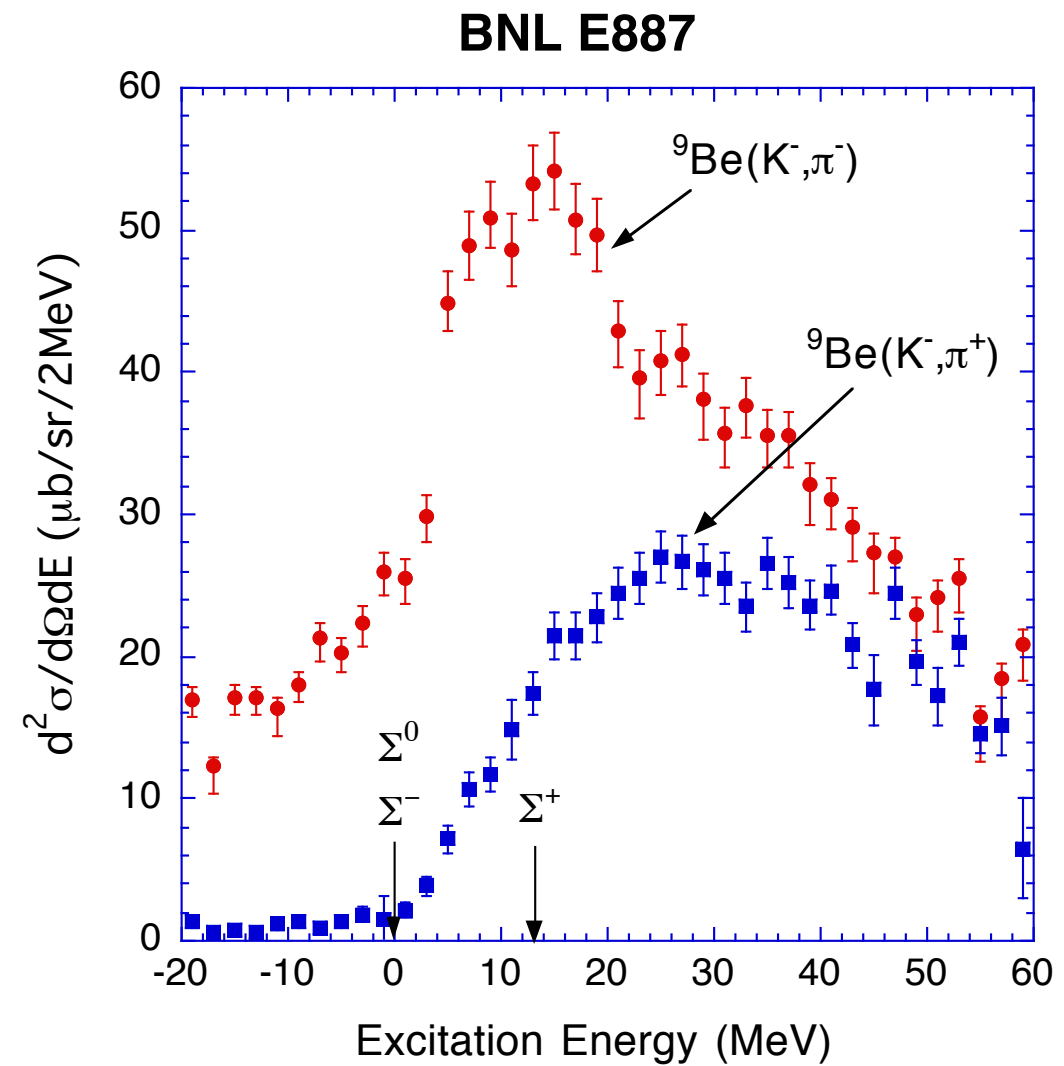
Narrow width problem in 1980s

- ${}^9\text{Be}(\text{K}^-, \pi^-)$ at CERN(1980)
 - Narrow peak($\sim 7 \text{ MeV}$) in unbound region
 - BNL, KEK

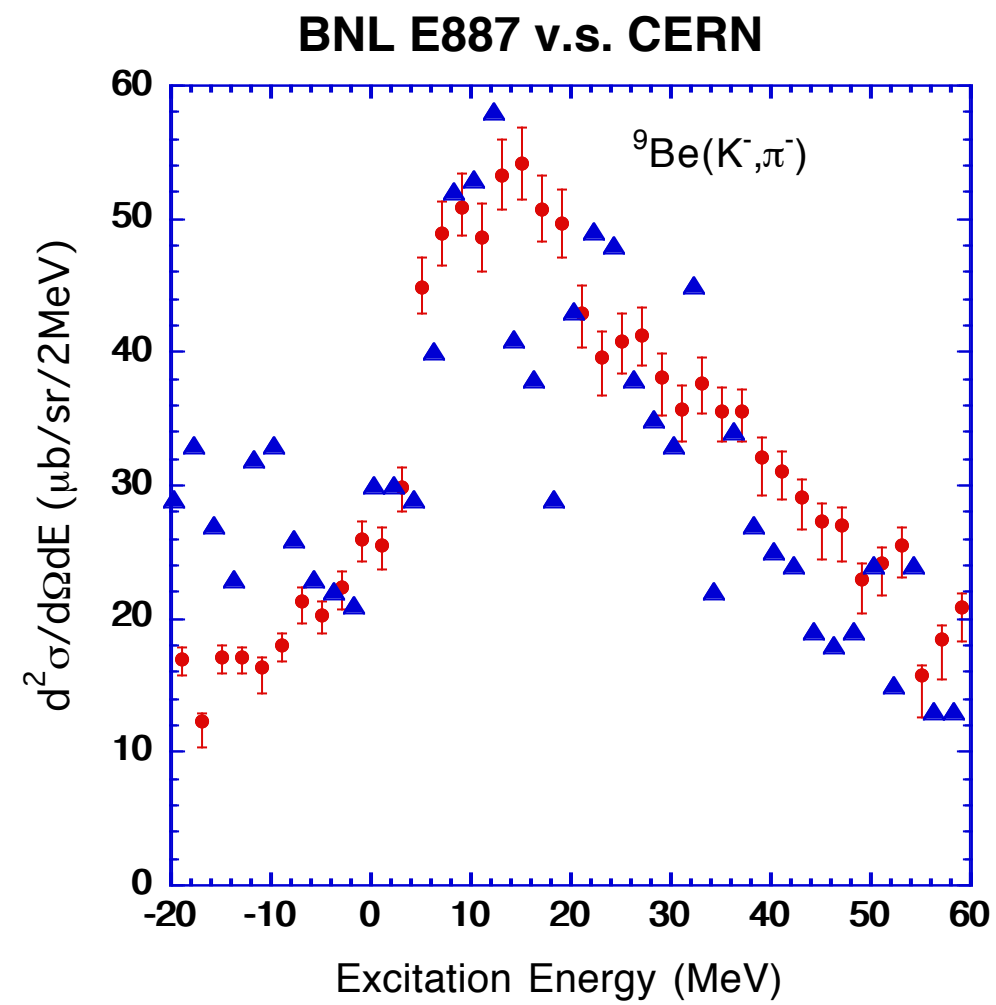


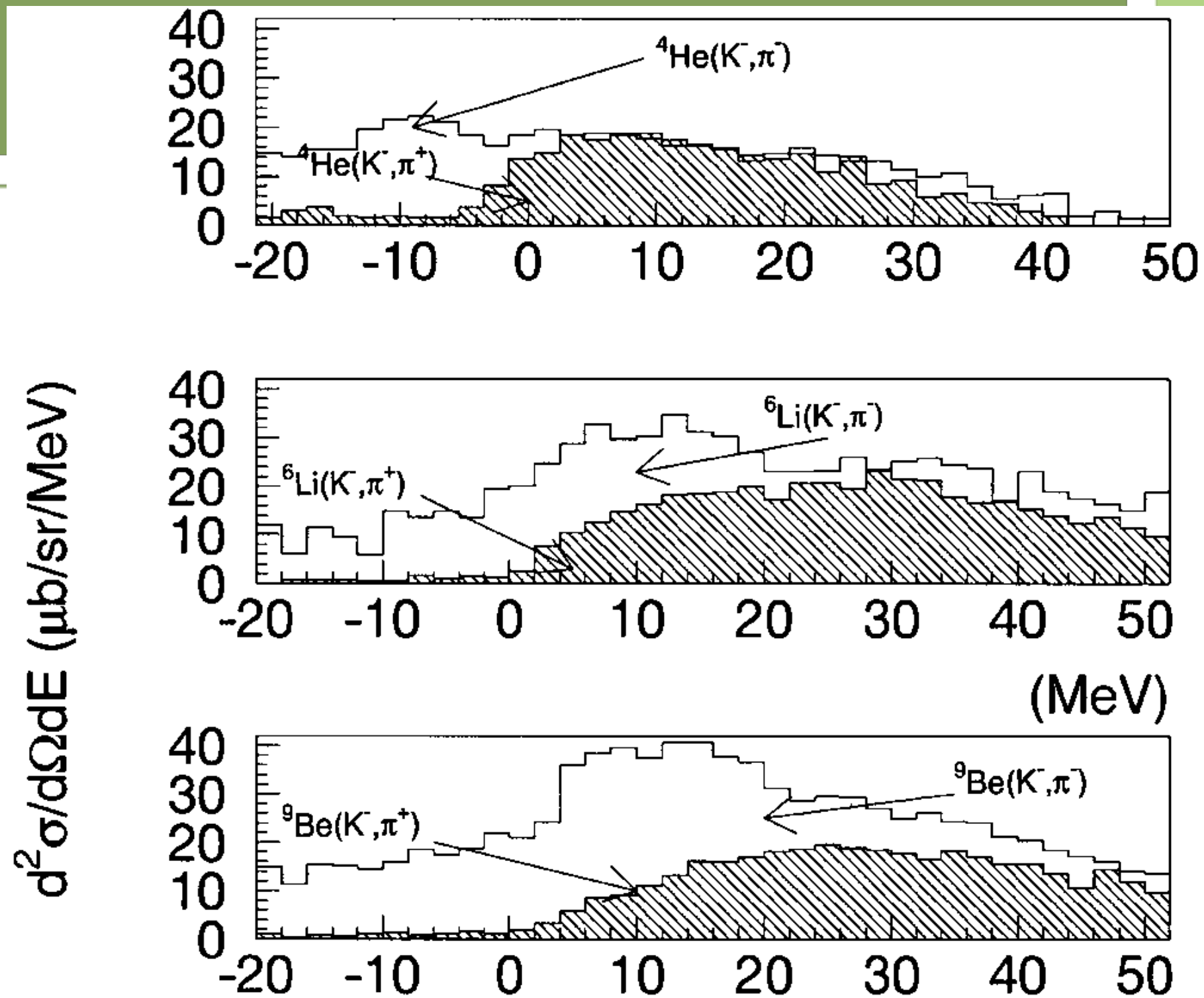
BNL E887

- 600 MeV/c
- 4 degrees
- No Peaks !!



E887 vs. CERN Data





束縛状態の問題

- ポテンシャルの実部の深さ？
- Σ 原子のX線データの密度依存型ポテンシャル

による再解析

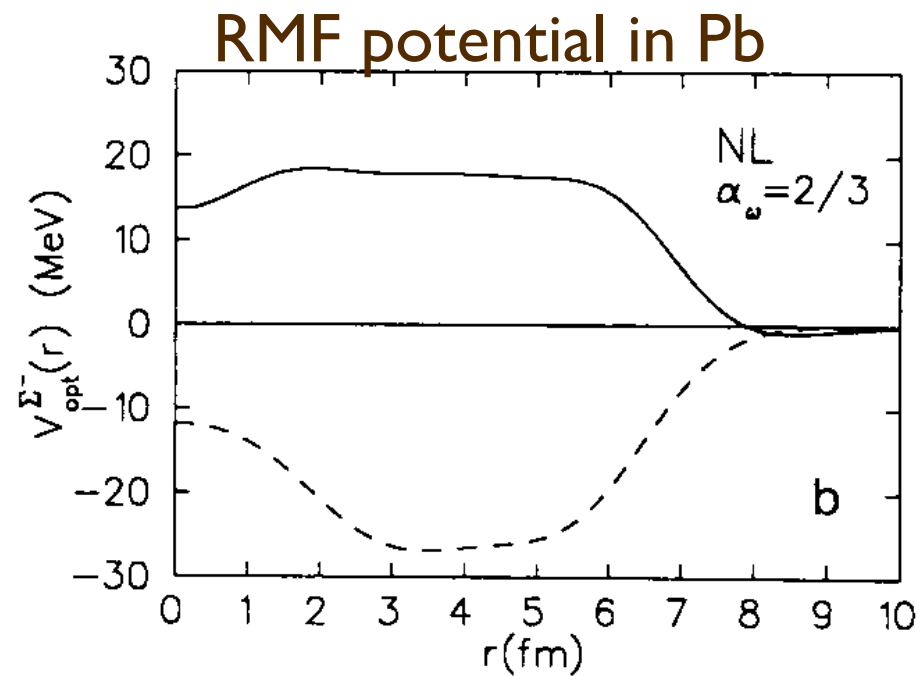
- 弱い引力：原子核外部の長距離
- 強い斥力：原子核内部

$$2\mu V_{opt}(r) = -4\pi \left(1 + \frac{\mu}{m_n}\right) \left\{ \left[b_0 + B_0 \left(\frac{\rho(r)}{\rho(0)} \right)^\alpha \right] \rho(r) + \left[b_1 + B_1 \left(\frac{\rho(r)}{\rho(0)} \right)^\alpha \right] \delta\rho(r) \right\}$$

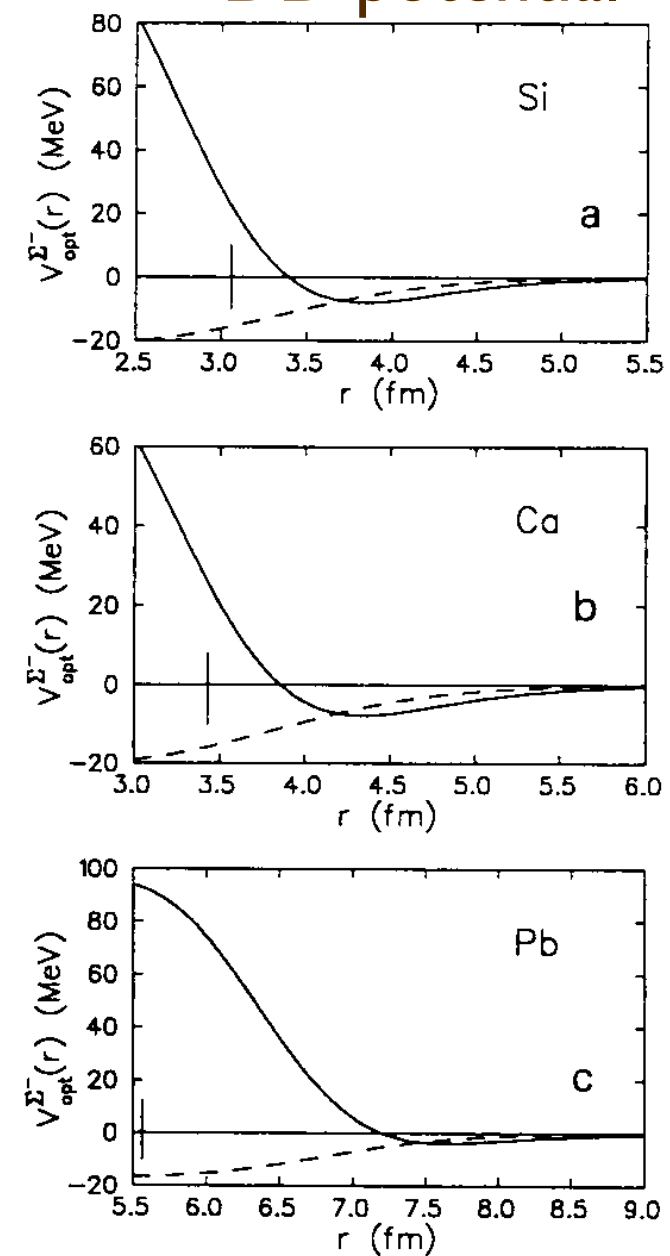
- 軽い核を除いて、束縛状態は存在しない!?

Repulsive ??

- C.J.Batty,E.Friedman,A.Gal,
Phys.Lett.B335(94)273;
PTP Suppl.117(94)227.
- J.Mares et al., NP A594(95)311.

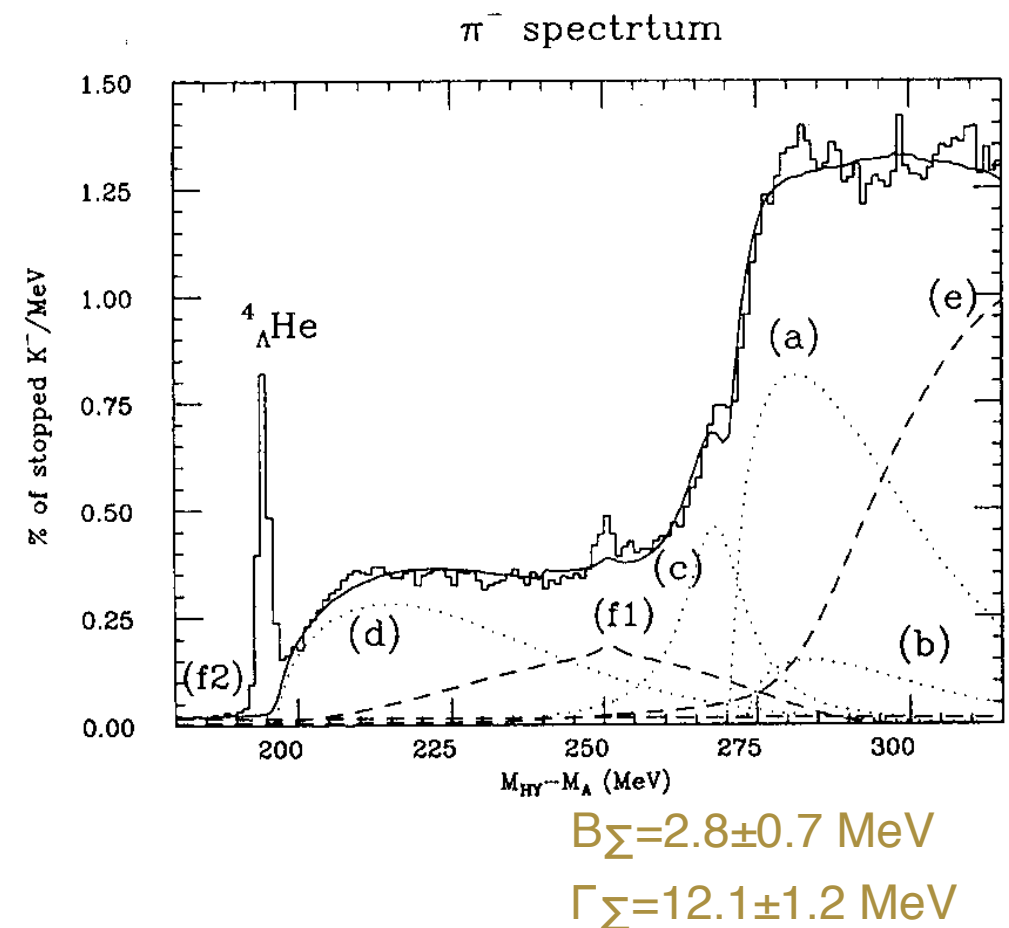


DD potential



Existence of any bound states ?

- Only candidate
 - ${}^4\text{He}(\text{K}^-_{\text{stop}}, \pi^-)$: R.S.Hayano et al.
 - predicted by Harada and Akaishi
- Definitive evidence ?
 - Large background
 - K^- orbit
 - *S or P ?*



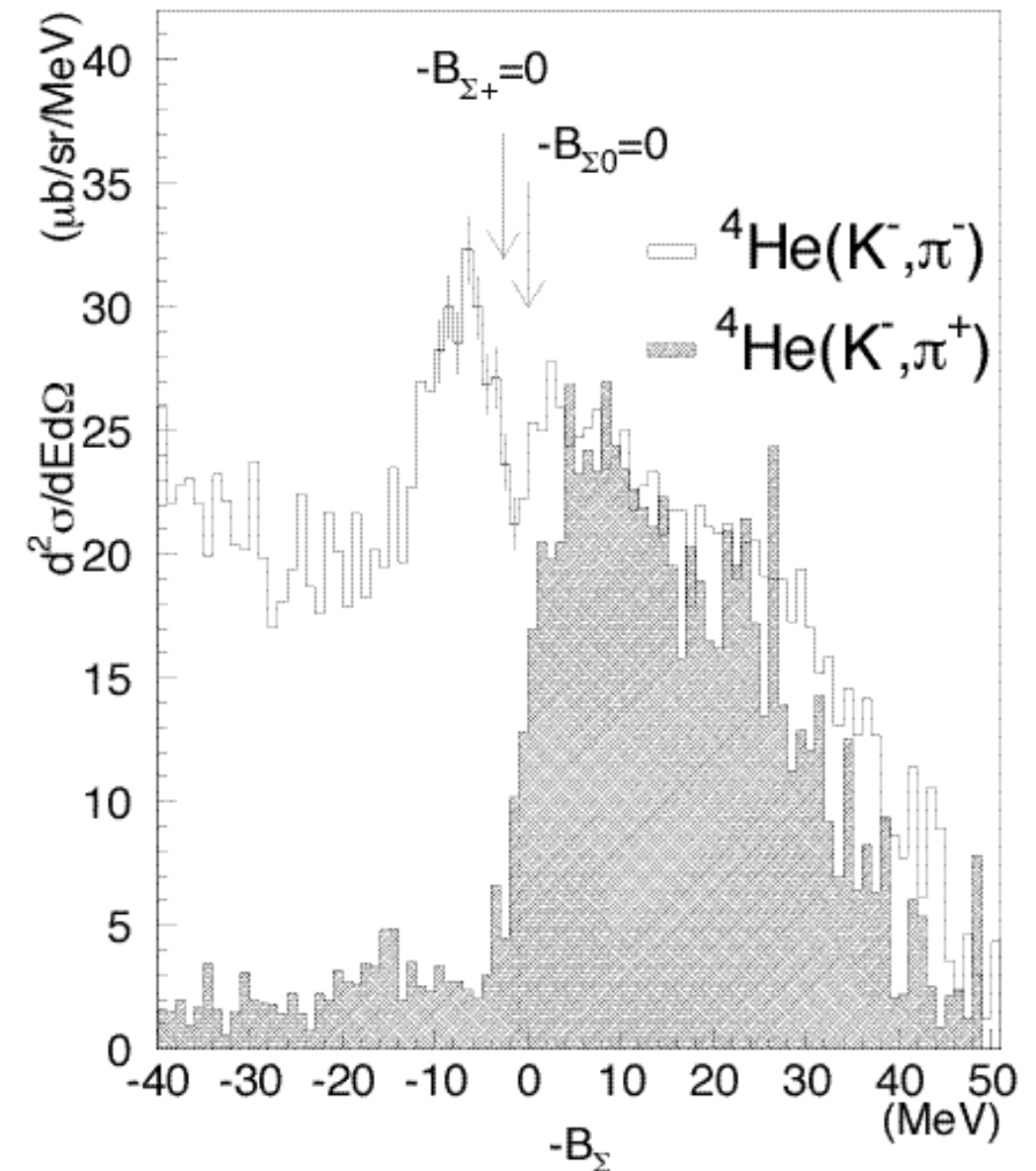
R.S. Hayano et al., PL B231 (1989).

H.Outa et al., Prog. Theor. Phys. Suppl. 117 (1994) 177.

BNL E905: In-flight (K^- , π^-)

- 600 MeV/c, 4 deg.
- Simple analysis: DWIA
- Established the existence of a bound state
 - B_Σ : $4.4 \pm 0.3 \pm 1$ MeV
 - Width : $7 \pm 0.7 + 1.2 / -0.0$ MeV (FWHM)

T. Nagae et al., PRL 80 (1998) 1605.



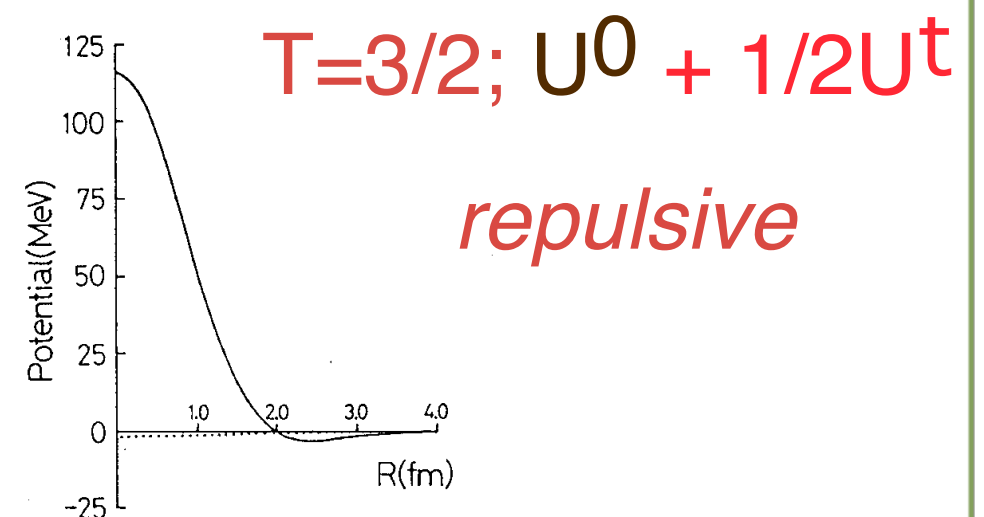
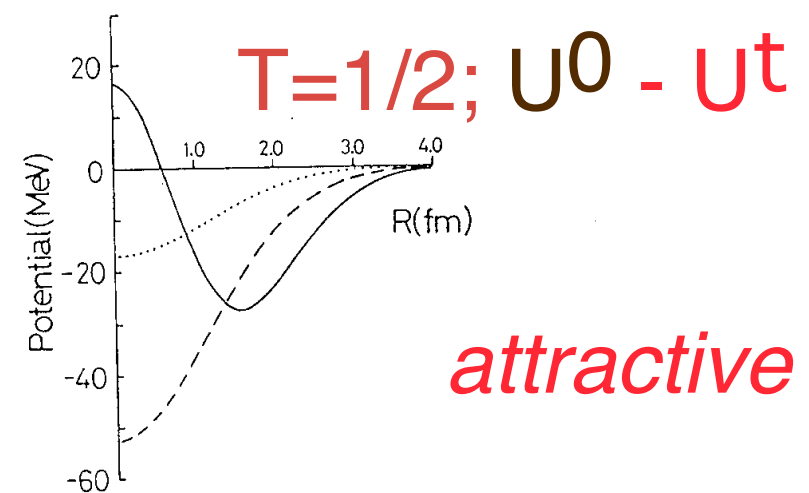
Harada and Akaishi

- Strong Isospin dependence

- Lane term

- $U_{C\Sigma} = U^0 + U^t T_C \cdot t_\Sigma / A$

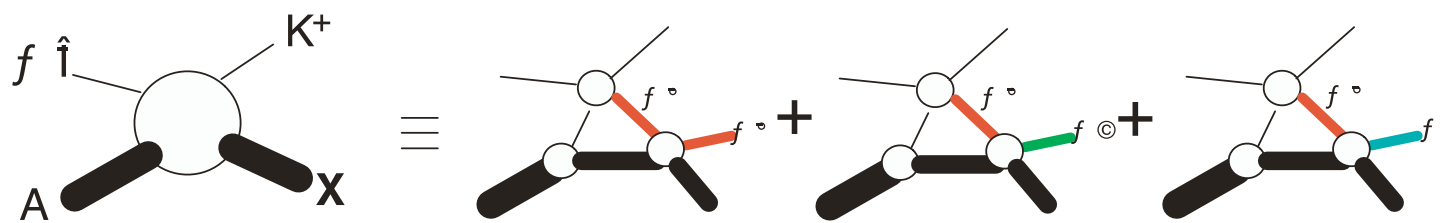
- T. Harada et al., Nucl. Phys. A507(1990) 715.
- T. Harada, PRL 81 (1998) 5287.



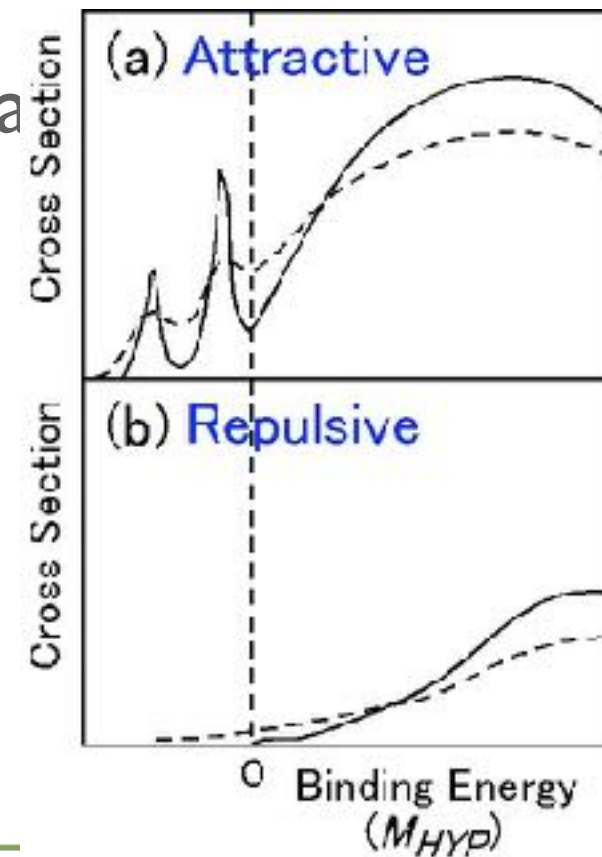
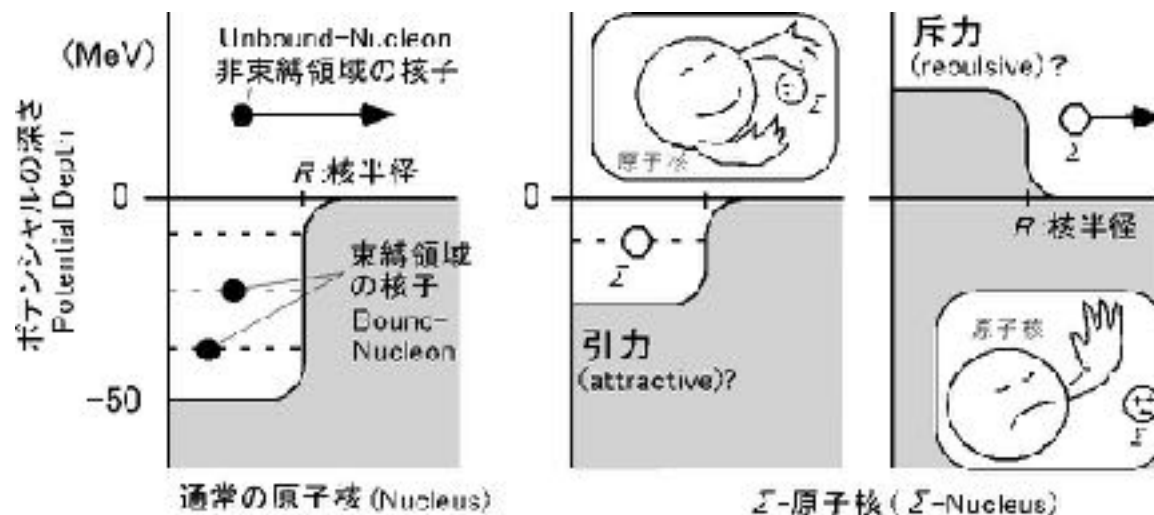
E438: Study of Σ -nucleus potential by the (π^-, K^+) reaction on heavy nuclei

$$U_{\Sigma} = V_{\Sigma} + iW_{\Sigma}$$

No Σ -hypernuclear bound states, but ${}^4_{\Sigma}\text{He}$



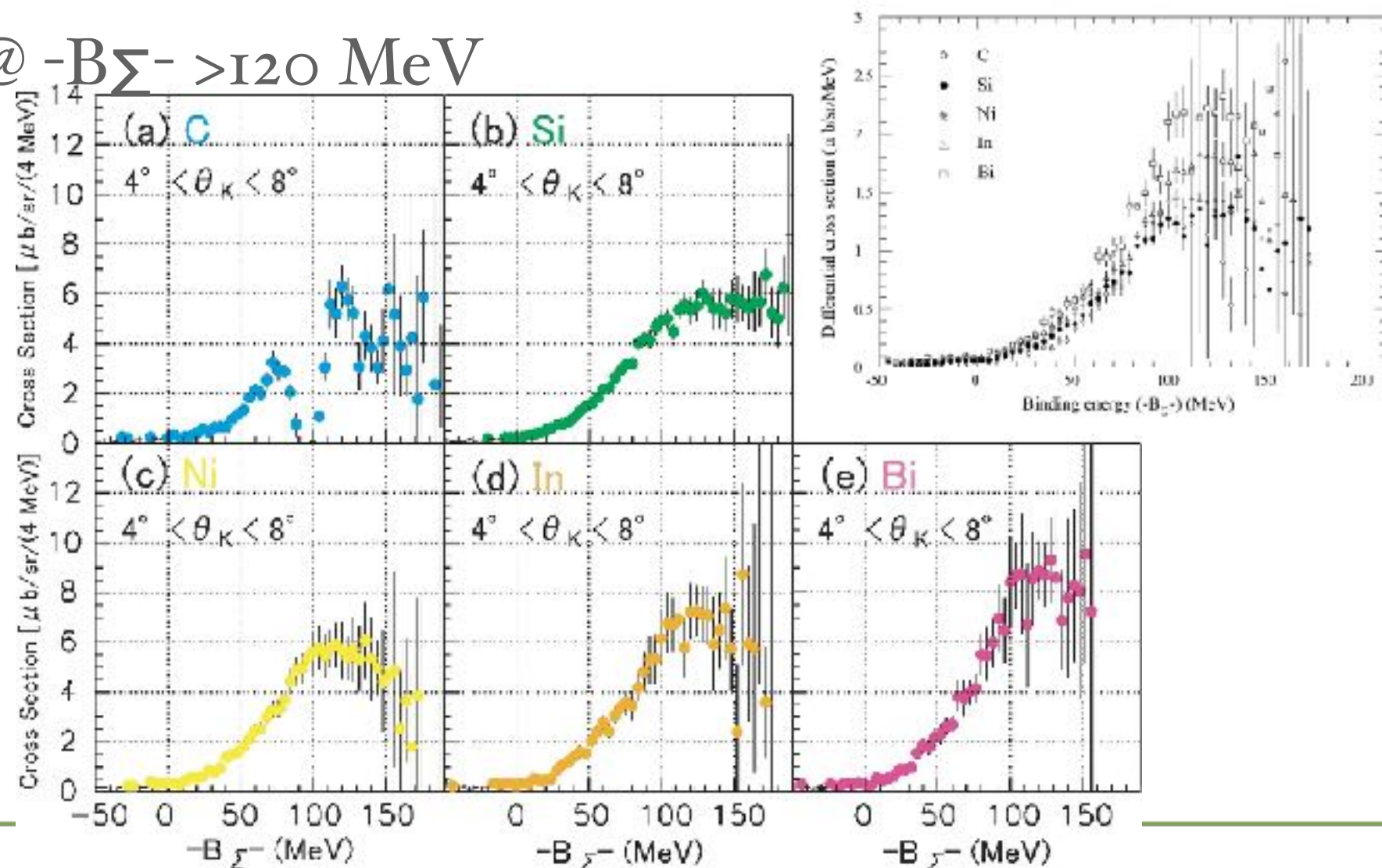
Inclusive spectrum tells the Σ potential

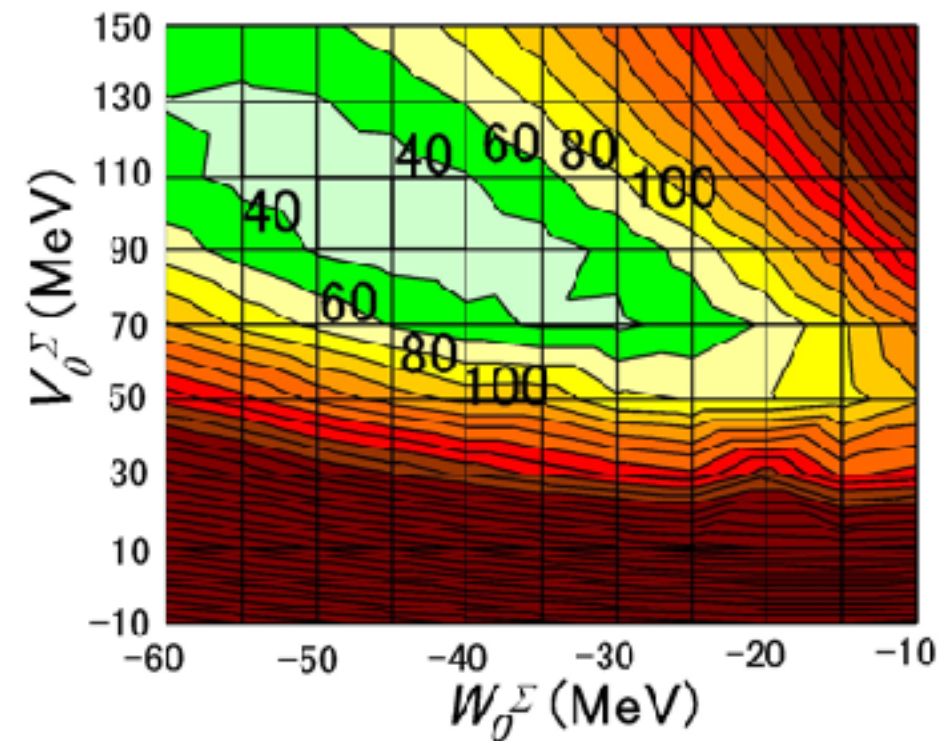
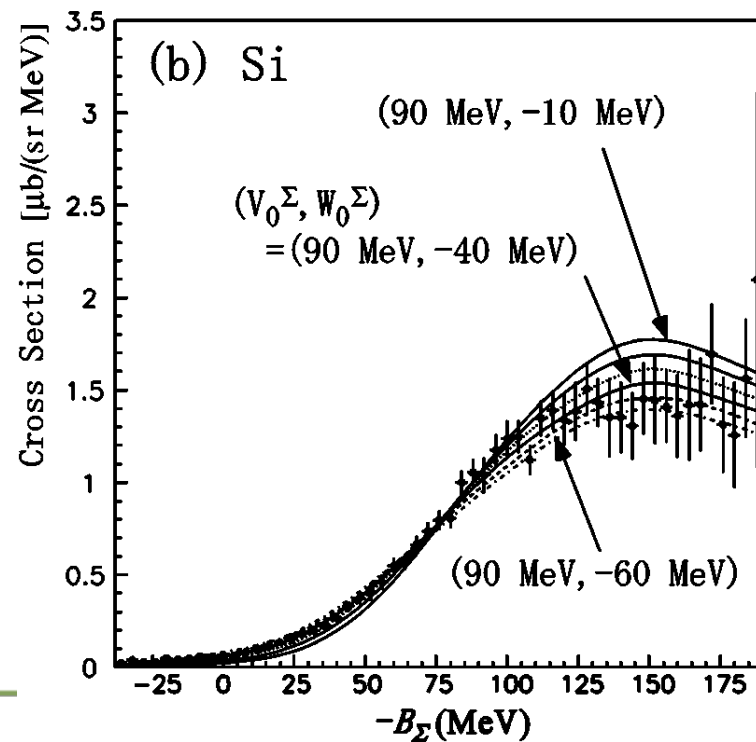
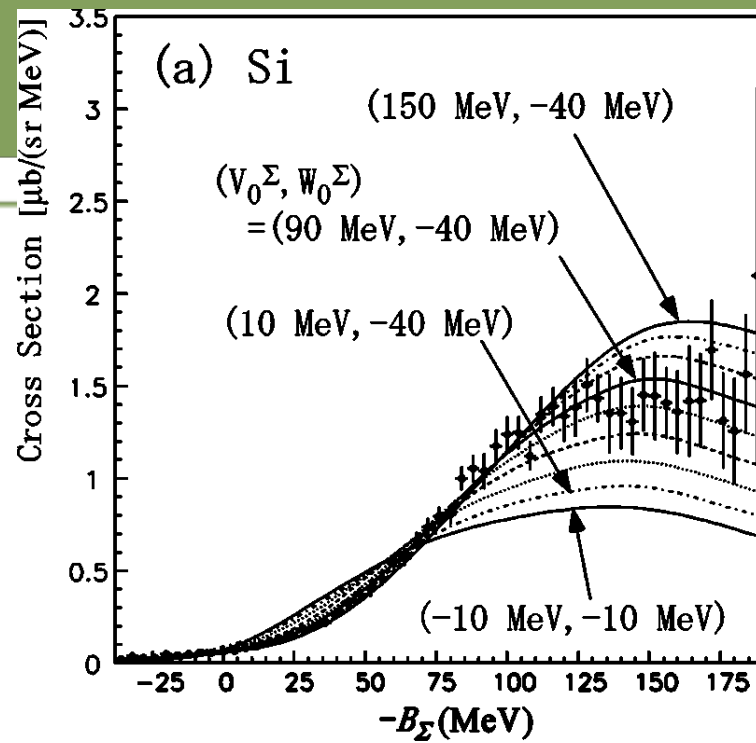


Measured Inclusive (π^- , K^+) Spectra on C, Si, Ni, In, & Bi

- Similar Shape
- No peak in $-B_{\Sigma^-} < 0$ MeV
- Maximum @ $-B_{\Sigma^-} > 120$ MeV

P.K. Saha et al., Phys. Rev. C 70 (2004) 044613.



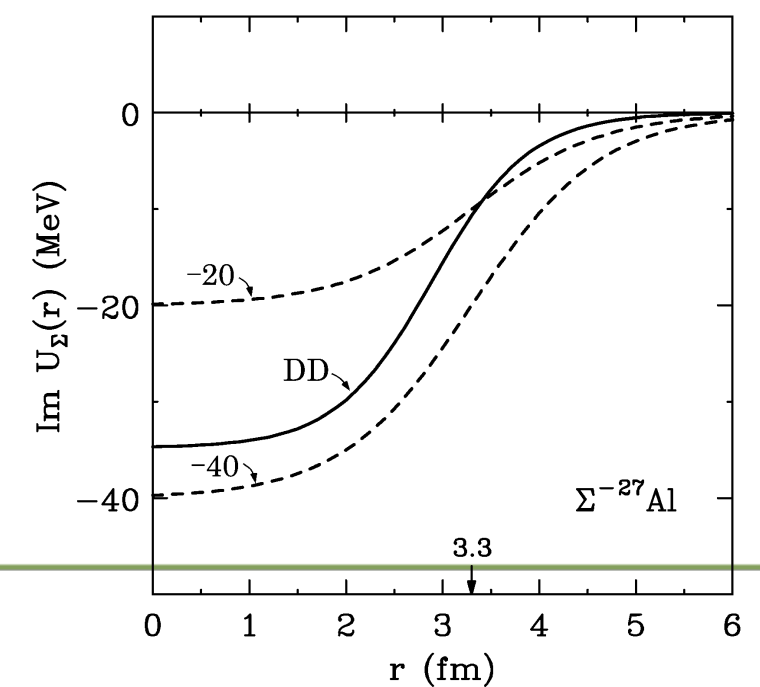
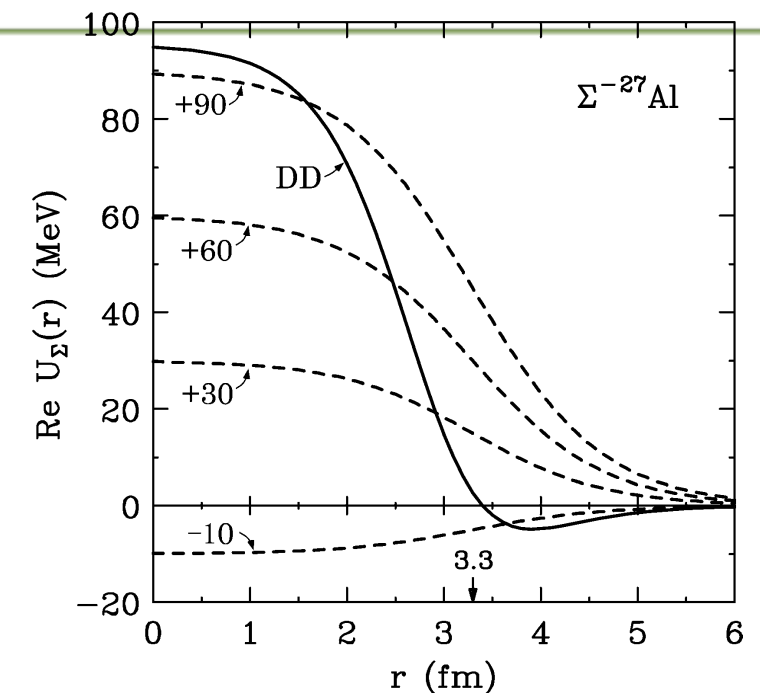
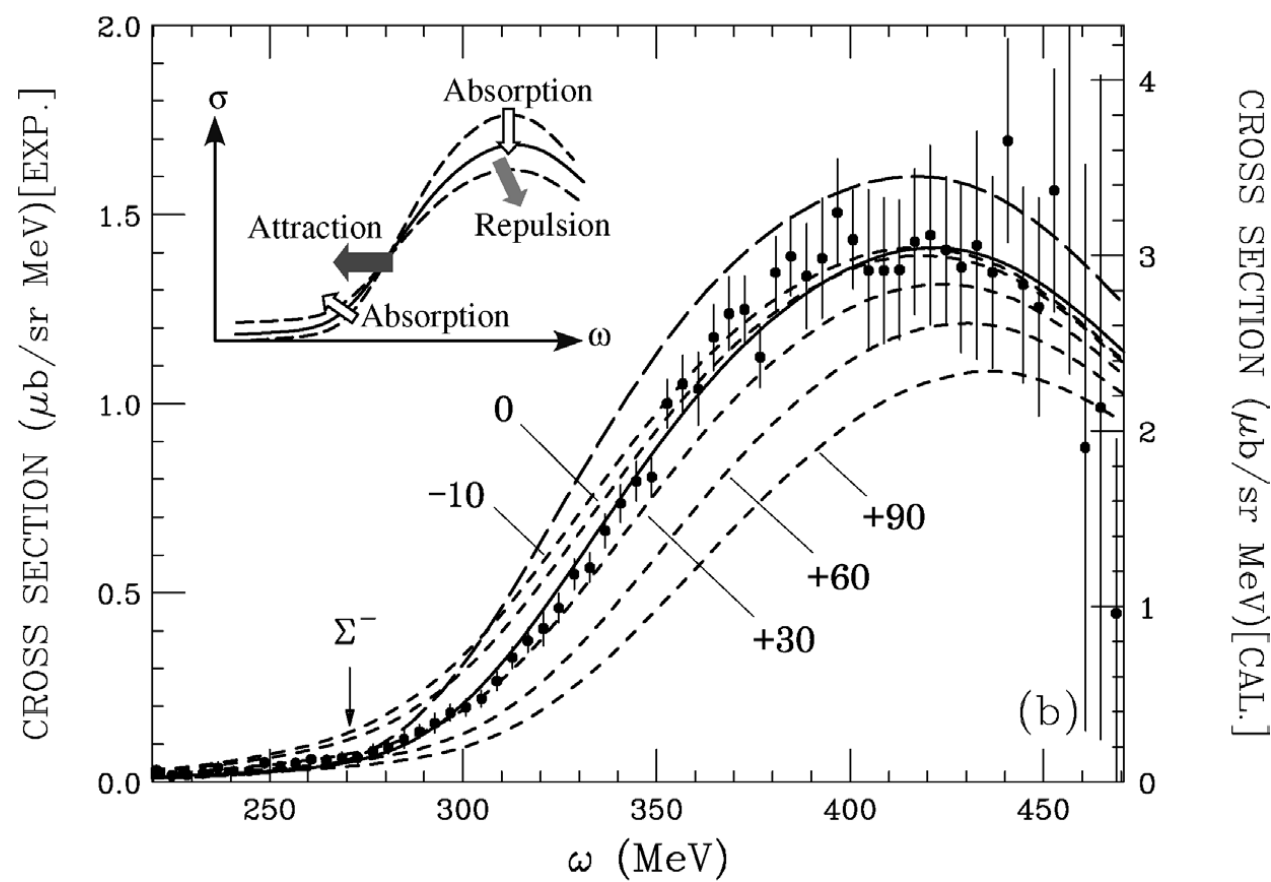


$V_0 = +90 \text{ MeV}, W_0 = -40 \text{ MeV}$

Theoretical analysis by Harada & Hirabayashi

T. Harada, Y. Hirabayashi / Nuclear Physics A 759 (2005) 143–169

► $V_0 = +30$ MeV, $W_0 = -40$ MeV



Summary on Σ hypernuclei

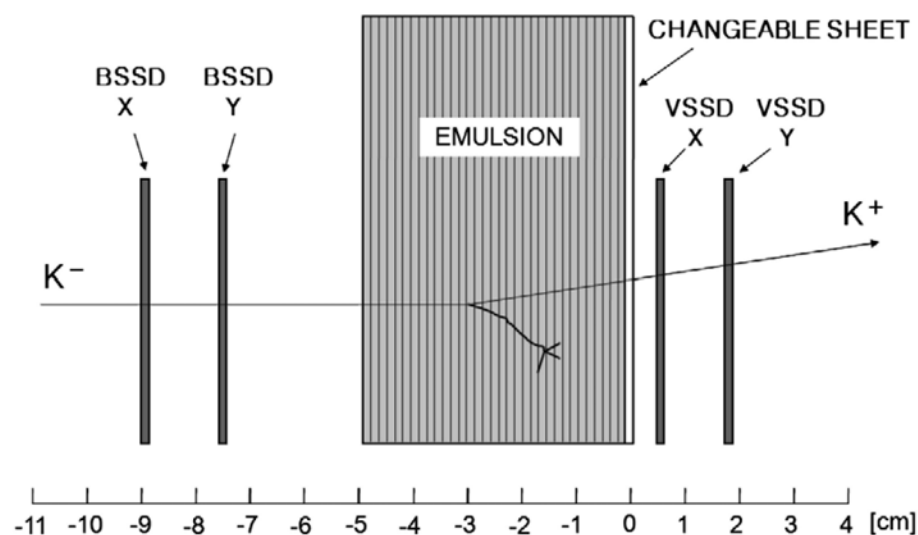
- ▶ No narrow states in unbound region
- ▶ One bound state in $^4_{\Sigma}\text{He}$
 - ▶ $^7_{\Sigma}\text{Li}$? Nucl. Phys. A 547 (1992) 175c.
- ▶ Σ -Nucleus potential is repulsive in medium-heavy system.

$S=-2$ Systems

Hybrid Emulsion Experiments

by K. Nakazawa

KEK E176



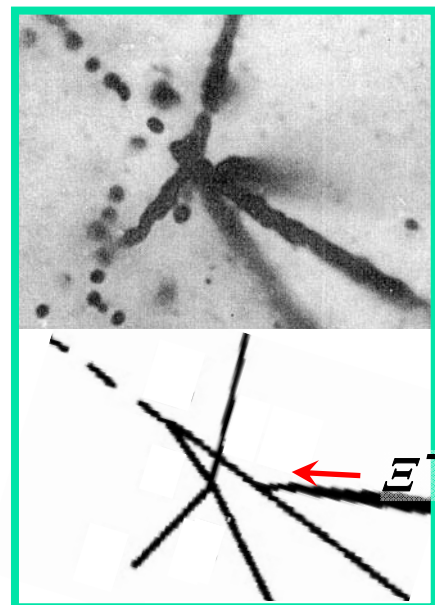
Introduction of experimental method

1. select Q.F. (K-,K+) reaction & reconstruct K⁺.
2. following up K⁺ meson in emulsion.
3. following down Ξ^- cand. track.
4. check seq. topology of DHY at end point.

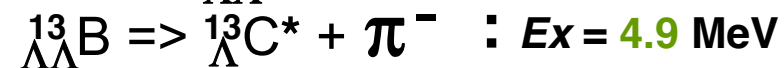
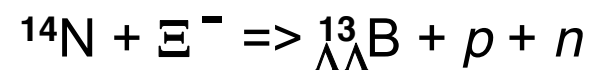
⇒ Ξ^- stops : **77.6 +/- 5.1 events captured by**

light elem. (C,N,O) : $42.3^{+4.5}_{-9.6}$ %

heavy elem. (Ag, Br): $57.7^{+6.1}_{-9.6}$ %



most probable case



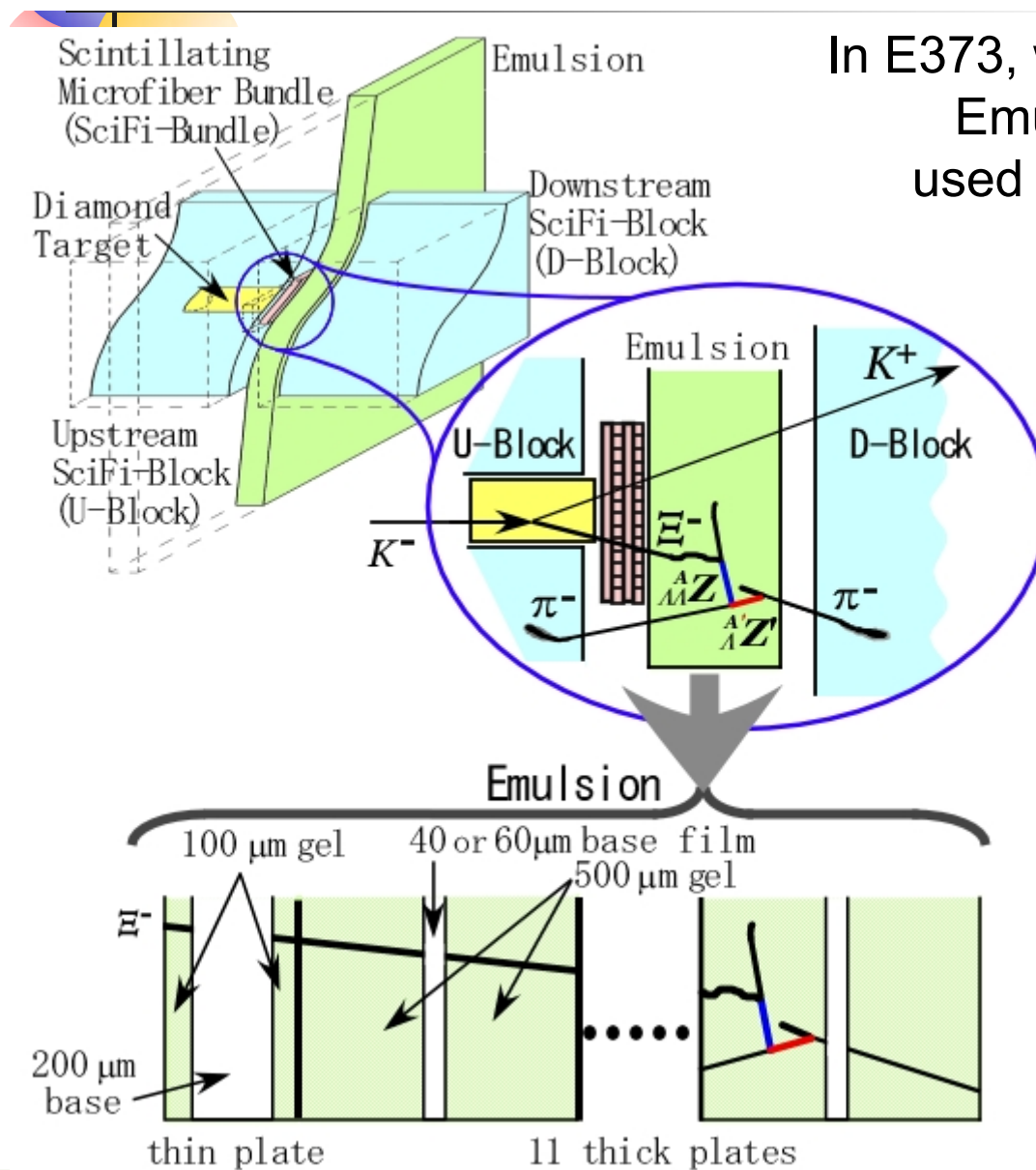
$$\boxed{\Lambda\Lambda^{13}\text{B}} \quad B_{\Lambda\Lambda} = 23.3 \pm 0.7 \text{ MeV}$$

$$\Delta B_{\Lambda\Lambda} = 0.6 \pm 0.8 \text{ MeV}$$

[Assumption]

$$B_{\Xi^-} = 0.17 \text{ MeV (atomic } \mathbf{3D} \text{ in } ^{14}\text{N-}\Xi^-)$$

KEK E373



In E373, we changed the target Emulsion (E176) ==> Diamond, used SciFi-Block and -Bundle.

1. select Q.F. (K^- , K^+) reaction,
2. reconstruct Ξ^- cand. track,
3. following down Ξ^- cand. track,
4. careful analysis of the vertex.

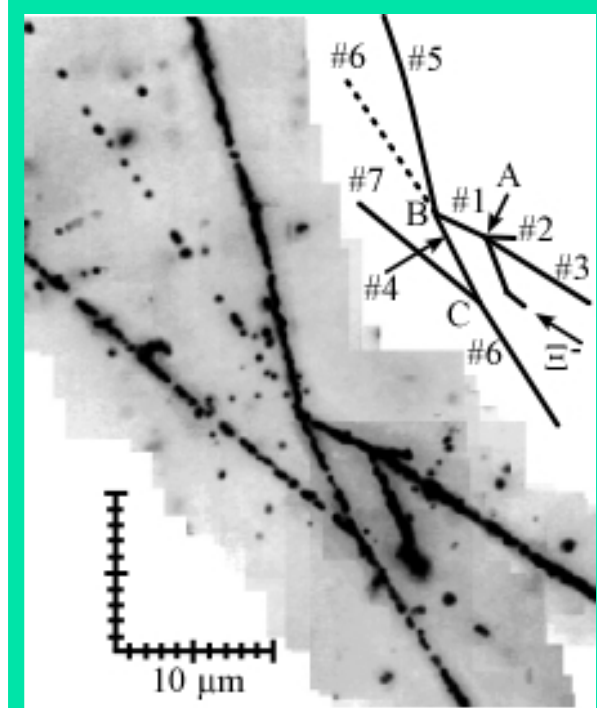
==> $\sim 10^3$ Ξ^- stops

“ the most significant result of the past 5 years in hypernuclear physics. ”

Final Report of the 2004 KEK PS External Review Committee (August 30, 2004), p5.

for NAGARA event

► Nagara Event



Unique assignment $^{12}\text{C} + \Xi^- \rightarrow \Lambda\Lambda^6\text{He} + ^4\text{He} + t$
 $\hookrightarrow \Lambda^5\text{He} + p + \pi^-.$

1. From Consistency in A & B : $B_{\Xi^-} < 1.86 \text{ MeV}$
2. By kinematical fitting : $B_{\Lambda\Lambda} = 6.79 + 0.91 B_{\Xi^-} (+/- 0.16) \text{ MeV}$
 $\Delta B_{\Lambda\Lambda} = 0.55 + 0.91 B_{\Xi^-} (+/- 0.17) \text{ MeV}$

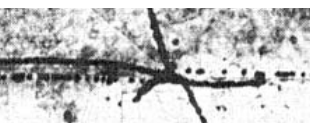
if we take into account $B_{\Xi^-} = 0.13 \text{ MeV}$ [atomic 3D : $^{12}\text{C} - \Xi^-$]

$\Lambda\Lambda^6\text{He}$ $B_{\Lambda\Lambda} = 6.91 +/- 0.16 \text{ MeV}, \Delta B_{\Lambda\Lambda} = 0.67 +/- 0.17 \text{ MeV}$

cf. in the paper PRL(2001) $B_{\Lambda\Lambda} = 7.25 +/- 0.19 \text{ MeV}, \Delta B_{\Lambda\Lambda} = 1.01 +/- 0.20 \text{ MeV}$

This discrepancy was come from the mass change of Xi- hyperon in PDG.

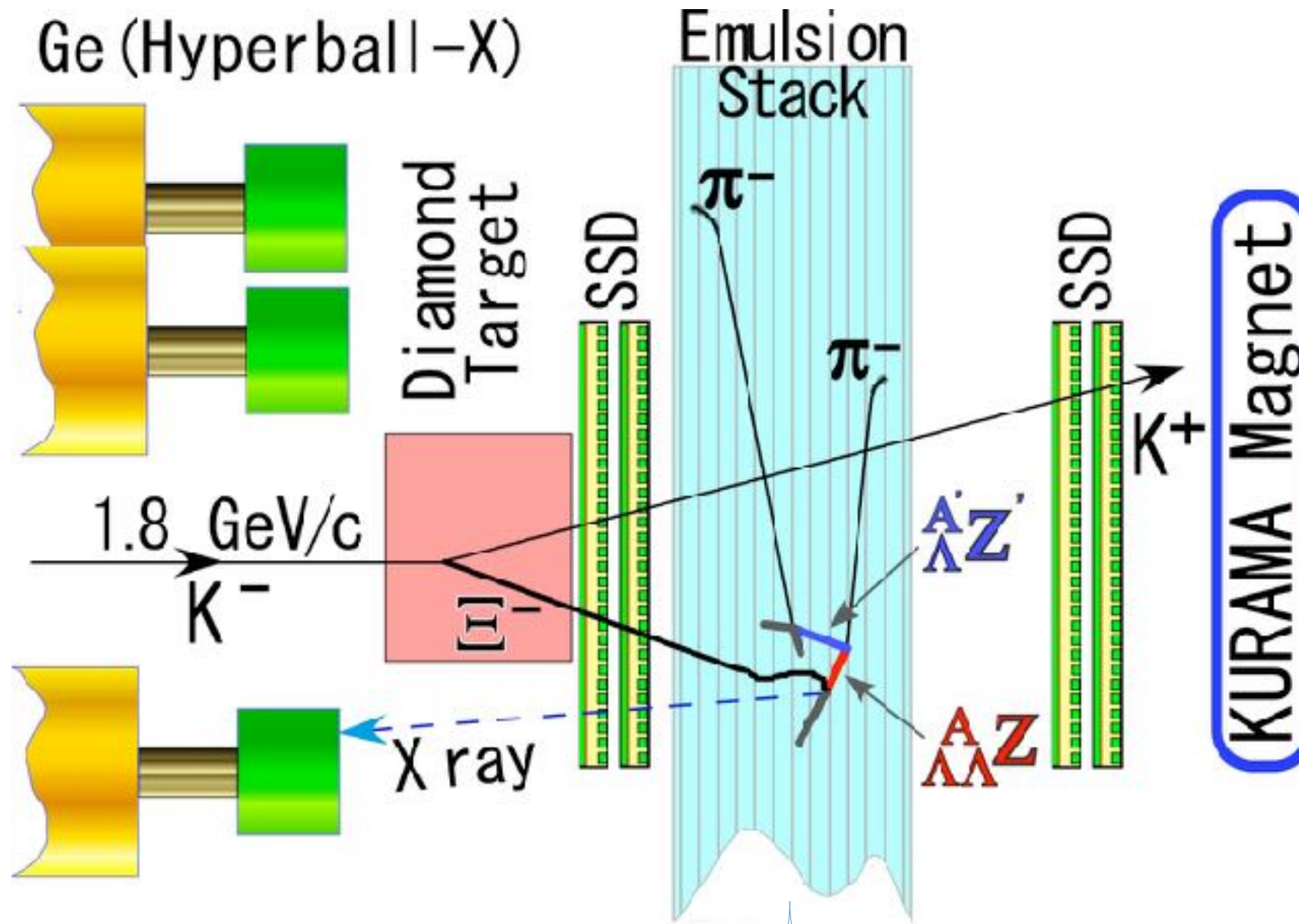
Summary of Emulsion events

	$\Lambda\Lambda Z$ Captured:	$B_{\Lambda\Lambda} - B_{\Xi^-}$ [MeV]	$\Delta B_{\Lambda\Lambda} - B_{\Xi^-}$ [MeV]	Assumed level	$B_{\Lambda\Lambda}$ [MeV]	$\Delta B_{\Lambda\Lambda}$ [MeV]
NAGARA	$\Lambda\Lambda^6\text{He}^{12}\text{C}$	$B_{\Lambda\Lambda} = 6.79 + 0.91 B_{\Xi^-}$ (+/- 0.16) $\Delta B_{\Lambda\Lambda} = 0.55 + 0.91 B_{\Xi^-}$ (+/- 0.17) $B_{\Xi^-} < 1.86$		3D	6.91 +/- 0.16	0.67 +/- 0.17
MIKAGE	$\Lambda\Lambda^6\text{He}^{12}\text{C}$	9.93 +/- 1.72	3.69 +/- 1.72	3D	10.06 +/- 1.72	3.82 +/- 1.72
DEMACHI-YANAGI	$\Lambda\Lambda^{10}\text{Be}^{*12}\text{C}$	11.77 +/- 0.13	-1.65 +/- 0.15 <i>cf. Ex = 3.0</i>	3D	11.90 +/- 0.13	-1.52 +/- 0.15 <i>cf. Ex = 3.0</i>
HIDA	$\Lambda\Lambda^{11}\text{Be}^{16}\text{O}$	20.26 +/- 1.15	2.04 +/- 1.23	3D	20.49 +/- 1.15	2.27 +/- 1.23
	$\Lambda\Lambda^{12}\text{Be}^{14}\text{N}$	22.06 +/- 1.15	-----	3D	22.23 +/- 1.15	-----
E176	$\Lambda\Lambda^{13}\text{B} \rightarrow \Lambda^{13}\text{C}^*$	----- <i>Ex = 4.9</i>	-----	3D	23.3 +/- 0.7	0.6 +/- 0.8
	 $\Lambda\Lambda^{10}\text{Be} \rightarrow \Lambda^9\text{Be}^*$	----- <i>Ex = 3.0</i>	-----	not checked, yet.	14.7 +/- 0.4	1.3 +/- 0.4

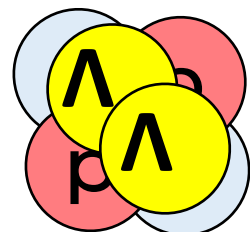
M.Danyasz et al., PRL.11(1963)29;
R.H.Dalitz et al., Proc. R.S.Lond.A436(1989)1

J-PARC E07

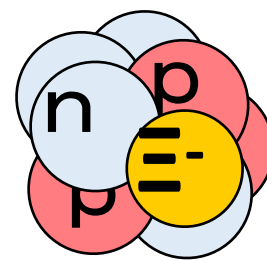
Systematic study of double strangeness nuclei with Hybrid emulsion method



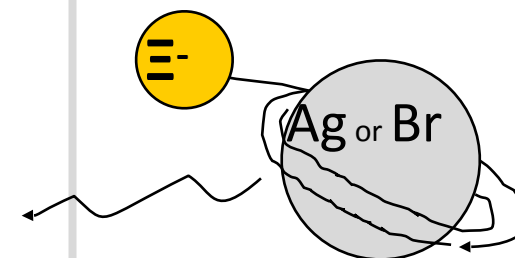
$\Lambda\Lambda$ hypernucleus



Ξ hypernucleus



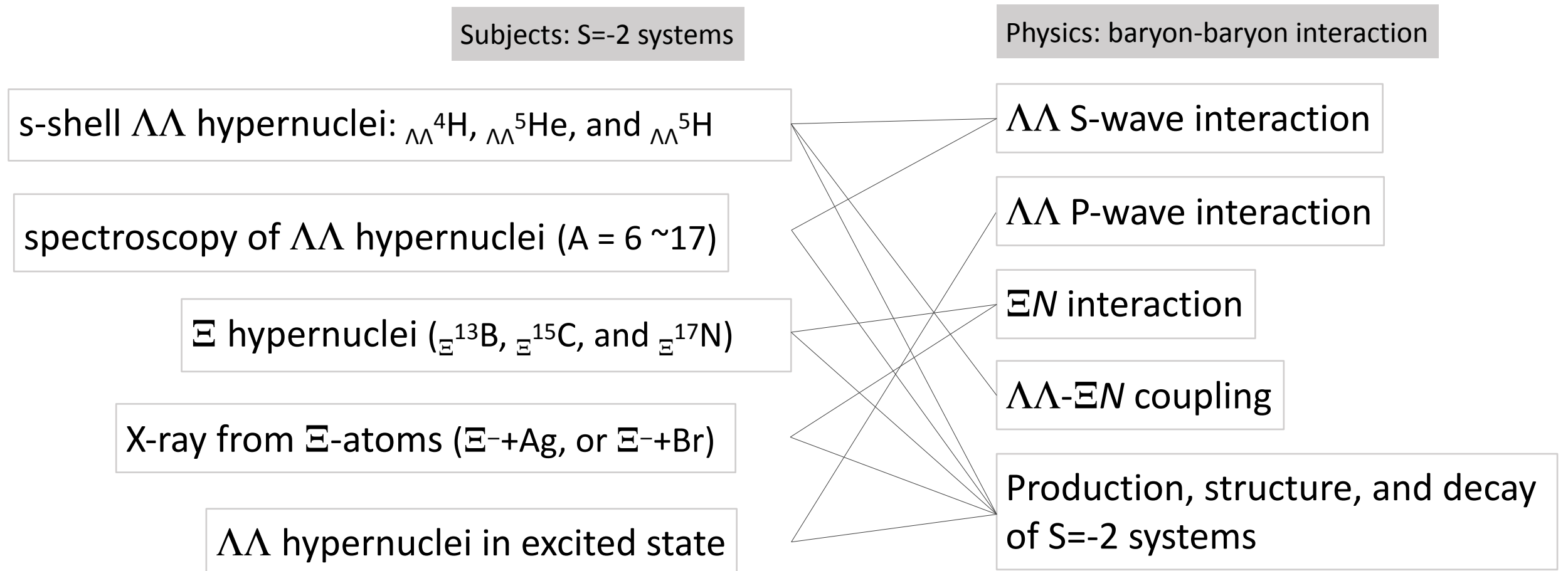
X-ray from Ξ^- atom



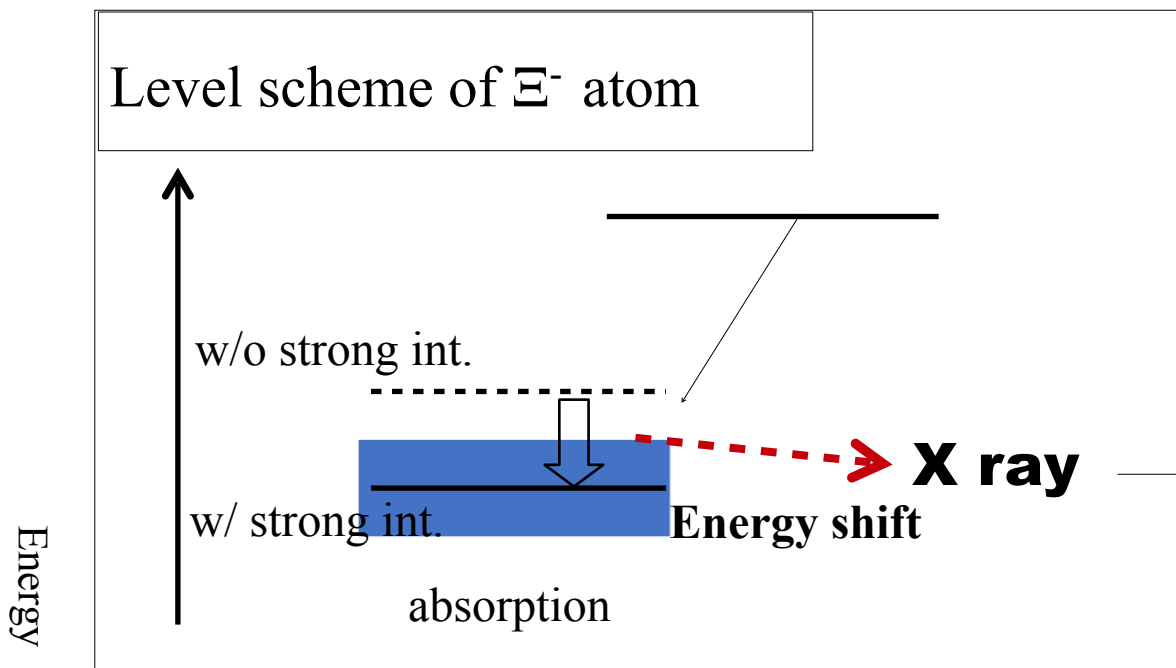
Concept: 10k Ξ^- stop events, which is 10 times statistics more than that of KEK-PS E373

	KEK-PS E373	J-PARC E07 (in proposal)
Emulsion gel	0.8 tons	2.1 tons
Purity of K- beam	25%	~85%
Ξ^- stop yield	~650	10k
S=-2 hypernuclei	9	~10 ²

Physics motivations



Ξ^- atom X-ray spectroscopy at J-PARC (E07)

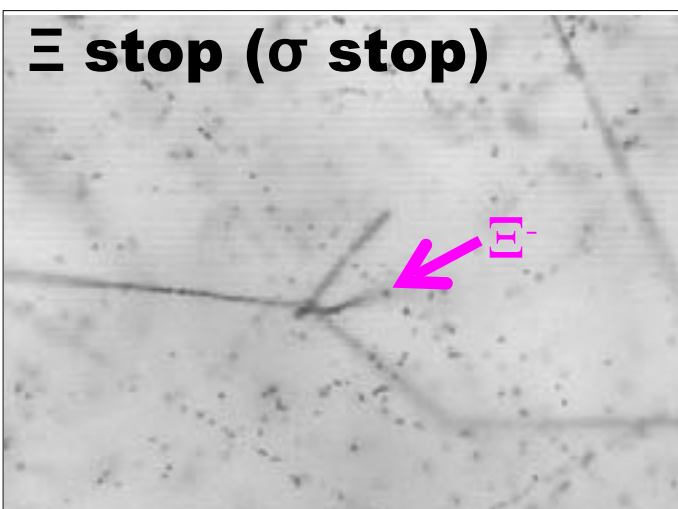


Hybrid emulsion method

Select (K^- , K^+) reaction by spectrometers



Select Ξ^- stop event by emulsion image



Coincidence with Hyperball-X data

Analysis status

Ξ^- Ag atom, Ξ^- Br atom data (from the emulsion)

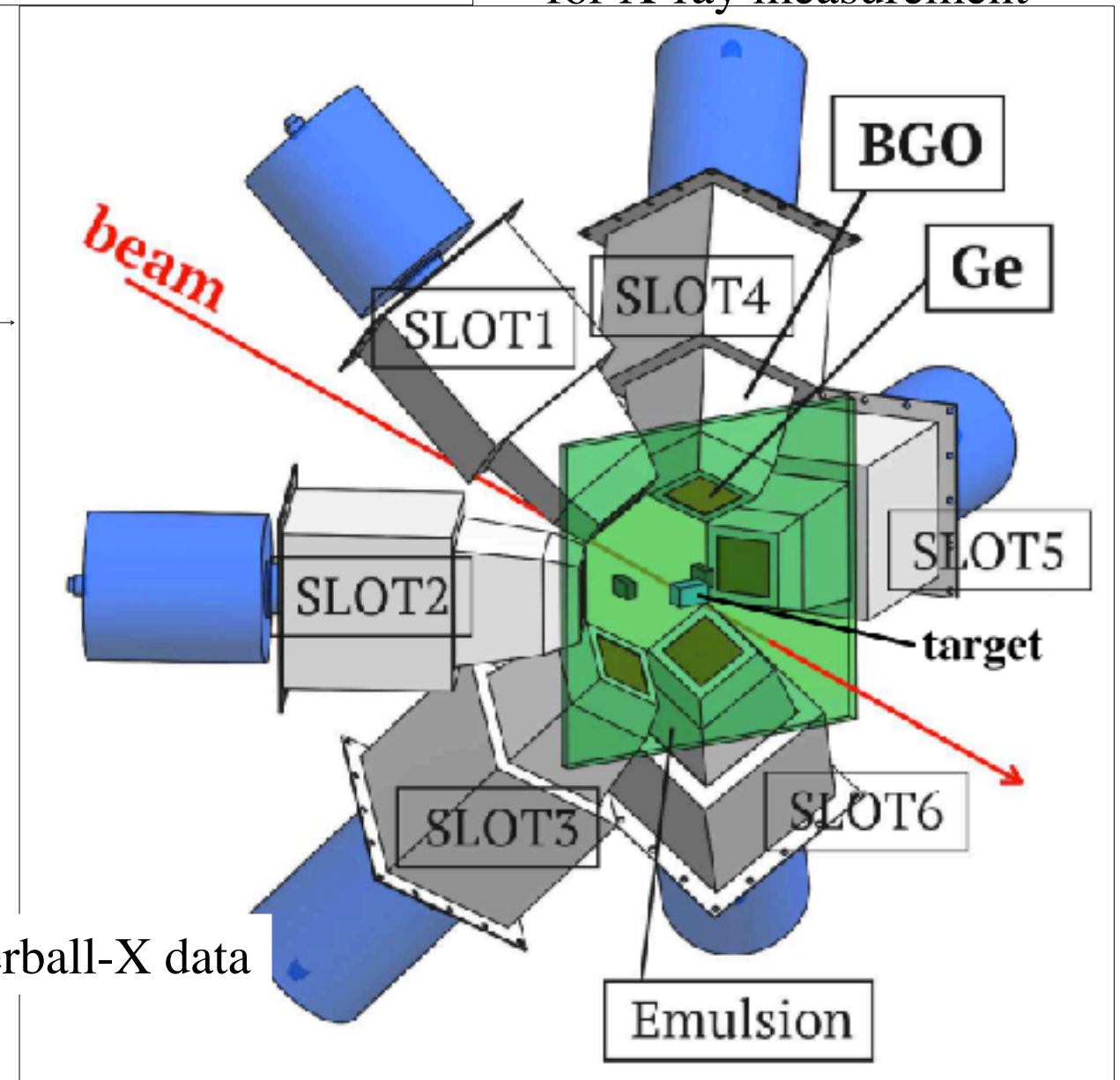
→ 20% coincidence analysis is finished

Ξ^- C atom data (from the diamond target)

→ On going

Hyperball-X

Ge detector array for X-ray measurement



Beam exposure

May-Jun. 2016

KURAMA Commissioning : 5.0 days

Physics : 4.9 days

4/15 - 4/19, 2017 (44kW)

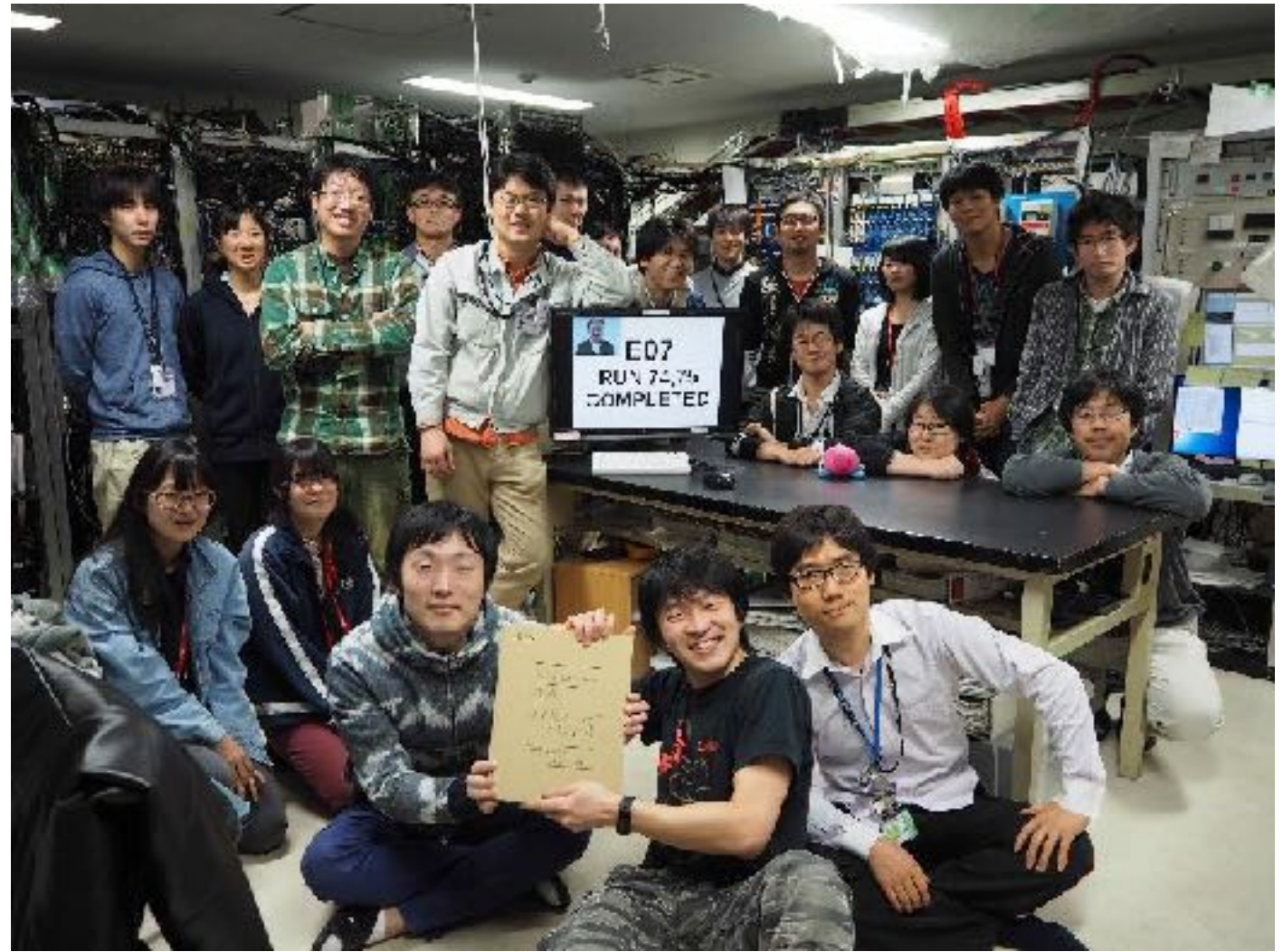
Emulsion exposure : 50 h

calibration : 19 h

5/25 - 6/29, 2017 (10 - 37.5kW)

Emulsion exposure : 23.4 days

calibration : 8.5 h



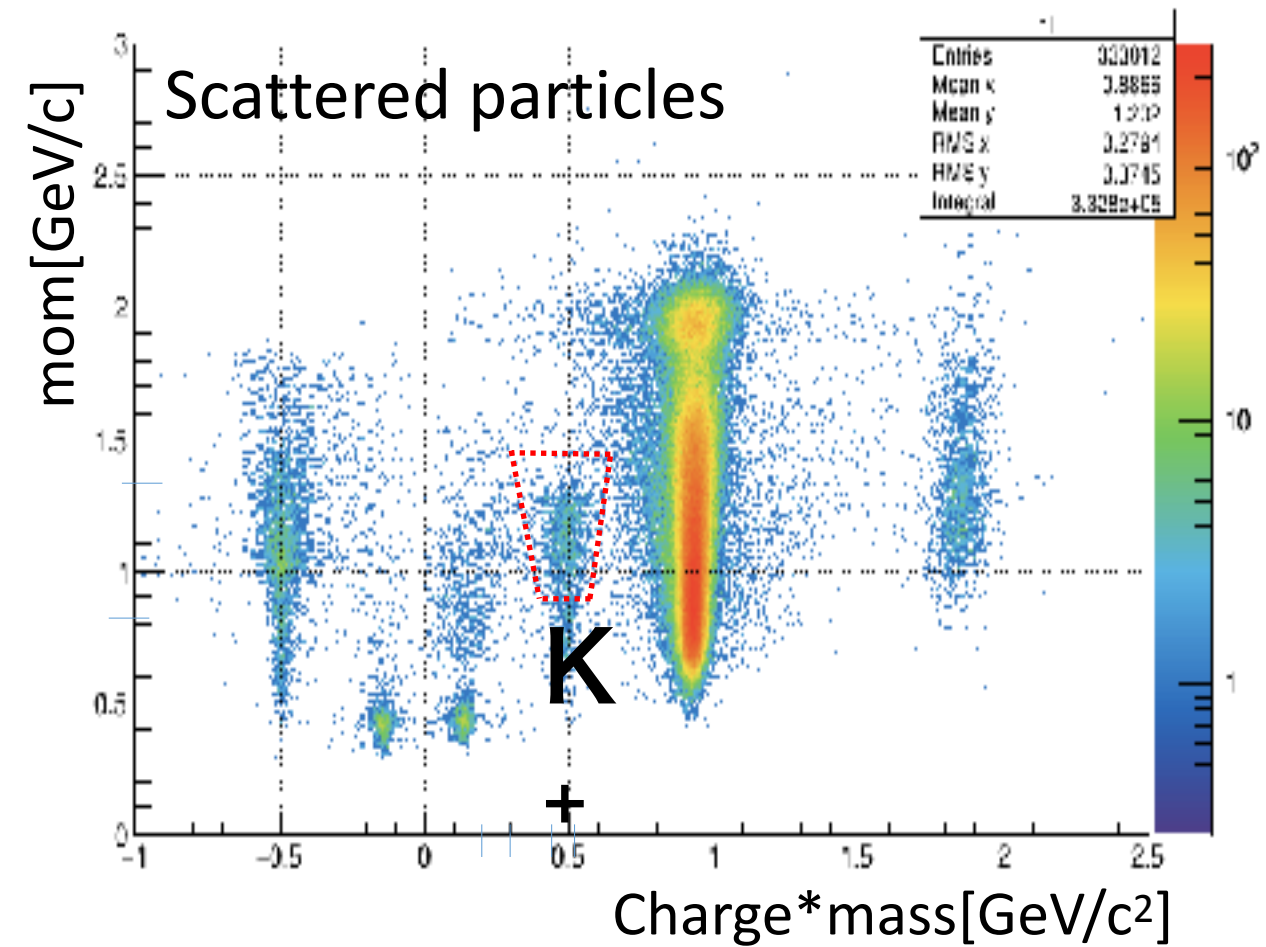
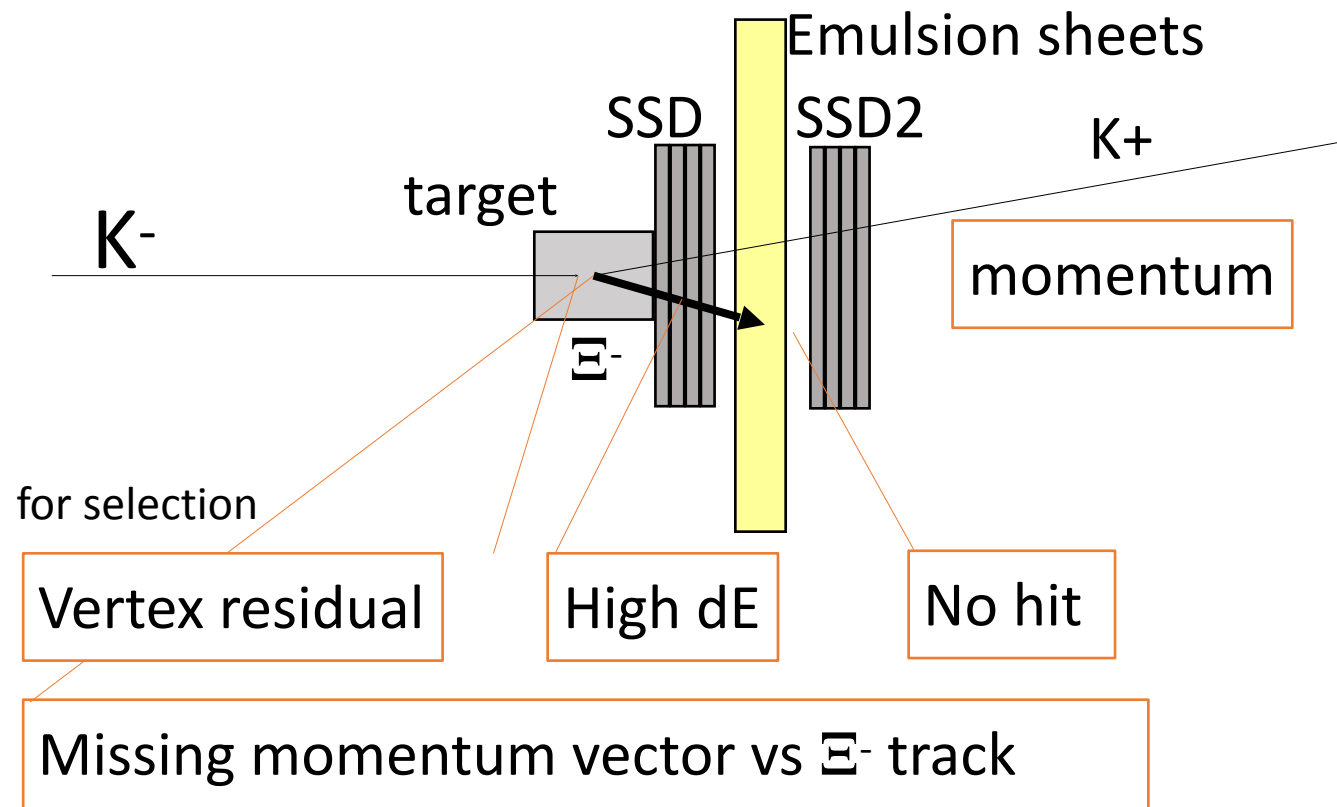
Jul. 1st 2017, Run end photo @K1.8 counting room

Year	Beam power [kW]	K- intensity [/spill]	K- purity	Time [h/mod.]
2016	42	260k	81%	6.5
2017	44	310k	83%	5.6
2017	37.5	280k	82%	6.0
2017	10 - 35	120k – 270k	50% - 82%	6.5 - 9.9

118 emulsion modules

Photographic processing: completed in Feb. 2018 in Gifu-U.

Ξ^- selection from the (K-, K+) reaction by off-line analysis



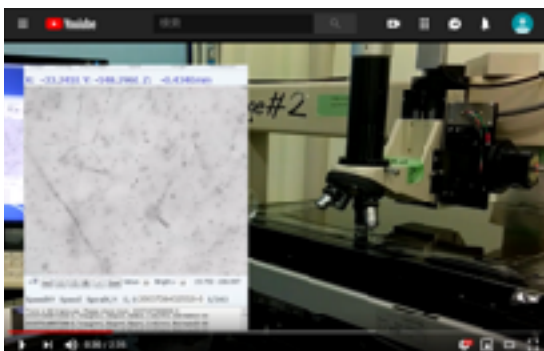
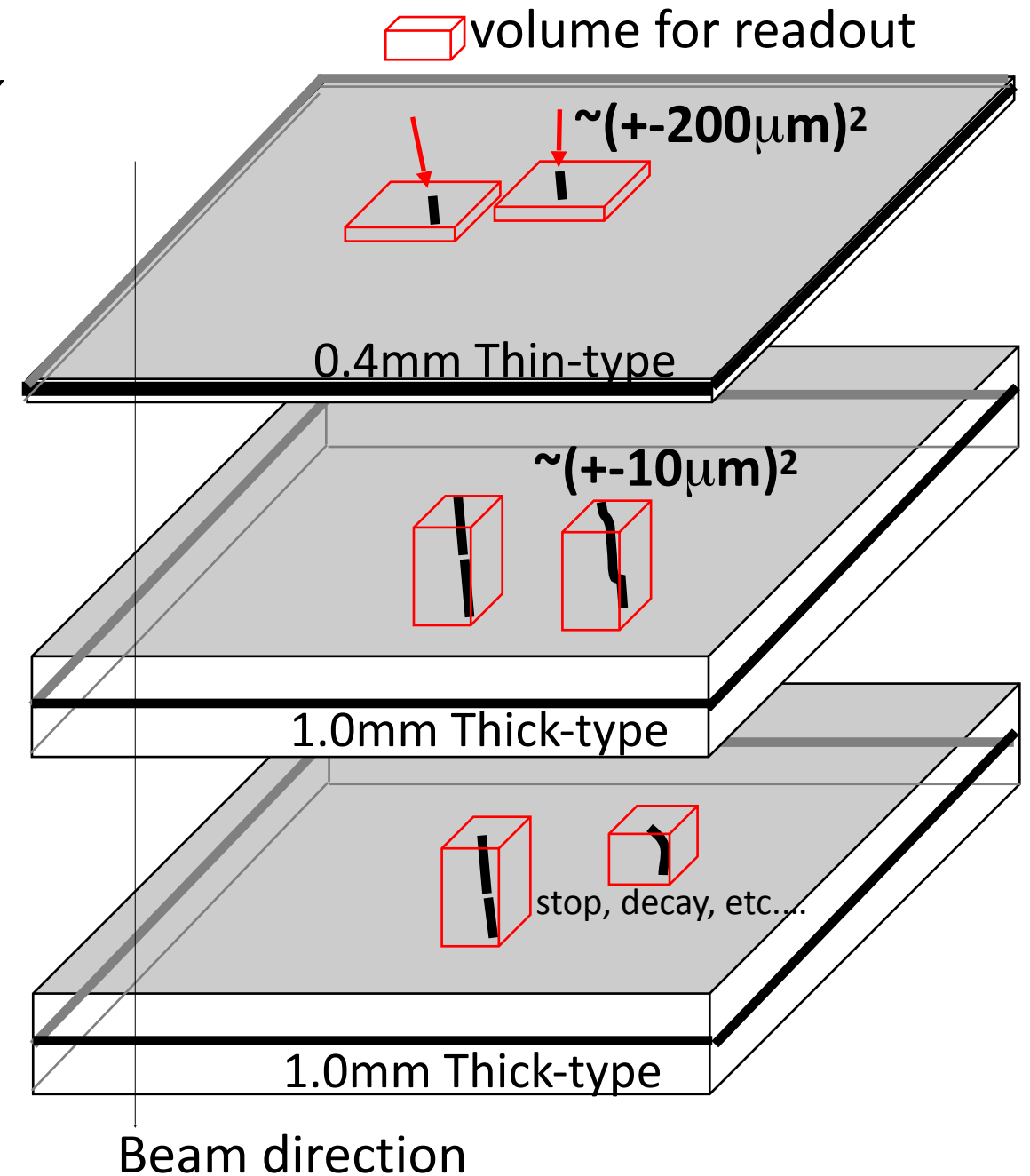
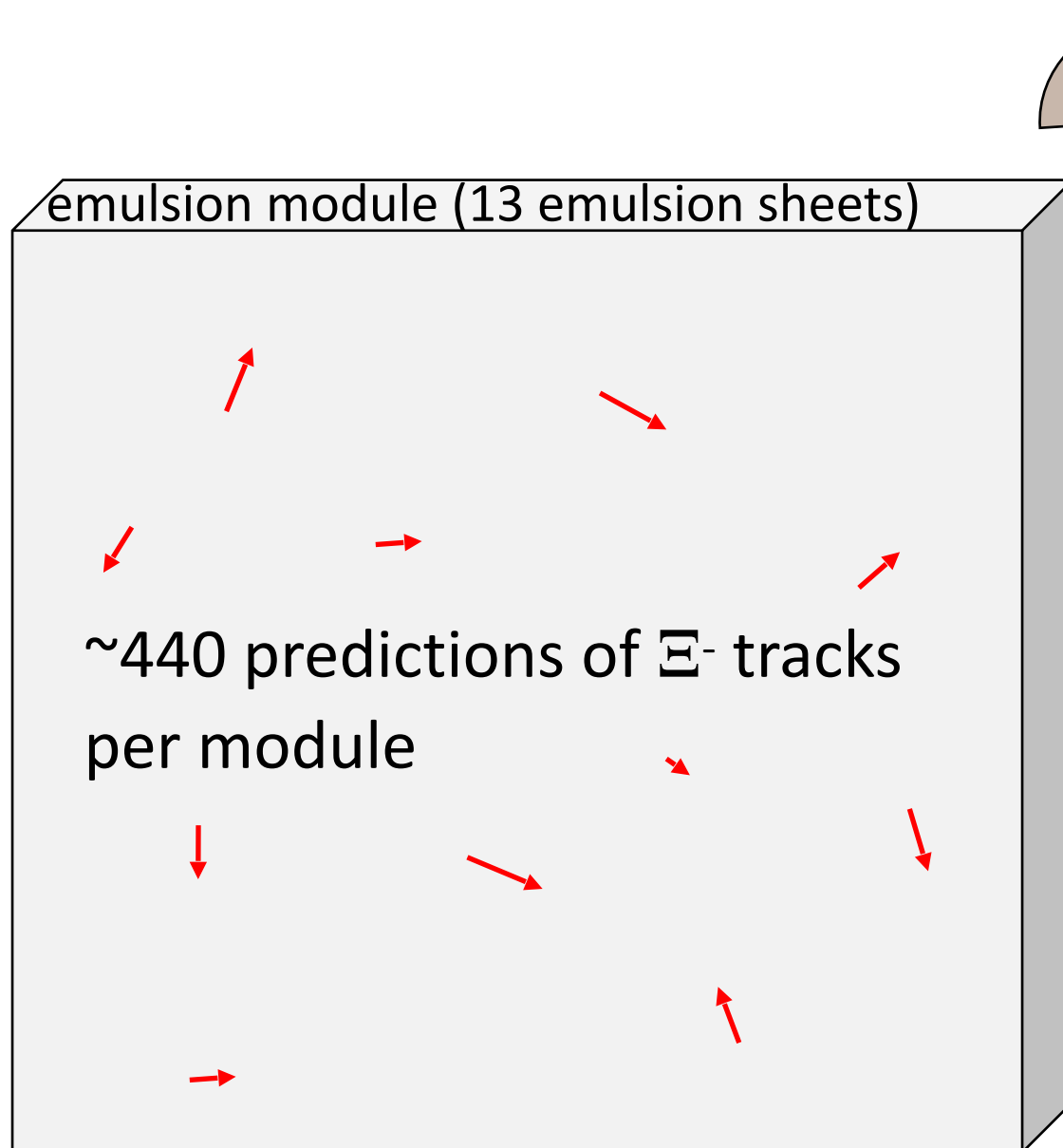
Criteria for Ξ^- track selection

by simulation for 118 modules

Level	Ξ^- stop	prediction/mod.		
1	9k	~440	High S/N & stop ratio	1 st priority
2	1k	~850	Realistic selection	
3	1k	6.2k	All Ξ^- stop	
4	negligible	16k	All combination	

Track following for Ξ^- stop event

- * Disassembling
- * Photographic developing



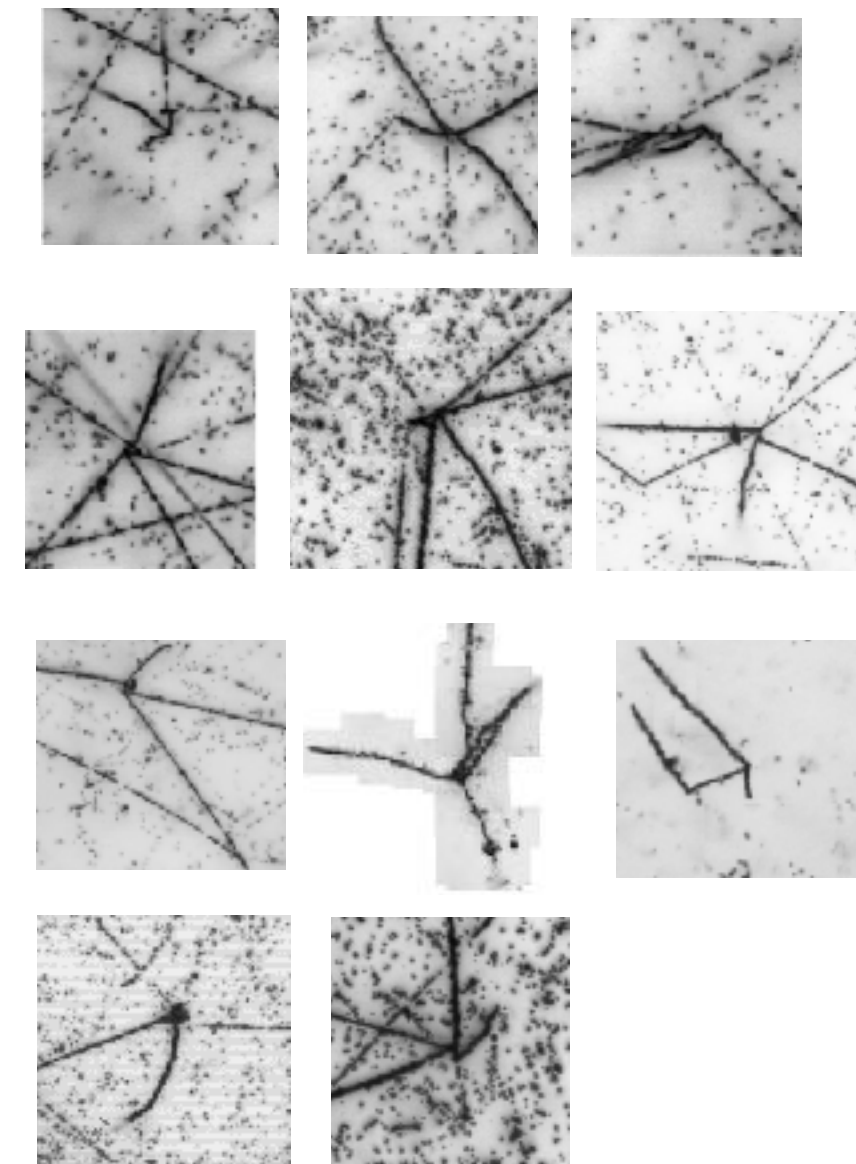
Automated Track Following (Sample Movie)
<https://youtu.be/3fiWI5tDx2U>

2019 May

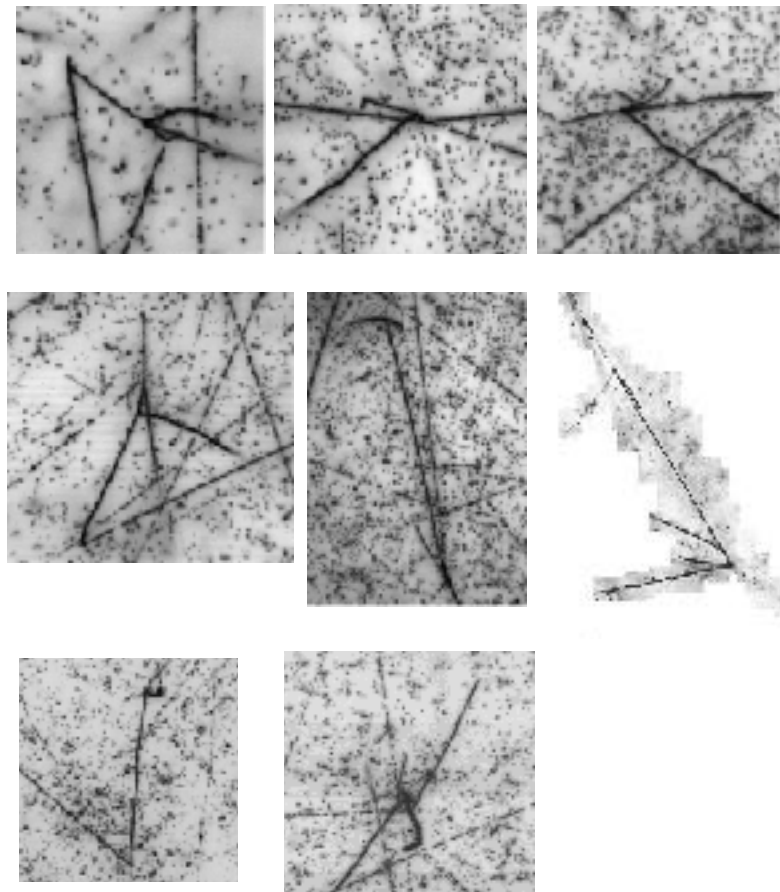
So far, 70% of emulsion sheets has been scanned at least once.

	KEK-PS E373	E07 (current)
E^- stop with nuclear fragment	430	1.6k (1.6k/430 = 3.8)
S=-2 system	9	26

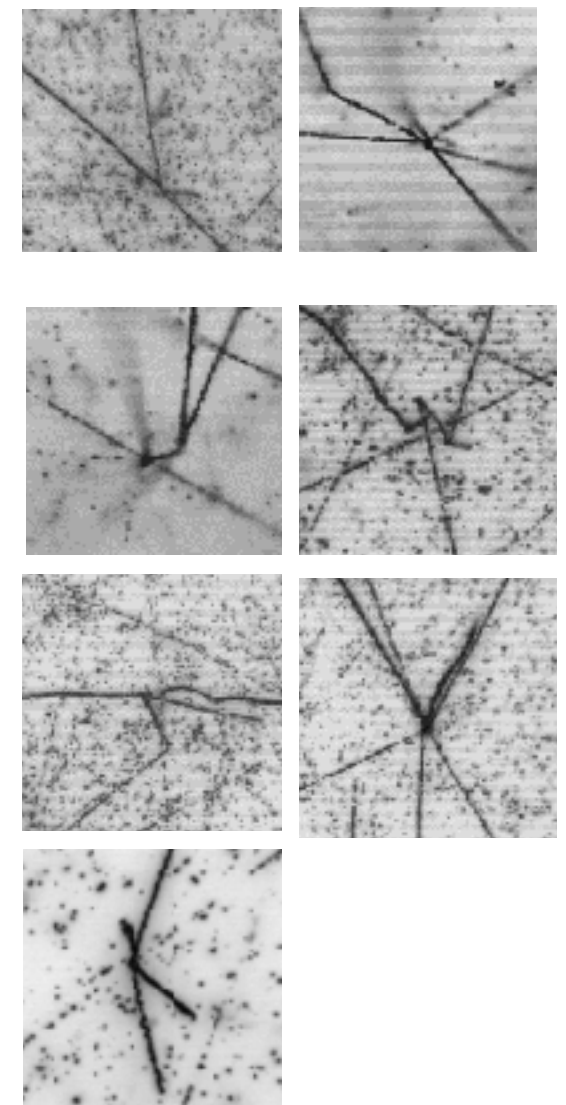
11 double Lambda events



8 twin events



7 others



2019 May

So far, 70% of emulsion sheets has been scanned at least once.

	KEK-PS E373	E07 (current)
Ξ^- stop with nuclear fragment	430	1.6k (1.6k/430 = 3.8)
S=-2 system	9	26

11 double Lambda events

D001 98-4 $\Lambda\Lambda$ ^8Li or $\Lambda\Lambda$ ^{10}Be	D002 42-10 Many candidates	D003 90-6 $(\Lambda\Lambda\text{C})$
D004 112-7 $(\Lambda\Lambda\text{C})$	D005 48-5 $(\Lambda\Lambda\text{C})$	D006 32-9 Many candidates
D007 69-7 $\Lambda\Lambda$ Be MINO π^-	D008 87-4 Many candidates	D009 30-6 $\Lambda\Lambda$ Li or $\Lambda\Lambda$ Be
D010 37-2 Found recently	D011 79-2 Found recently	

8 twin events

T001 104-3 Many candidates	T003 75-7 Many candidates	T005 61-7 Many candidates
T002 117-7 $(^{14}\text{N} + \Xi^-)$ in progress	π^- T004 62-11 $^{16}\text{O} + \Xi^-$ atomic	π^- T006 47-10 Ξ^- ^{15}C IBUKI
T007 43-4 $(^{14}\text{N} + \Xi^-)$ in progress	T008 43-7 $(^{12}\text{C} + \Xi^-)$ in progress	

7 others

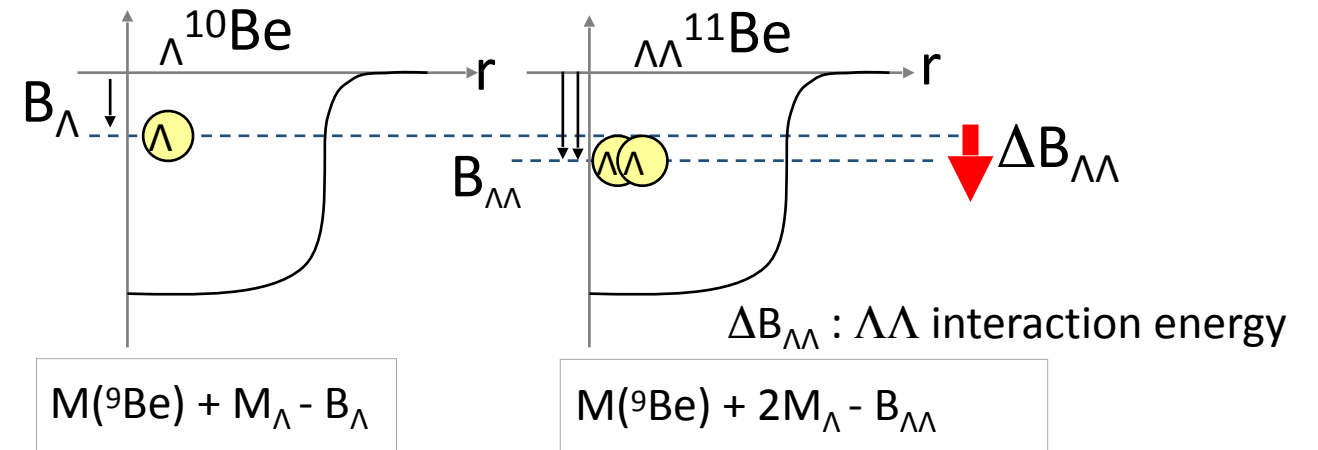
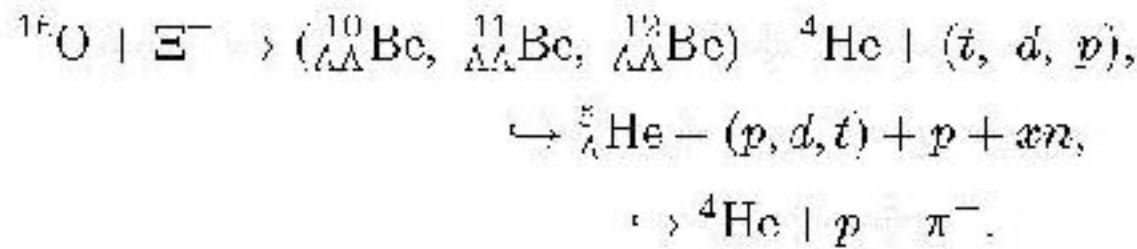
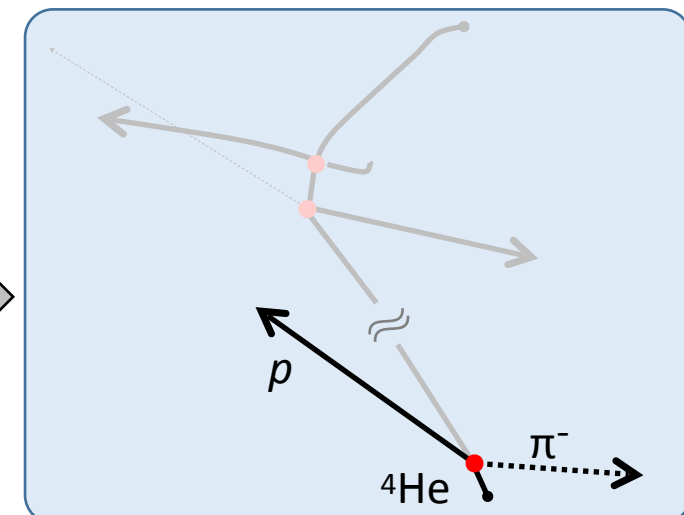
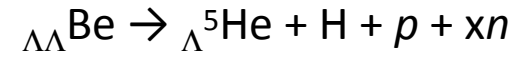
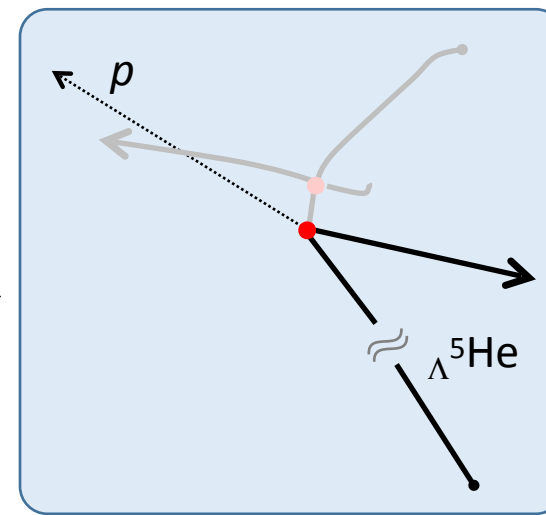
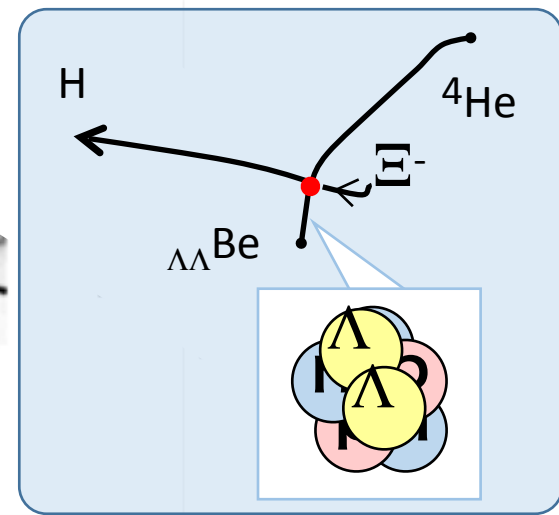
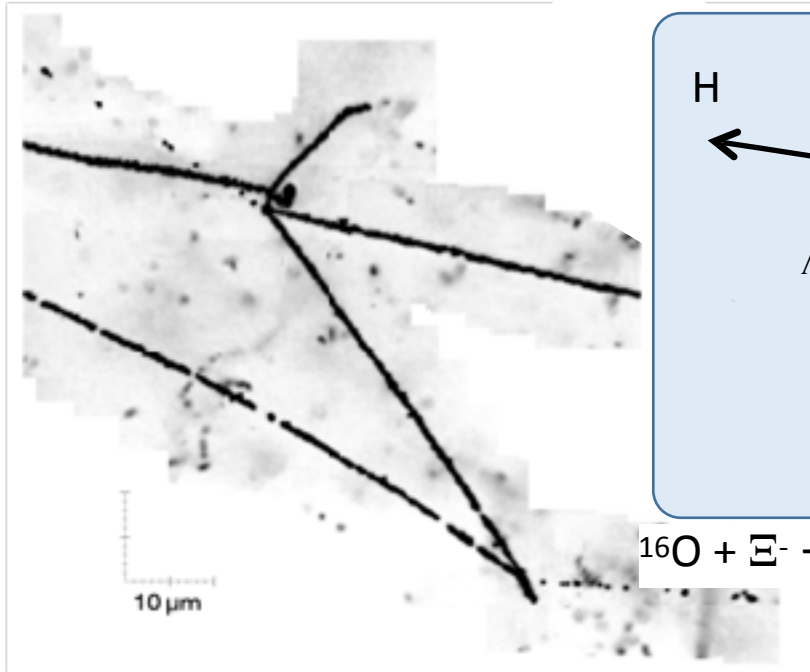
2018/11/12 77-7	2018/11/19 43-5 DoubleCenterd
2018/12/04 68-12	2018/12/09 45-11 2v+kink
2019/01/14 37-6 DoubleL?	2019/01/16 35-3 DoubleCenterd
2019/03/04 39-5 Twin?	

* Nuclear species of some event are identified.

* B_{Ξ^-} or $\Delta B_{\Lambda\Lambda}$ are measured quantitatively in several events (red framed). 152

Double- Λ Hypernucleus MINO event

H. Ekawa et al., Prog. Theor. Exp. Phys. 2019, 021D02



Possible interpretations	$B_{\Lambda\Lambda}$ [MeV]	$\Delta B_{\Lambda\Lambda}$ [MeV]	kinematic fitting χ^2	p-value[%]
$\Xi^- + {}^{16}\text{O} \rightarrow \Lambda\Lambda^{10}\text{Be} + {}^4\text{He} + t$	15.05 +- 0.11	1.63 +- 0.14	11.5	0.9
$\Xi^- + {}^{16}\text{O} \rightarrow \Lambda\Lambda^{11}\text{Be} + {}^4\text{He} + d$	19.07 +- 0.11	1.87 +- 0.37	7.3	6.4
$\Xi^- + {}^{16}\text{O} \rightarrow \Lambda\Lambda^{12}\text{Be}^* + {}^4\text{He} + p$	13.68 +- 0.11 + E_{ex}	-2.7 +- 1.0 + E_{ex}	11.3	1.0

$\Lambda\Lambda^{11}\text{Be}$ is most probable by kinematic fitting χ^2 (DOF=3)

where, $B_{\Xi^-} = 0.23$ MeV, 3D orbit of ^{16}O

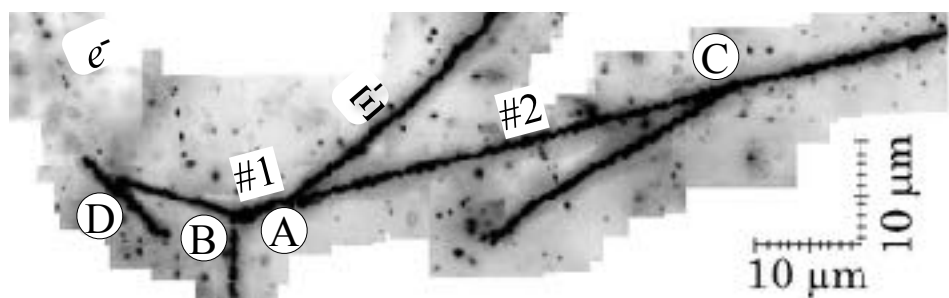
In a new nuclide event of $\Lambda\Lambda\text{Be}$, a $\Delta B_{\Lambda\Lambda}$, $\Lambda\Lambda$ interaction energy, has been obtained successfully.

Deeply bound Ξ^- - ^{14}N systems

0.1/4 MeV:3D atomic state
 Prog. Theor. Phys. 105 (2001) 627.

$B_{\Xi^-}(\Xi^- + ^{14}\text{N})$

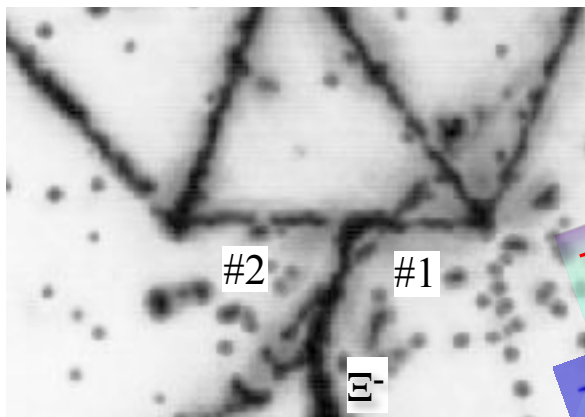
KISO
 event
 (KEK-E373)



$B_{\Xi^-} 1.03 \pm 0.18$
 (MeV) or
 3.87 ± 0.21

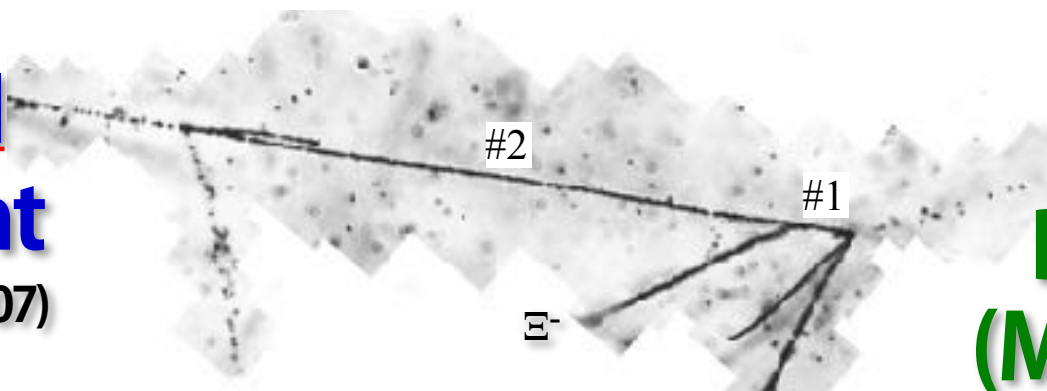
E.Hiyama, K. Nakazawa, Annu. Rev. Nucl. Part. Sci. 2018.68.131

KINKA
 event
 (KEK-E373)



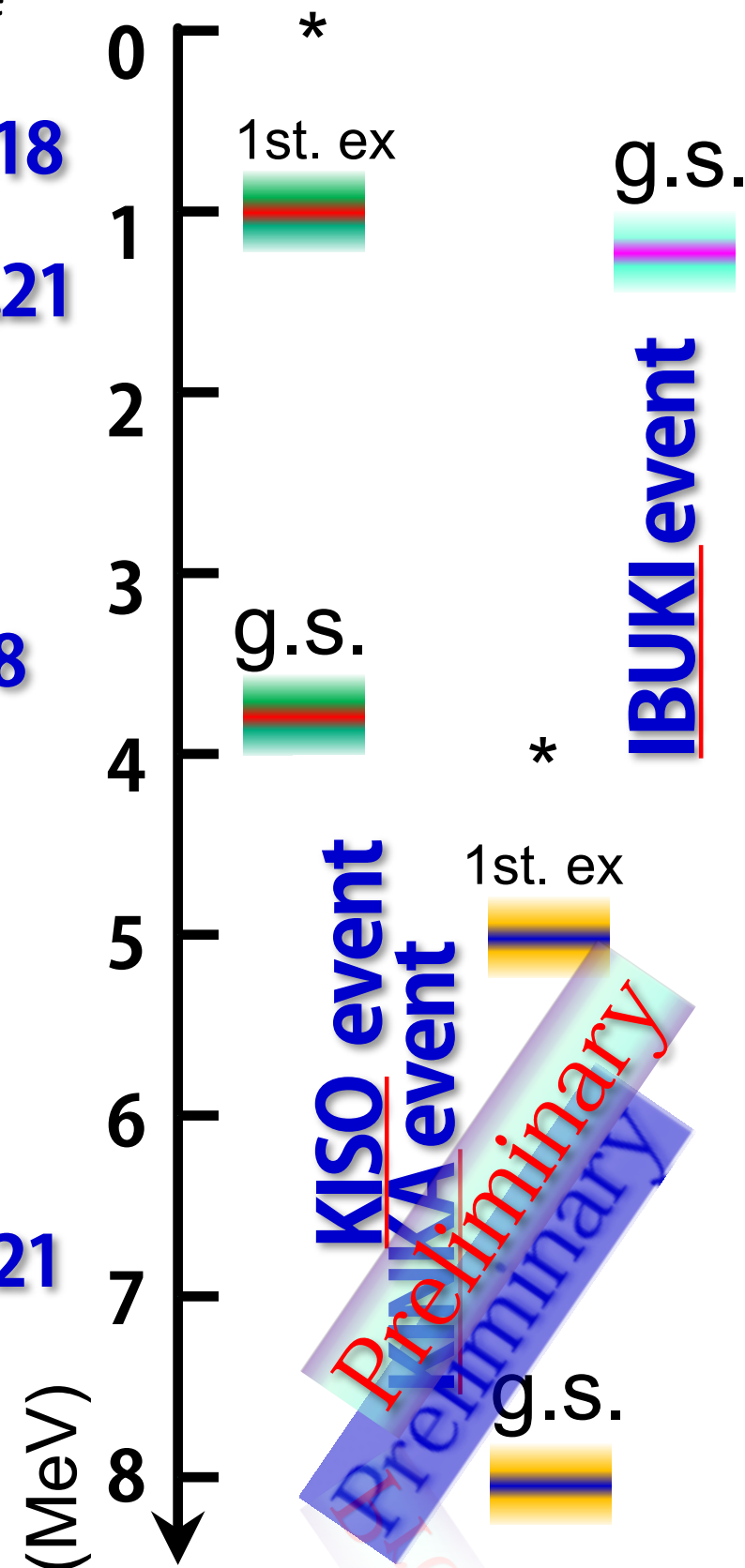
B_{Ξ^-}
 (MeV) 5 or 8
 Preliminary
 Preliminary

IBUKI
 event
 (J-PARCE07)



$B_{\Xi^-} 1.27 \pm 0.21$
 (MeV)

S. Hayakawa, PhD thesis (2019) Osaka Univ., Unpublished



* Multiple candidates of Ξ hypernucleus with B_{Ξ^-} beyond 3D atomic level in Ξ^- - ^{14}N systems

* We expect more examples through further analysis in E07.

Search for Double- Λ with Sequential Weak Decay

- ▶ Large Branch of Mesonic Weak Decay in Light hyperfragments
- ▶ Characteristic π^- emission



$$P_{\pi^{-}} \sim 130 \text{ MeV}/c$$

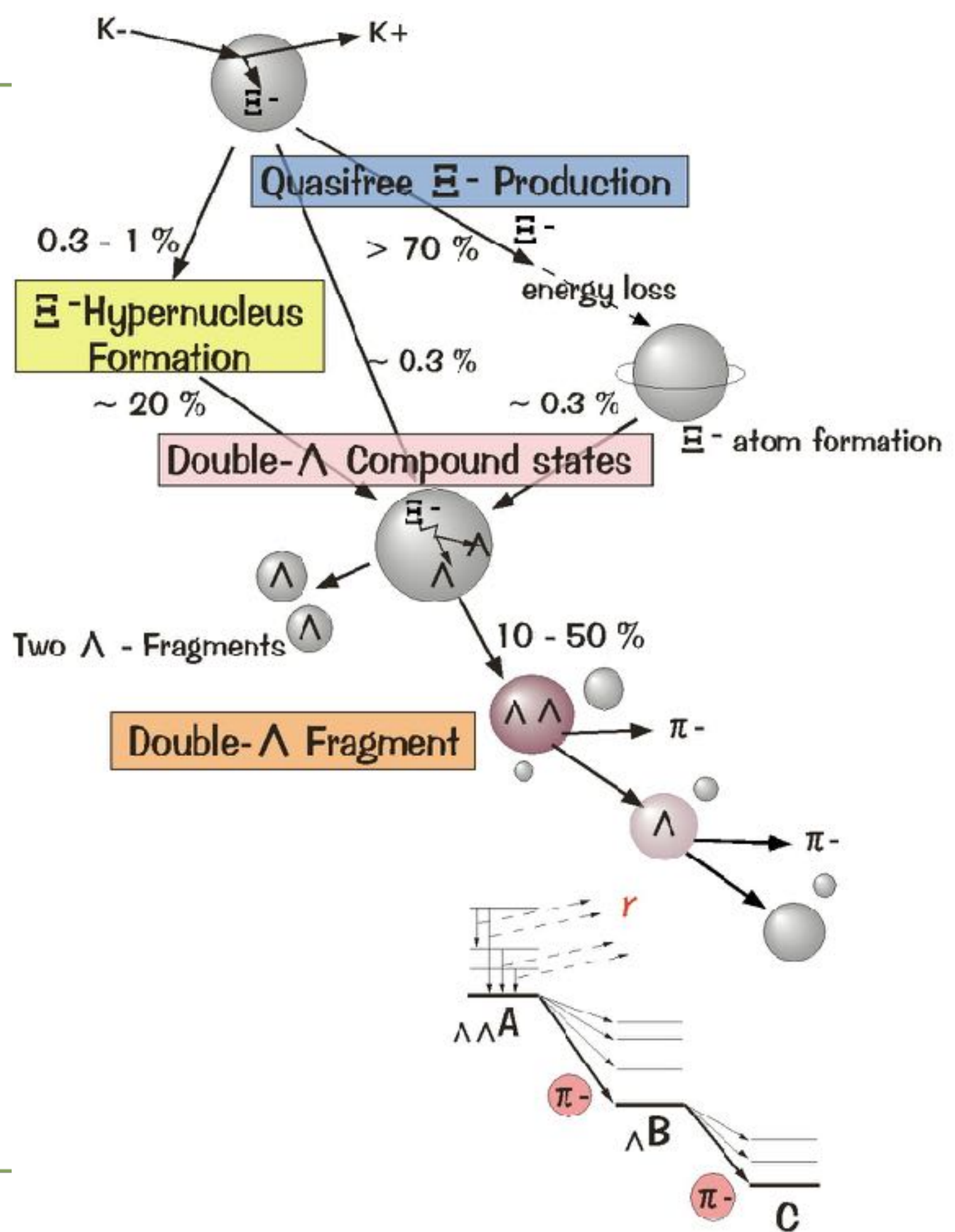
$$\Gamma_{\pi^{-}}/\Gamma_{\text{tot}} \sim 0.21$$



$$P_{\pi^{-}} = 99.2 \text{ MeV}/c$$

$$\text{Width} = 1 \text{ MeV}/c$$

$$\Gamma_{\pi^{-}}/\Gamma_{\text{tot}} \sim 0.39$$



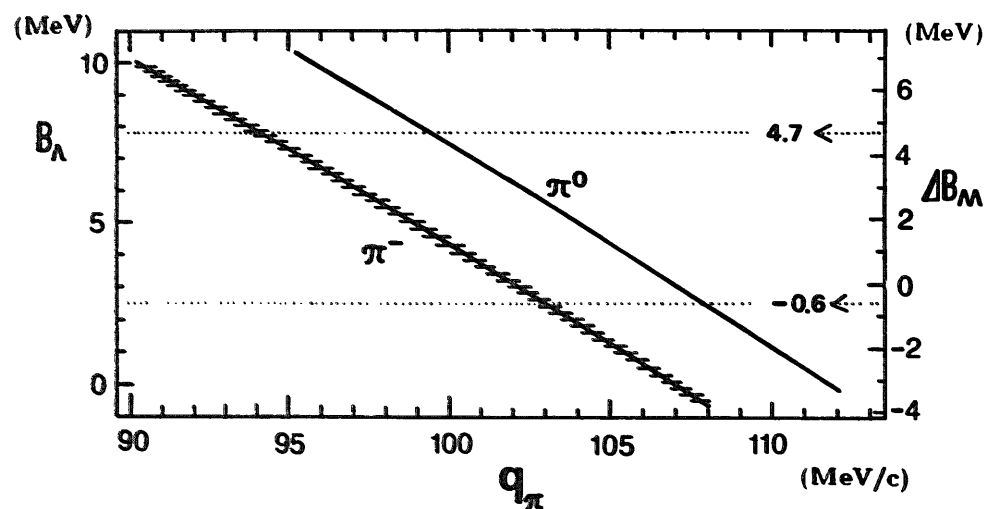


Fig. 8. The Λ -binding energy $B_\Lambda(^6\Lambda\text{He})$ is plotted as a function of the weak decay pion momentum q_π . The corresponding $\Lambda\Lambda$ interaction matrix element $\Delta B_{\Lambda\Lambda}$ is also shown on the right scale. The hatch for the π^- decay indicates the predicted pion momentum width $\Delta q = 0.45$ MeV/c.

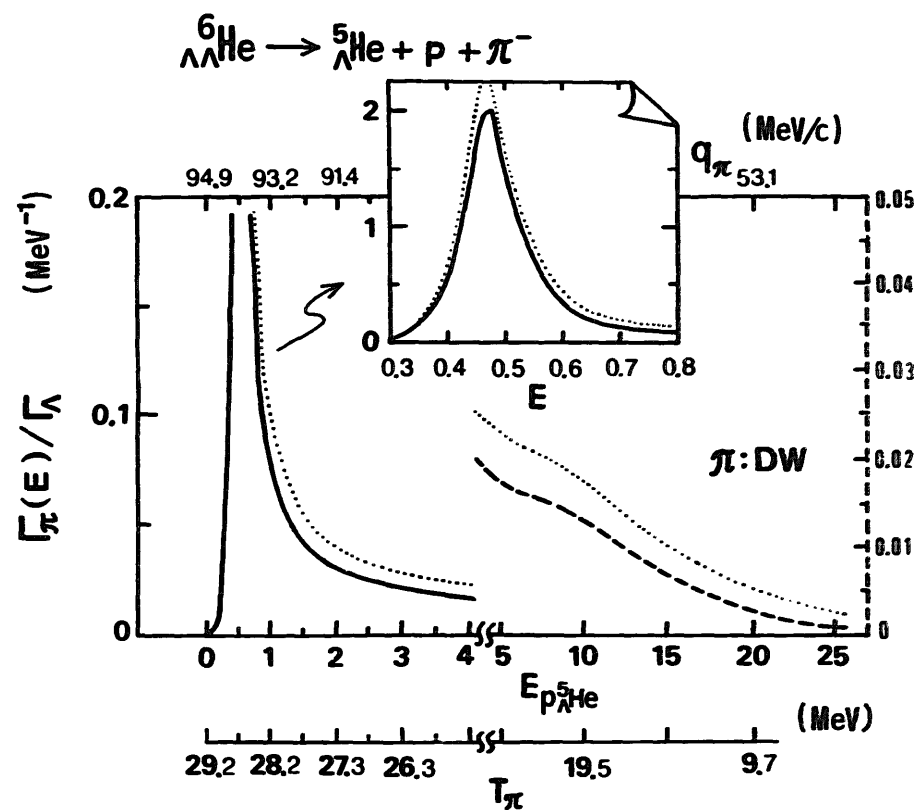
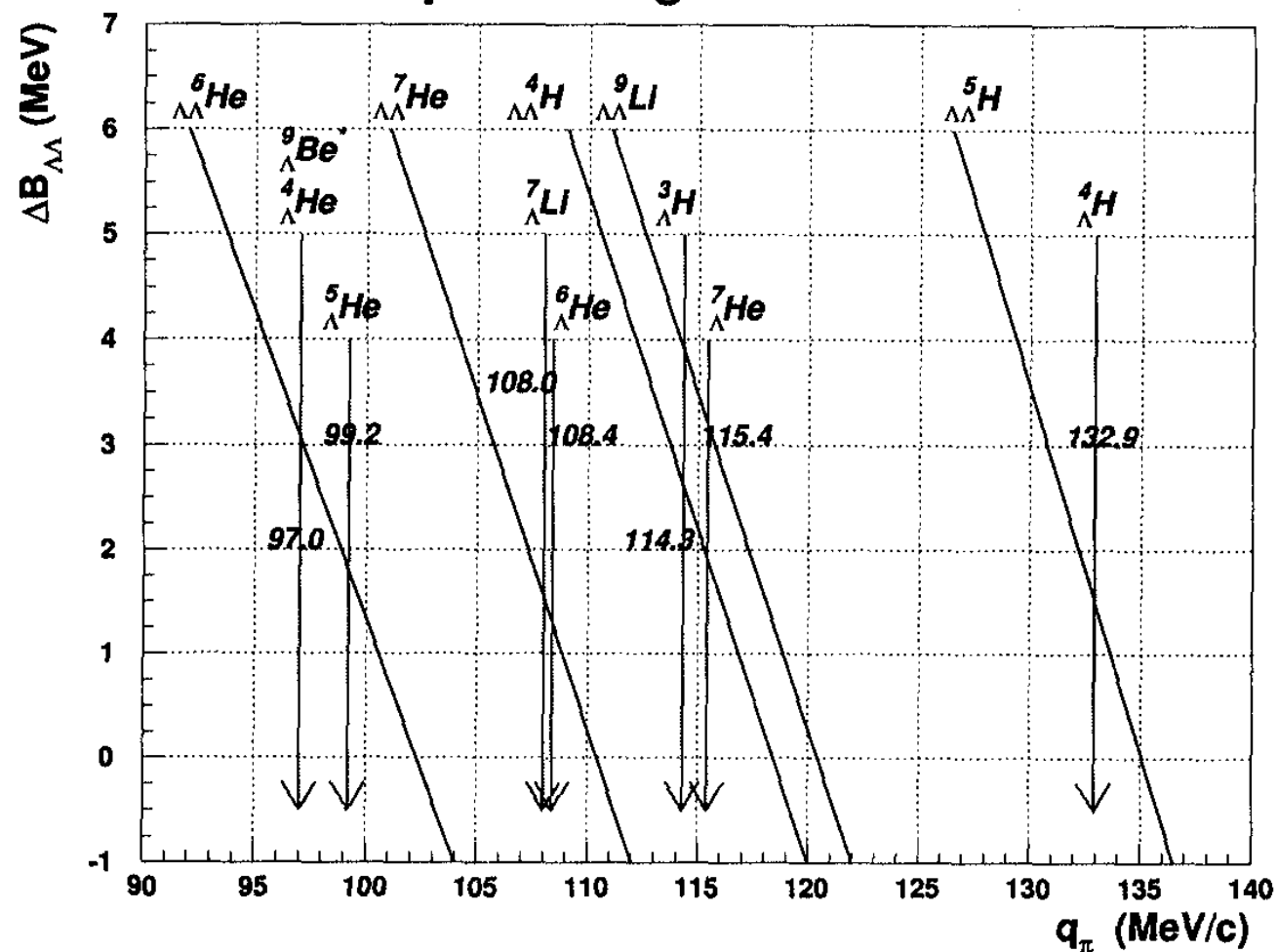


Fig. 7. The theoretical π^- decay spectrum $\Gamma_\pi(^6\Lambda\text{He})/\Gamma_\Lambda$ with YNG is drawn by solid line as a function of the proton- $^5\Lambda\text{He}$ relative energy $E \equiv E_{p^5\Lambda\text{He}}$. The shallow Λ -binding energy case described in sect. 4.2 results in the dotted curve in which case the pion momentum and energy should be shifted (cf. fig. 8).

Expected Signals and Lines



BNL E906

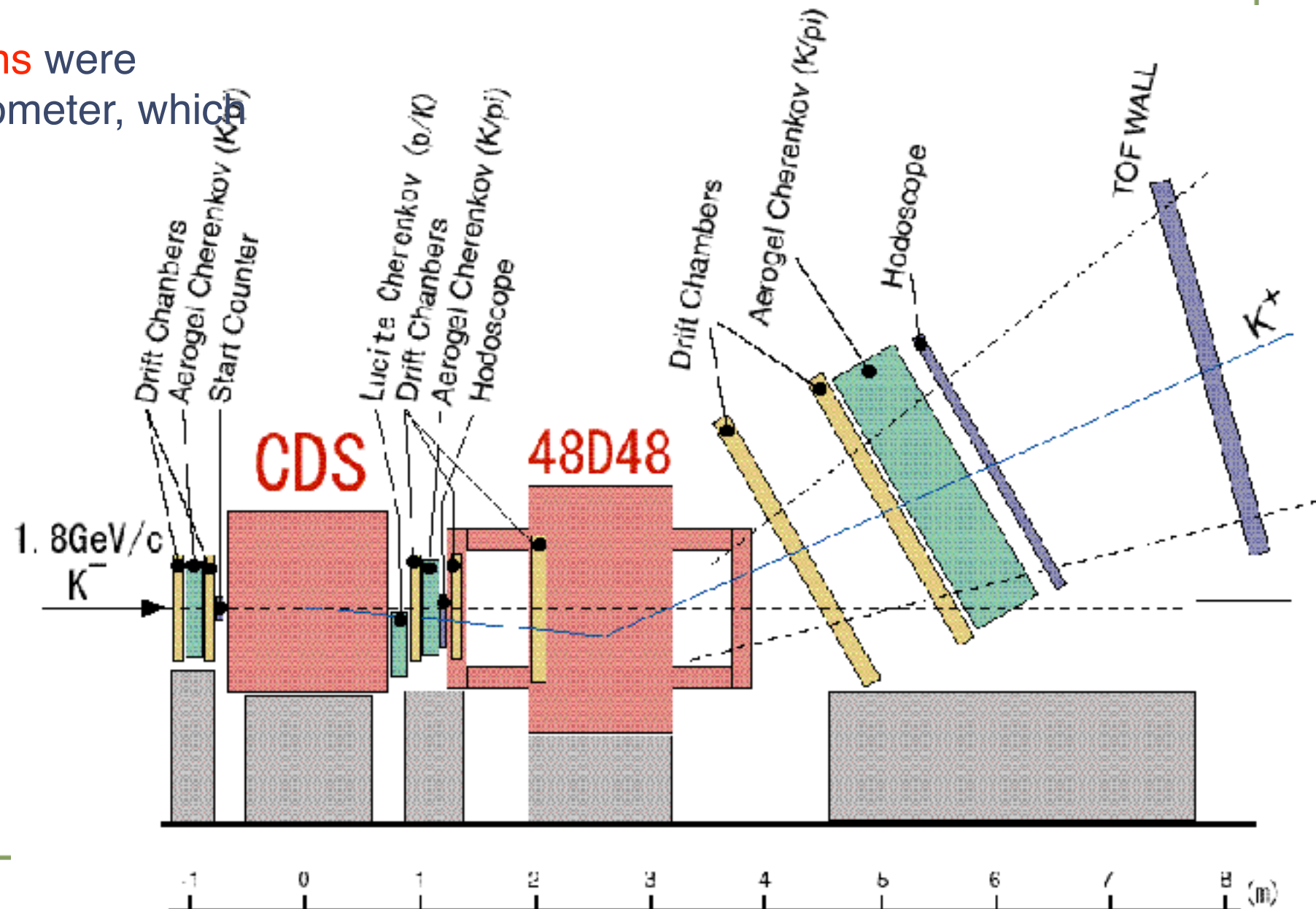
- 1998 Run Summary

- $0.9 \times 10^{12} K^-$ (1.8 GeV/c) was irradiated

- Target was a ^9Be plate (6"x 2"x1/2" high)

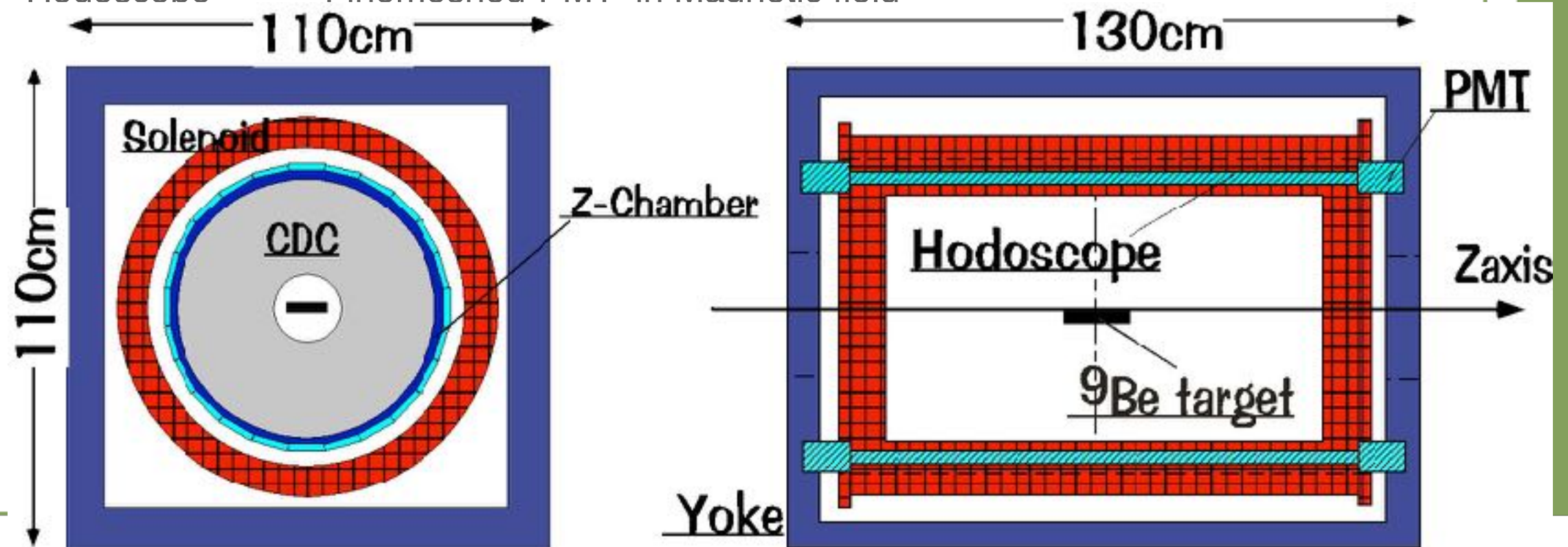
48D48 spectrometer system and CDS

- $1.1 \times 10^5 (K^-, K^+)$ reactions were identified by 48D48 spectrometer, which covers 2-10 deg.

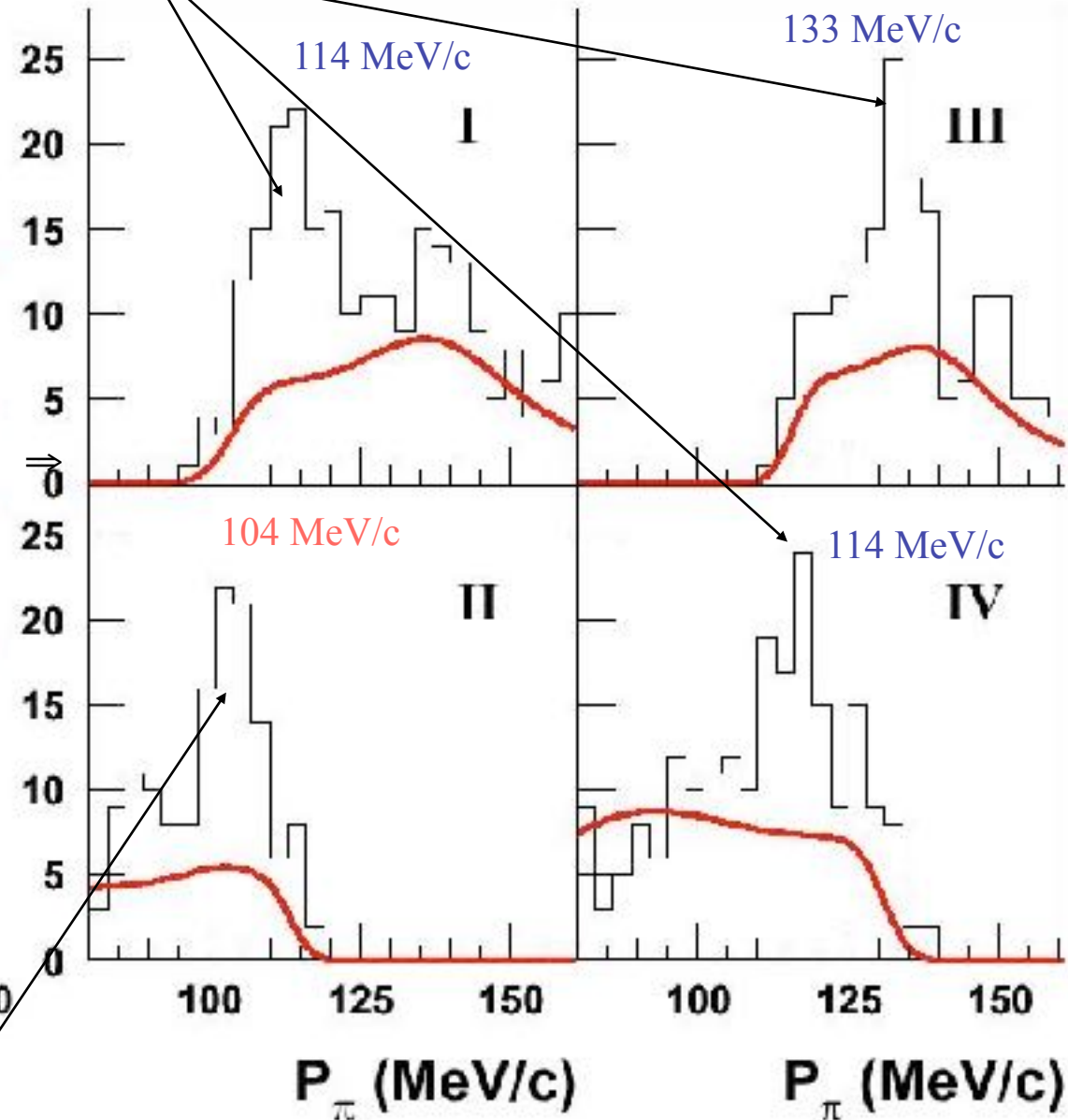
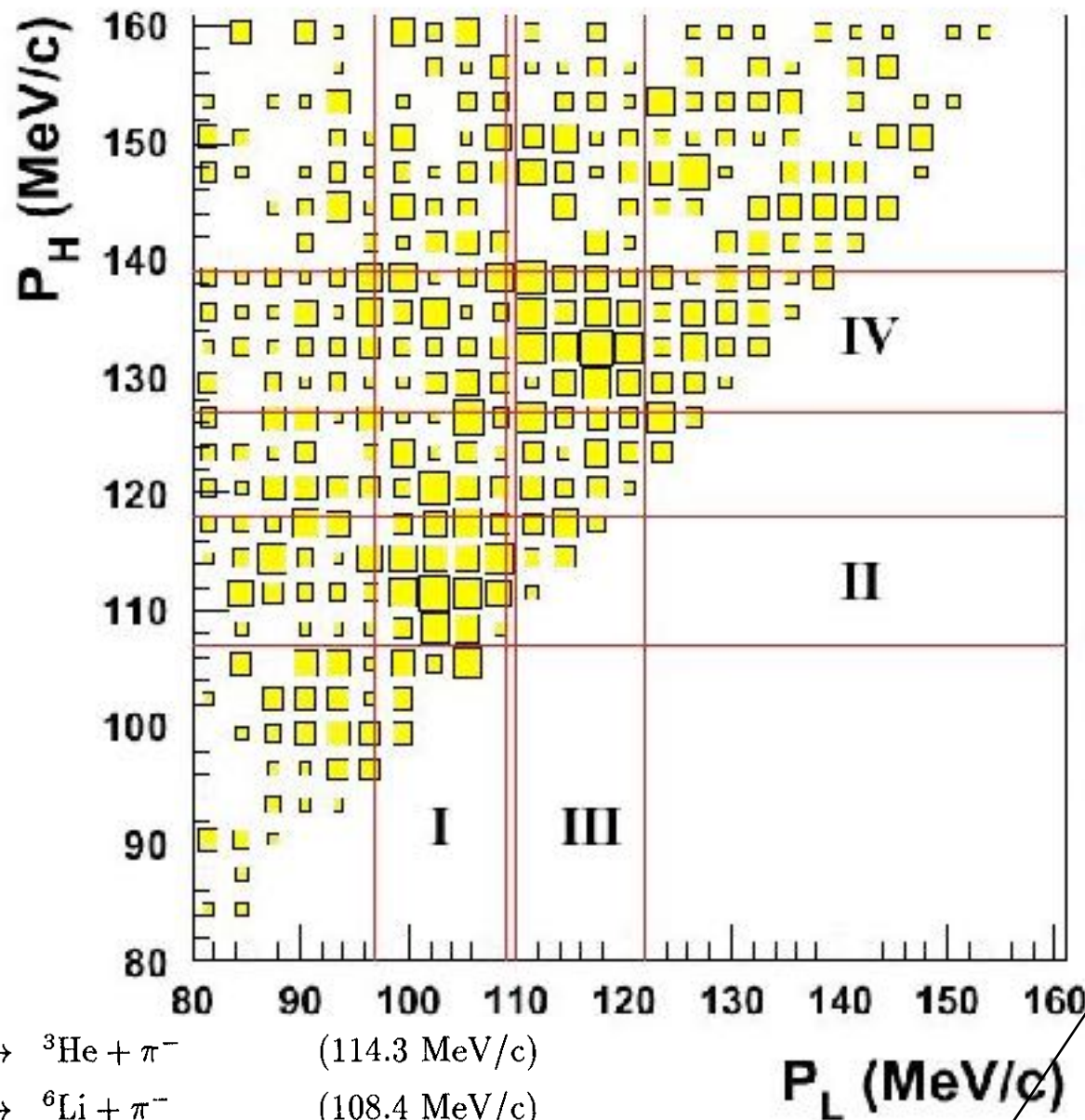


Cylindrical Detector System

- Large solid angle 72% of 4π
- Momentum resolution for 100MeV/c π 9-10MeV/c(FWHM)
- Solenoid magnet Uniform field variation less than 0.5%
- Cylindrical Drift Chamber (CDC)
 - Low Z materials
 - gas ; He:C₂H₆=50%:50%
 - field-wire ; gold plated aluminium
 - 12 layers ; 6 stereo layers, 6 axial layers, 576 cells
- Z-Chamber 5.5mm pitch Cathode strip readout-MWPC
- Hodoscope Finemeshed-PMT in Magnetic field



Consistent with known single Λ hypernuclei



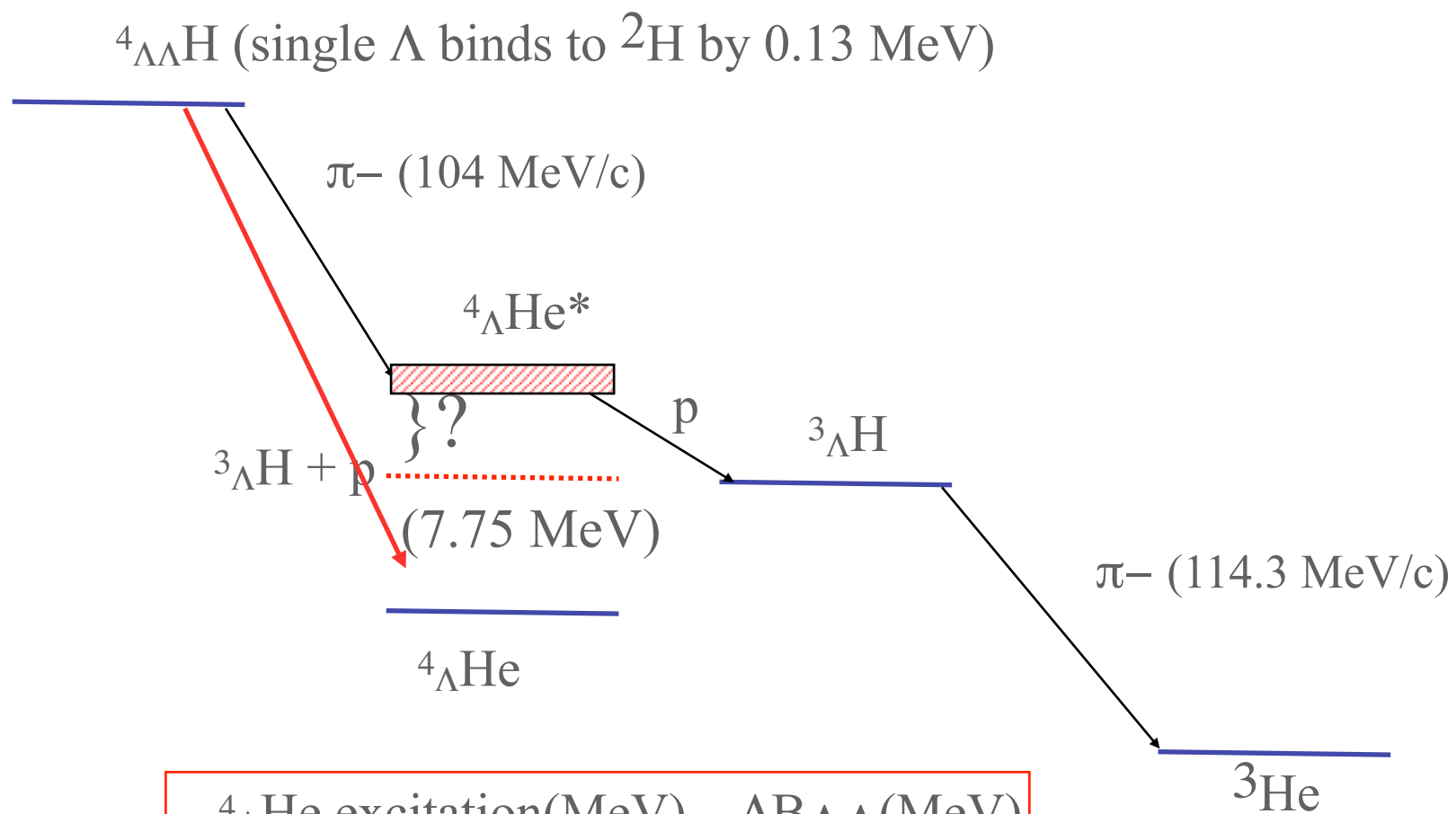
- (i) $\begin{cases} {}^3_{\Lambda}\text{H} \rightarrow {}^3\text{He} + \pi^- & (114.3 \text{ MeV}/c) \\ {}^6_{\Lambda}\text{He} \rightarrow {}^6\text{Li} + \pi^- & (108.4 \text{ MeV}/c) \end{cases}$
- (ii) $\begin{cases} {}^3_{\Lambda}\text{H} \rightarrow {}^3\text{He} + \pi^- & (114.3 \text{ MeV}/c) \\ {}^4_{\Lambda}\text{H} \rightarrow {}^3\text{H} + \text{p} + \pi^- & (\sim 98 \text{ MeV}/c) \end{cases}$
- (iii) $\begin{cases} {}^4_{\Lambda\Lambda}\text{H} \rightarrow {}^4_{\Lambda}\text{He} + \pi^- & (\sim 116 \text{ MeV}/c) \\ \quad \quad \quad \downarrow & \\ \quad \quad \quad {}^3\text{He} + \text{p} + \pi^- & (\sim 97 \text{ MeV}/c) \end{cases}$
- (iv) $\begin{cases} {}^4_{\Lambda\Lambda}\text{H} \rightarrow {}^4_{\Lambda}\text{He}^* + \pi^- & (\sim 103 \text{ MeV}/c) \\ \quad \quad \quad \downarrow & \\ \quad \quad \quad {}^3_{\Lambda}\text{H} + \text{p} & \\ \quad \quad \quad \downarrow & \\ \quad \quad \quad {}^3\text{He} + \pi^- & (114.3 \text{ MeV}/c) \end{cases}$

Phys. Rev. Lett. 87, 132504 (2001)

Candidate for $\Lambda\Lambda$ hypernucleus decay

new interpretation by S. Randeniya: ${}^7_{\Lambda\Lambda}\text{He}$

Suggested decay mode of ${}^4_{\Lambda\Lambda}\text{H}$ and limits on $\Delta B_{\Lambda\Lambda}$



${}^4_{\Lambda}\text{He}$ excitation(MeV)	$\Delta B_{\Lambda\Lambda}$ (MeV)
7.75	1.8

Search for **two body decay mode** ${}^4_{\Lambda\Lambda}\text{H} \rightarrow {}^4_{\Lambda}\text{He}(1^+) + \pi^-$

K中間子原子核

Contents

- ❖ Past measurements on “ K^-pp ”
 - ❖ FINUDA, E549 : $K^-_{\text{stop}}A$ reactions $(K^-pp) \rightarrow \Lambda p$
 - ❖ DISTO : $pp \rightarrow \Lambda p K^+$
 - ❖ HADES, LEPS, E15 ${}^3\text{He}(K^-, n)$
- ❖ Recent measurements on “ K^-pp ”
 - ❖ J-PARC E27 : $d(\pi^+, K^+ pp)X$
 - ❖ J-PARC E15 : ${}^3\text{He}(K^-, \Lambda p)n$ in the first data taking in 2013
- ❖ Discussion : Role of $\Lambda(1405)$ as a doorway Recent high-statistics data by T. Yamaga
- ❖ Summary

AY02

PHYSICAL REVIEW C, VOLUME 65, 044005

Nuclear \bar{K} bound states in light nuclei

Yoshinori Akaishi¹ and Toshimitsu Yamazaki²

¹*Institute of Particle and Nuclear Studies, KEK, Tsukuba 305-0801, Japan*

²*RI Beam Science Laboratory, RIKEN, Wako 351-0198, Japan*

(Received 21 August 2001; published 1 April 2002)

The possible existence of deeply bound nuclear \bar{K} states is investigated theoretically for few-body systems. The nuclear ground states of a K^- in ${}^3\text{He}$, ${}^4\text{He}$, and ${}^8\text{Be}$ are predicted to be discrete states with binding energies of 108, 86, and 113 MeV and widths of 20, 34, and 38 MeV, respectively. The smallness of the widths arises from their energy-level locations below the $\Sigma\pi$ emission threshold. It is found that a substantial contraction of the surrounding nucleus is induced due to the strong attraction of the $I=0$ $\bar{K}N$ pair, thus forming an unusually dense nuclear medium. Formation of the $T=0$ $K^- \otimes {}^3\text{He} + \bar{K}^0 \otimes {}^3\text{H}$ state in the ${}^4\text{He}$ (stopped K^- , n) reaction is proposed, with a calculated branching ratio of about 2%.

YA02



Physics Letters B 535 (2002) 70–76

PHYSICS LETTERS B

www.elsevier.com/locate/npe

(K^-, π^-) production of nuclear \bar{K} bound states in proton-rich systems via Λ^* doorways

Toshimitsu Yamazaki^a, Yoshinori Akaishi^b

^a *RI Beam Science Laboratory, RIKEN, Wako, Saitama-ken, 351-0198 Japan*

^b *Institute of Particle and Nuclear Studies, KEK, Tsukuba, Ibaraki-ken, 305-0801 Japan*

Received 2 January 2002; received in revised form 13 February 2002; accepted 13 February 2002

Editor: J.P. Schiffer

Abstract

We propose to use the (K^-, π^-) and (π^+, K^+) reactions to produce deeply bound nuclear \bar{K} states in proton-rich systems, in which an elementary formation of $\Lambda(1405)$ and $\Lambda(1520)$ plays the role of a doorway state. Exotic discrete \bar{K} bound systems on unbound nuclei, such as K^-pp , K^-ppp and K^-pppn , are predicted to be produced, where a high-density nuclear medium is formed as a result of nuclear contraction due to the strong K^-p attraction. © 2002 Elsevier Science B.V. All rights reserved.



ELSEVIER

Invariant-mass spectroscopy for condensed single- and double- \bar{K} nuclear clusters to be formed as residues in relativistic heavy-ion collisions

Toshimitsu Yamazaki ^a, Akinobu Doté ^b, Yoshinori Akaishi ^b

^a *RI Beam Science Laboratory, RIKEN, Wako, Saitama 351-0198, Japan*

^b *Institute of Particle and Nuclear Studies, KEK, Tsukuba, Ibaraki 305-0801, Japan*

Received 26 September 2003; received in revised form 9 January 2004; accepted 9 January 2004

Editor: J.P. Schiffer

Abstract

Using a phenomenological $\bar{K}N$ interaction, we predict that few-body double- \bar{K} nuclei, such as $pp\bar{K}^-K^-$ and $ppn\bar{K}^-K^-$, as well as single- \bar{K} nuclei, are tightly bound compact systems with large binding energies and ultra-high nucleon densities. We point out that these \bar{K} nuclear clusters can be produced as residual fragments in relativistic heavy-ion collisions, and that their invariant masses can be reconstructed from their decay particles.

© 2004 Elsevier B.V. Open access under [CC BY license](https://creativecommons.org/licenses/by/4.0/).

The unique signature for \bar{K} cluster formation is a clear peak to be revealed in the invariant-mass spectra of its decay particles, if all of the decay particles with their energies and momenta are correctly identified. This method applies to limited cases, where \bar{K} clusters can decay to trackable particles, such as

$$(i) \quad pp\bar{K}^- \rightarrow \Lambda + p, \quad (12)$$

$$(ii) \quad ppn\bar{K}^- \rightarrow \Lambda + d, \quad (13)$$

Bound States of Baryon number=2

- ❖ $S=0$: One bound state
 - ❖ deuteron = p+n with $T=0, J^P=1^+$ $\Delta\Delta, T=0, J^P=3^+$
- ❖ $S=-1$: No bound states ?
 - ❖ Λ hypernuclei : $A \geq 3$ (${}^3_{\Lambda}\text{H}$)
 - ❖ Σ hypernuclei : $A \geq 4$ (${}^4_{\Sigma}\text{He}$)
- ❖ $S=-2$: ??
 - ❖ $\Lambda\Lambda$ -H dibaryon, ΞN

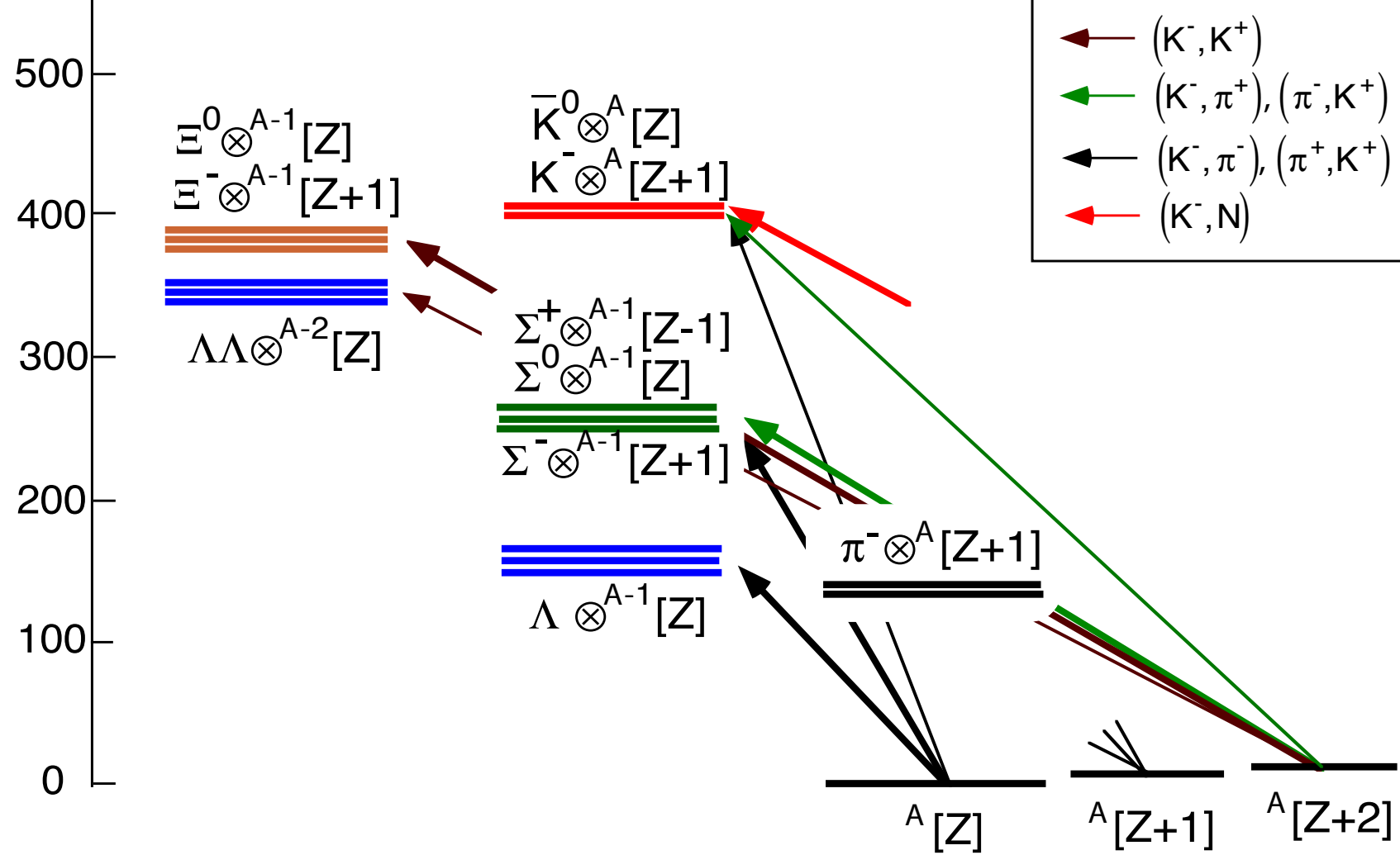


New type of Strange matter

❖ Strange meson (K^- , K^{bar}) in Nuclei.

Excitation Energy

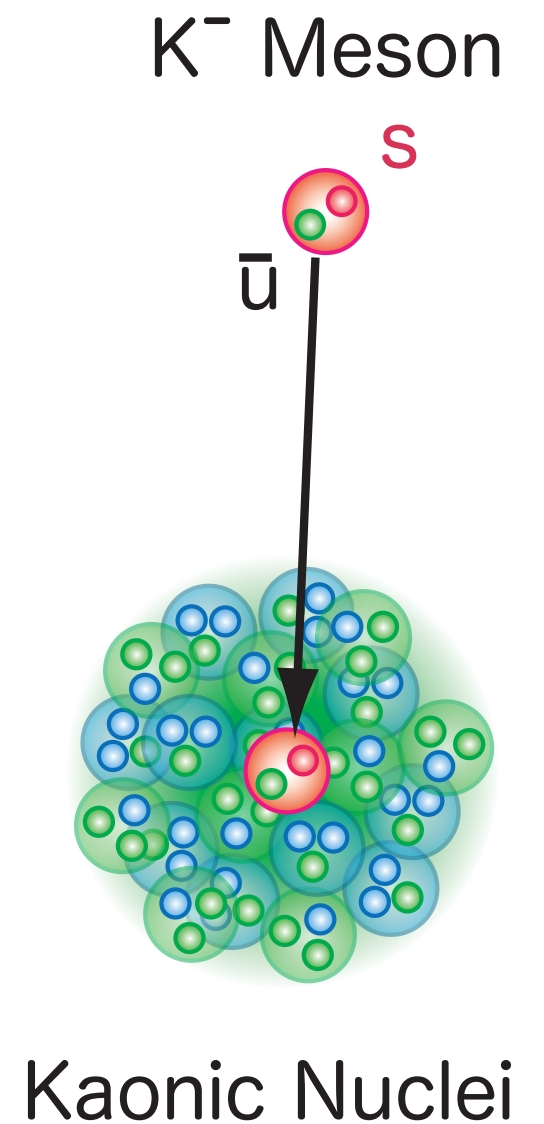
(MeV)



S = -2 Nuclei

S = -1 Nuclei

S = 0 Nuclei



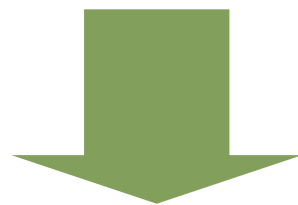
$\bar{K}N$ Bound States

► Prediction by Akaishi and Yamazaki

► $\bar{K}N$ scattering lengths

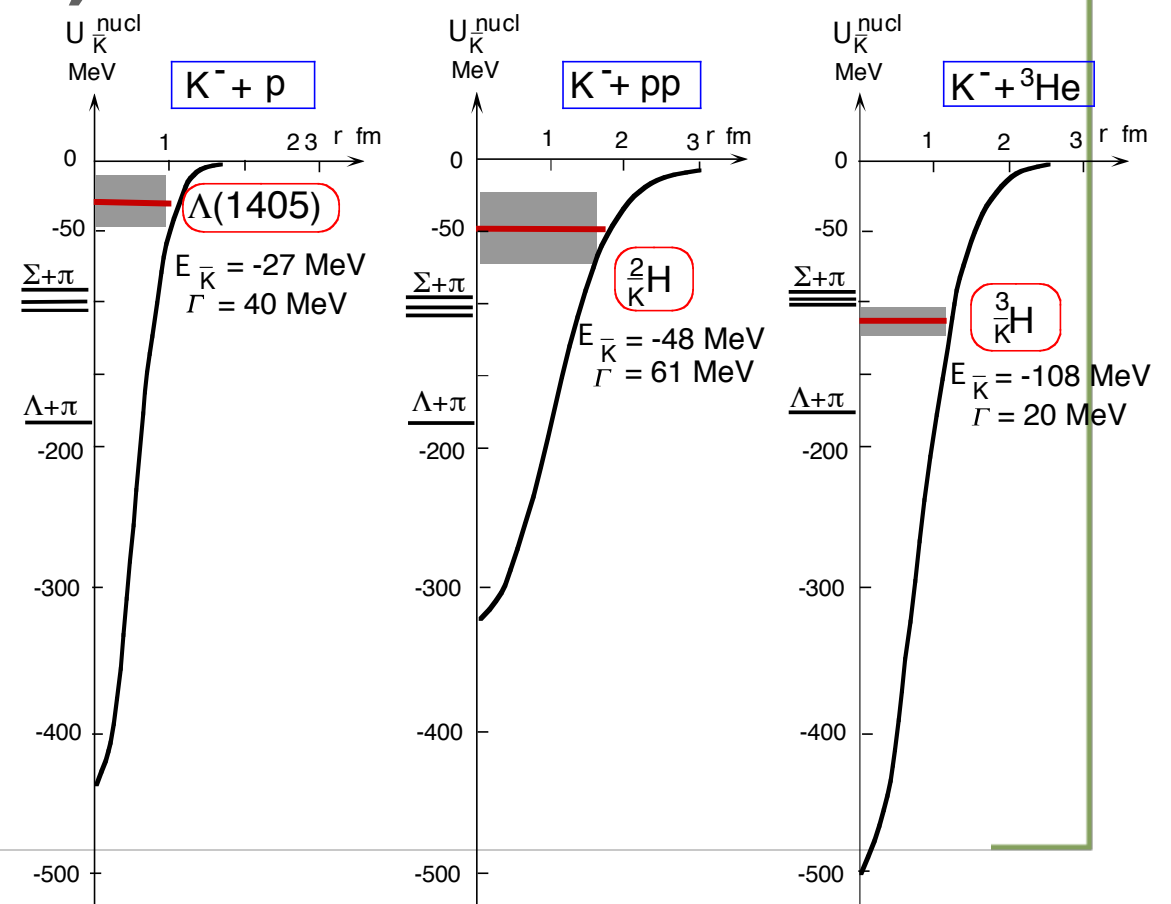
► K^-p atomic shift (KEK E228)

► Mass & width of $\Lambda(1405)$



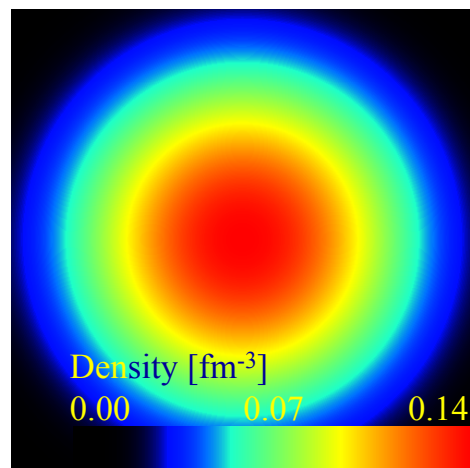
► **Strong attraction in $I=0$ $\bar{K}N$ interaction**

► K^-pp , K^-ppp , K^-pppn , ...

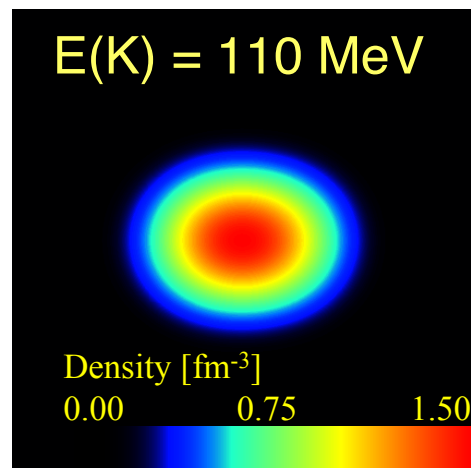


Formation of High Density State

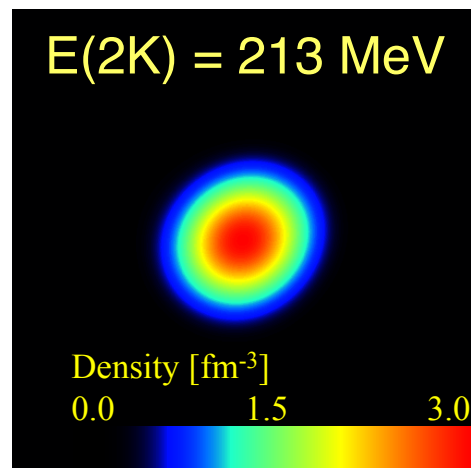
← 4 fm → ← 4 fm → ← 4 fm →



ppn
total B.E. = 6.0 MeV
central density = 0.14 fm^{-3}
 $R_{\text{rms}} = 1.59 \text{ fm}$



ppnK⁻
total B.E. = 118 MeV
central density = 1.50 fm^{-3}
 $R_{\text{rms}} = 0.72 \text{ fm}$

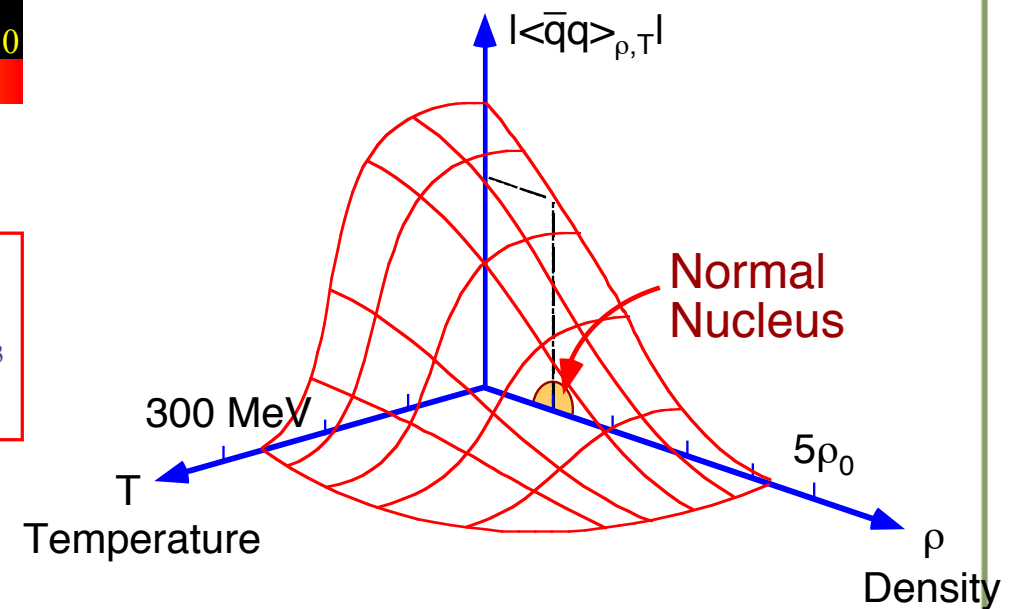


ppnK⁻K⁻
total B.E. = 221 MeV
central density = 3.01 fm^{-3}
 $R_{\text{rms}} = 0.69 \text{ fm}$

$\rho > \rho_0 \times 10$!?

Dote et al.

- ▶ Formation of **Cold**($T=0$) and **Dense**($\rho > 5 \rho_0$) nuclear matter
- ▶ Chiral symmetry restoration
- ▶ Kaon condensation



T. Hatsuda and T. Kunihiro, Phys. Rev. Lett. 55 (1985) 158.
W. Weise, Nucl. Phys. A443 (1993) 59c.

\bar{K} interaction

- ▶ $\bar{K}N$ interaction
 - strongly attractive in the isospin $I=0$ term
(A. D. Martin, kaonic hydrogen X-ray @ KpX)
- 
- ▶ How about \bar{K} -Nucleus interaction ?
 - ▶ Very deep attractive ? (150—200MeV)
 - ▶ Shallow attractive ? (50—75MeV)
 - ▶ *Ambiguity remains with kaonic atom data ($Q \ll Q_0$)*

Hadronic Atoms

E. Friedman, A. Gal / Physics Reports 452 (2007) 89–153

► Klein-Gordon equation

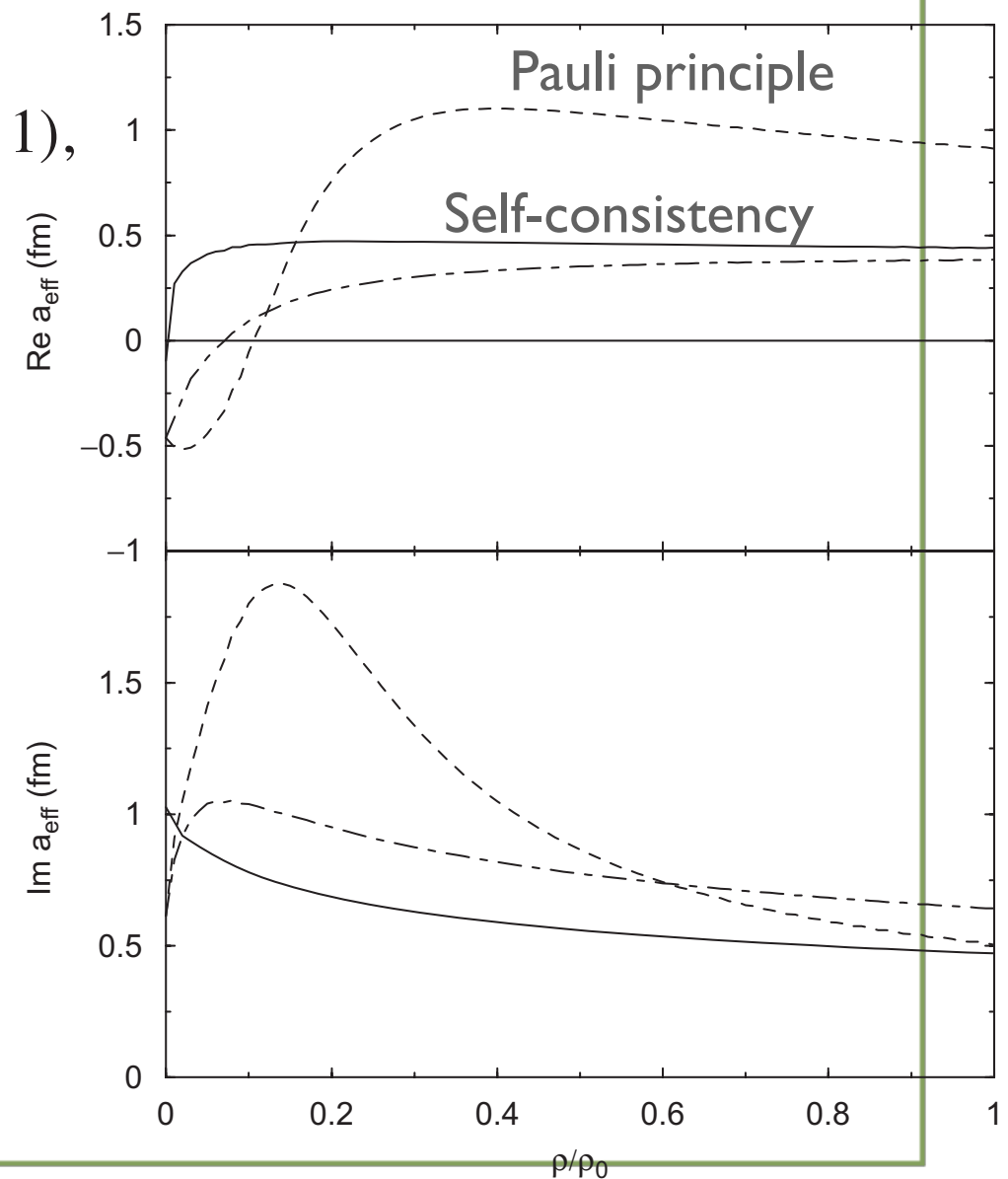
$$[\nabla^2 - 2\mu(B + V_{\text{opt}} + V_c) + (V_c + B)^2]\psi = 0 \quad (\hbar = c = 1),$$

$$2\mu V_{\text{opt}}(r) = -4\pi \left(1 + \frac{A-1}{A} \frac{\mu}{M}\right) \{b_0[\rho_n(r) + \rho_p(r)] + \tau_z b_1[\rho_n(r) - \rho_p(r)]\}.$$

$$2\mu V_{\text{opt}}(r) = -4\pi \left(1 + \frac{\mu}{M}\right) [a_{K-p}(\rho)\rho_p(r) + a_{K-n}(\rho)\rho_n(r)],$$

where

$$a_{K-p} = b_0 - b_1, \quad a_{K-n} = b_0 + b_1$$



K-p interaction near threshold

► Threshold branching ratios

$$\gamma = \frac{\Gamma(K^- p \rightarrow \pi^+ \Sigma^-)}{\Gamma(K^- p \rightarrow \pi^- \Sigma^+)} = 2.36 \pm 0.04,$$

$$R_c = \frac{\Gamma(K^- p \rightarrow \pi^+ \Sigma^-, \pi^- \Sigma^+)}{\Gamma(K^- p \rightarrow \text{all inelastic channels})} = 0.664 \pm 0.011,$$

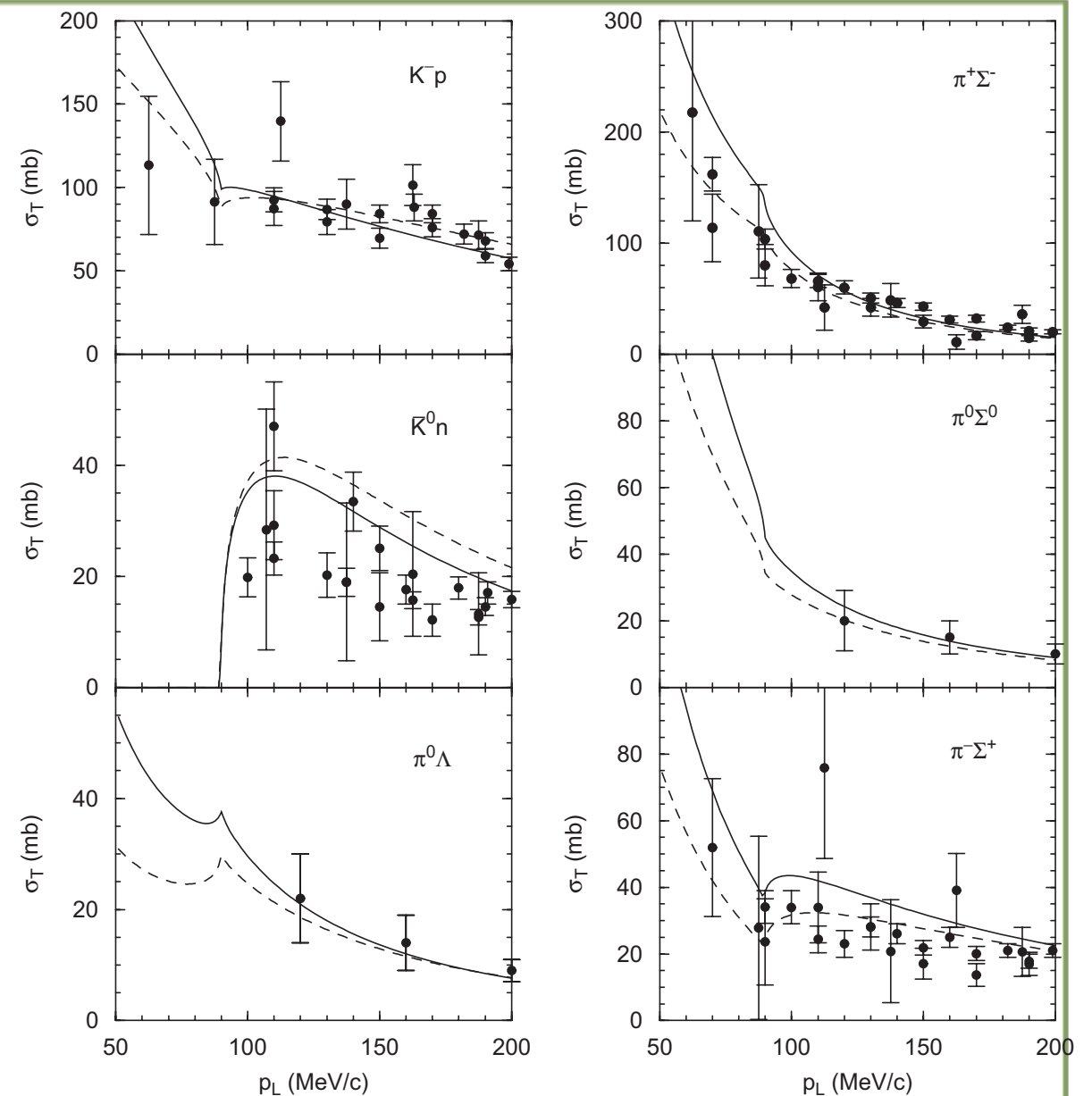
$$R_n = \frac{\Gamma(K^- p \rightarrow \pi^0 \Lambda)}{\Gamma(K^- p \rightarrow \pi^0 \Lambda, \pi^0 \Sigma^0)} = 0.189 \pm 0.015.$$

► K-p Scattering data

► Kaonic hydrogen

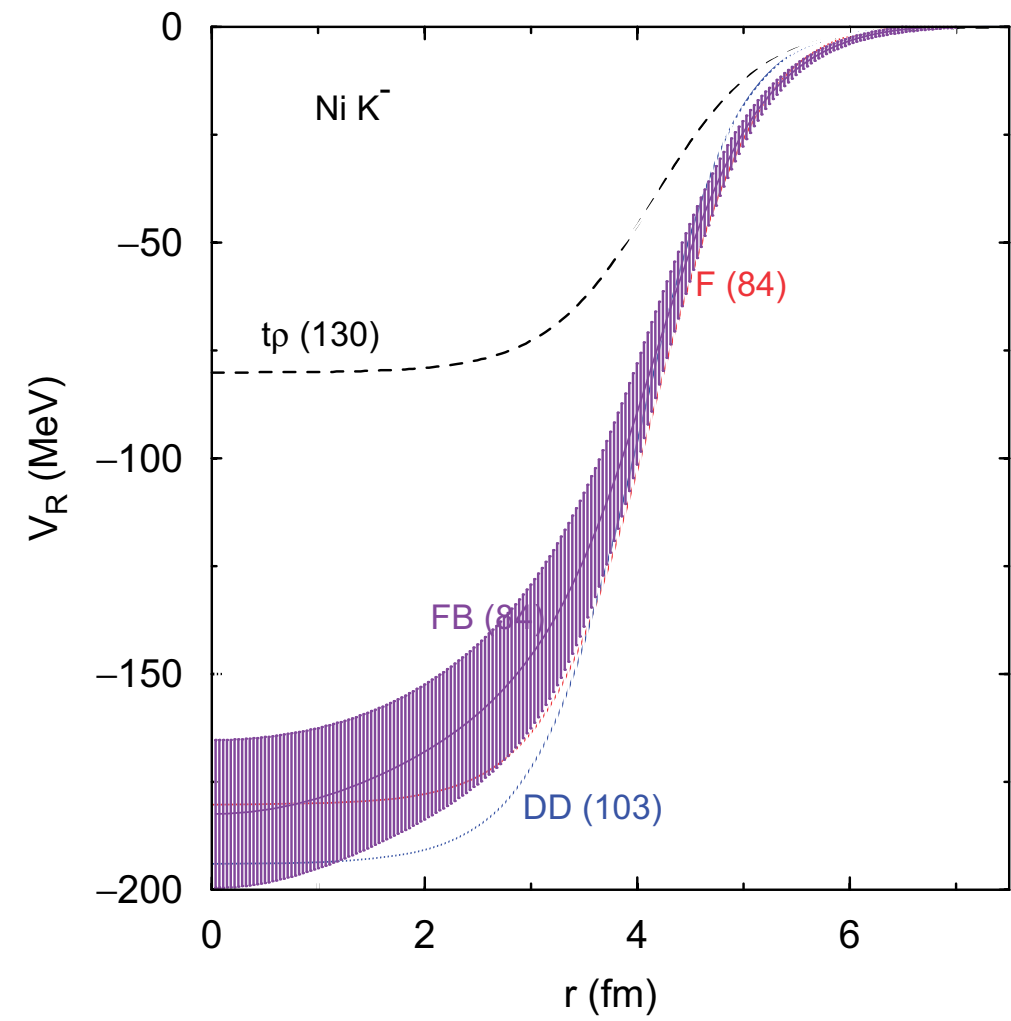
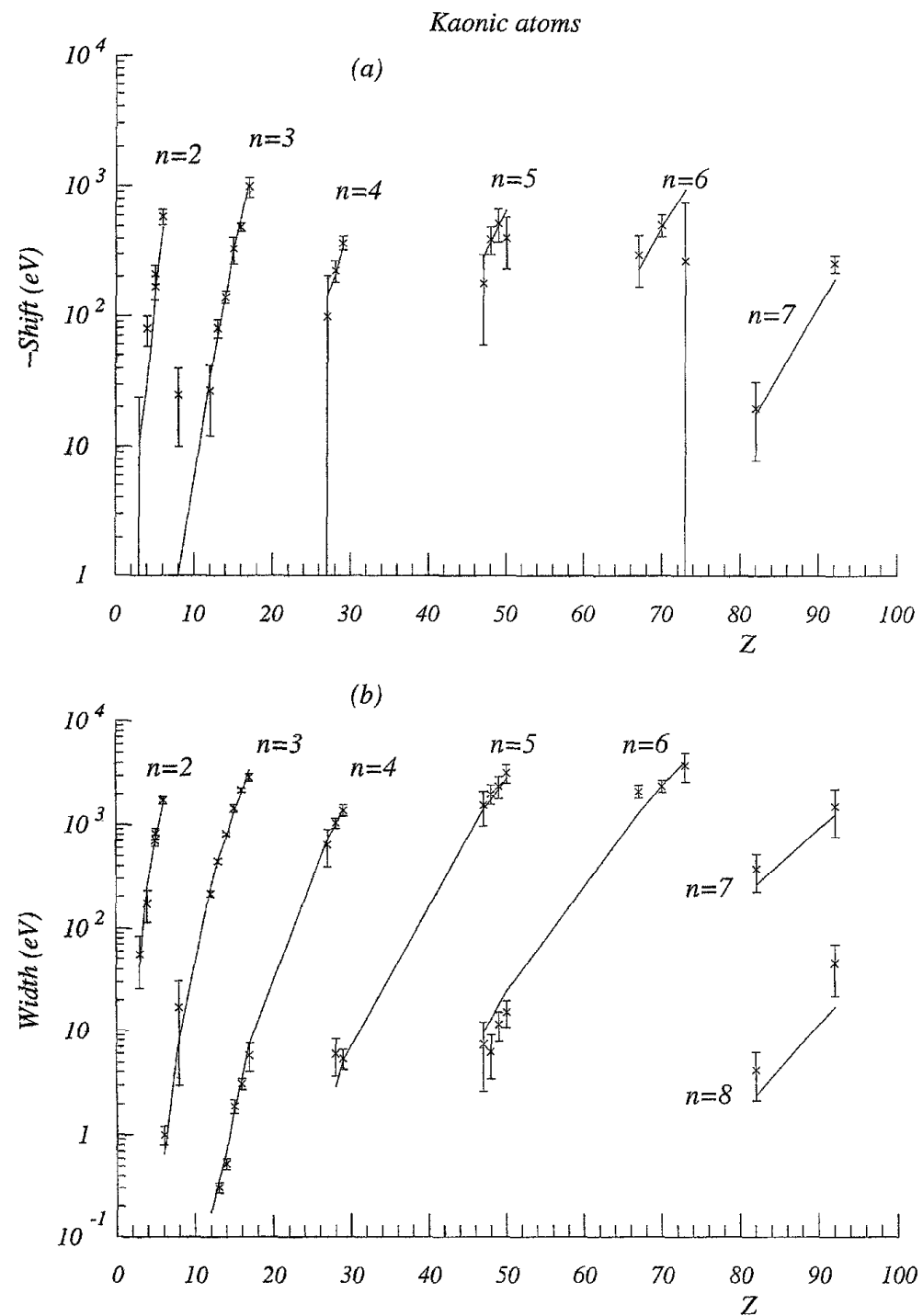
$$\epsilon_{1s} - i \frac{\Gamma_{1s}}{2} \approx -2\alpha^3 \mu_{K-p}^2 a_{K-p} (1 - 2\alpha \mu_{K-p} (\ln \alpha - 1) a_{K-p})$$

$$a(K-p) = (-0.78 \pm 0.15 \pm 0.03) + (0.49 \pm 0.25 \pm 0.12) i \text{ fm}$$



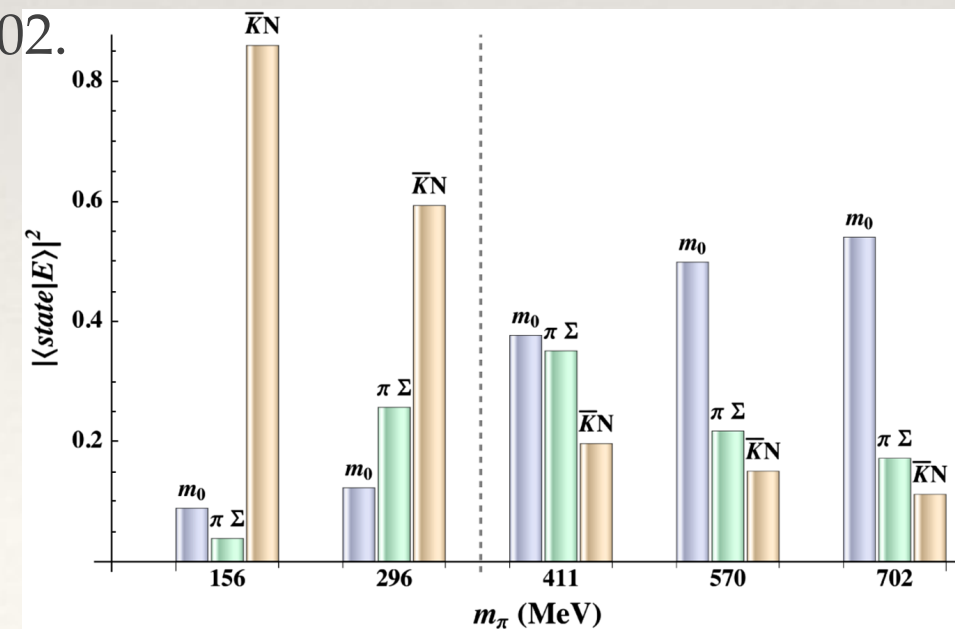
Kaonic Atoms

C.J. Batty et al. / *Physics Reports* 287 (1997) 385–445



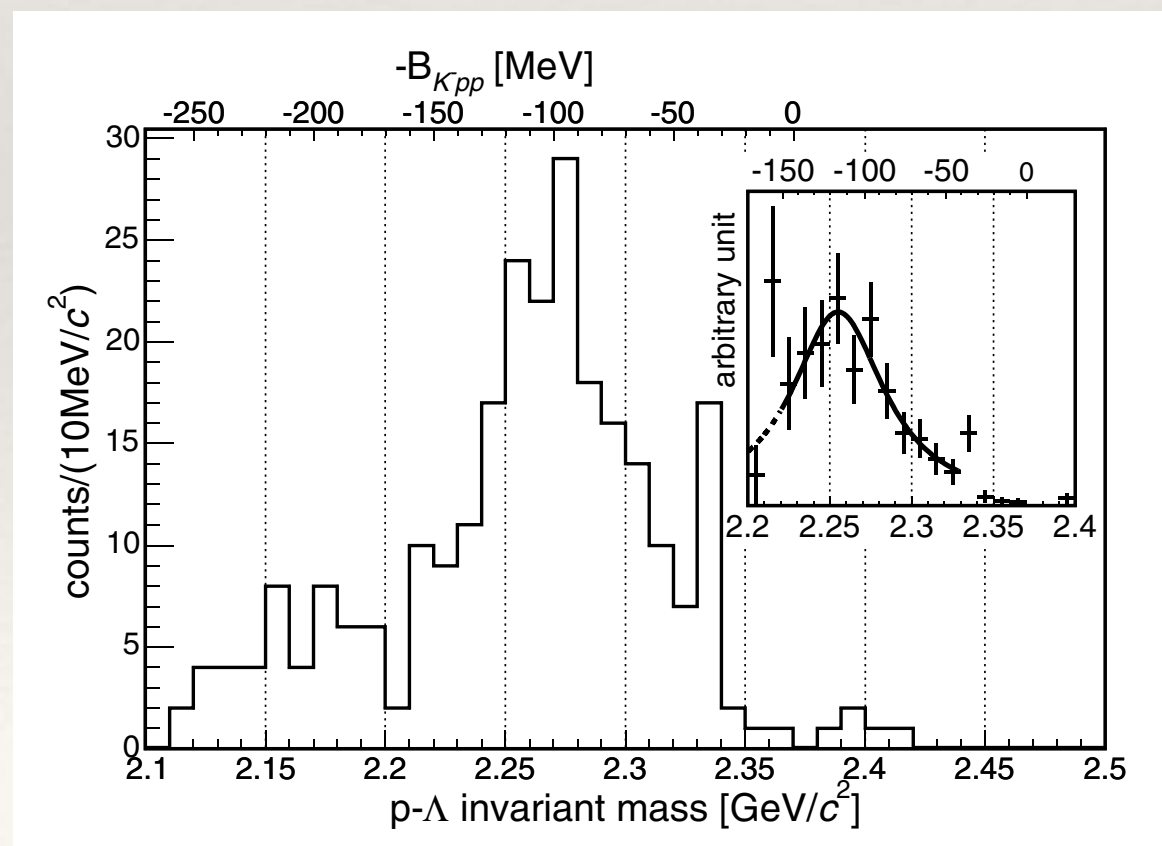
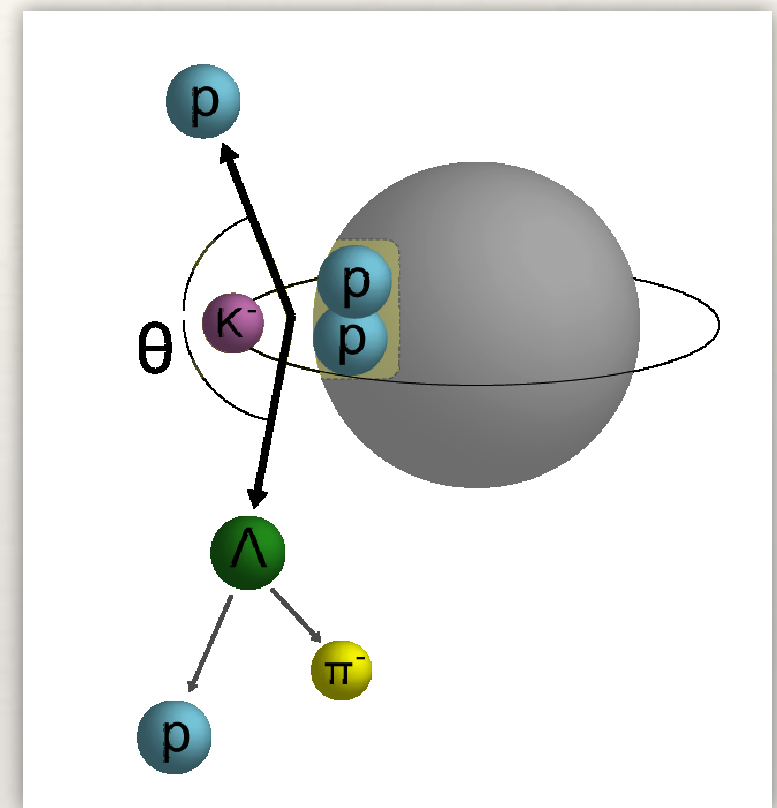
K^-pp

- ❖ $\bar{K}N$: attraction in Isospin=0
 - ❖ Kaonic hydrogen X-ray ; SIDDHARTA
M. Bazzi et al., NPA 881 (2012) 88-97.
 - ❖ Low-energy scattering measurements + Branching ratios at threshold
 - ❖ $\Lambda(1405)$ below the K^-p threshold
 - ❖ $J^\pi=1/2^-$; Moriya et al., Phys. Rev. Lett. 112 (2014) 082004.
 - ❖ Antikaon-Nucleon Molecule from Lattice QCD
; J.M.M. Hall et al., Phys. Rev. Lett. 114 (2015) 132002.
- ❖ Possible existence of “ K^-pp ” : $Y=1, I=1/2, J^\pi=0^-$



Past Measurements on Kpp #1

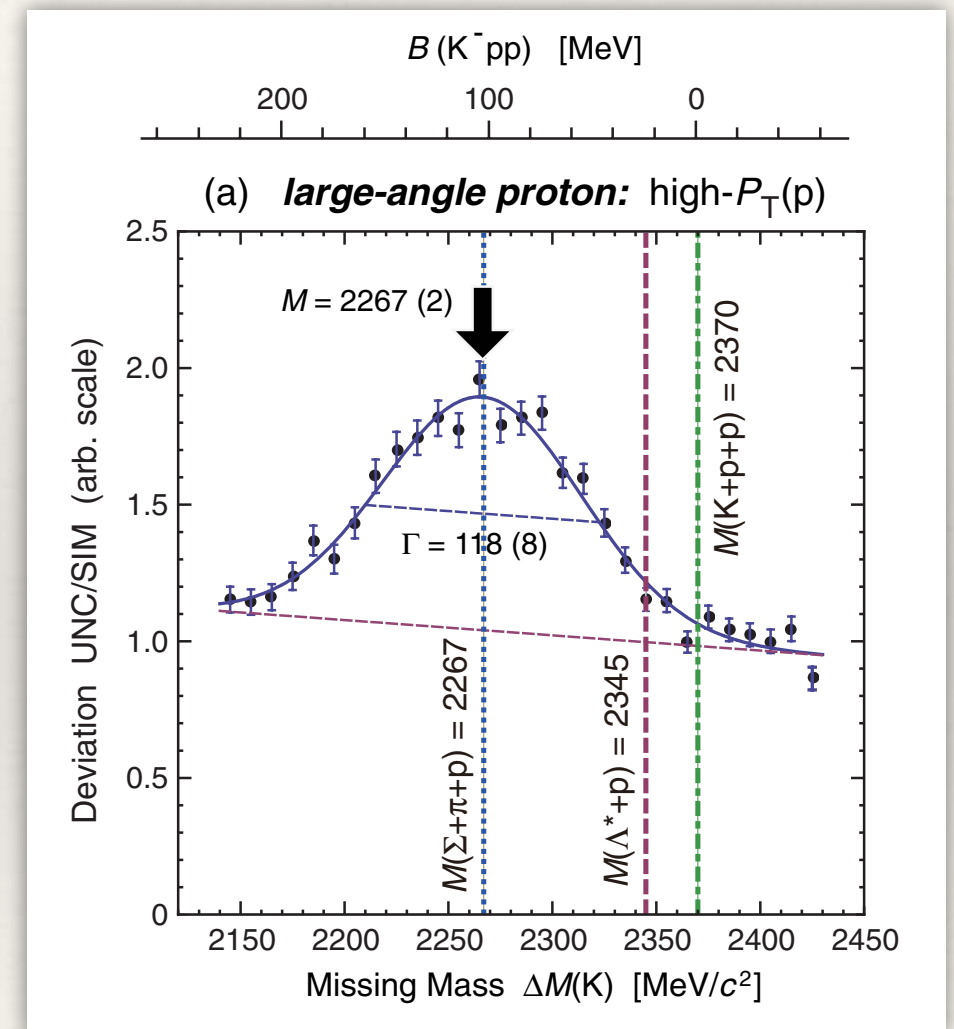
- ❖ First evidence of Kpp with ${}^6\text{Li}+{}^7\text{Li}+{}^{12}\text{C}$ by FINUDA
- ❖ A lot of back-to-back Λp pairs with small invariant mass



$$B = 115^{+6}_{-5} + 3_{-4} \text{ MeV}$$
$$\Gamma = 67^{+14}_{-11} + 2_{-3} \text{ MeV}$$

Past Experiments on K^-pp #2

- ❖ DISTO data: $p+p \rightarrow p\Lambda(K^-pp) + K^+$ at 2.85 GeV
 - ❖ $M = 2267 \pm 3 \pm 5 \text{ MeV}/c^2$
 - ❖ $\Gamma = 118 \pm 8 \pm 10 \text{ MeV}$
- ❖ Not observed at 2.5 GeV
 - ❖ small Λ^* production cross section



Past Measurements on K - pp #3

❖ HADES

G. Agakishiev et al., Phys. Lett. B 742 (2015) 242-248.

❖ $p+p \rightarrow K^+ p \Lambda$ @3.5 GeV; $S/N \ll 1$

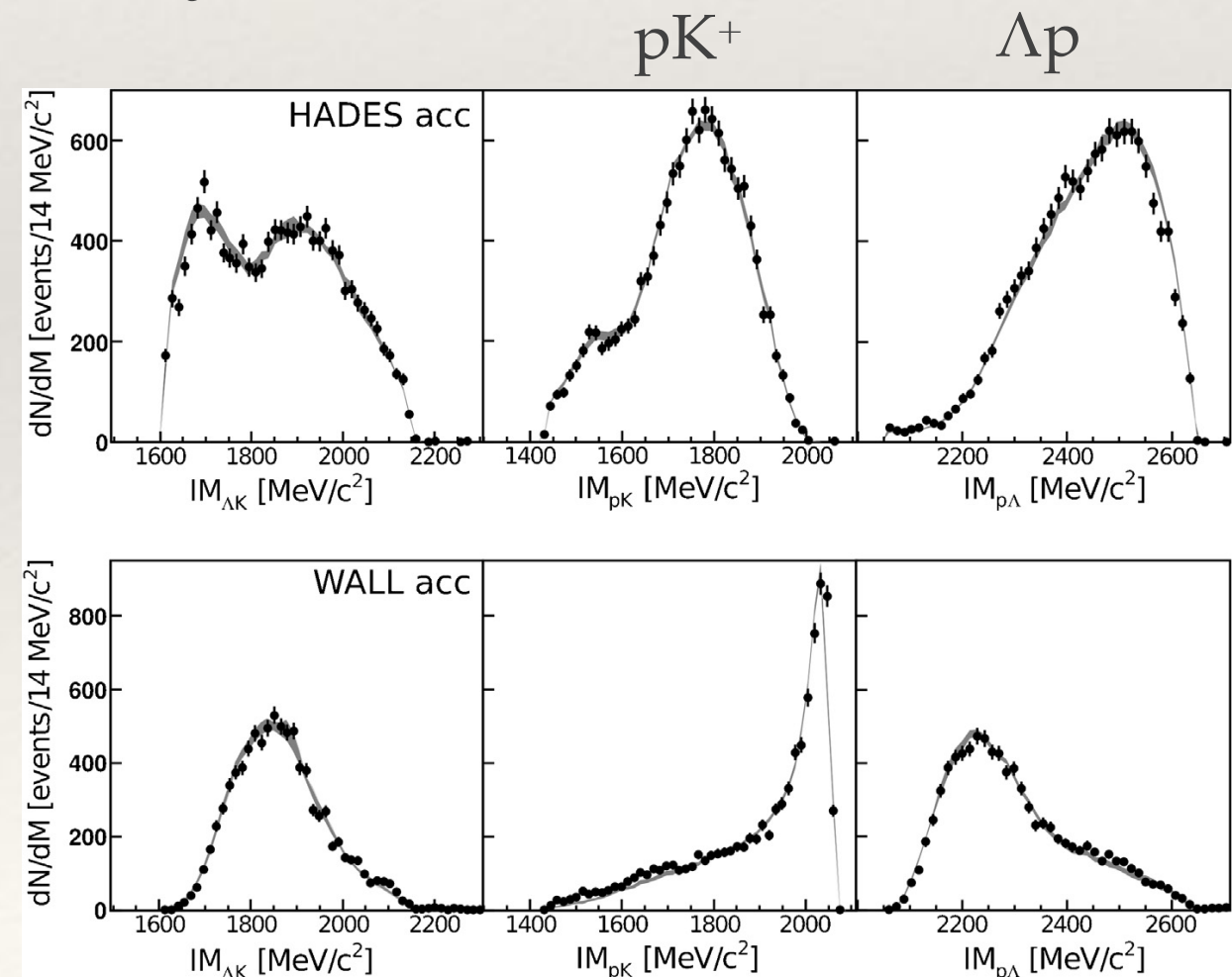
❖ Bonn-Gatchina Partial Wave Analysis
well reproduces the data

❖ K - pp production upper
limit $\sim 4 \mu\text{b}$ for $\Gamma = 70 \text{ MeV}$
(2.22 - $2.37 \text{ GeV}/c^2$)



$\Lambda(1405)$ production $\sim 10 \mu\text{b}$

Sensitivity ?



Past Measurements on $K\text{-}pp$ #4

❖ LEPS / SPring-8

A.O. Tokiyasu et al., Phys. Lett. B 728 (2014) 616-621.

❖ $d(\gamma, K^+\pi^-)$ reaction ($E_\gamma=1.5\text{-}2.4$ GeV)

❖ **Inclusive** missing-mass

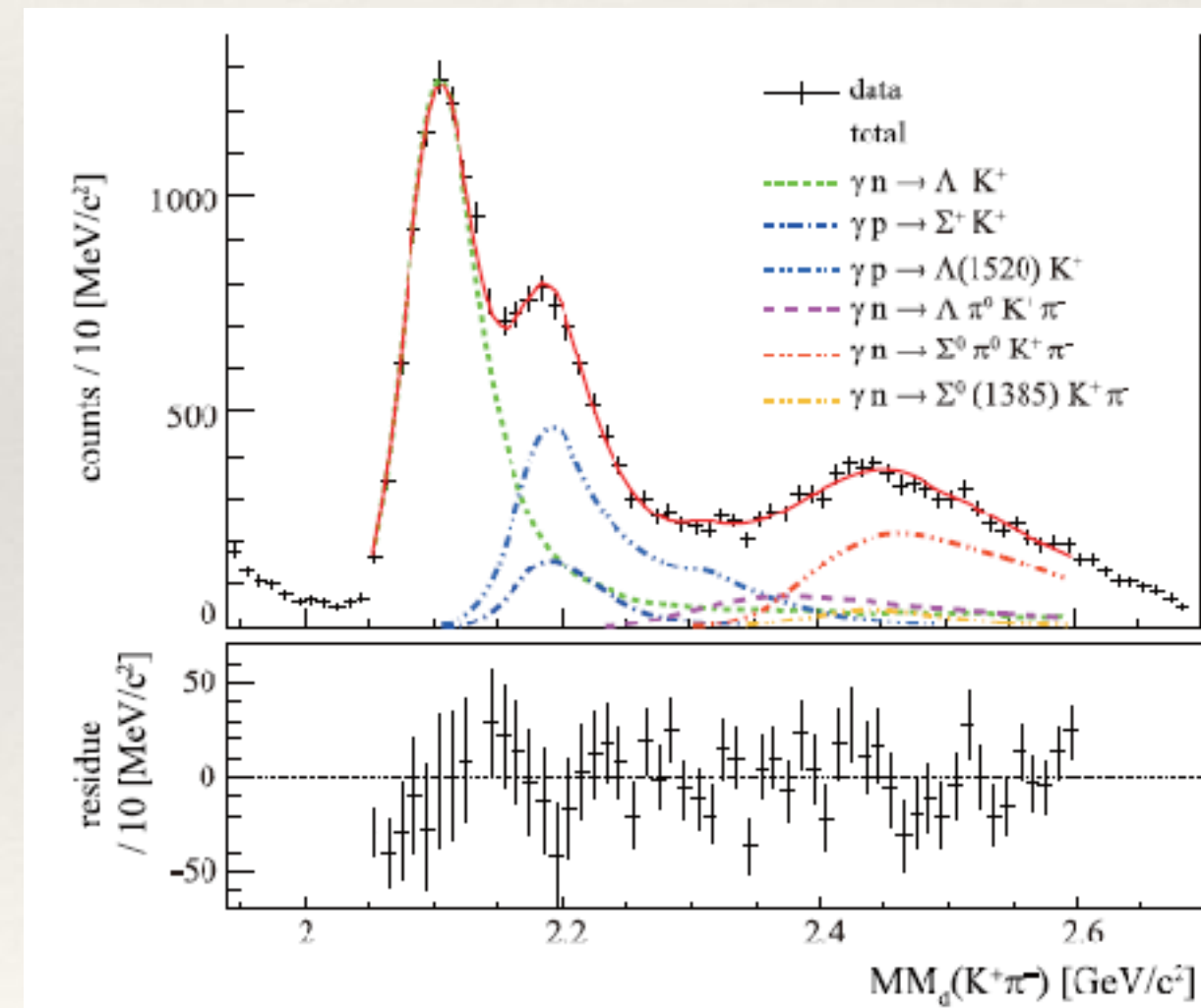
$$\sigma_m \sim 10 \text{ MeV}$$

❖ Background

$$K^+\Lambda(1520), K^+\pi^-\pi^0 Y$$

❖ Upper limits: $2.22\text{-}2.36 \text{ GeV}/c^2$ $< 1.1\text{-}2.9 \mu\text{b}$ for $\Gamma=100 \text{ MeV}$, $9.9\text{-}26\%$ of $K\pi Y$ productions

Sensitivity ?



Past Measurements on K^-pp #5

❖ J-PARC E15

T. Hashimoto et al., PTEP (2015) 061D01.

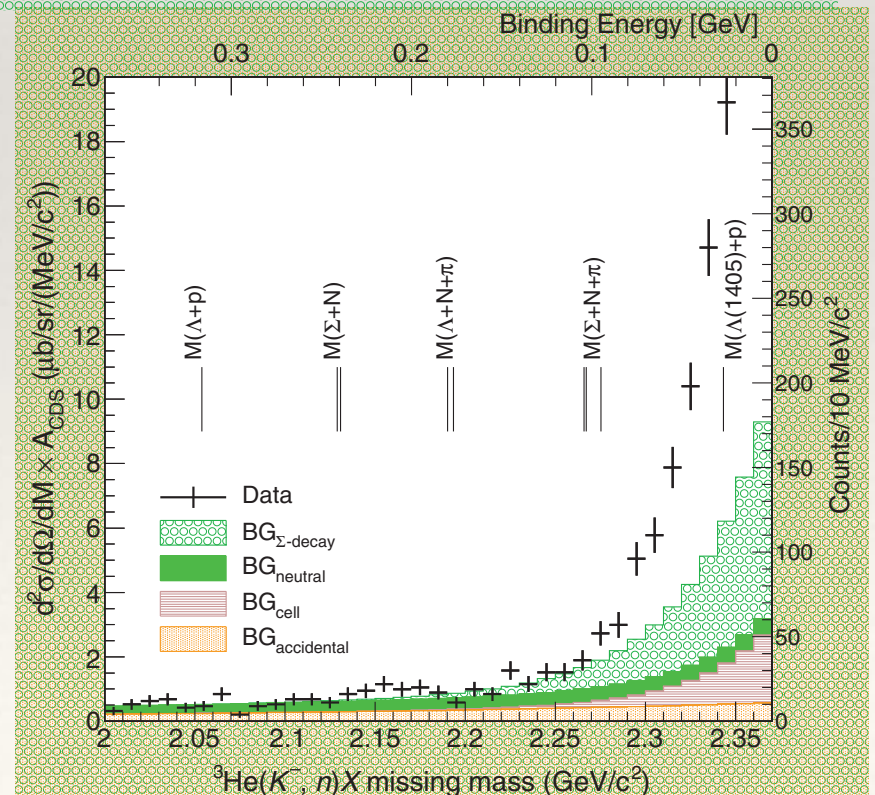
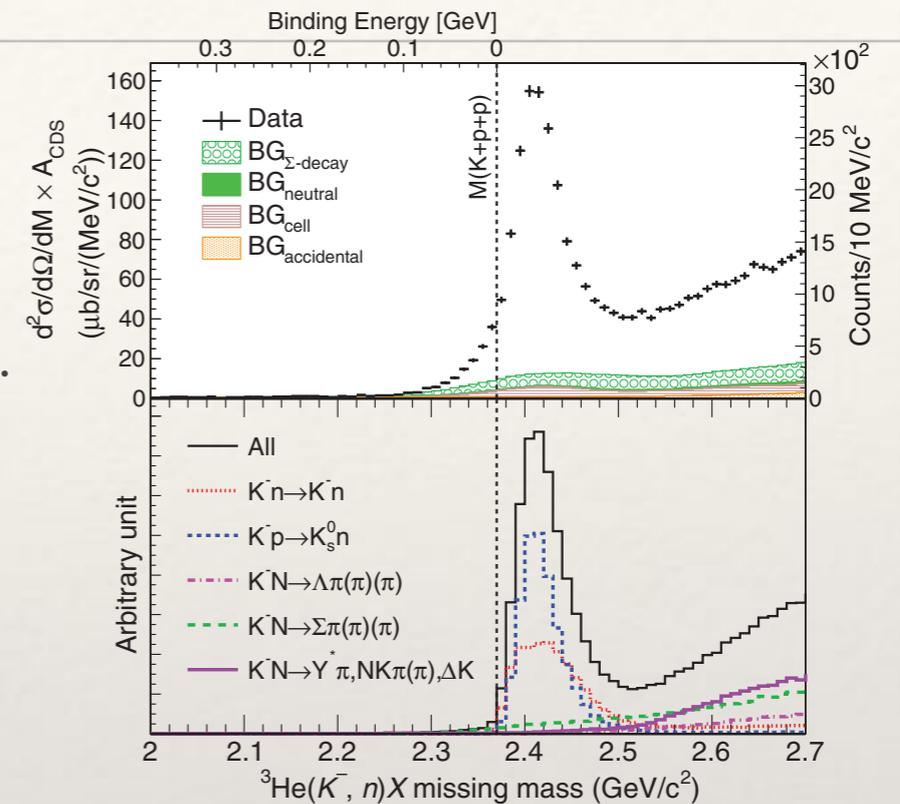
❖ ${}^3\text{He}(K^-,n)$ reaction @ 1 GeV/c

❖ Semi-inclusive missing-mass

σ_m : 5-15 MeV

❖ K^-pp production upper limit 100-270 $\mu\text{b}/\text{sr}$ for $\Gamma=100$ MeV (~5% of QF K^-n elastic)

Sensitivity ?



Theoretical calculations on K - pp

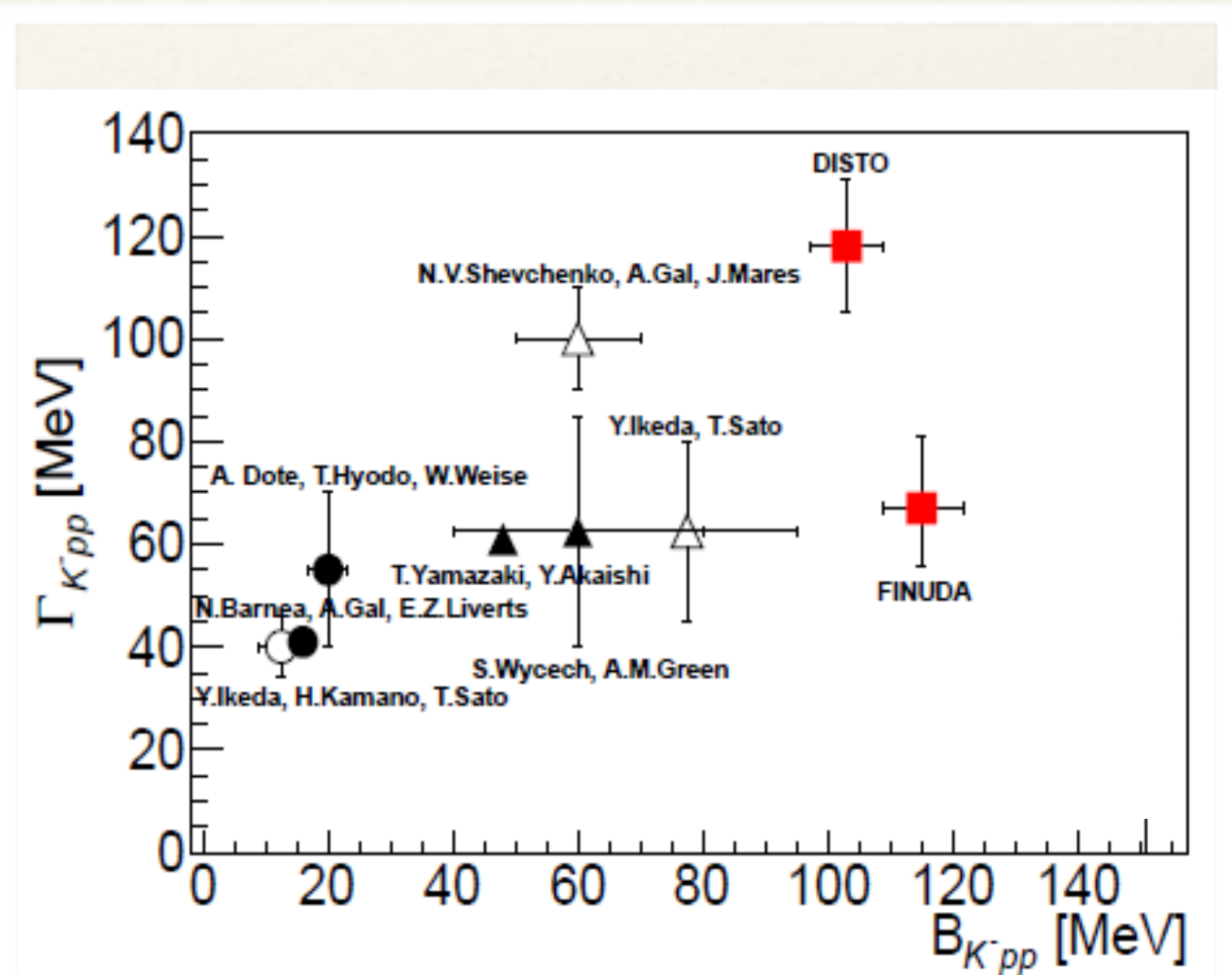
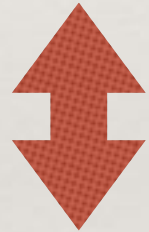
- ❖ Methods : Variational vs. Faddeev
 - Almost same results by using the same interaction model
- ❖ $\bar{K}N$ Interaction Models :
 - Chiral SU(3)-based (Energy dependent) → Shallow ~20 MeV
 - Phenomenological (Energy independent) → Deep ~40-70 MeV

	Dote,Hyodo, Weise	Akaishi, Yamazaki	Barnea, Gal, Liverts	Ikeda, Sato	Ikeda, Kamano,Sato	Schevchenko ,Gal, Mares	Revai, Schevchenko	Maeda, Akaishi, Yamazaki
B (MeV)	17-23	48	16	60-95	9-16	50-70	32	51.5
Γ (MeV)	40-70	61	41	45-80	34-46	90-110	49	61
Method	Variational	Variational	Variational	Faddeev- AGS	Faddeev- AGS	Faddeev- AGS	Faddeev- AGS	Faddeev- Yakubovsky
Interaction	Chiral	Phenom.	Chiral	Chiral	Chiral	Phenom.	Chiral	Phenom.

FSI effects? (V.K. Magas et al.), Λ^*N bound state (T. Uchino et al.)

Comparison between Theory and Exps.

- ❖ Binding energy
 - ❖ Shallow case: $B \sim 20$ MeV
 - ❖ Deep case: $B \sim 40-70$ MeV
- ❖ Observations: $B \sim 100$ MeV
- ❖ Width
 - ❖ agreement: $\Gamma \sim 30-100$ MeV



By Y. Ichikawa

Lessons

- ❖ It looks hard to observe the K - pp signal in inclusive measurements. (LEPS, J-PARC E15 fwd “n”)
- ❖ Small and Broad signature ; ~ 1
two-step reaction (two nucleons be involved)
- ❖ Large and Widely distributed QF background ; $>10\sim 100$
single-step reaction

Recent Measurements on K - pp

★ J-PARC E27 : $d(\pi^+, K^+ pp)X$

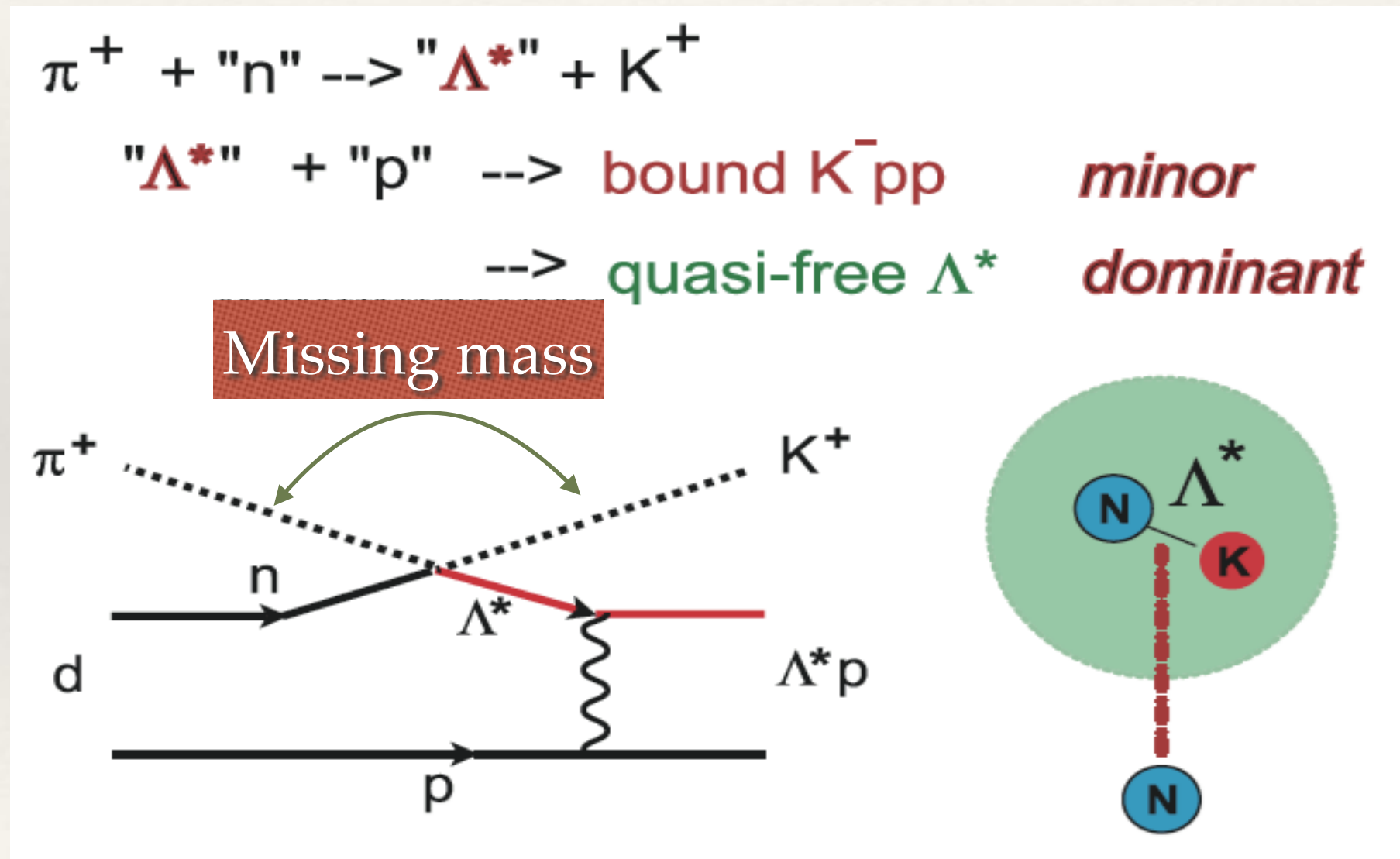
★ J-PARC E15 : ${}^3\text{He}(K^-, \Lambda p)n$

J-PARC E27

❖ $d(\pi^+, K^+)$ reaction @1.69 GeV/c

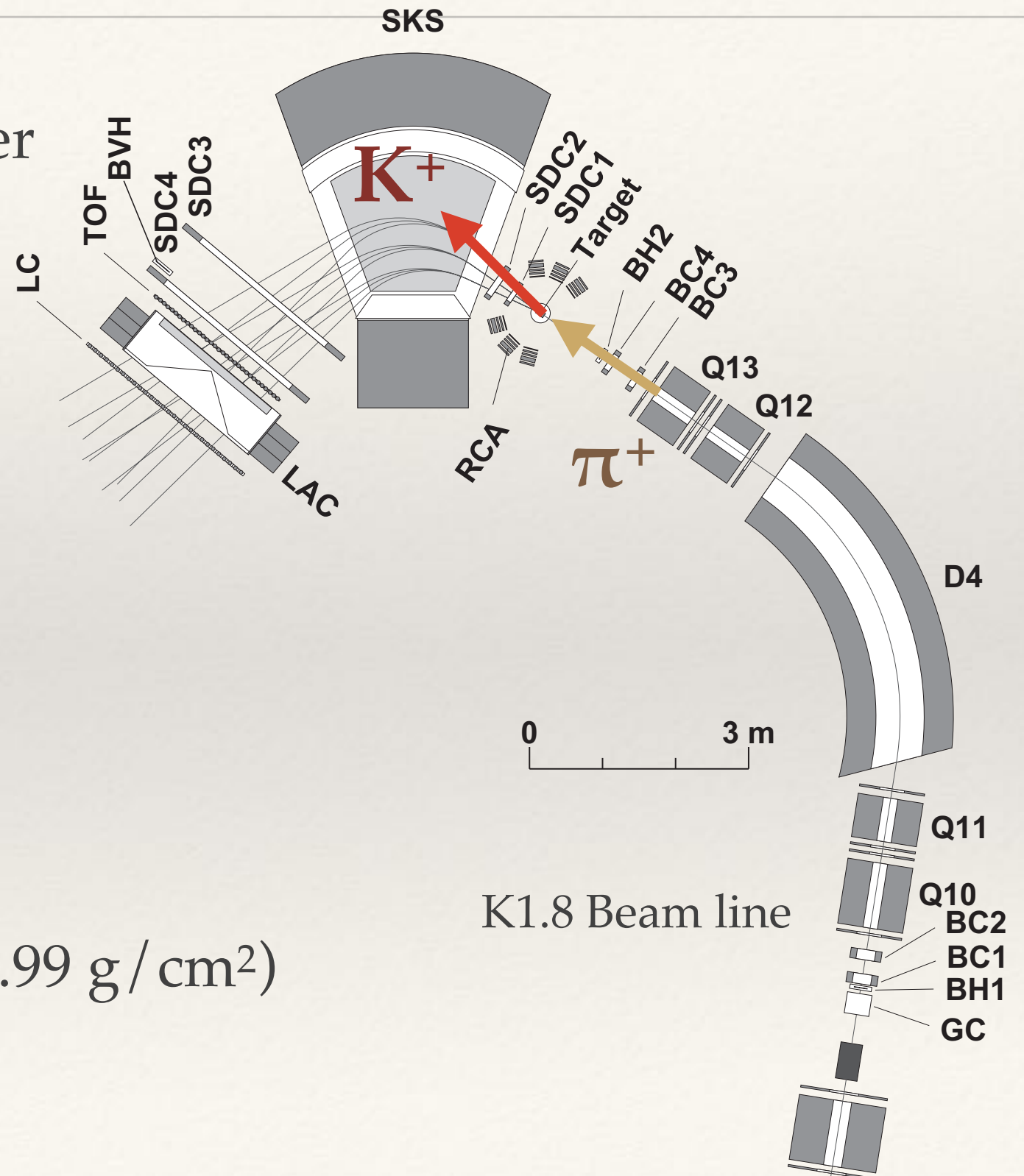
Y. Ichikawa et al., PTEP (2014) 101D03.

Y. Ichikawa et al., PTEP (2015) 021D01.

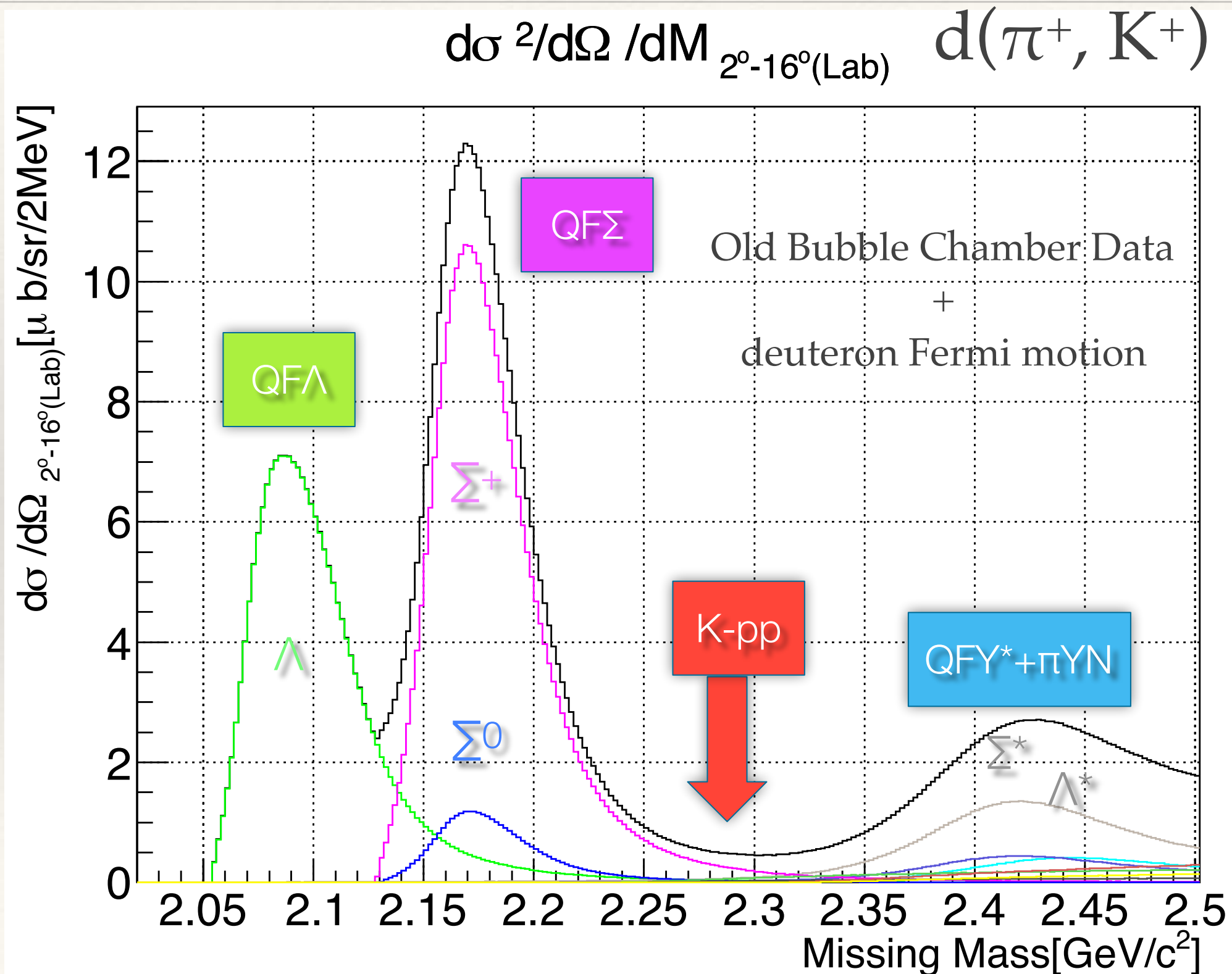


Experimental Setup

- ❖ K1.8 beam line spectrometer
 - ❖ $1.69 \text{ GeV}/c \pi^+$
 - ❖ $\Delta p/p \sim 2 \times 10^{-3}$
- ❖ SKS spectrometer
 - ❖ $0.8\text{-}1.3 \text{ GeV}/c K^+$
 - ❖ $\Delta p/p \sim 2 \times 10^{-3}$
 - ❖ $\Delta\Omega \sim 100 \text{ msr}$
- ❖ Target : liquid deuterium ($1.99 \text{ g}/\text{cm}^2$)

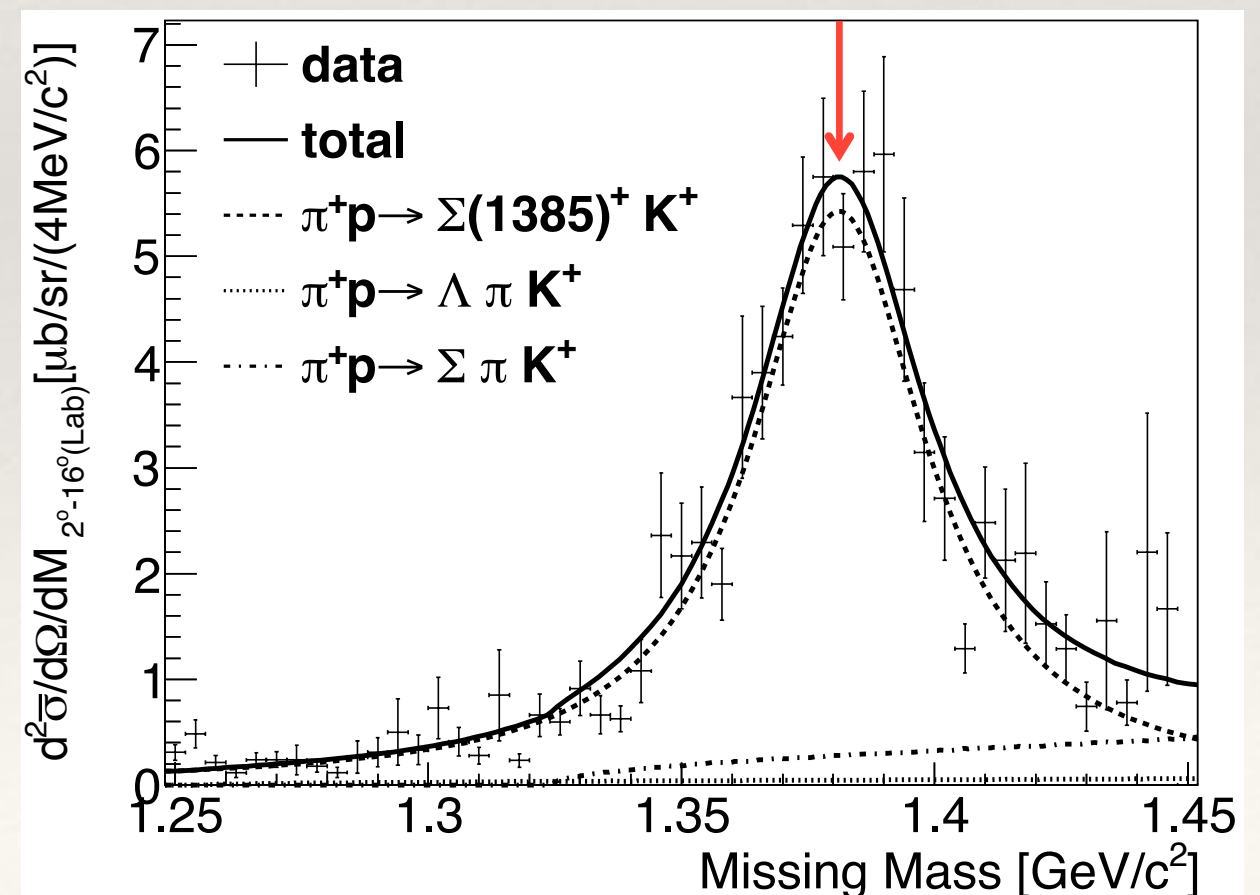
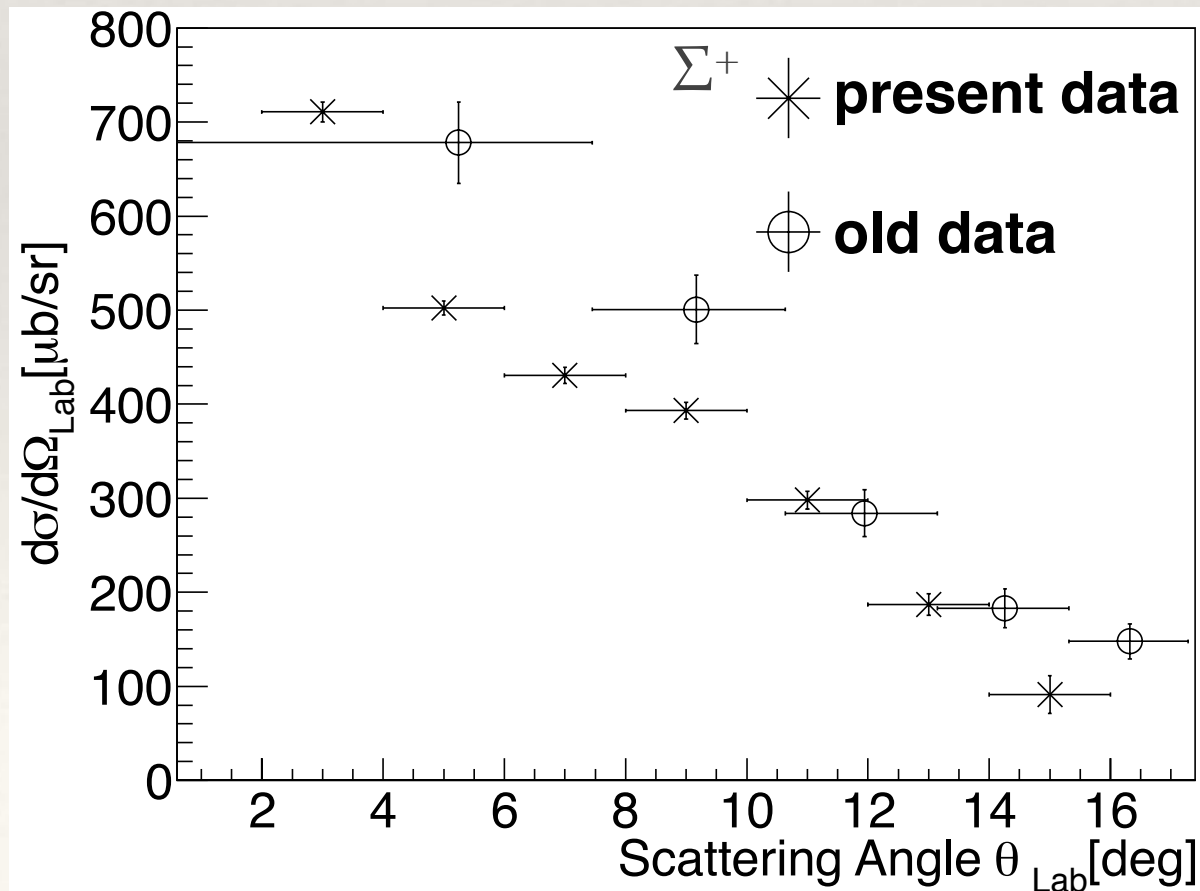
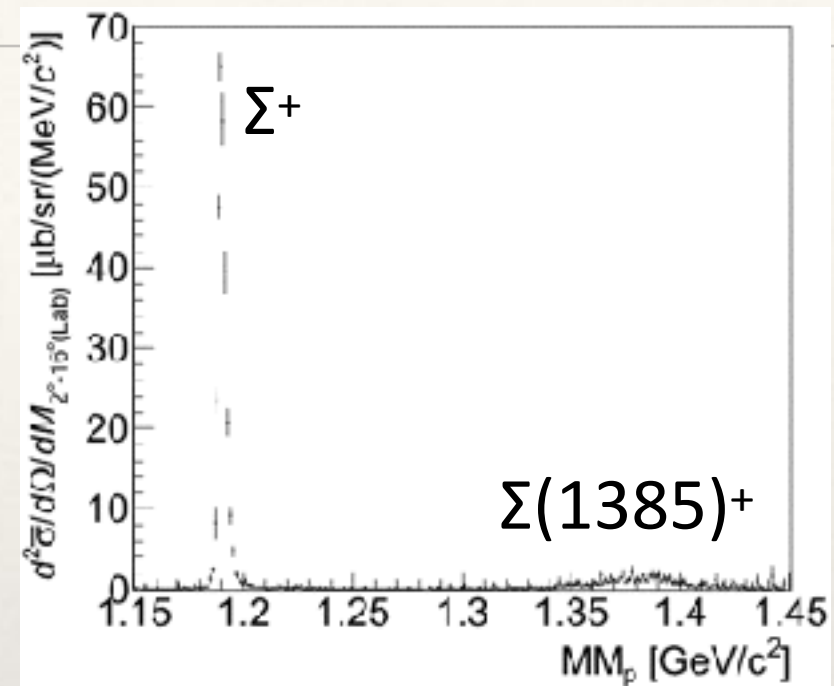


Expected Inclusive Spectrum

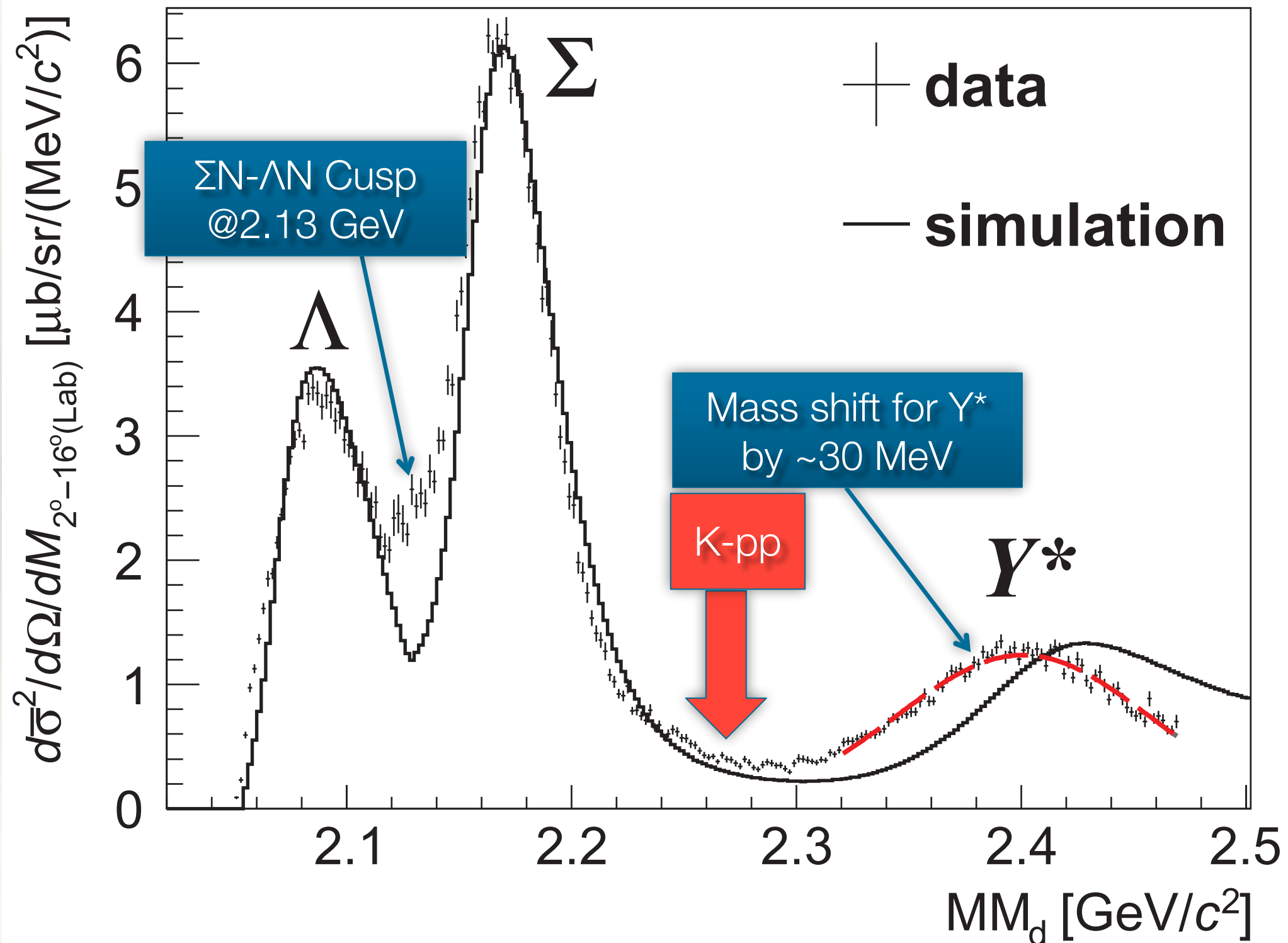


$p(\pi^+, K^+) \Sigma^+ / \Sigma^* @ 1.69 \text{ GeV}/c$

- ❖ Σ^+ and $\Sigma^+(1385)$:
mass & width are consistent with PDG
- ❖ $\Delta m_{\text{FWHM}} = 2.8 \pm 0.1 \text{ MeV}/c^2$



Measured $d(\pi^+, K^+)X$ spectrum



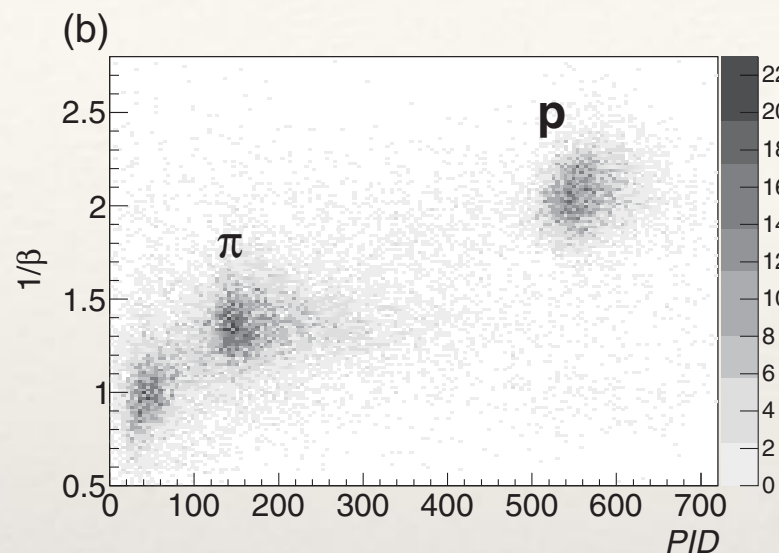
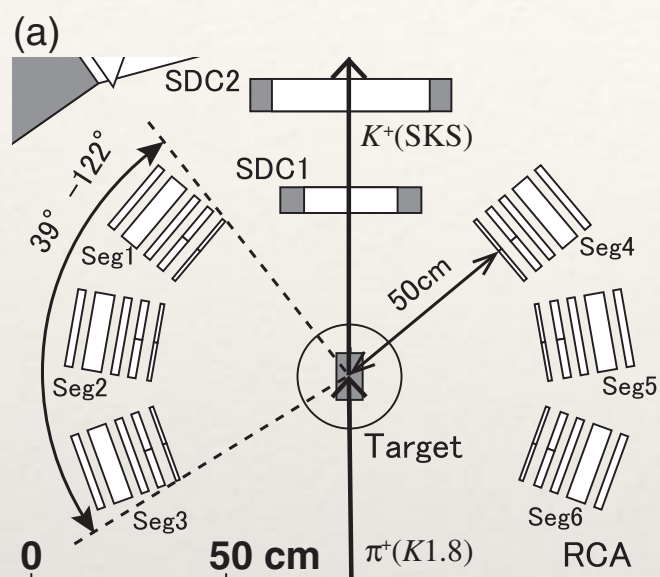
Range counter for Proton tagging

- ❖ Range Counter Arrays (RCA)

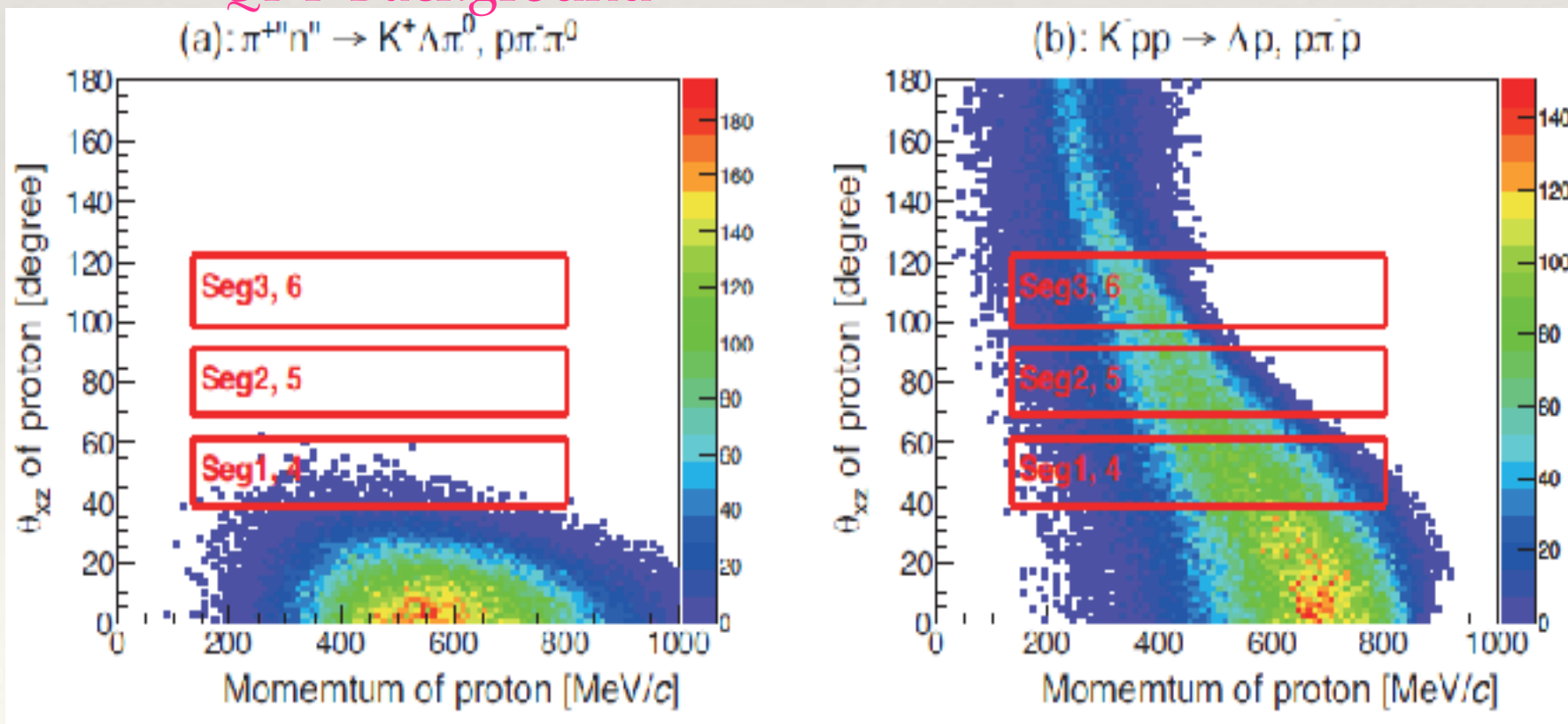
- ❖ 5 layers (1+2+2+5+2 cm) of Plastic scinti.

- ❖ 39-122 deg. (L+R)

- ❖ 50 cm TOF $\rightarrow \beta_p$



QFY Background



K-pp Signal

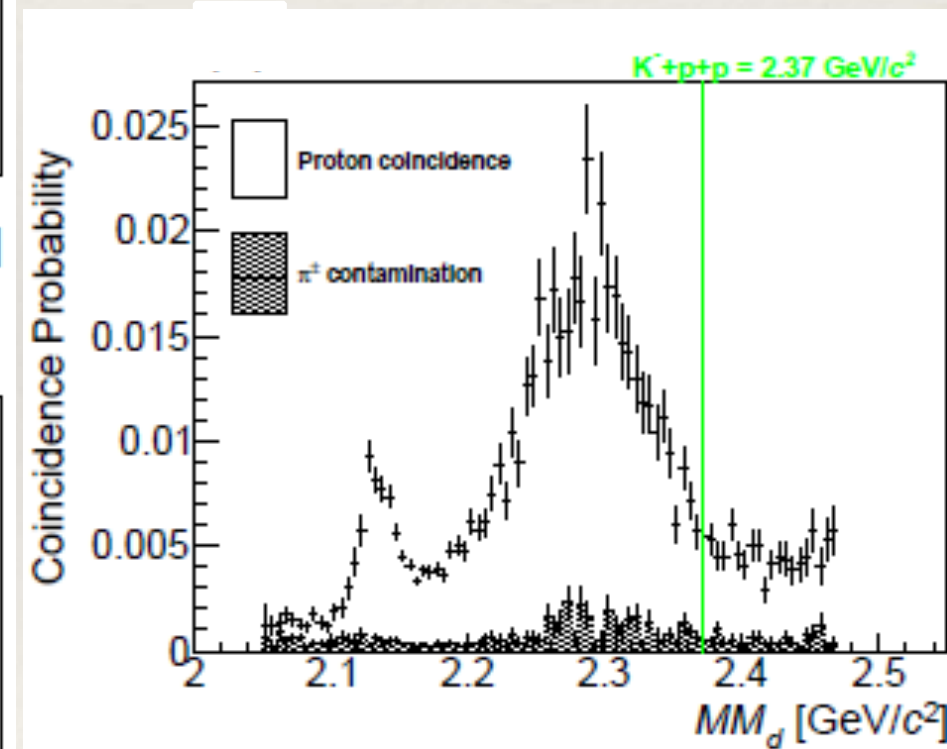
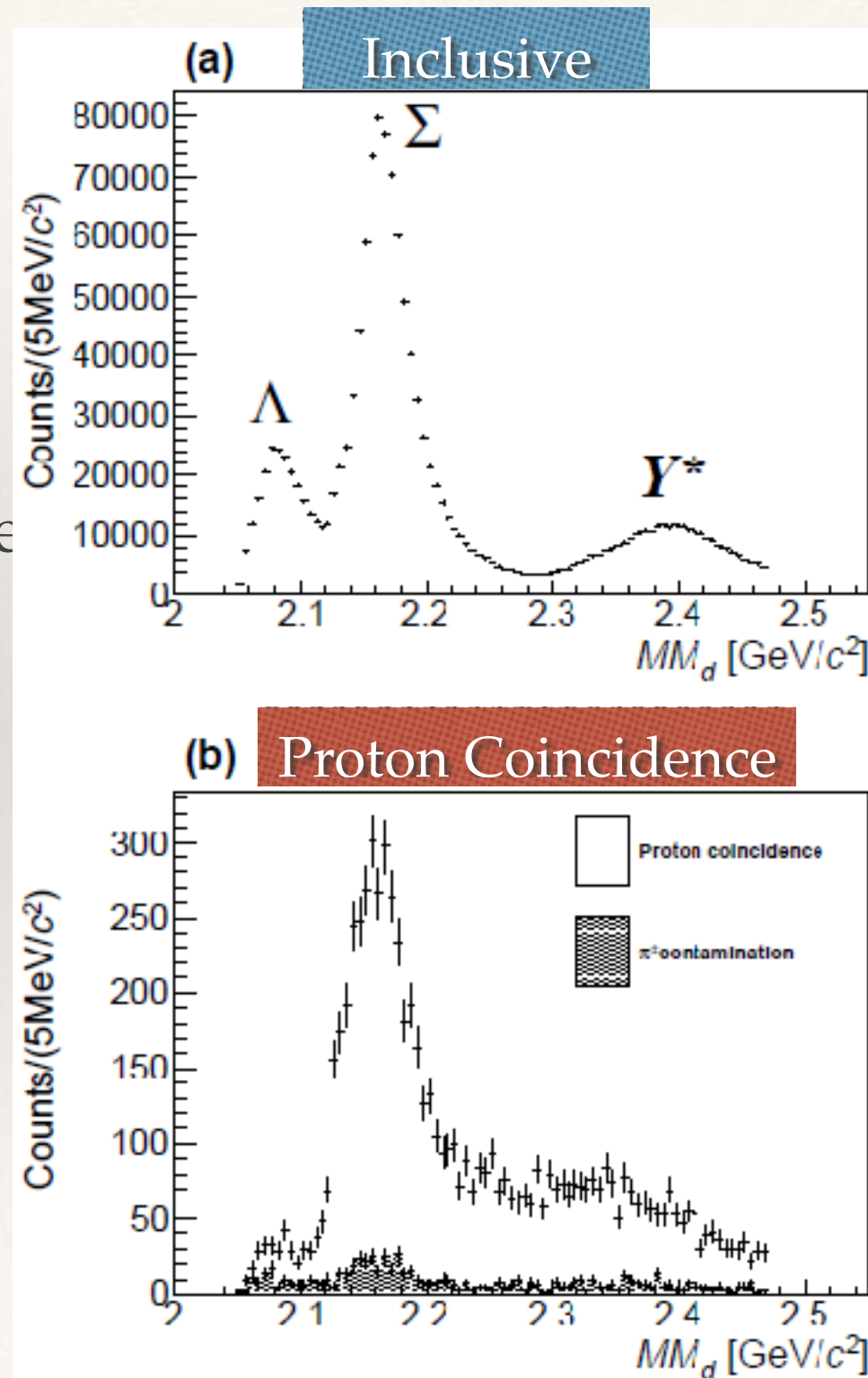
Coincidence Study

Proton mom. ≥ 250
MeV/c

❖ QF Λ , QF Σ , QFY*s are
suppressed as
expected !!

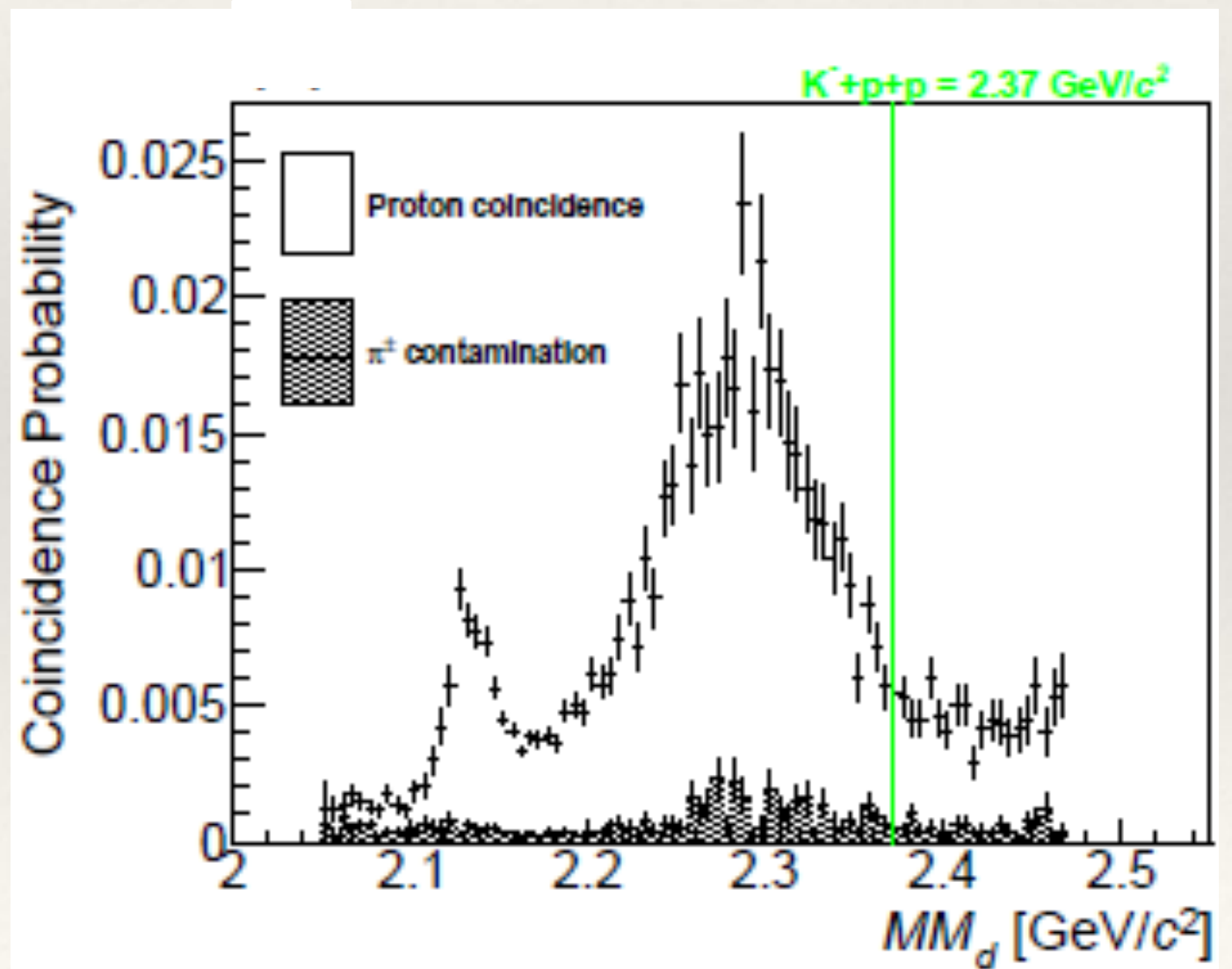
❖ What's left ?

❖ $Y, Y^* + N \rightarrow p + X$

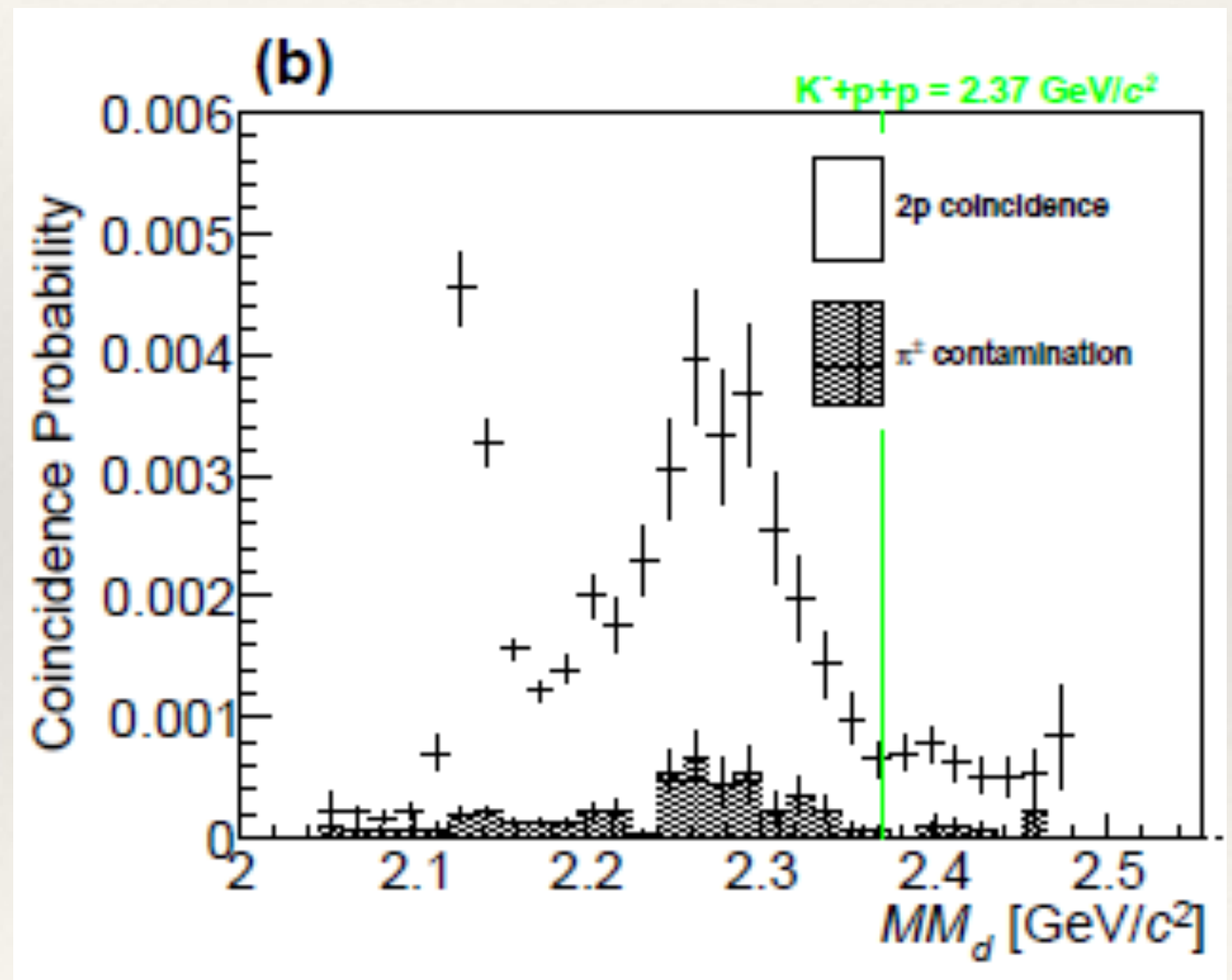


One-proton coincidence

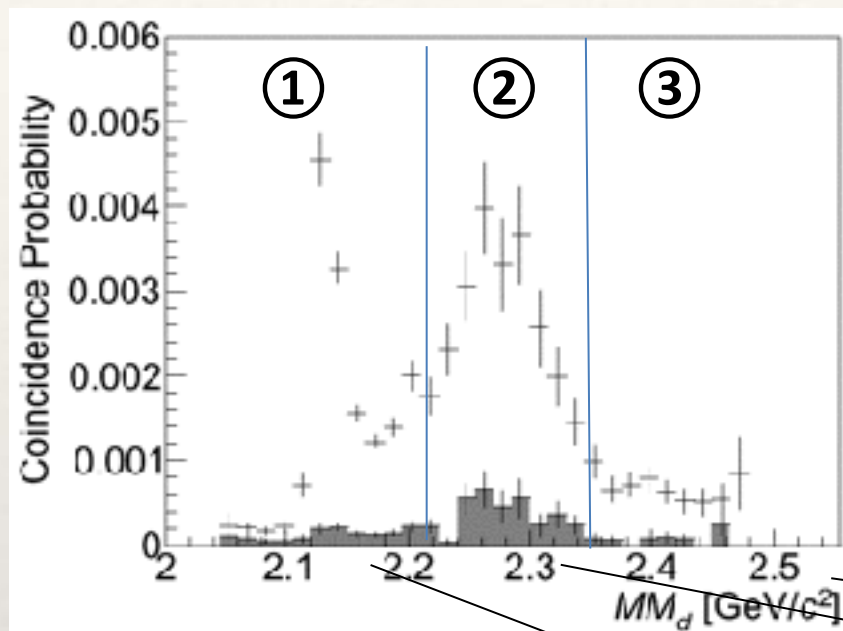
- ❖ Coincidence Probability(MM)
= One-proton coincidence(MM) / Inclusive(MM)
- ❖ Enhancement near the ΣN threshold ($2.13 \text{ GeV} / c^2$)
- ❖ Broad bump at $\sim 2.28 \text{ GeV} / c^2$



Two-proton coincidence



Two-proton coin. & Decay mode



- Two-protons in the final state :
 $K^-pp \rightarrow \Lambda p, \Sigma^0 p, \Upsilon p$
 $pp\pi, pp\pi\gamma, pp\pi\pi(\gamma)$
- $d(\pi^+, K^+ pp)X$

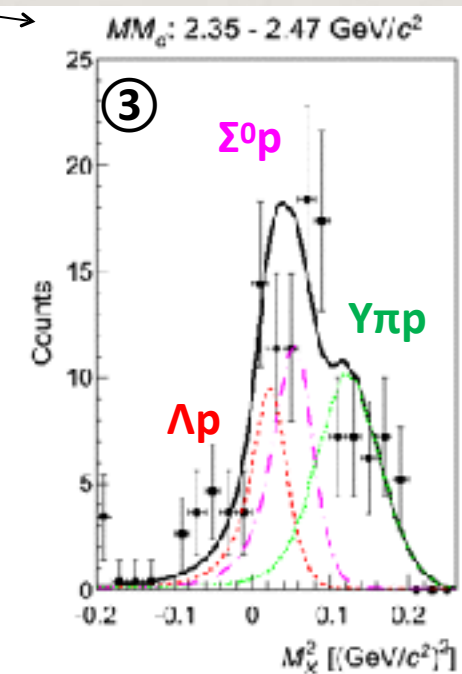
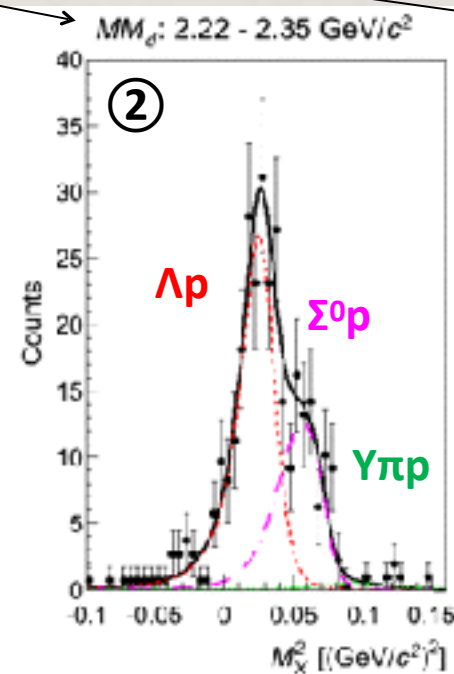
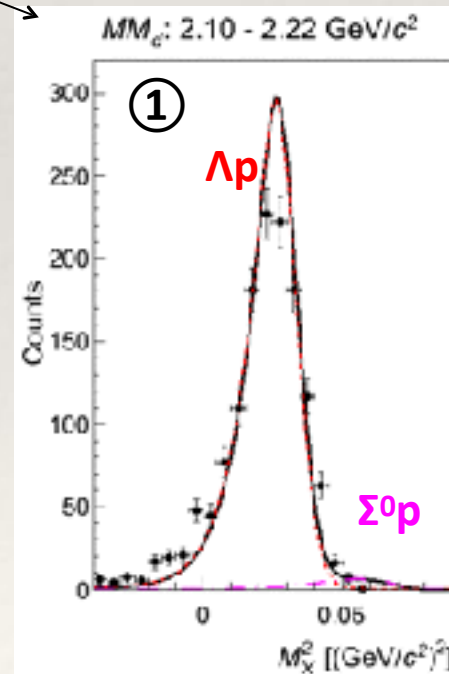
+ Data

— $X = \pi$ (FS: Λp)

— $X = \pi\gamma$ (FS: $\Sigma^0 p$)

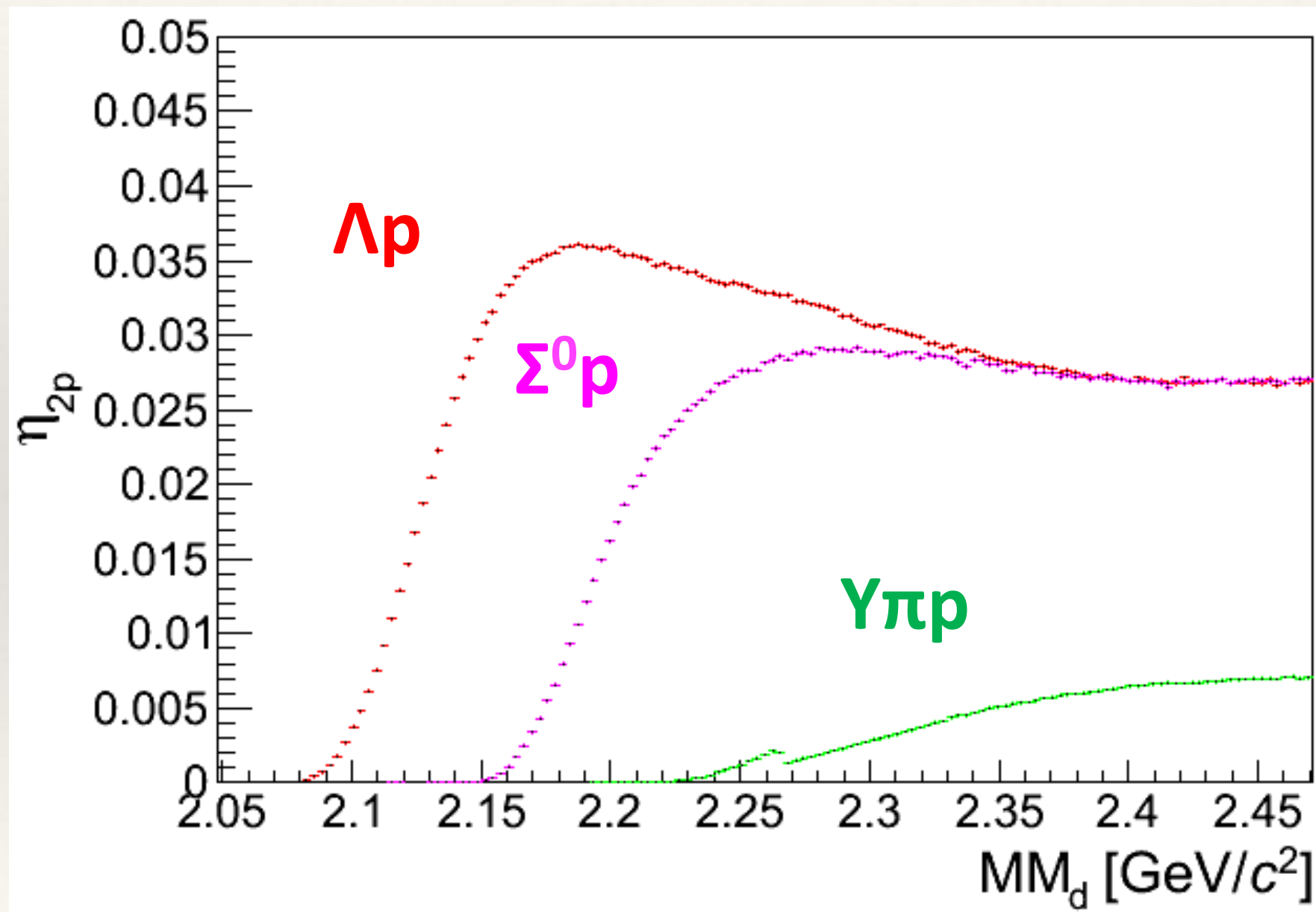
— $X = 2\pi(\gamma)$ (FS: Υp)

— Sum



Kinematically almost-complete measurement !

Mass-acceptance for each decay mode



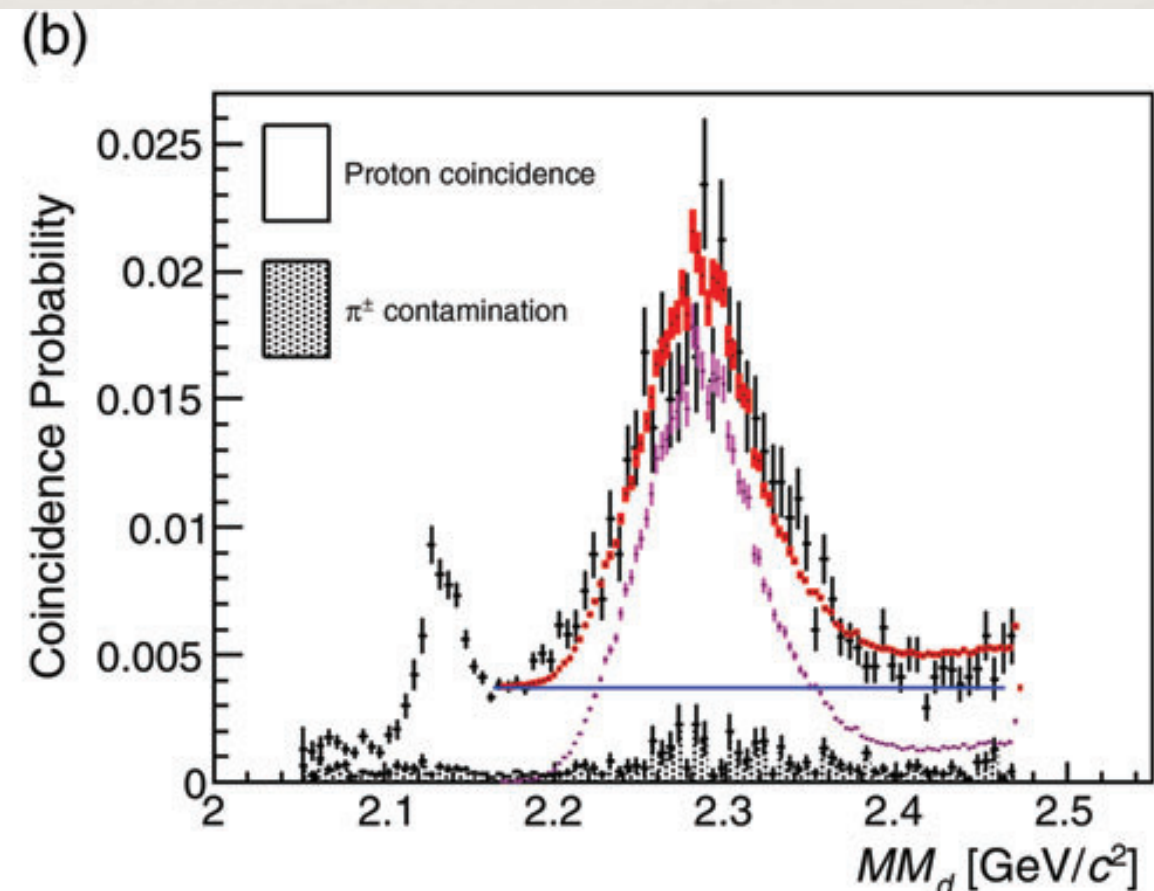
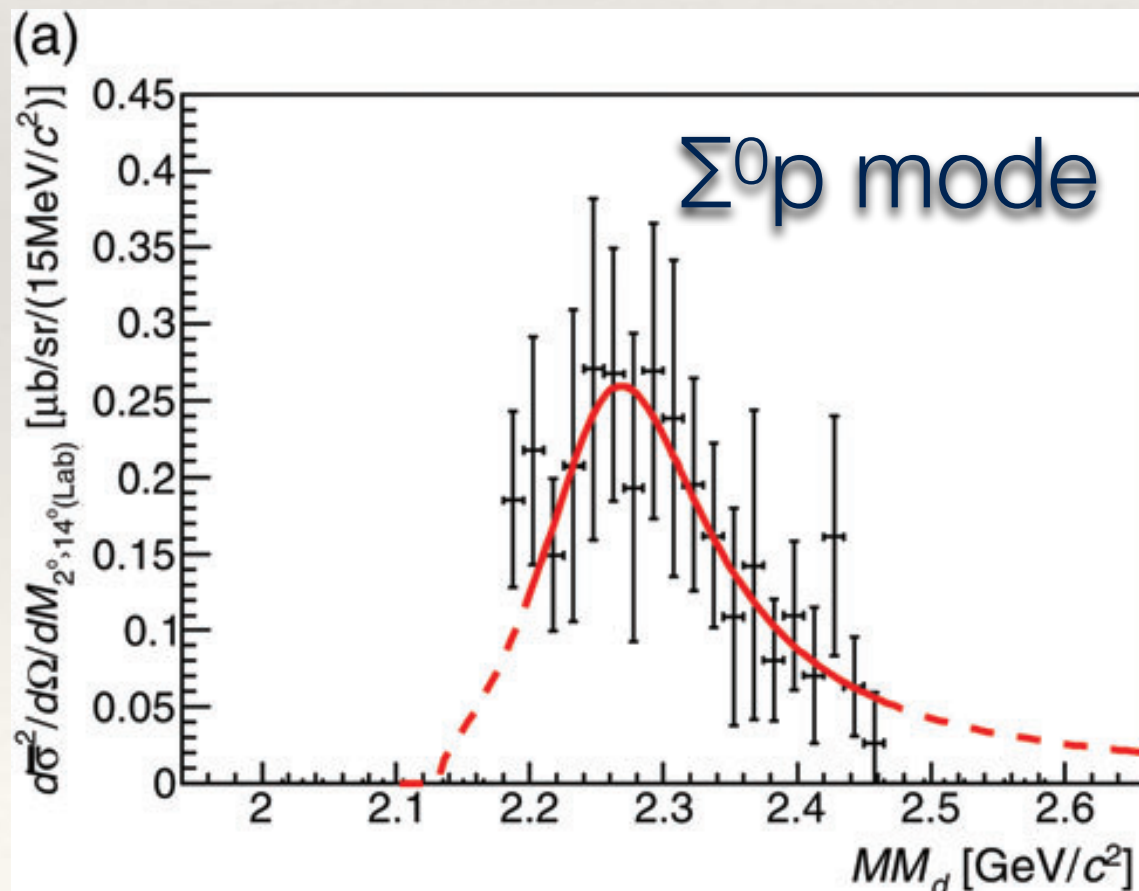
Kpp -like Structure

❖ Mass : 2275_{-18}^{+17} (stat.) $_{-30}^{+21}$ (syst.) MeV/ c^2

❖ Width : 162_{-45}^{+87} (stat.) $_{-78}^{+66}$ (syst.) MeV

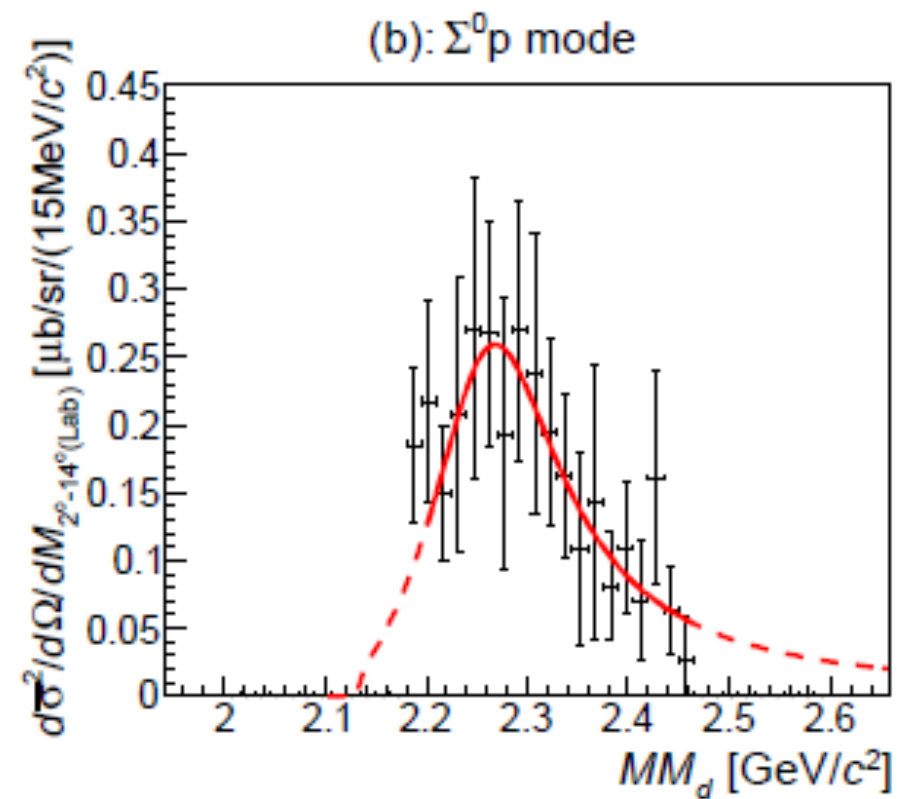
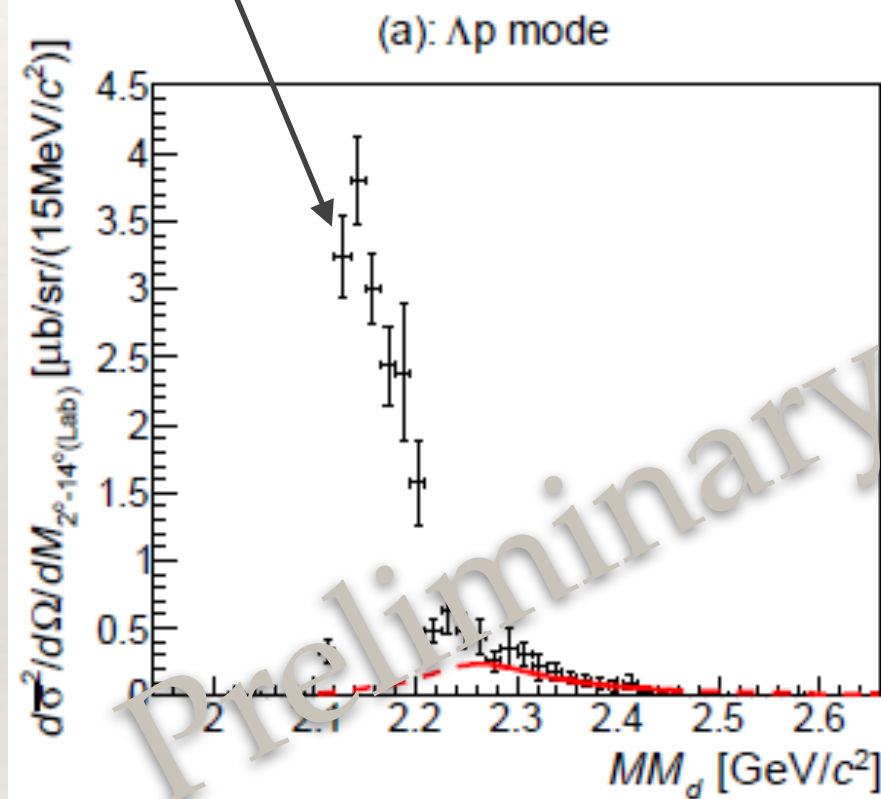
❖ Binding Energy 95_{-17}^{+18} (stat.) $_{-21}^{+30}$ (syst.) MeV

Relativistic Breit-Wigner



$\Lambda p / \Sigma^0 p$ Branching Fraction

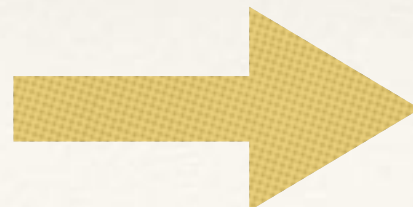
ΣN cusp +
 $\Sigma N \rightarrow \Lambda N$ conversion



$$\frac{\Gamma_{\Lambda p}}{\Gamma_{\Sigma^0 p}} = 0.92^{+0.16}_{-0.14}(\text{stat})^{+0.60}_{-0.42}(\text{syst})$$

$$\frac{d\sigma}{d\Omega}_{K^- pp \rightarrow \Sigma^0 p} = 3.0 \pm 0.3(\text{stat})^{+0.7}_{-1.1}(\text{syst}) \mu\text{b}/\text{sr}$$

$$\frac{d\sigma}{d\Omega}_{\Lambda(1405)} = 36.9 \mu\text{b}/\text{sr}$$



$$\frac{d\sigma}{d\Omega}_{K^- pp \rightarrow \Lambda p / \Sigma^0 p} / \frac{d\sigma}{d\Omega}_{\Lambda(1405)} \approx 15.7\%$$

E15: ${}^3\text{He}(K^-, p\Lambda)n$

Y. Sada et al., PTEP 2016, 051D01.

- ❖ $\Lambda p(pp\pi^-)$ in CDS.
 $\sigma_{\Lambda p} \sim 10 \text{ MeV}$
- ❖ “n” in missing-mass
 $\sigma_n \sim 40 \text{ MeV}$

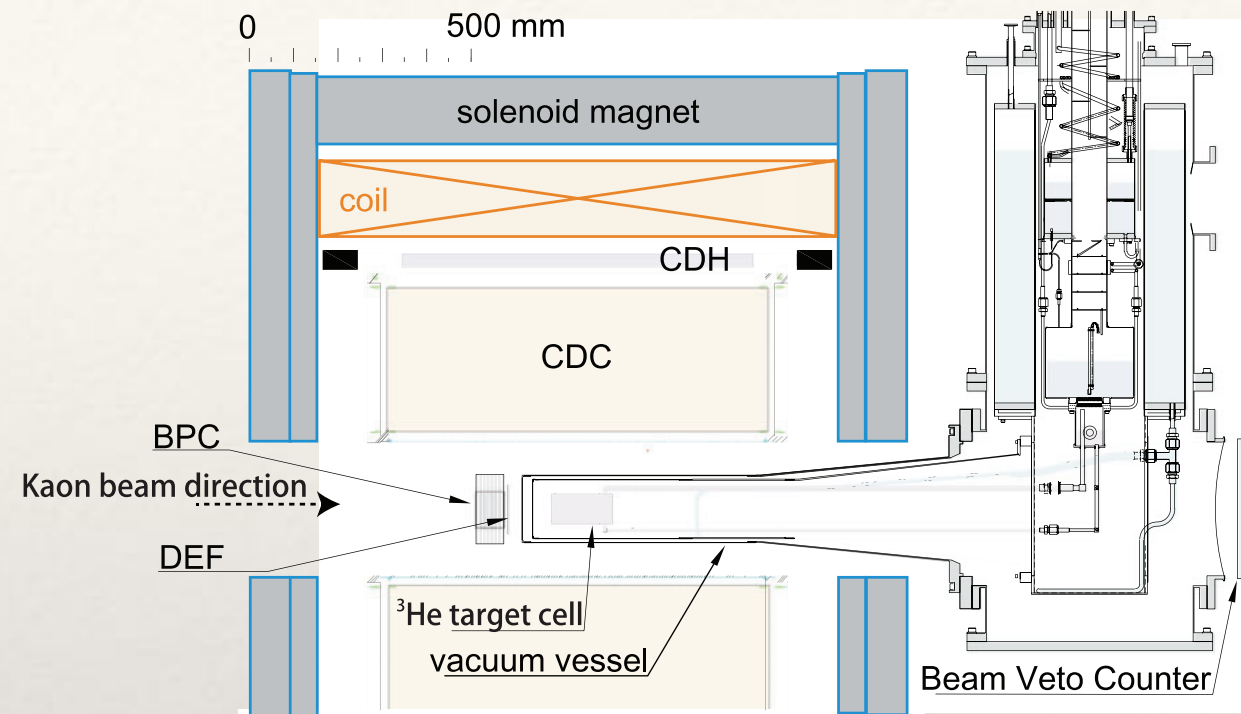
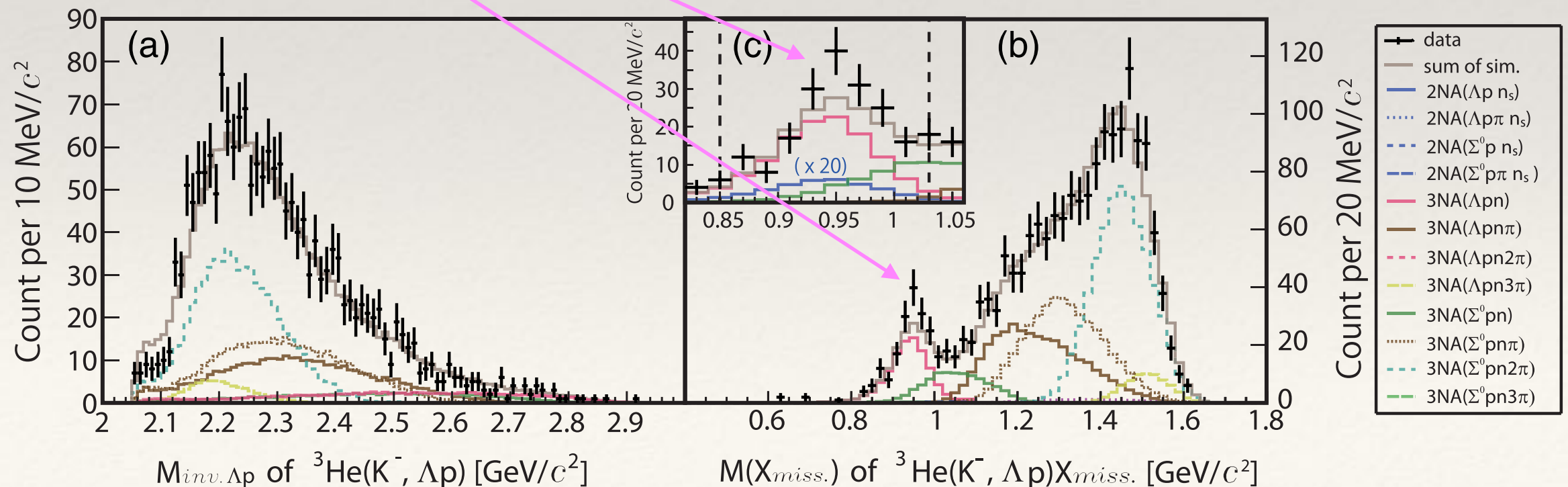
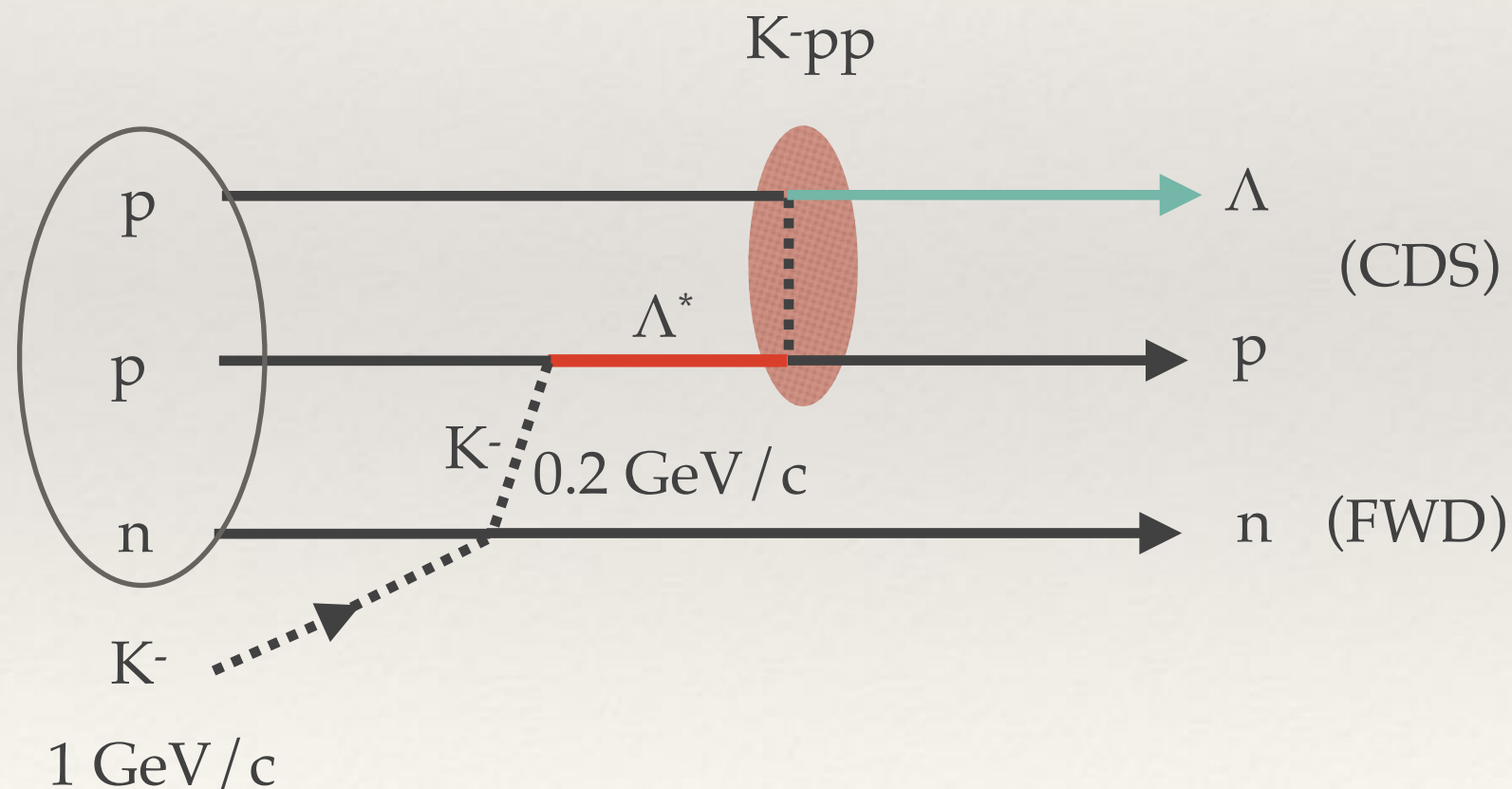


Fig. 1. Schematic diagram of detectors in the CDS and of the target system [22].



K^-pp Production through Λ^*

- ❖ $K^- + n \rightarrow n + K^-$; $1 \text{ GeV}/c \rightarrow 0.2 \text{ GeV}/c$
- ❖ $K^- + p \rightarrow \Lambda^*$, $\Lambda^* + p \rightarrow (K^-pp) \rightarrow \Lambda + p$

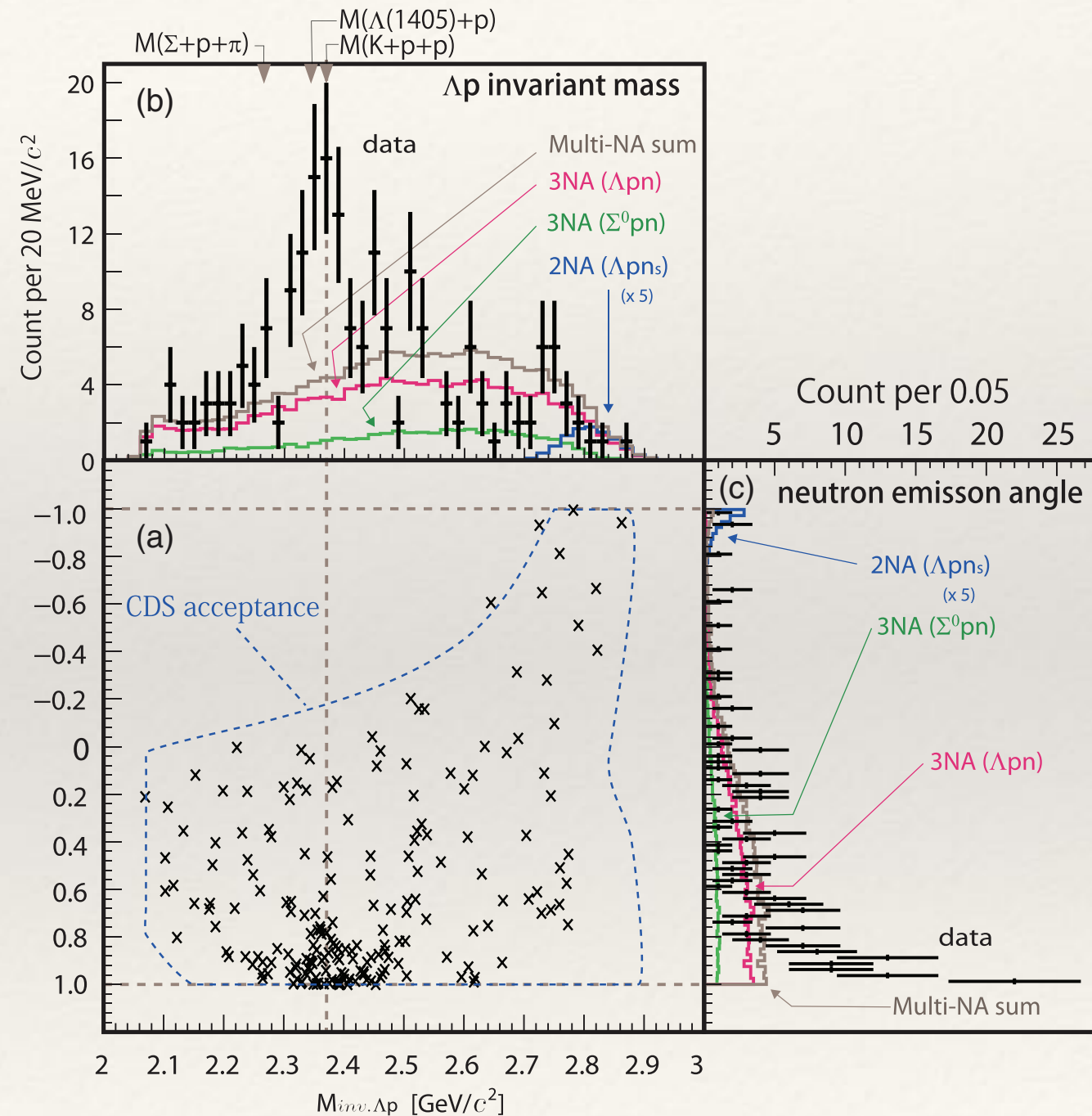


pΛ vs. “n”

- ❖ A uniform distribution in 3-body phase space ?!
- +
- ❖ A structure near the K+p+p threshold.
- ❖ “n” in the very forward $\cos\theta_n^{\text{CM}}$

$$M_X = 2355_{-8}^{+6} \text{ (stat.)} \pm 12 \text{ (syst.) MeV}/c^2$$

$$\Gamma_X = 110_{-17}^{+19} \text{ (stat.)} \pm 27 \text{ (syst.) MeV}/c^2$$



$$\frac{d^2\sigma_X}{dM_{\text{inv.}\Lambda p}dq_{\Lambda p}} \propto \rho_3(\Lambda pn) \times \frac{(\Gamma_X/2)^2}{(M_{\text{inv.}\Lambda p} - M_X)^2 + (\Gamma_X/2)^2} \times \left| \exp\left(-q_{\Lambda p}^2/2Q_X^2\right) \right|^2$$

Remarks

- ❖ $\Lambda(1405)$ production seems to be necessary,
 - ❖ (OK for DISTO, HADES, J-PARC E27; Δ for FINUDA, ? for E15)
 - ❖ **but, not enough !**
- ❖ Need to understand the $\Lambda^*(E)p \rightarrow K-pp$ dynamics
 - ❖ \rightarrow sensitivity of the measurements
 - 7% of $\Lambda(1405)$ in E27 \Leftrightarrow < 40% in HADES

Discussion on “ K^-pp ”

❖ $B(\text{FINUDA}) > B(\text{DISTO}) \sim B(\text{E27}) \gg B(\text{E15})$

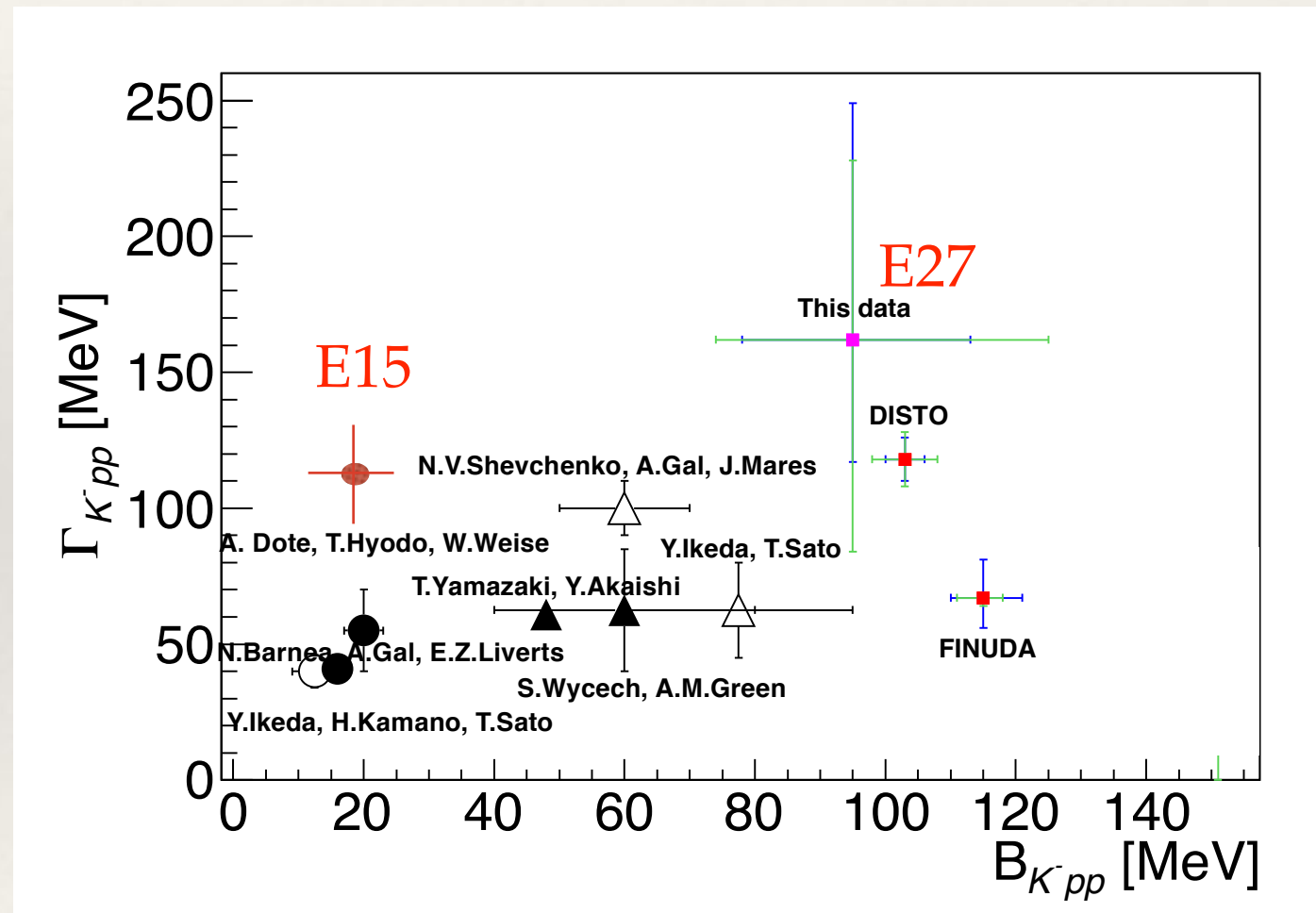
115 100 95 15

❖ We have two states ?

❖ Width is broad (> 70 MeV)

❖ $\Gamma_{\text{Mesonic}} \sim 50$ MeV

❖ $\Gamma_{\text{Non-Mesonic}} > \Gamma_{\text{Mesonic}}$?



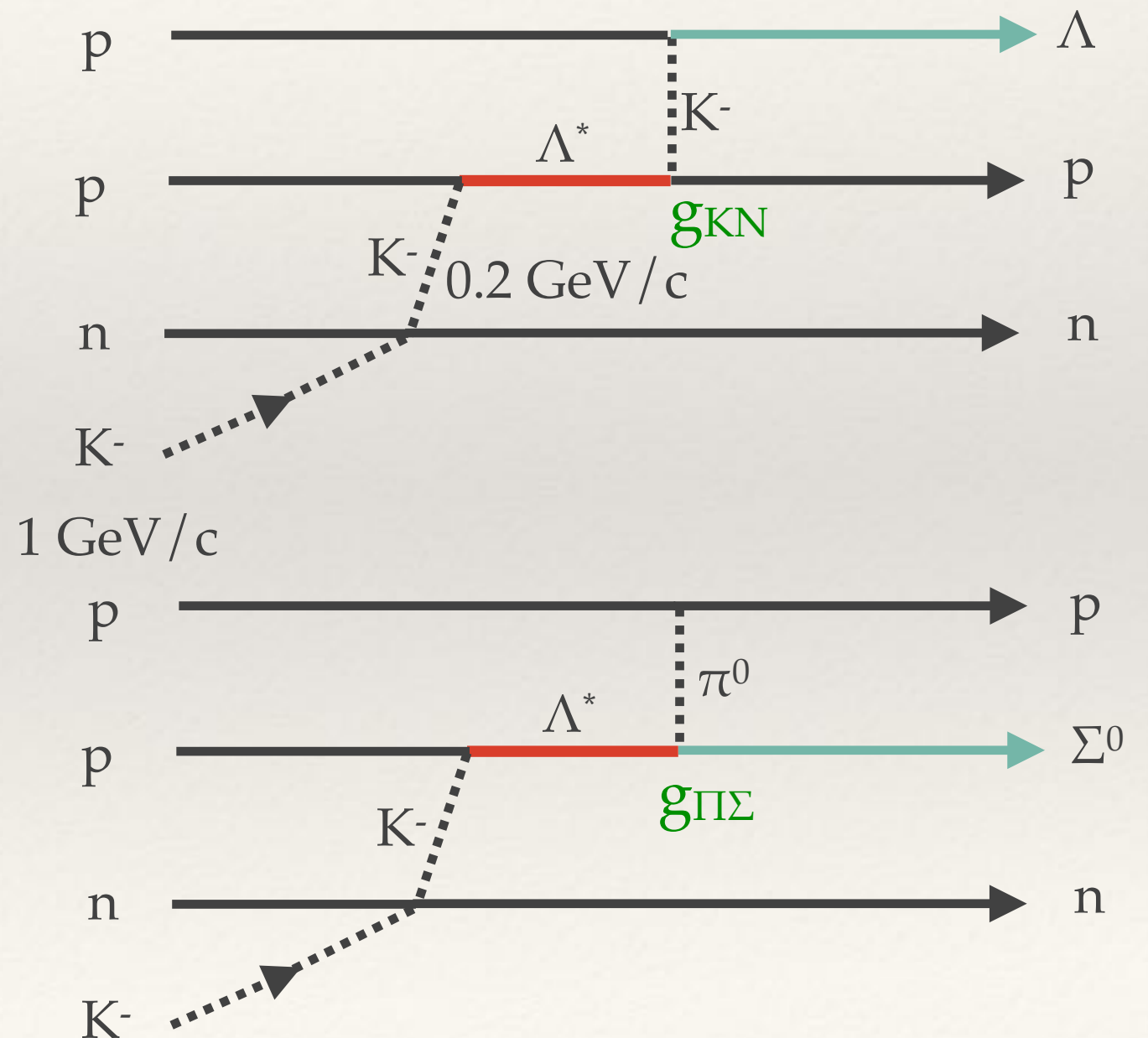
Mysteries of K^-pp

- ❖ Main decay mode is theoretically expected to be $\Sigma\pi N$ channel.
 - ❖ *if $B > 100$ MeV, $\Sigma\pi N$ mode is closed.*
- ❖ *However ...*
 - ❖ No observations in $\Sigma\pi N$ channel.
 - ❖ Signals are in non-mesonic ($\Lambda p, \Sigma^0 p$).
- ❖ Binding energies:
 - ❖ Two states ? Shallow(E15) and Deep(E27, DISTO).
 - ❖ Momentum Transfer ~ 0.2 GeV/c ~ 0.6 GeV/c

Role of $\Lambda(1405)$ as a doorway

- ❖ $\Gamma_{\Lambda p} / \Gamma_{\Sigma p} \sim 0.92$ (E27),
 $= 1.2$ (ChUA)
- ❖ depends on $g_{KN} / g_{\pi\Sigma} \gg 1$.
- ❖ $\Gamma_{\text{Mesonic}} : \Gamma_{\text{Non-Meso.}} \sim 7 : 3$.
- ❖ $\Lambda^* \rightarrow \Sigma^*$
- ❖ $\Gamma_{\Lambda p} / \Gamma_{\Sigma p} \gg 1$
- ❖ $\Gamma_{\text{Mesonic}} : \Gamma_{\text{Non-Meso.}} \sim 1 : 1$.

T. Sekihara et al., PRC 86 (2012) 065205.
 PRC 79 (2009) 062201(R).



Other possibilities

- ❖ Dibaryon as $\pi\Lambda N$ - $\pi\Sigma N$ bound states

H. Garcilazo, A. Gal, NPA 897 (2013) 167-178.

$$Y=1, I=3/2, J^\pi=2^+$$

- ❖ $\Lambda(1405)N$ bound state

T. Uchino et al., NPA868 (2011) 53.

$$I=1/2, J^\pi=0^- ; \quad \text{not so large binding}$$

- ❖ A lower $\pi\Sigma N$ pole of “ K - pp ”

a broad resonance near the $\pi\Sigma N$ threshold

A. Dote, T. Inoue, T. Myo, PTEP (2015) 043D02.

- ❖ Enhanced $\bar{K}N$ interaction due to

Partial restoration of Chiral symmetry;

S. Maeda, Y. Akaishi, T. Yamazaki, Proc. Jpn. Acad., B 89 (2013) 418-437.

Summary

- ❖ Two measurements suggest two bound states: Shallow(~ 20 MeV) and Deep(~ 100 MeV).
- ❖ At least, there exists a K - pp bound state.
- ❖ Whether both states co-exist ?
 - ❖ Deep : K - pp_{gs} , and Shallow : K - $pp_{excited}$?
 - ❖ or
 - ❖ Shallow : K - pp_{gs} , and Deep : $\pi\Sigma N$ bound state ?
- ❖ Measure the Spin-Parity and Isospin of K - pp !